Application of Electrodialysis into Nutrient Recovery and Antibiotics Removal for Pig Manure Management

by **Lin Shi**

Civil Engineering, College of Engineering & Informatics, National University of Ireland, Galway, Ireland

Research Supervisors:

Prof. Xinmin Zhan, Civil Engineering, National University of Ireland, Galway, Ireland

Prof. Zhenhu Hu, Municipal Engineering, Hefei University of Technology, China

Professor of Civil Engineering: Padraic E. O'Donoghue

A thesis submitted to the National University of Ireland in fulfilment of the requirements for the degree of Doctor of Philosophy.

Submission date: 22/07/2019

Abstract

Animal manure should be regarded as a resource rather than a waste as it contains abundant nutrients (nitrogen and phosphorus) available for plants. Land spreading of animal manure is a common practice while it has to be limited not exceeding the land carrying capacity. Nutrient recovery from excess animal manure, either in the form of raw manure or anaerobic digestate, is important and necessary for the sustainable development of animal farming. Since animal manure is a reservoir of veterinary antibiotics, the biosafety regarding antibiotics during nutrient recovery should be taken into account.

In this Ph.D. research, the application of electrodialysis (ED) technologies to recover the nutrients from pig manure was assessed. The research objectives were to: (1) assess the feasibility of nutrient recovery from pig manure digestate using electrodialysis reversal (EDR); (2) assess the recovery of nutrients and volatile fatty acids (VFAs) from pig manure hydrolysate using bipolar membrane electrodialysis (BMED); (3) investigate the fate of antibiotics in relation to membrane fouling in an EDR process for nutrient recovery; and (4) investigate in-situ anodic oxidation in EDR for antibiotics removal and fouling mitigation.

The results showed that the EDR removed all ammonium nitrogen (NH_4^+-N) and 84% of phosphorus (PO_4^{3-}-P) from the feed solution. Particle and chemical fouling were mitigated through the reversal of electrodes during EDR. Organic matter was the main cause of membrane fouling, while this fouling levelled off gradually, indicating the potential of long-term operation of EDR for nutrient recovery.

Bipolar membrane electrodialysis was able to separate NH_4^+-N into the base product and PO_4^{3-}-P and VFAs into the acid product. It was observed that there was a diffusion of ions through the bipolar membranes, causing the low recovery of NH_4^+-N and impurity of products. A BMED model was established to quantify the ion flux balance and a novel two-stage BMED was developed based on the 'inflection point' of the voltage profile. The research results proved that this two-stage BMED can efficiently improve the product yield and purities.

Antibiotics can be concentrated in the product solution during nutrient recovery, causing the risk to the people, animals, and ecology when using the product as fertilizer. Using synthetic wastewater, it was found that 90% of the sulfadiazine (SD) and tetracycline (TC) in EDR were removed from the feed solution due to membrane sorption, and transported to the product solution and membrane matrices. SD can pass through the membranes, while TC accumulated in the membrane-solution interface, showing an association with particle and organic fouling. Comparing with the synthetic wastewater, lower removal efficiencies of SD and TC were observed due to the membrane fouling when treating real pig manure.

The anode in ED was utilized in-situ for the oxidation of antibiotics, fouling mitigation, and pathogen inactivation. Anodic oxidation had negligible effects on the Cl^-, NH_4^+-N, and PO_4^{3-}-P, but rapidly removed the SD and TC from the feed solution. The particle fouling was significantly mitigated due to gas bubbling, and *E. coli* and *Enterococcus* were efficiently inactivated in the initial 30 minutes. Despite a high generation potential of disinfection by-products (DBPs), trihalomethanes and haloacetic acids in the feed solution were only 134 and 192 μg/L, respectively, proving that the effluent (feed solution) generated is far safe for water reclamation.

The results in this research indicate that EDR and BMED are efficient in nutrient recovery from pig manure. In-situ anodic oxidation in ED reactors can remove antibiotics, mitigate fouling, and inactivate pathogens, with low concentrations of DBPs produced. The data obtained will provide with alternatives for pig manure management regarding nutrient recovery and biosafety.

Table of Contents

List of Tables

List of Figures

Declarations

This thesis or any part thereof, has not been, or is not currently being submitted for any degree at any other university.

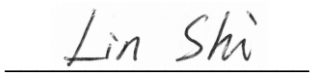

Lin Shi

The work reported herein is as a result of my own investigations, except where acknowledged and referenced.

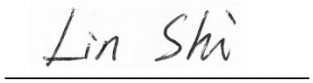

Lin Shi

Acknowledgments

Firstly I would like to thank Prof. Xinmin Zhan for his supervision, support, and encouragement throughout my 4 years' research work. I sincerely appreciate his valuable advice on my research direction, experiment conduction, and paper/thesis writing.

I would like to thank Prof. Zhenhu Hu and Dr. Yuansheng Hu for their guidance and advice on my experimental design and paper writing. Thank Prof. Olivier Thomas for the guidance on the determination of oxidation intermediates. Thank Prof. Piet Lens and his research group for the help on the sample analysis. Thank Prof. Peter Croot, Prof. Donal Leech and Dr. Liam Morrison for their help on fouling characterization. I also would like to thank Dr. Sihuang Xie for his review and revision of my draft papers.

I'd like to thank the China Scholarship Council (Ref: 201506690025) for funding my Ph.D. research work from 2015 to 2019.

I would like to thank Prof. Padraic O'Donoghue, Dr. Annette Harte, and Dr. Eoghan Clifford for their insightful comments on my annual GRC reports.

I would like to thank all the friends and colleagues in our group, who made my last 4 years not only professional work but full of warmth and joy. I also would like to thank all the staff and technicians in the Engineering Building, for their help throughout my research work.

Finally, I would like to sincerely thank my parents and all my friends in Galway. Thanks for all the encouragement and accompany, thanks for the happiness you brought me during my study.

List of Abbreviations

AD: anaerobic digestion

AM: anion-exchange membrane

ARG: antibiotic resistant gene

BM: bipolar membrane

BMED: bipolar membrane electrodialysis

BSA: bovine serum albumin

CH: chloral hydrate

CM: cation-exchange membrane

COD: chemical oxygen demand

DBP: disinfection by-product

DC: direct current

DCAA: dichloroacetic acid

DCAN dichloroacetonitrile

DM: dry matter

DOM: dissolved organic matter

ECD: electron capture detector

ED: electrodialysis

EDR: electrodialysis reversal

EDX: energy dispersive X-ray detector

EEM: excitation-emission matrix

EPA: environmental protection agency

FO: forward osmosis

GC: gas chromatography

HA: humic acid

HAA: haloacetic acid

HPLC: high performance liquid chromatography

HTC: hydrothermal carbonization

IEC: ion-exchange capacity

MCR-ALS: multivariate curve resolution – alternating least squares

MD: membrane distillation

MF: microfiltration

MFD: multistage flash distillation

MS: mass

NF: nanofiltration

PC: penicillin

RD: reverse osmosis

SA: sulphonamide

SC: single-compartment

SD: sulfadiazine

SEM: Scanning electron microscope

SPE: solid phase extraction

SS: suspended solids

TC: tetracycline

TCAA: trichloroacetic acid

TCM: trichloromethane

THM: trihalomethane

*t*BuOH: tert-butyl alcohol

UF: ultrafiltration

VFA: volatile fatty acid

Chapter 1

Introduction

1.1 Background

Global pork production has reached more than 120 million tonnes in 2018 [1], resulting in not only the intensification of large-scale pig farms but also a significant increase in manure production. Pig manure is a mixture of flushed faeces, urine, strewing material and spilled food [2]. As a natural fertilizer, pig manure has been extensively applied on farmlands to favour plant growth [3]. Prior to land application, pig manure is commonly collected and stored in animal houses for several weeks to several months (it is not rare that manure has been stored for one year), leading to the release of nitrogen (N), phosphorus (P), and volatile fatty acids (VFAs) to the liquid fraction as hydrolysis occurs. In large-scale pig farms, it is common that pig manure is anaerobically digested for the purpose of biogas production, odour elimination, and pathogen inactivation [4-6]. This approach can also maximize the fertilizer effect of pig manure due to the complete release of nutrients to the liquid phase. However, land application of pig manure either in the form of raw manure or anaerobic digestate at a rate exceeding the crops uptake threshold can pose significant environmental impacts, particularly in large-scale pig farms where manure generated exceeds the land carrying capacity [7]. The European Union Nitrates Directive Action plan has restricted the use of animal manure on grassland and cereals [8]. In Ireland, the maximum amount of N that can be applied annually to land is 170 kg/ha [9]. Many farms are no longer suitable for land spreading of pig manure or digestate because organic N loading from grazing livestock is already at or approaching this limit. The application of P fertilizer to the lands in Ireland is limited by P indexes, which have been classified into four indexes (Index 1 – 4) based on the P contents in soil [10]. Only the land with P index below 3 can be fertilized (below 5.0 mg/L for grassland). The land availability will be reduced further due to the imposed P loading in future. Therefore, alternative options become essential to the disposal of excessive pig manure, in order to avoid over-fertilization and mitigate environmental impacts.

Nutrient recovery from pig manure is one of the most promising alternatives, through which soluble N and P are extracted from the liquid phase. Nutrient recovery can be achieved either in the form of hydrolysate or digestate, since most of N and P are released from the organic matter to the liquid phase during hydrolysis. In large-scale pig farms, pig manure digestate can be regarded as a by-product after complete biogas

production. It is preferable to be used as the raw material for nutrient recovery since the digestate is less in odour and pathogens. Pig manure hydrolysate presents a lower pH than digestate, thus a higher concentration of P being mobilized in the liquid phase [11, 12]. Hydrolysate contains a very high concentration of VFAs, a carbon source widely used in the production of bioplastics and bioenergy, as well as in biological nitrogen removal from low C/N wastewater [13, 14]. Apart from being organic matter for biogas production through anaerobic digestion (AD), VFAs can be alternatively harvested as by-products, which can be incorporated potentially into the recovery processes of N and P. The compositions of pig manure hydrolysate and digestate are mostly identical but with some differences. Water, suspended solids (SS), salts, and humic acid (HA) in the hydrolysate are all present in the digestate after AD, in addition to the degradation of organic matter. The selection of raw materials for nutrient recovery (hydrolysate or digestate) may vary depending on recovery purposes, yet there is no big difference in the recovery mechanism.

Most recently, researchers have focused on nutrient recovery from pig manure using membrane technologies, including microfiltration (MF), ultrafiltration (UF), nanofiltration (NF), reverse osmosis (RO), membrane distillation (MD), and ED [15, 16]. In particular, some of the membrane technologies (e.g. RO, MD, and ED) can separate and concentrate N and P from the feed solution into a solution with a higher fertilizer value. Prior to the membrane processes, pig manure (either in hydrolysate or digestate) has to be pretreated to remove the SS, namely solid-liquid separation. This is often performed in a thickener or decanter centrifuge where flocculants or coagulants are supplemented. However, flocculation is insufficient to remove colloidal particles, and coagulation is also limited by the high dosage of coagulants due to the high concentrations of SS, carbonate, and phosphate [2, 17]. As such, the separated liquid fraction of pig manure is still turbid (rich in colloidal particles, Appendix A), which can clog the membranes very quickly. Ca^{2+} and Mg^{2+} in the liquid phase may cause chemical deposition on the membranes, and certain dissolved organic matter (DOM) can cause organic fouling via the molecular interaction between foulants and membrane matrix [18, 19]. By far, most of the studies have used synthetic hydrolysate or digestate as the feed solution to assess the viability of nutrient recovery using membrane technologies, while the usage of real pig manure has insufficient demonstrations.

Electrodialysis reversal (EDR) and bipolar membrane electrodialysis (BMED) are emerging ED technologies offering great potential in nutrient recovery. EDR is effective in the mitigation of membrane fouling caused by particle aggregation because of the frequent reversal of electrodes. This provides feasibility for nutrient recovery using only EDR rather than integrating MF and UF. In addition, chemical deposition can be dissolved periodically during the reversal operation of electrodes, thereby remitting the risk of membrane scaling. BMED is normally designed for the enhancement of product diversity. It couples functionally the solvent dissociation of bipolar membrane (BM) and the salt dissociation of conventional ED. In other words, BMED takes advantage of the specific property of a BM and effectively splits water into hydroxide ions (OH^-) and protons (H^+) under an applied electric field, thus separating cations and anions to different compartments. Inorganic and organic salts can be converted to the corresponding acids and bases in BMED, thereby allowing the diversity of the products without chemical dosing. In terms of nutrient recovery from pig manure, a high pH in the base compartment creates suitable conditions for NH_4^+ recovery via subsequent air stripping, while P and VFAs migrating to the acid compartment in BMED can be recovered as weak acids for industrial use. EDR and BMED have been frequently applied to the desalination of industrial water and wastewater [18, 20-25], while there have been no studies conducted on the treatment of pig manure that have high concentrations of SS, Ca^{2+}, Mg^{2+}, and DOM. Simultaneous recovery of NH_4^+, P, and VFAs has never been reported in the literature. The mechanism and evolution of membrane fouling in a long-term nutrient recovery process remain unclear.

Pig manure is a reservoir of veterinary antibiotics. In addition to nutrient recovery, biosafety regarding antibiotics during the treatment of pig manure should be of concern. Since the administered antibiotics are poorly absorbed in the animal gut, the majority of the dose (30 – 90%) is excreted unchanged to the animal manure via urine and faeces [26]. The concentrations of antibiotics in fresh animal manure can reach the level of mg/L depending on feeding manners and seasons. It is noteworthy that certain antibiotics are extremely hard to degrade in biological processes, such as sulphonamides (SAs) and tetracyclines (TCs) (they are extensively used in Europe). Chronically exposure to these antibiotics can generate antibiotics resistance genes (ARGs) in bacteria, causing the risk to the human, animals, and ecology. Previous

studies have reported that long-term application of animal manure to farmlands can cause the enrichment of antibiotics and ARGs in soil [27, 28]. The application of struvite recovered from wastewater also caused this issue [29]. The enrichment of antibiotics in the recovered fertilizer makes its land application questionable. In relation to ED technologies, the ionized antibiotics are able to migrate under the electric field, forming the possibility of being transported to the product [30-33]. It has been reported that certain organic trace pollutants, e.g. steroid hormones and endosulfan, can be adsorbed by the ion-exchange membrane [34, 35]. However, there have been no studies investigating the migration and sorption of antibiotics in ED technologies so far. The studies on antibiotics will provide the industry with valuable information on manure management.

In the ED technologies, antibiotics are only physically transported to the membranes and product solution. Additional approaches are required for further destruction of the antibiotics in pig manure. Anodic oxidation is effective in the destruction of bio-refractory compounds, e.g. antibiotics, dyes, phenols, and perfluoroalkyl substances [36-39]. It has been applied to the treatment of toilet wastewater for water reclamation, with acceptable DBPs generated [40]. Since certain pathogens cannot be removed efficiently in anaerobic digesters, such as *E. coli*, *Enterococcus*, and *Salmonella* [41-44], anodic oxidation shows a possibility to inactivate these pathogens so as to meet the criteria on biosafety and water reclamation. However, this technology is normally regarded as an independent process requiring additional electric energy, while it can be achieved in the ED system by sharing one pair of electrodes. The commonly used anodes, e.g. Pb/PbO_2, dimensionally stable anode, graphite, and boron-doped diamond electrodes, are showing good compatibilities in the ED system, and the current density in ED enables efficient oxidation. It has been reported that gas bubbling can mitigate the membrane fouling caused by particles due to the increase of fluid turbulence [45-47]. In this regard, the generated gas bubbles in ED has the potential of fouling mitigation. By applying anodic oxidation in ED, the surplus energy on electrodes can be utilized, thus leading to a decrease in the total energy consumed on desalination.

1.2 Objectives

In this research, the application of emerging ED technologies, including EDR and BMED, to the nutrient recovery from pig manure was demonstrated. Pig manure digestate and hydrolysate were tested as raw materials for recovery in EDR and BMED for different purposes, respectively. The objectives of this Ph.D. research were to: (1) assess the viability of long-term nutrient recovery from pig manure digestate using EDR, with a semi-continuous operation and a periodical acid cleaning protocol; (2) assess the simultaneous recovery of N, P, and VFAs from pig manure hydrolysate using BMED and the improvement of product purities; (3) investigate the distribution and migration of antibiotics in ED and EDR during the nutrient recovery from pig manure; (4) utilize the anode in the ED system for in-situ antibiotics oxidation, fouling mitigation, and pathogen inactivation during the nutrient recovery from pig manure digestate.

1.3 Research boundary

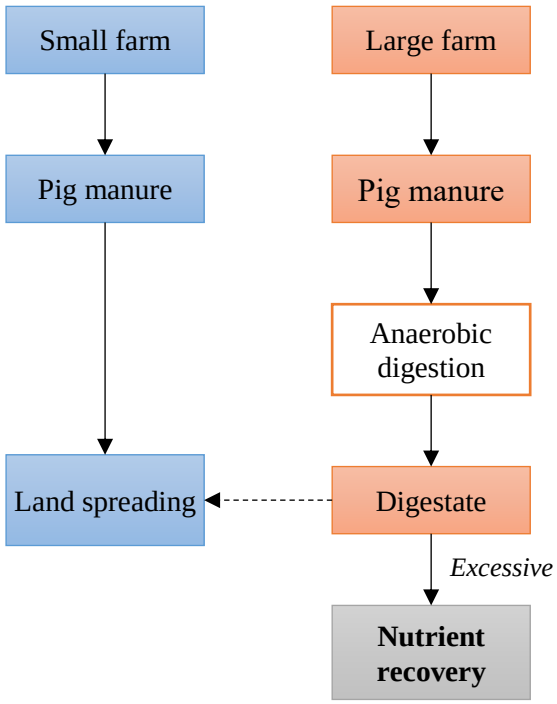

Figure 1-1. Research boundary of this thesis.

The boundary of this research is shown in Figure 1-1. As to small pig farms, the adjacent lands are sufficient for direct land application of animal manure. As to large pig farms,

the adjacent lands are not enough for direct land application. The transportation of animal manure to the lands distant from animal farms causes a high transportation cost. In this case, nutrient recovery from pig manure should be considered. The reason of using this research boundary will be further discussed in Chapter 2.

1.4 Methodologies

Pig manure digestate and hydrolysate are both organic fertilizer available for plants. They can be acquired in one AD system but from different digestion stages. The compositions of digestate and hydrolysate are largely identical, but with minor differences. In this context, nutrient recovery from pig manure was regarded as the recovery of N and P from either the digestate or hydrolysate forms of pig manure. Pig manure digestate and hydrolysate were both tested as the raw materials for nutrient recovery. The roadmap of this Ph.D. research is shown in Figure 1-2.

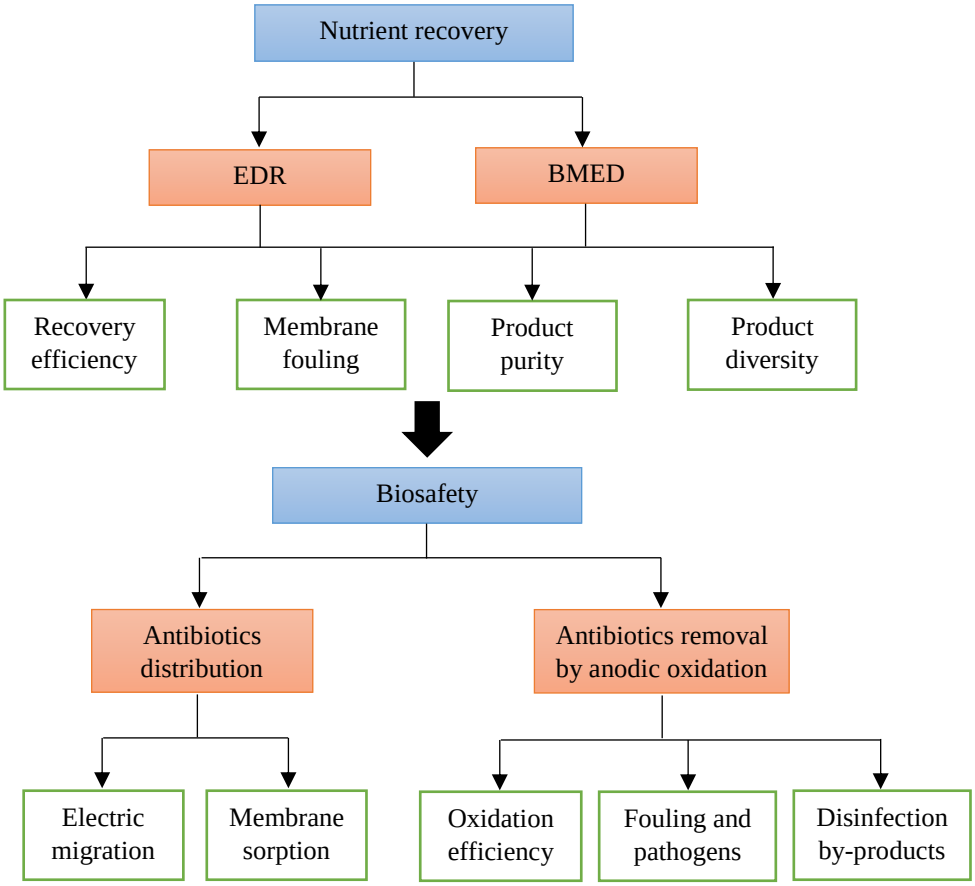

Figure 1-2. Research roadmap of this thesis.

Pig manure digestate and hydrolysate both contain a high concentration of SS, Ca^{2+}, Mg^{2+}, and DOM. These compounds can cause severe membrane fouling in the membrane processes. EDR is known for its high resistance to membrane fouling. Considering this, the application of EDR to nutrient recovery from pig manure using digestate was assessed. Prior to EDR, a solid-liquid separation consisting of acidification and low-speed centrifugation was carried out to remove the coarse particles and increase the concentration of P in the liquid phase. The concentrations of NH_4^+-N and PO_4^{3-}-P (sum of P in the form of PO_4^{3-}, HPO_4^{2-}, and $H_2PO_4^-$) in the feed and product solutions were measured. The feasibility of long-term operation was assessed via monitoring membrane fouling, including particle aggregation, chemical scaling, and DOM-caused fouling. The long-term stability of ion-exchange membranes was assessed by monitoring the conductivity and ion-exchange capacity (IEC) of membranes. In addition, a conventional ED process was set up as the control group, in order to demonstrate the benefits of electrode reversal.

The application of BMED to nutrient recovery from pig manure hydrolysate was then assessed, in order to recover N, P, and VFAs as different products. The recovered acid and base can potentially be used as industrial materials. The experiment was conducted using synthetic wastewater first to probe the feasibility of nutrient recovery from the hydrolysate. A mathematic model was established to quantify the ion flux balance in BMED. Because the diffusion loss of ions became intensive in the late period of BMED, a novel two-stage BMED was proposed to increase the recovery efficiency and product purity. Real pig manure hydrolysate after solid-liquid separation was tested in BMED for the consolidation of results.

Alongside the nutrient recovery from pig manure (either digestate or hydrolysate), antibiotics can be transported to the product solution. The fate of antibiotics in EDR during nutrient recovery from synthetic pig manure was investigated, including the electric migration and membrane sorption. SD and TC were selected as target antibiotics for study since they are widely used in pig farms. Using real pig manure, the association between antibiotics migration and membrane fouling was profiled.

Since the antibiotics were only physically transported or adsorbed by membranes in ED technologies, additional techniques are needed for the elimination of antibiotics. In this research, the anode in ED was utilized in-situ for the oxidation of antibiotics. Briefly,

the feed solution was pumped to the anode compartment and flowed into the dilute compartment subsequently, so that the gas generated was bubbled in the feed solution, which can oxidize the antibiotics. Membrane fouling was assessed and *E.coli* and *Enterococcus* were measured to study the fouling mitigation and pathogen inactivation of this anode-ED process. The concentrations of trihalomethanes (THMs) and haloacetic acids (HAAs) were determined, so as to assess the risk of using the effluent for water reclamation.

1.5 Thesis structure

Chapter 1 is the introduction. The background of the research, primary objectives, and research methodologies are presented.

Chapter 2 reviews the recent studies related to this Ph.D. research, including the composition of pig manure, solid-liquid separation, conventional and emerging technologies regarding nutrient recovery, as well as common antibiotics in pig manure.

Chapter 3 assesses the application of EDR to the nutrient recovery from pig manure digestate. The recovery efficiency, membrane fouling, and stability of long-term operation were investigated.

Chapter 4 assesses the application of BMED to the nutrient recovery from pig manure hydrolysate. A novel two-stage BMED was established in order to improve the recovery efficiency and product purity.

Chapter 5 investigates the fate of antibiotics in EDR for nutrient recovery from pig manure. Membrane sorption, electric migration, and distribution associated with membrane fouling were investigated.

Chapter 6 demonstrates the in-situ anodic oxidation in EDR for antibiotics removal, fouling mitigation, and pathogen inactivation. The concentrations of generated DBPs were determined, so as to assess the risk to the environment and the possibility of water reclamation.

Finally, Chapter 7 presents the conclusions drawn from all the studies in Charter 3-6. Recommendations for future research are put forward.

1.6 Publications

Published:

Chapter 2: **Lin Shi**, Walquiria Silva Simplicio, Guangxue Wu, Zhenhu Hu, Hongying Hu, Xinmin Zhan. Nutrient recovery from digestate of anaerobic digestion of livestock manure: a review. *Current Pollution Reports* 2018 4, 74-83.

Chapter 3: **Lin Shi**, Sihuang Xie, Zhenhu Hu, Guangxue Wu, Liam Morrison, Peter Croot, Hongying Hu, Xinmin Zhan. Nutrient recovery from pig manure digestate using electrodialysis reversal: membrane fouling and feasibility of long-term operation. *Journal of Membrane Science* 2019, 573, 560-569.

Chapter 4: **Lin Shi**, Yuansheng Hu, Sihuang Xie, Guangxue Wu, Zhenhu Hu, Xinmin Zhan. Recovery of nutrients and volatile fatty acids from pig manure hydrolysate using two-stage bipolar membrane electrodialysis. *Chemical Engineering Journal* 2018, 334, 134-142.

Ready for submission:

Chapter 5: **Lin Shi**, Zhenhu Hu, Walquiria Silva Simplicio, Songkai Qiu, Brendan Harhen, Liwen Xiao, and Xinmin Zhan. Antibiotics in electrodialysis reversal for nutrient recovery from pig manure: sorption and migration influenced by membrane fouling.

Chapter 6: **Lin Shi** and Xinmin Zhan. In-situ anodic oxidation in electrodialysis for antibiotics removal, fouling mitigation, and pathogen inactivation during nutrient recovery from pig manure digestate.

Chapter 2

Literature review: nutrient recovery from animal manure

Chapter 2

Animal manure can be applied onto farmlands to enhance crop yields as it is abundant in nutrients. However, intensive livestock farming brings about manure exceeding the carrying capacity of lands nearby. Technologies focused on nutrient recovery from animal manure have been studied recently, while many problems and challenges still remain unsolved. In this chapter, these recovery technologies are reviewed and compared, and challenges are deliberated. Ammonia stripping and struvite formation are easily operated technologies in comparison with membrane technologies. Amongst membrane technologies, EDR and forward osmosis are promising due to their high resistance to membrane fouling. Further studies should be focused on the operational cost, disposal of solid and liquid residuals, and marketization of the recovered products.

This chapter has been published on *Current Pollution Reports:*

Lin Shi, Walquiria Silva Simplicio, Guangxue Wu, Zhenhu Hu, Hongying Hu, Xinmin Zhan. Nutrient recovery from digestate of anaerobic digestion of livestock manure: a review. *Current Pollution Reports* 2018 4, 74-83.

2.1 Introduction

Livestock products are critical dietary sources in people's daily lives. In particular, meat and milk supply essential animal proteins, iron, zinc, and vitamins to human bodies [48, 49]. Nowadays, the world population is growing by 1.7% annually and it is estimated to reach 9.7 billion by 2050 [50], which will, therefore, lead to increasing demand for livestock products. According to the census organized by the Food and Agriculture Organization of the United Nations, global meat and dairy products have reached 335.0 and 826.9 million tonnes in 2018, respectively [1]. The development of livestock production brings huge economic benefits but massive livestock manure is generated. The disposal of animal manure in livestock farms has unquestionably become a worldwide issue by far.

Animal manure can be regarded as a resource rather than a waste as it contains plenty of nutrients biologically available for plants. Land application is a conventional method of manure management, which is often adopted by farmers to increase crop yields. During land application, fresh or hydrolysed manure is directly applied on lands so as

to reuse the nutrients. Its history dates back to thousands of years ago when farmers in certain countries (e.g. China) started to spread animal manure and human excreta to less arable lands [51, 52]. The United States have started to extensively spread animal manure on farmlands since mid-20th century [3]. However, the overuse of raw animal manure can damage plants and lead to a series of environmental problems. In this regard, dedicated technologies, such as composting and AD, have to be adopted to minimize the environmental hazards of animal manure prior to land application. Composting is a traditional method of manure management which transforms organic matter to a safe and stabilized fertilizer, i.e. compost. However, only the solid manure with low water content can be used for composting, and additional carbon materials are required to increase the C/N ratio of composting piles [53-55]. The advantage of AD is the production of renewable biogas, being methane share of around 65% [7, 56, 57]. It is able to increase the fertilizer effect, eliminate odor, and reduce pathogen levels and greenhouse gas emissions [4, 5, 7]. Up to now, plenty of anaerobic biogas plants have been developed within many European countries, e.g., Germany, Denmark, Austria, Netherlands, France, United Kingdom, Spain, and Italy [4]. Over 52.3 TW of electricity in Europe was produced from the biogas in 2014 [58]. In developing countries, China, India, and Nepal contribute most of the domestic anaerobic digesters in the world [59]. Over 40 million biogas reactors have been set up in rural areas of China for cooking and lighting purposes [60]. The energy of biogas generated from animal manure is 424 MJ per ton of cattle manure, and 447 MJ per ton of pig manure [61]. In the AD system, due to the decomposition of organic matter, most of the nutrients existing in solids can be released to the liquid phase. The digested manure (i.e. digestate) is more eco-friendly and effective for land application [62].

The nutrients in animal manure include nitrogen (N) and phosphorus (P). The application rate of animal manure (either the raw manure or digestate) to lands should comply with the land carrying capacities. In small farms, animal manure can be directly reused on lands nearby to close the nutrient loops. While in intensive farming areas where tons of surplus animal manure are produced daily, managers are impelled to pursue efficient, cost-effective, and eco-friendly disposal alternatives. The concept of nutrient recovery is therefore presented to cope with the excessive animal manure in farms. The major incentives of nutrient recovery from animal manure are summarized as follows:

- *Pollution prevention*. Reducing the nutrients emission to the environment and remitting air pollution. In the case of over-fertilization, most of the N and P in animal manure are lost via ammonia (NH_3) evaporation and water runoff [4, 15, 63]. It can cause serious air pollution and water eutrophication

- *Alternative fertilizer production.* Supplying renewable fertilizer to substitute mineral nutrients. In many countries, mineral P is not likely to be depleted immediately, while the majority of countries must import the mineral P to maintain domestic crop yields [64].

- *Industrial recovery values*. Producing raw materials for industrial use, such as detergents, food additives, and livestock feed additives [63].

This review offers the current state of nutrient recovery from animal manure, including the hydrolysed and digested manures, two common forms of manure in animal farms. The characteristics of animal manure, pretreatment methods, and nutrient recovery technologies are reviewed. Recovery technologies, including ammonia stripping, chemical precipitation, ion exchange, membrane separation, and thermal treatment are compared, and future research directions are deliberated.

2.2 Characteristics of animal manure

Although animal manure originates from different sources, such as pig, cattle, and chicken, or manures co-digested with food waste and agriculture straw, the composition of animal manure and final digestion products is mostly similar. In an AD system, most substances (e.g. water, nutrients, and other inorganic matter) in the digestate are inherited from fresh animal manure, but their quantities may vary depending on animal housing practices, feeding patterns, and manure collection and on-farm storage method [2, 65]. Hydrolysed and digested animal manure can be acquired from one AD system but different digestion stages. The characteristics of animal manure and digestate in recent studies are summarized in Table 2-1, and the transformation of animal manure in AD is shown in Figure 2-1.

Table 2-1. Characteristics of animal manure and digestate in recent studies.

Manure	TS (g/L)	VS (g/L)	Total N (g/L)	NH_4^+-N (g/L)	Total P (g/L)	K (g/L)	Reference
PM	46.0 – 91.0	28.0 – 72.0	-	-	-	-	[65]
PM	17.1 – 80.6	11.4 – 65.0	2.20 – 5.28	-	0.38 – 1.26	1.27 – 2.72	[66]
PM	56.6	-	4.10	-	1.40	-	[67]
PM	56.0	41.0	-	-	-	-	[68]
PM	22.0 – 83.4	13.8 – 65.1	2.35 – 5.74	-	0.38 – 1.68	-	[69]
PM	59.5	38.9	7.60	4.95	-	-	[70]
PM	53.0	35.2	5.63	3.39	-	-	[71]
PM	18.1 – 51.9	3.0 – 35.0	1.18 – 8.35	0.99 – 6.71	0.007 – 1.14	0.61 – 5.78	[72]
PM	35.4 – 45.5	22.1 – 32.0	4.58 – 6.47	3.71 – 5.54	1.04 – 1.63	2.13 – 2.61	[73]
CM	42.0	24.5	33.55	10.15	-	-	[74]
PM	37.1	26.1	-	1.64	-	-	[7]
PM	78.1	56.1	-	4.62	-	-	[14]
PM	73.0	56.0	-	4.80	-	-	[41]
PM	38.0 – 73.0	25 – 56	3.08 – 3.99	1.43 – 2.09	-	-	[44]
DM	44.9 – 63.7	30.8 – 46.1	-	2.50 – 2.90	0.48 – 0.69	3.06 – 4.26	[66]

DM	87.0	74.0	3.50	1.40	-	-	[75]
DM	71.0	-	-	3.80	0.80	-	[67]
DM	20.0 – 81.3	5.2 – 24.5	2.50	1.65	-	-	[76]
DM	125.0	101.1	1.80	1.40	-	-	[77]
PM digestate	35.5 – 65.3	24.8 – 37.0	-	3.8 – 5.00	0.89 – 1.67	2.31 – 2.71	[66]
PM digestate	19.3	4.0	-	1.45	-	-	[78]
PM digestate	31.7	17.2	4.73	3.68	-	-	[71]
Mix digestate	26.1 – 38.2	14.9 – 25.4	1.06 – 4.50	0.24 – 2.38	-	-	[79]
PM digestate	15.0 – 18.0	-	-	1.39 – 1.45	-	1.21	[80]
PM digestate	71.5	-	3.68	1.78	0.77	2.90	[81]
DM digestate	60.0	46.0	3.60	2.10	-	-	[75]
DM digestate	70.0	49.0	3.35	1.73	1.64	-	[82]
Overall	17.1 – 125.0	3.0 – 101.1	1.06 – 8.35	0.24 – 6.71	0.38 – 1.68	0.61 – 5.78	-

Note: PM, DM, and CM are the abbreviations of pig manure, dairy manure, and chicken manure, respectively.

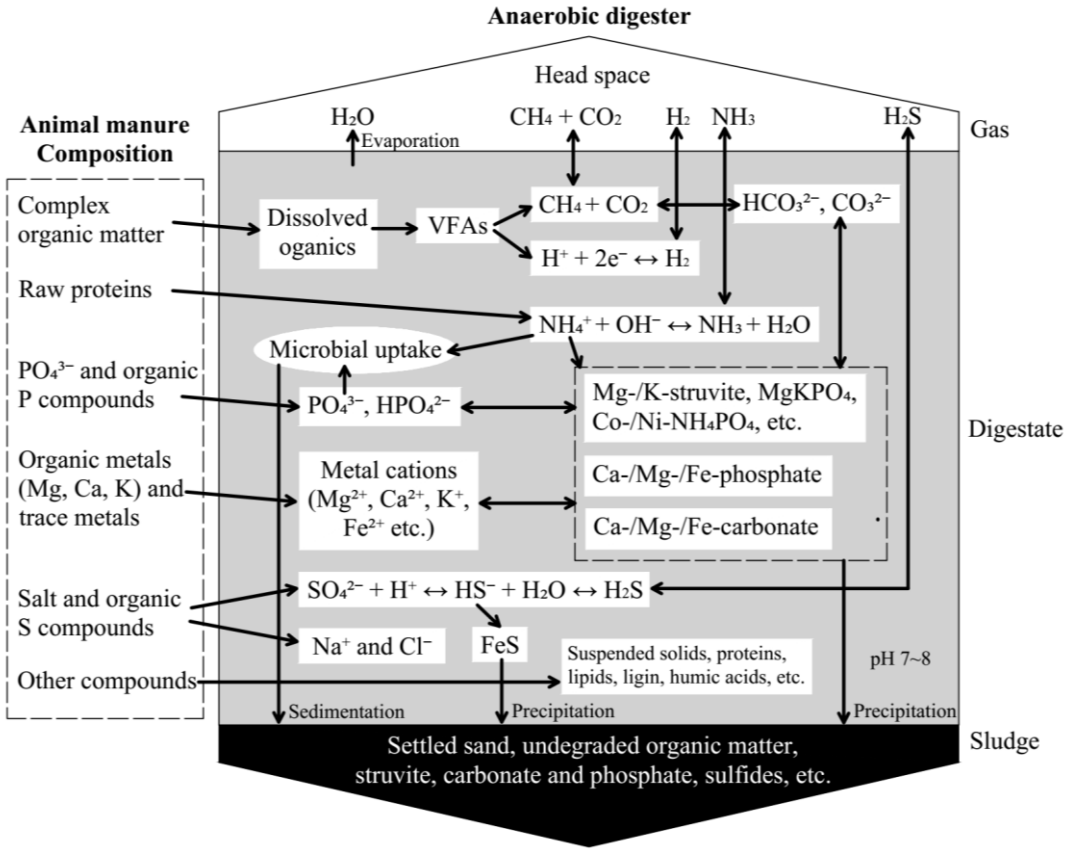

Figure 2-1. Composition and transformation of animal manure in anaerobic digester [17].

2.2.1 Water content

The water content of animal manure and manure digestate is highly dependent on the method of animal housing. Currently, solid manure can be only found in small- and medium- sized farms (Asian farms in particular), where the farmers scrape faeces manually from the floor in houses and the wastewater is drained in the gutter behind the animals [2]. This mode of animal housing generates solid manure so that composting and dry AD can be processed. In order to reduce the labour intensity, animal excreta in animal houses (e.g. pig farms) are flushed using water down to the pits or tanks beneath the slatted house, thereby forming liquid manure containing 95 – 98% of water [5]. In this circumstance, the generated liquid manure, which can be also called slurry elsewhere, is collected as a mixture of faeces, urine, spilt food, and flushed water that can support wet AD. Therefore, the water content of animal manure varies depending on the quantities of water used for manure flushing. In poultry farms, dry

manure is collected mechanically using a belt beneath chicken houses, while it is normally mixed with daily wastewater after collection for the sake of wet AD. Although dry AD has many advantages (e.g. small digester capacity, free of stirring, and less foam), wet AD is worldwide adopted because of its stable performance. Therefore, nutrient recovery from animal manure is normally regarded as the recovery of N and P from wet AD systems. The nutrient recovery from dry manure is difficult to apply.

2.2.2 Particles

"Particles" in animal manure, which is also called suspended solids elsewhere, is commonly investigated by researchers and engineers with the intensions of providing with important information on solid-liquid separation. The particles between 1 nm and 1 μm settle very slowly due to the Brownian motion, thus the poor efficiencies in solid-liquid separation and nutrient recovery processes. Particles distribution in manure is highly dependent on the animal feeding patterns. Fed with large grind sized and higher fiber content materials, high solids content and more particles in the range of 2 – 25 μm can be detected in animal manure [65]. It has been reported that the dry matter (DM) of particles smaller than 25 μm in pig manure was higher than that in cattle manure because of the feeding difference [66, 83]. In general, particles larger than 100 μm can be regarded as the feed residues, while particles smaller than 100 μm are microbial flocs, single cells, and digested residues being decomposed from the feeding materials. However, large particles can be further disassembled due to the high temperature, mechanical agitation, and organic matter decomposition, resulting in the alternations in particle size distribution during AD. It has been reported that the particles smaller than 10 μm increased by 20% after AD, while the particles smaller than 1.6 μm decreased [66, 84]. The particle size distribution in animal manure has been reported in the range of 1 nm – 1mm with one or two peaks observed in distribution patterns, while most of the particles remain around 25 μm. Much fewer data in relation to animal manure digestate are available, but the particles in digestate are normally a bit smaller than those in the raw manure before AD due to the decomposition of organic matter [41, 85].

2.2.3 Nutrients

During AD, the nutrients in raw animal manure remain in the digesters, regardless of a small part of N being released to the biogas. The nutritional composition of animal manure and digestate may vary depending on animal types and feeding patterns. It is associated with animal diet, intestinal microorganisms, and manure degradability [55]. In general, cattle manure contains a high content of fiber, thus lower degradability and methane yield during AD, while pig manure contains higher contents of N and P [54]. The concentrations of total N and P in pig manure are normally in the range of 1.2 – 6.7 g/L and 0.4 – 2.7 g/L, respectively [86]. It has been reported that one sow can generate approximately 21 m^3 of manure annually, resulting in up to 141 kg of N and 57 kg of P extracted to the manure [6]. The concentration of N in cattle slurry is in the range of 2.0 – 7.0 g/L, while it remains 2.0 – 21.0 g/L in poultry slurry [87-89]. The nutrients in animal manure hydrolysate are almost identical to those in digestate, because most of the nutrients are released to the liquid phase in the hydrolysis stage of AD.

Different from agricultural waste (e.g. food waste, straw, and corn), animal manure contains a high concentration of N. It has been reported that the C/N ratio in animal manure is in the range of 4 – 10, while this value increases to 14 – 37 in food waste [90]. The N in digestate originates from the N bonded proteins in the feeding materials, which occupies 55 – 95% of total dietary N [2]. The other N in feeding materials is absorbed by the intestinal tract and converted to animal proteins. Approximately 70% of total N in fresh manure is dissolved and mineralized in the hydrolysis stage of AD [11]. Regardless of a few nitrogen oxides and nitrous oxide, most of the N is mineralized to the ammonium (NH_4^+) and free ammonia (NH_3) and mobilized in the liquid phase of animal manure. However, this part of N can be lost to the atmosphere via evaporation easily. It has been estimated that 10 – 40% of NH_4^+-N was lost to the atmosphere during the manure storage, and this value increases to more than 50% after land application [12, 91]. NH_4^+ in animal manure can be converted to struvite in the presence of Mg^{2+} and PO_4^{3-}. However, the concentration of PO_4^{3-} in animal manure is far lower than that of NH_4^+, which is insufficient to convert all the NH_4^+ to struvite. A small part of N can be ingested by the anaerobic microorganisms, because N is an important element for cell synthesis, while this is negligible compared with the high

concentration of mobilized NH_4^+-N in animal manure. In summary, the fate of N in animal manure can be concluded as the (1) N in the form of NH_4^+ and NH_3; (2) N lost to atmosphere and biogas in the form of NH_3; (3) struvite formed; and (4) N ingested by microorganisms [17].

Phosphorus in animal manure derives from feeding materials and inorganic additives. Similar to N, the absorption of P in intestinal tract varies depending on animal types. For instance, the digestive system of cattle can absorb P very efficiently (more than 90% of P can be absorbed), while absorbed amount is much less (<50%) for pigs [2]. During AD, the surplus P in urine and faeces are released to the liquid phase along with the decomposition of organic matter, but most of them can precipitate with metals (e.g. Mg^{2+}, K^+, and Ca^{2+}) and form Mg-/K-struvite and Ca-phosphate compounds. It has been reported that around 80% of P exists in the solid fraction of animal manure [11]. Comparing with manure hydrolysate, complete AD can decrease the P availability because of the pH increase in the methanogenesis stage [17]. The dissolved P, which is mostly identified as orthophosphate, is highly associated with pH conditions. The P in the solid phase of animal manure starts to be significantly dissolved when the pH is lower than 6.5. Raising the pH moves the chemical reaction towards the precipitation of P and results in low availability for plants. The distribution of P is associated with the particles. Different from organic P, the mineralized P can precipitate on the surface of particles, causing the coagulation effect of particles. Similar to N, P is also an important element for cells, in particular for the synthesis of adenosine, nucleic acids, and phospholipids. The fate of P in animal manure can be concluded as (1) the mobilized P in the liquid phase; (2) the P in Mg-/K-struvite and Ca-phosphate; and (3) the P ingested by microorganisms.

2.2.4 Other components

Animal manure is a complex system containing various inorganic and organic matters. Apart from water and nutrients, the inorganic substances include mineralized metals (e.g. Na^+, K^+, Mg^{2+}, Ca^{2+}) and anions (e.g. Cl^-, SO_4^{2-}, carbonate) originating from roughage and salt intake, which can cause the high conductivity of animal manure. Mg^{2+} and Ca^{2+} have attracted increasing attention recently since they can form stable precipitates with PO_4^{3-}. The concentrations of Mg^{2+} and Ca^{2+} in the liquid phase are

also affected by the pH. It has been reported that the concentrations of Mg^{2+} and Ca^{2+} in pig manure digestate (pH = 8.4) were both 0.1 g/L, while their concentrations increased to 0.5 and 2.0 g/L when the pH was adjusted to 5.0, respectively [92]. The concentrations of Na^{+}, K^{+}, and Cl^{-} in animal manure digestate have been determined as 0.8, 2.0, and 1.5 g/L, respectively [93]. However, there are few studies concerning these ions since the negligible impact on the methane production and nutrient recovery. Carbonate (HCO_3^{-} and CO_3^{2-}) derives from the dissolution of produced CO_2 and carbonate intake from the feeding stock, which is normally present in the digestate in large quantities [94]. The degradation of organic S compounds can release SO_4^{2-} to the liquid phase, while it cannot persist in anaerobic conditions for a long time. The absence of O_2 leads to the generation of H_2S and metal sulfide precipitate (e.g. FeS). Organic compounds in animal manure include VFAs, lipids, proteins, HA, carbohydrates, lignin, and additives residues co-existing in both liquid and solid phases [2]. These organic compounds contribute to the colour and odour of animal manure. Certain compounds, e.g. humic acids and lignin, can persist for a very long time in the AD system as they are bio-refectory. The inorganic ions and non-degraded organics in anaerobic digesters can form a buffer solution containing multiple chemical reactions. There are two peaks of buffer capacity in animal manure, being pH in 4 – 6 caused by fatty acids and metal precipitates, and pH in 8 – 12 caused by ammonia, respectively [12].

Overall, almost all of the nutrients remain in the solid and liquid fractions during AD. The N in animal manure is originated from the N-bonded proteins in the feeding materials. The concentration of NH_4^{+}-N in animal manure is normally in the range of 0.8 – 5.0 g/L, which is equal to 55 – 95% of total dietary N. P derives from both feeding materials and inorganic additives, which can reach 1.21 g/L in animal manure but mostly exists in the solid fraction. The dissolvable P can be mostly identified as orthophosphate, which is highly associated with pH conditions.

2.3 Pretreatment methods

2.3.1 Solid-liquid separation

Animal manure and manure digestate are often processed with solid-liquid separation, so as to reduce the volume of liquid manure and increase the fertilizer values [2]. Based

on the composition of animal manure, solid-liquid separation is capable of producing a solid fraction containing P, large residues, and biomass, and liquid part rich in N, salts, and colloidal particles. The separated solid and liquid fraction can be used for different purposes. For instance, the liquid fraction can be used for crops cultivation nearby, while the solid fraction can be transported to the lands farm from animal houses. In terms of nutrient recovery, solid-liquid separation is essential as the particles can block machines and reactors. The expected situation is that the separated liquid fraction does not contain any particles, but is rich in nutrients.

Different techniques basically utilizing gravity or filters have been applied to the separation of fresh, ages, and digested manure in farms. Table 2-2 summarizes the performance of solid-liquid separation of animal manure. It is observed that the separation efficiency of DM and P is higher than that of N. The P in animal manure is mostly present in the solid faction, which can be removed together with the solids during the solid-liquid separation. The overall separation efficiencies for animal manure can be ranked as follows: centrifugation > sedimentation > filtration > pressurized filtration [2, 95].

Amongst the separation technologies, decanter centrifuge is the most efficient. It is believed that centrifugation can remove all the particles larger than 20 μm and up to 50% of the particles smaller than 4 μm. As shown in Table 2-2, the decanter centrifuge has satisfactory separation efficiencies – up to 95% of DM, 49% of total N, and 90% of total P. Decanter centrifuge is encouraged due to the high efficiency in treating animal manure with high solid content. A high centrifuge force and long retention time can significantly improve the separation efficiency, while only up to 4100 g of centrifuge force was applied in these studies. High speed centrifugation is unrealizable in practice due to the high energy consumption. The particles smaller than 1 μm cannot be separated using low centrifuge force, therefore, additional techniques should be adopted for the removal of small particles.

Table 2-2. Solid-liquid separation of animal manure.

Methods	Techniques	Manure type	Retention time	Particles removed	DM (%)	Separation efficiency (%)			References
						DM	Total N	Total P	
Sedimentation	Slurry thickener	Pig and cattle	0.2 – 1200 h	-	1 – 3.2	30 – 63	30 – 35	42 – 70	[96, 97]
Centrifugation	Decanter centrifuge (2050–2200 g)	Pig and cattle	8 – 30 s	>20 µm	2 – 8.9	47 – 70	17 – 34	55 – 87	[66, 98-100]
	Decanter centrifuge (1500–4100 g)	Pig, cattle and digestate	600 s	>20 µm	2.6 – 8.0	33 – 95	13 – 49	48 – 90	
Filtration	Sieves (0.25–2 mm)	Cattle	-	>0.25 mm	6.9 – 8.7	20 – 62	10 – 25	10 – 26	[75, 101, 102]
	Brushed screen (1.6 mm)	Pig and cattle	720 s	>1.6 mm	4.5	19 – 36	6 – 18	7 – 26	
Pressurized filtration	Belt separator (0.1mm)	Pig and cattle	<2 min	>100 µm retained by filters >1 µm retained by cake	1.5 – 8.0	50 – 87	33 – 51	34 – 62	[67, 100, 103-107]
	Belt separator (0.5–3 mm)	Pig and cattle	<2 min		1.1 – 7.7	11 – 62	3 – 49	2 – 49	
	Screw press (0.7–3.0 mm)	Cattle	<2 min		1.8 – 7.1	13 – 64	4 – 36	3 – 46	

Sedimentation is cost-effective because it can treat a large quantity of animal manure in one settling tank. In general, the higher viscosity of animal manure, the longer settling times. It has been reported that a gravity thickener separated the animal manure with 2 – 4% of DM in 1 hour, while it had longer retention time when treating the animal manure of high viscosity up to 6% of DM [108]. Settling velocity decreases when treating animal manure containing 0.5% of DM due to fewer flocs formed. In general, sedimentation cannot remove solids as efficiently as the decanter centrifuge. It has been reported that the highest removal efficiency of sedimentation is 72% when treating animal manure containing 1% of DM [97]. More attention should be paid to the temperature during sedimentation. Animal manure can generate gas bubbles if the temperature is higher than 16 ℃, causing the high buoyancy of particles and reduced separation efficiency [109].

Filtration is not efficient in solid-liquid separation. In a full-scale belt or screw press separator, the pore size of filters varies from 0.1 to 3 mm. Particles larger than the pores can be retained, adhering to or clogging the media, thereby forming a layer of filtration cake. Subsequently, small particles (smaller than the pores, 1 – 100 μm) can retain within the filtration cake, increasing the specific filter cake resistance [2]. This requires a frequent cleaning of filtration cake via scraping or blushing. The application of filtration is tough when treating the animal manure containing high concentration of SS, particularly for the filters with small pore size. Although particles can be retained efficiently, the application of filtration is problematic due to the severe blockage of filters.

2.3.2 Coagulation and flocculation

To shorten the retention time of solid-liquid separation, certain chemicals can be added to the liquid manure, so as to aggregate the small particles towards large flocs benefiting separation. By far the mechanisms of coagulation and flocculation have been sufficiently studied, being charge neutralization by Fe/Al/Ca-salt and particles bridging by polymers, respectively. The effect of coagulants for animal manure can be ranked as follows: using calcium as cation, $CaO > Ca(OH)_2$; using iron as cation, $FeCl_3 > Fe_2(SO_4)_3 > FeSO_4$; and using aluminum as cation, $Al_2(SO_4)_3 > AlCl_3$ [2]. Fe/Al salt is normally better than Ca salt when treating animal manure. It is noteworthy that the

chemical dosage of coagulants is very high due to the high concentration of SS and PO_4^{3-} in animal manure. In a P-rich solution, the dosed coagulants will not only aggregate the particles but also transfer P to the solid part via precipitation. The high dosage of coagulants greatly limits the application of coagulation in full-scale plants. In addition, chemical dosing can change the pH of animal manure. Fe/Al salt can reduce the pH and generate massive bubbles due to the dissolve of carbonate. These bubbles can hinder the formation and sedimentation of flocs, causing an unexpected decrease in separation efficiency.

Polymers are encouraged to be used in solid-liquid separation due to their high efficiency and low dosage. Studies proved that cationic polymers with 20 – 40% charge are the most efficient, and the branched polymer shows high retention of nutrients in press screw separator [68, 110]. However, polymer can only bridge the large particles, while it fails in separating small particles and colloids (0.1 – 1 μm). The separated liquid fraction after flocculation is still turbid compared with the clean solution that after coagulation. Polymers can be used individually or together with coagulants, while no polymer can remove the colloids in animal manure efficiently. In addition, the toxicity of polymers and the impact of Fe/Al to the lands need to be further assessed.

2.3.3 Acidification

Most recently, researchers have studied the acidification of animal manure prior to land application. In Denmark, full-scale acidification of animal manure has been built up and tested on farms for over 30 years [12]. Animal manure can be acidified by HCl, HNO_3, H_2SO_4, lactic acid, and other acidic salts, for the purpose of (1) reducing NH_3 emission after land application, and (2) increasing P concentration in the liquid phase of animal manure. For the digested animal manure, acidification will bring the same benefits. As aforementioned, acidification can change the ionic composition of animal manure. Figure 2-2 shows the nutrient dissolution in pig manure under different pH conditions, according to Piveteau et al.'s study [69]. Lowering the pH of animal manure can shift the NH_4^+/NH_3 equilibrium toward NH_4^+, resulting in a higher concentration of NH_4^+ in the liquid phase. It has been observed that NH_3 loss was up to 60% after the land application of animal manure, and the field NH_3 emissions in winter can reach up to 33% [89, 111, 112]. Acidification of either the raw or digested manure is able to save

up to 80% of NH_3 from evaporation loss [12]. Acidification can lead to a sudden release of CO_2 due to the dissolution of carbonate, however, besides a small increase in N_2O emission, the emission of NH_3, CO_2, H_2S, and CH_4 are all reduced due to acidification over the whole storage period [76, 113-116]. The acidification of animal manure can dissolve the crystallized phosphate, thus a concentration increase of P in the liquid phase. As shown in Figure 2-2, P started to dissolve when the pH is lower than 7.0, and it almost reached the maximum concentration at pH=5.5. Given this fact, the acidification of animal manure is an effective way to increase the P concentration prior to land application, and it will also cause a high recovery yield of P in terms of nutrient recovery [117, 118].

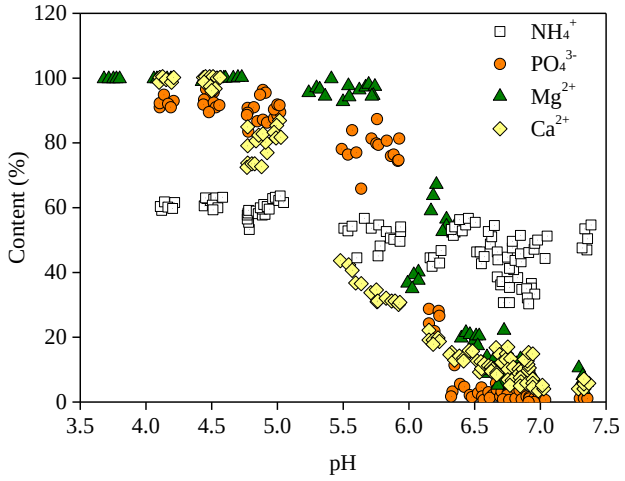

Figure 2-2. The concentration of mobilized nutrients in pig manure under different pH conditions, according to Piveteau et al.'s study [69].

Note: PO_4^{3-} represents the phosphate in the form of PO_4^{3-}, HPO_4^{2-}, and $H_2PO_4^-$.

Acidification may change the particle size distribution in animal manure. The particles in acidified manure can aggregate easier because of the low zeta-potential at low pH; meanwhile, they may become smaller due to the dissolution of carbonate and phosphate. To date, the variation of particle size during acidification has not been sufficiently investigated, with some studies reporting increase but the others reporting decrease [12]. Long-term use of acidified animal manure can lower the pH of soil, and the large consumption of acids is problematic. One option to replace chemical acids is to use food waste as the medium for the purpose of co-digestion, which can increase the concentration of VFAs during AD and cause a low pH and high concentration of P in the liquid phase [69]. From the perspective of nutrient recovery, acidification is necessary if P is expected to be separated from the solids.

2.4 Nutrient recovery technologies

In this study, nutrient recovery is a process that soluble N and P are extracted from manures and converted to chemical fertilizers, while direct land-spreading refers to the reuse of raw manure on lands rather than being recovered. In this section, nutrient recovery technologies involving ammonia stripping, struvite formation, ion-exchange and adsorption, membrane technologies, as well as thermal treatments are compared and deliberated, from the perspectives of recovery efficiency, yield and cost.

2.4.1 Ammonia stripping

Ammonia stripping allows air or steam to be introduced into stripping towers equipped with compressors, with the liquid flowing in a converse direction, causing NH_3 emission from the liquid to the gas phase [95, 119]. Up to now, approaches based on NH_3 stripping from animal manure and manure digestate have been established and extended from lab-scale to full-scale around the world. In the United States, 9-10 full-scale stripping installations are implemented to recover NH_3 from the digested sludge. Germany also had at least 15 stripping plants by 2015 [95]. Table 2-3 summarizes the recent studies of NH_3 stripping from different animal manure.

Followed by acid trapping (mainly H_2SO_4), ammonia can be recovered as $(NH_4)_2SO_4$, a frequently used fertilizer for crop cultivation. The efficiency of NH_3 stripping is dominated by multiple parameters, such as NH_4^+ concentration, temperature, pH, retention time, as well as the flow rates of gas and liquid in the stripping towers. High pH, temperature, air flow rate, and NH_4^+ concentration would benefit the equilibrium of NH_4^+/NH_3 moving towards NH_3. It has been observed increasing pH could improve the NH_3 stripping rate more efficiently than the other parameters [120]. Therefore, alkali addition is normally adopted in practical plants. Lime is frequently used due to its low cost. However, a high dosage of lime is needed, w hich can lead to an unexpected high cost. For instance, Liu et al. [78] have used up to 22.15 g of lime to reach pH 12.5 when treating 3 L of pig manure dig estate. The increase of pH also leads to metal precipitation in animal manure. In addition, the application of NH_3 stripping is challenged by the heating process, which requires a high-energy input to keep the high temperature of animal manure. Given this, many researchers pursue simultaneous NH_3

stripping by N_2 without pH control during AD, which can also utilize the surplus heat in AD [77]. However, the removal efficiency is not satisfactory and the consumption of N_2 would be problematic. Many studies have tested the laboratory-scale thermal evaporation of NH_3 from animal manure [121]. It requires huge energy input to evaporate NH_3 while it allows less alkali dosage.

2.4.2 Chemical precipitation

One alternative to recover both N and P from animal manure is to form struvite [$Mg(NH)_4PO_4 \cdot 6H_2O$]. Struvite is a slow-release fertilizer for agriculture and horticulture. The struvite precipitation can be expressed as follows:

$$Mg^{2+} + NH_4^+ + H_nPO_4^{3-n} + 6H_2O \rightarrow Mg(NH)_4PO_4 \cdot 6H_2O + nH^+$$

where n is 0, 1, or 2. Up to now, the lab- and pilot-scale struvite reactors are extensively established. A few full-scale plants have been built up to fertilize fruits and vegetables in certain countries (e.g. Japan, the Netherlands, and Italy) [122]. Amongst these applications, fluidized bed, or air-agitated struvite reactors are most frequently used.

As shown in Table 2-4, struvite formation is affected by pH, ions concentration, temperature, liquid turbulence, and suspended particles [122-124]. The precipitation of PO_4^{3-} occurs when pH increases from 5.0 to 7.5, while the optimal pH has been addressed in the range of 8.5 – 9.5. Because H^+ is produced during struvite formation, pH has to be kept in this optimal range by continuously alkali addition. Optimally, a higher concentration of ions favours this reaction, and the mole ratios of N/P and Mg/P have to be kept above 3/1 and 1/1, respectively [123]. In comparison with PO_4^{3-}, NH_4^+ in animal manure is normally abundant for struvite formation, whereas Mg^{2+} is insufficient. For this reason, MgOH, $MgCl_2$, or $MgSO_4$, has to be supplemented to induce struvite formation. In addition, a high concentration of Mg^{2+} would remit the precipitation caused by Ca^{2+}, which can negatively impact the recovery yield of struvite [125, 126].

Table 2-3. Studies on NH_3 stripping from animal manure and digestate.

Media	pH	Flow rate (L/min)	Temperature (℃)	NH_4^+-N (g/L)	Retention time (h)	Quantities treated (L)	Removal efficiency (%)	References
PM	11.5/9.5	90/45	22	0.8	7/55	10	90	[120]
PM	9.5 – 10	0.5	37	5	24	20	31– 70	[70]
PM	9.5/11.5	0.02	80	3.4	4	4	69/98.8	[71]
PM	9.5	20 – 45	40 – 50	4.2 – 6.7	3.75	2	50 – 90	[72]
PM digestate	8.5 – 11	333 – 2000	30 – 70	2.2	2	100	27.3 – 98.9	[127]
PM digestate	9.5/11.5	0.02	80	3.7	4	4	96	[71]
PM digestate	9.5	20 – 45	40 – 50	1.8 – 2.7	3.75	2	>90	[72]
PM digestate	8.6 – 12.5	6 – 10	36	1.4	-	3	75 – 97	[78]
PM digestate	7.8 – 8.9	5	65	6	4	0.5	34 – 86	[128]
DM digestate	9 – 11	-	97	0.8	4	0.3	50	[129]
DM digestate	7.8 – 9.8	5 – 35	35 – 70	1.4	3-12	-	20 – 90	[130]
DM digestate	8.4	1 – 5	55	1.8 – 2.4	50 h	3	44 – 64	[77]
PM+FW digestate	11	10	15	1.5	12	1	95.3	[131]
DM+PM+CM digestate	8.8 – 12	-	23	4 – 5	24	0.2	88.7	[132]
DM+PM+CM digestate	7.81 – 9	10	30 – 40	1.84 – 2.38	10 d	40	21 – 89	[79]

Note: PM, DM, CM, and FW are the abbreviations of pig manure, dairy manure, chicken manure, and food waste, respectively.

Table 2-4. Impact factors for struvite formation according to previous studies [122-124, 133].

Parameter	Impacts	Impact level	Optimal conditions	Improving methods
pH	High pH reduces the solubility	High	8.5 – 9.5	Alkali addition; CO_2 stripping
Mg^{2+} and PO_4^{3-}	High concentration causes shorter induction time and higher growth rate	High	N/P/Mg > 3/1/1	Mg supplementation; maximum P release during pretreatment
Foreign ions	Precipitation competition caused by Ca^{2+}, K^+, carbonate, and other ions	High	Mg:Ca > 2.25	Mg supplementation; Ca^{2+} chelation; CO_2 stripping
Temperature	High temperature causes low solubility and the change of crystal morphology	Low	Around 25℃	-
Liquid turbulence	High turbulence is positive for nucleation, while negative for crystal growth	Low	-	Proper turbulence
Suspended particles	Negatively blocks the crystallization	Low	<1 g/L	Efficient solid-liquid separation

Recent studies have been focused on the maximization of the recovery yield and purification of struvite. The NH_4^+-N in animal manure is sufficient to support struvite formation. However, only 10% of P is available in the liquid faction due to the high pH of animal manure (approximate 8). For instance, a trial of struvite recovery from pig manure digestate has been operated by Song et al., while the recovered P only represented a small portion of total P [134]. Besides struvite, increasing attentions have been drawn to the other P-precipitates in the solid fraction, which can be identified as $MgHPO_4 \cdot 3H_2O$ (newberyite), $MgKPO_4$, $MgHPO_4$, $K_2NH_4PO_4$, $Ca_5(PO_4)_3OH$, $Ca_3(PO_4)_4 \cdot 5H_2O$, $CaHPO_4$, and $CaHPO_4 \cdot 2H_2O$ [121]. In terms of P, increasing the concentration of PO_4^{3-} in the liquid fraction is vital for the improvement of struvite yield [69]. Various pretreatment methods have been proved effective to enhance the soluble P in animal manure, including acidification, microwave, heating, ultrasonic treatment, and orbital shaking [135]. Amongst these approaches, acidification is the most powerful one. The purification of struvite would still be tough due to the existence of Ca^{2+} and suspended particles. Although Ca^{2+} can be chelated by EDTA or selectively reduced by oxalic acid, the high content of Ca^{2+} would lead to a huge chemical cost, and the toxicity of EDTA in animal manure has not been evaluated by far [136, 137]. Struvite formation causes the aggregation of small particles, forming larger particles suspended in the liquid. Therefore, struvite is always harvested as a complex mixture of precipitates and solids.

2.4.3 Ion exchange and adsorption

Ion exchange and adsorption are similar as they both utilize solid materials (i.e. sorbents) filled in a column bed to extract the target compounds (e.g. PO_4^{3-} or NH_4^+) from the feed solution. After a certain period of time, the sorbent reaches its capacity and has to be regenerated so a new cycle can be started. The adsorption process is driven by intermolecular forces, while ion exchange is held by ionic forces. These two processes may occur simultaneously in one media, such as zeolites and resins.

Zeolites are the most frequently studied materials in terms of adsorption. They contain massive cavities and negative charges that can adsorb cations efficiently. Zeolites can potentially release the adsorbed NH_4^+ to soil after l and application. Many studies have

successfully used zeolites to remove and recover NH_4^+ from animal manure. It has been observed the adsorption capability for NH_4^+ is 19 g/kg by natural zeolite and 21 g/kg by Na-zeolite, being the initial removal efficiency varying in the range of 71 – 91% [138]. Tao et al. incorporated clinoptilolite and resins to the anaerobic digesters with the purpose of lowering the concentration of NH_4^+, leading to a significant increase in the methane yield [139]. Phosphorus can be likewise adsorbed by zeolite, while the removal efficiency is much lower than that of NH_4^+. Most recently, the adsorption of nutrients using biochar and hydrochar has been demonstrated. The adsorption capacities of NH_4^+ and PO_4^{3-} by biochar are normally in the range of 100 – 160 and 0 – 30 g/kg, respectively [140]. This adsorption is favoured at pH 6.5 – 7.0, while very acidic (pH <4) and alkaline (pH >8) conditions can significantly reduce the adsorption capability [141].

Ion exchange and adsorption are challenging techniques. For instance, the cavities in sorbent materials can be easily blocked by suspended particles and precipitates, so the removal of particles is necessary. In addition, the competition of foreign ions, i.e. NH_4^+ and PO_4^{3-} ions, has to be considered, because zeolites can adsorb metals (e.g. Mg^{2+} and Ca^{2+}) along with NH_4^+. Zarebska et al. have compared the chemical cost of zeolites adsorption, NH_3 stripping, and struvite formation [95]. The result showed the chemical cost of zeolites was much higher than the other two technologies, as more zeolites were required than lime and MgO. However, ion exchange and adsorption are easy to be operated, which may result in lower energy consumption and labour cost.

2.4.4 Pressure-driven membrane technologies

Microfiltration and UF consist of a solid-liquid separation process in which the liquid to be purified passes through a porous membrane. With a driven pressure applied, porous membranes can retain particles larger than a particular size while allowing smaller ones to pass through. As shown in Table 2-5, MF is able to remove the particles larger than 0.1 – 1 μm, while UF retains the particles between 0.01 – 0.2 μm (colloids). Two types of membranes can be used in both MF and UF, i.e. ceramic membrane and polymeric membrane. A higher flux can be achieved in the former, while the latter allows a higher quality of permeate [95]. It is believed the dissolved compounds cannot be removed by MF and UF. Thus, a liquid fraction rich in NH_4^+-N and a solid fraction

rich in P can be harvested after these separations. For NF and RO, water is freely diffused but salts and organic matter are retained. These technologies can be adopted for on-farm water reuse, e.g. animal houses flushing, and irrigation purposes [2]. Meanwhile, the ions in the feed solution can be concentrated due to the decrease in volume. Researchers found NH_4^+-N can be concentrated to 7 – 10 g/L by RO and the retention efficiency achieved was up to 99 – 99.8% [81, 142]. As reported by Gerardo et al., NF has a lower separation efficiency of NH_4^+-N compared to P, being 5 – 23% and 97 – 98%, respectively [143]. However, a lower pressure is required for NF.

Once animal manure is directly fed to NF and RO, the membranes would be completely fouled in minutes [2]. Even if the particles are efficiently removed by MF and UF first, the membrane fouling of NF and RO is still severe. A layer of gel can be formed on the surface of membranes which can hinder the subsequent permeate pass through. Membrane fouling is unavoidable as it occurs naturally when particles are retained by filters. Severe membrane fouling is undesired, as it can greatly limit the long-term operation. The membranes of MF and UF can be fouled in a short time due to the high content of SS in animal manure [82, 144, 145]. One way to mitigate fouling is intermittent backwashing by water or air during the operation. It has been observed ultrasound is effective to clean UF membranes, which can be classified as a physical method to increase the liquid turbulence [146]. Chemical cleaning is necessary to regenerate the fouled membranes in the case that physical methods are insufficient to clean them. Various chemicals, e.g. acids, alkalis, oxidants, surfactants, chelants, enzymes, or a mixture of them, have shown remarkable regenerations [147]. However, MF and UF have not been successful in the treatment of animal manure.

Table 2-5. Comparison of membrane technologies adopted for nutrients recovery [148-151].

Technology	Membrane	Pore size	driven pressure	Capabilities	Retained compounds	Impact factor
MF	Porous	0.1 – 10 μm	0.1 – 2.0 bar	>50 $L/m^2/h/bar$	Suspended particles >0.1 μm	Pressure and suspended solids
UF	Porous	0.01 – 0.2 μm	1.0 – 5.0 bar	10 – 50 $L/m^2/h/bar$	Colloids	
NF	Dense	-	5.0 – 20 bar	1.4 – 12 $L/m^2/h/bar$	Organics and most of ions	Pressure and organics
RO	Dense	-	10 – 100 bar	0.5 – 1.4 $L/m^2/h/bar$	Ions and molecules	
ED	Ion-exchange	-	<60 mA/cm^2 electrical force	appr.3 $L/m^2/h/A$	Non-charged compounds	Ionic charge
MD	Porous (hydrophobic)	0.2 – 20 μm	0.02 – 0.2 bar vapour gap, 45-75 ℃	5 – 80 $L/m^2/h$	Non-vapour compounds	pH and temperature
FO	Dense	-	0 – 30 bar Osmotic pressure	<12 $L/m^2/h$	Ions and molecules	Osmotic pressure gap

2.4.5 Non-pressure membrane technologies

Electrodialysis is an electrically driven membrane technology. In the electrical field, anions move towards anode, while cations move heading for cathode. With ion-exchange membranes equipped, ED allows the transportation of ions from the feed to the product. Currently, only lab-scale ED has been established on the recovery of nutrients from animal manure. However, the advantage of ED is that NH_4^+-N can be concentrated to 16 – 21 g/L, a relatively high level compared to RO [73, 152]. BMED is an emerging ED technology equipped with BM. It enables the dissociation of water in the middle boundary of BM and releases OH^- and H^+ to adjacent compartments, forming base and acid. The produced by-products (i.e. base and acid) can be used for multiple purposes. For instance, the acid can be used for membrane cleaning, while the base can offer abundant OH^- for NH_3 stripping. In a selective ED system, PO_4^{3-} can be retained by mono-selective membranes, which can favour the subsequent struvite formation [153, 154]. Likewise, ED related technologies all have fouling problems. It is proposed that the fouling can be reduced by Cl_2 produced by the anode, however, it may cause pitting and cracking of membranes [155, 156]. EDR allows the frequent reverse of electrode polarities. It causes the foulants on the membranes to disassemble during the operation.

Membrane distillation utilizes vapour pressure gradient across a porous membrane to extract water and volatile compounds from the feed. In the MD process, a heat source elevates the temperature of feed solution (40 – 70 ℃), causing a high vapour pressure compared to the ambient. The liquid and gas phases are isolated by a hydrophobic membrane (0.2 – 20 μm pores), which only allows vapour molecules to pass through [150]. MD has a wide application on seawater desalination and food industry. The recovery of NH_3 from animal manure using MD has already been demonstrated in the laboratory. Water and NH_3 in animal manure can evaporate and diffuse towards the cold side, where NH_3 can be trapped along with water condensing. A high pH (>9.7) and high temperature (>45 ℃) can favour the evaporation rate of NH_3 during MD, and the concentration of NH_4^+ in permeate could reach up to 18.3 g/L [157]. The membrane fouling during MD has been evaluated by Kim et al. [158]. A serious drop of permeate flux from 17.5 to 5 L/m^2/h has been observed over 72 h of continuous operation.

However, the membranes can be regenerated after 90 min of citric acid rinse. As the feed solution does not flow through membranes, membrane fouling of MD is less than that of pressure-driven membranes [150]. The recovery efficiency of NH_3 is lower than 20% when the pH is lower than 9.0 [159]. In addition, MD cannot recover P and other non-volatile compounds. This may limit the further application of MD if P is targeted to be recovered.

Forward osmosis, an emerging technology, has attracted increasing attention over the past decade. In the FO process, a semipermeable membrane is placed between the feed and draw solutions (the salinity of draw solution is higher than that of the feed solution). Driven by the osmotic pressure difference, water in the feed diffuses spontaneously to the draw solution, thereby causing the enrichment of nutrients in the feed and the dilution of draw solution [160]. Different from the pressure-driven membrane technologies, foulants in FO are not compacted but loose and easy to be cleaned. The membranes in FO can be regenerated by flushing water, while the membranes in RO and MD are hardly regenerated without chemical cleaning [151, 161, 162]. The energy consumption of FO is far lower than the other membrane technologies. However, after one circle of FO, the diluted draw solution has to be treated by other technologies, e.g. RO and MD, so that its salinity can be maintained at a high level [160]. In this regard, the energy density of FO-RO is higher than that of standalone RO. Nonetheless, the application of FO is promising due to its unique advantages, i.e., high resistance of membrane fouling, and high performance in treating high-salinity wastewater. Up to now, FO is only assessed in laboratory-scale studies, and pilot- and full-scale demonstration should be conducted.

2.4.6 Thermal treatments

Thermal treatments include incineration, pyrolysis, and hydrothermal carbonization (HTC), depending on the thermal conditions. Ashes can be produced from the incineration of biomass. In Europe, many full-scale incineration plants have been built up for the disposal of municipal sludge, such as in Finland, Belgium, Sweden, Switzerland and Austria [163]. However, incineration is considered energy-extensive, which is not suitable for manure disposal. Pyrolysis and HTC have been applied to the treatment of fresh and digested animal manure. Pyrolysis enables the carbonization of

biomass under 350 – 700 ℃, while three products can be produced, i.e. gas and vapours, liquid (bio-oil and tar), and solid (biochar) [164]. Under anoxic conditions, the majority of carbon substance (e.g. cellulose, starch, lignin, and glucose) can be hydrolysed and converted to biochar with non-vapour elements co-existing. HTC of biomass has got increasing attention in recent ten years. It allows the hydrolysis of feeding materials under 170 °C followed by the carbonization under 170 – 250 °C, during which less energy is consumed [165]. The produced chars either from pyrolysis and HTC can be regarded as potential biofuels or materials for soil amendment, which can adsorb contaminants, retain nutrients, and immobilize CO_2.

During carbonization, certain nutrients can be retained and recovered from the char, such as P and K. It has been observed that 100% of P is transported to the char with a significant concentration increase during the pyrolysis of animal manure [164]. However, more than 90% of N is lost along with the carrier gas. As for HTC, it has been observed that half of the N and most of the K are mobilized in the aqueous phase after this treatment [166]. Compared to pyrolysis, HTC is able to retain N to the liquid phase, which favours the following recovery with filtration. In addition, the feeding material is free of drying (necessary for pyrolysis), which may further its application to livestock slurry [167].

Thermal treatments are able to eliminate odour and pathogens, suggesting that the produced char (either biochar or hydrochar) can be used on lands. The morphology of nutrients in char can provide vital information to nutrient recovery and land application. The phosphates in biochar have been identified as orthophosphate, pyrophosphate, and polyphosphate [168]. Long chain P compounds (pyrophosphate and polyphosphate) are not directly bioavailable, while they may serve as a P reservoir in soil. In contrast, HTC can only produce orthophosphate. Most recently, the slow released fertilizer has been reported to be more recyclable than soluble inorganic fertilizer [169]. Phosphorus in hydrochar can be furtherly recovered for multiple purposes as it is dissolvable under acidic conditions. The liquid fraction after HTC can be regarded as a liquid fertilizer due to the abundant NH_4^+. However, it has to be understood that certain bio-oil compounds co-existing in the liquid fraction are harmful to plants, e.g. aldehydes, phenols, ketones, acids, and some small molecules and heterocyclic compounds [170]. The solid-liquid separation turns to be easier after HTC, since the decomposition of

organic matter and hydrophobicity of char [171]. Huang et al. proposed the air stripping of NH_3 after hydrothermal process [74]. Other techniques may also work efficiently on the N recovery from this liquid.

However, thermal treatments are energy-intensive. Slurry heating needs massive energy input from fossil fuel. It has been predicted that the energy consumption is 1330 kWh/ton of dry hydrochar when treating compost residuals, resulting in a cost of 157 €/t [172]. Suppose 20 kg dry hydrochar is produced from 1 m^3 of slurry, the total energy consumption of treating slurry could be up to 27 kWh/m^3.

2.5 Critical comparison of recovery technologies

Table 2-6 compares the advantages and weakness of different technologies. To recover the nutrients from the liquid fraction, conventional approaches (i.e. NH_3 stripping and struvite formation) can be applied. Ammonia stripping can recover NH_4^+ efficiently (the efficiency can reach 98.9% as shown in Table 2-2), while P is retained in the solid fraction. The high cost of this technique is mainly from alkali addition. Meanwhile, after stripping, animal manure has to be neutralized for final disposal, causing additional acid consumption. Struvite formation is promising due to the low operational cost, while the formation of struvite is limited by the low concentration of PO_4^{3-} in animal manure. The low concentration of PO_4^{3-} in the liquid phase of animal manure indicates that a large amount of NH_4^+ would not be recovered. Ion exchange and adsorption are not encouraged, since sorbents can be easily fouled by the high SS, and the competition of foreign ions is severe. Particles and foreign ions can significantly reduce the recovery efficiencies, and the regeneration of sorbents is also problematic.

Table 2-6. Critical comparison of technologies related to nutrients recovery.

Technologies	materials needed	Advantages	Limits	Product	Further recovery process
Ammonia stripping	Lime or NaOH	easy operation	pH	$(NH_4)_2SO_4$	P in the solids
Struvite formation	Mg-salts	low cost	Surplus NH_4^+ cannot be recovered	Struvite	most of the N and P
Ion exchange and adsorption	Sorbents	easy operation	particles blockage, ions competition		P in the solids
MF/UF	membranes	clean filtered solution	membrane fouling	Filtered solution	N and P needs further recovery
NF RO	membranes	nutrients enrichment	membrane fouling	concentrated N and P, clean water	-
ED	membranes	nutrients enrichment	membrane fouling	concentrated N and P	-
MD	membranes, lime or NaOH	ammonia enrichment	pH and heating source	$(NH_4)_2SO_4$	P
FO	membranes	high resistances of membrane fouling	-	concentrated feed	RO, ED or MD process
Pyrolysis	fuels for drying and heating	char production	huge energy input	biochar	P in the char, N loss
HTC	fuels for heating	char production	huge energy input	hydrochar and liquid	P in the char, N in the liquid

Microfiltration and UF exhibit a high rejection of SS. However, neither pure chemicals nor concentrated products can be produced from them. For this reason, they can only be regarded as pretreatment methods prior to the other membrane processes. NF, RO, ED, and MD are able to concentrate the nutrients, and NF and RO can produce clean water for on-farm reuse, e.g. animal house flushing and irrigation. However, membrane technologies are energy-intensive. For instance, the operational cost of UF-RO has been proved higher than NH_3 stripping in full scale plants, being €6.97 compared with €5.40 per m^3 of digestate, as investigated by Bolzonella et al. in 2017 [82]. In addition, the application of membrane technologies is limited by membrane fouling. EDR and FO both exhibit high resistance to membrane fouling, while pilot- and full- scale studies should be assessed. The carbonization of animal manure (pyrolysis and HTC) requires huge energy input, which means thermal treatment can be only accepted if char is the expected product.

Figure 2-3 summarizes the potential application of different technologies to the nutrient recovery from animal manure. Each recovery technology plays a different role in different stages over the whole recovery process. The selection of pretreatment methods is dependent on the recovery purposes. It is found that solid-liquid separation is the key section before nutrient recovery, which can change the distribution of N and P in animal manure and digestate, thereby changing the nutrient recovery yield in the following processes. For instance, acidification can increase the P yield in struvite formation, ion exchange, adsorption, BF/RO, and ED technologies. Without acidification, P will mainly remain in the solid fraction of animal manure, which can be only spread on lands or transported to the biochar. Acidification will reduce the NH_3 emission to the atmosphere during animal housing, leading to a high recovery yield of N in the nutrient recovery processes. However, it cannot be applied to NH_3 stripping, struvite precipitation, and MD, because the low pH will reduce the efficiency of these technologies.

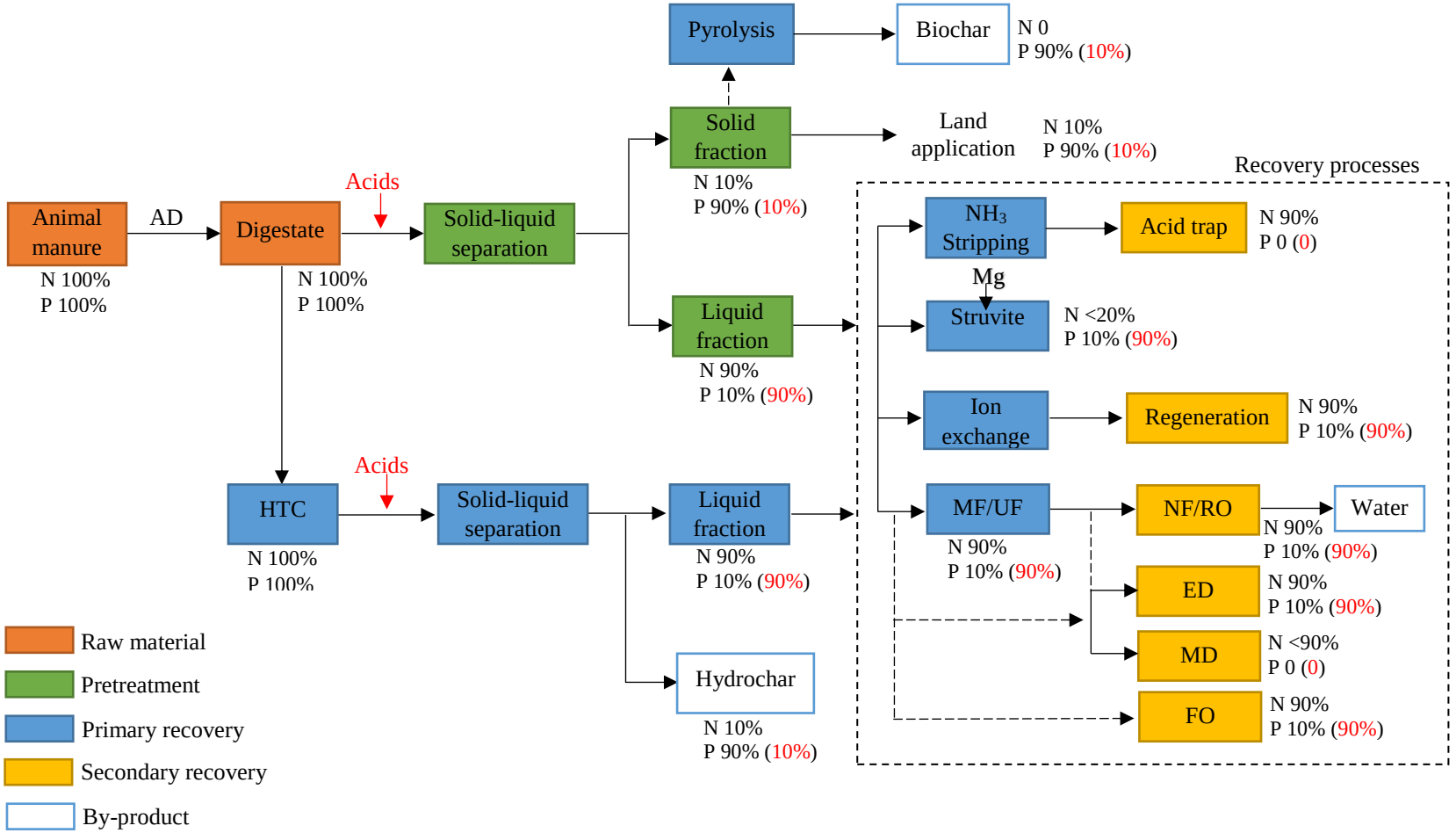

Figure 2-3. Application flow chart of different technologies in relation to nutrient recovery from animal manure.

Note: The percentages of N and P were calculated and estimated based on the results of manure acidification in Appendix A. It is hypothesized that 10% of N and 90% of P exists in the solid fraction of animal manure; the percentage under each box represents the ratio of N (or P) to total N (or P) in this technology. The red colour represents the percentage using acidification as pretreatment.

Amongst the recovery technologies, only the ion exchange and adsorption, NF/RO, ED, and FO can recover both N and P with a high recovery yield. These technologies can only use the liquid fraction of animal manure as feed. From the perspective of technical feasibility, membrane technologies are promising; however, their operational costs still need more investigation. The inputs on chemicals and energy, labour, transportation, as well as the fertilizer market demand, all impact the nutrient recovery chain [163]. It is noted that the nutrients in animal manure can be recovered as pure chemicals (e.g. $(NH_4)_2SO_4$ and struvite) or concentrated solutions. However, the concentrated solution contains other ions, and the concentrations of N and P are still lower than the chemical fertilizers on market. Therefore, how to purify and enrich nutrients should be taken into account in terms of product marketization. In addition, the disposal of solid residuals generated from solid-liquid separation and liquid residuals generated from recovery process should also be taken into account. The liquid residuals contain low concentrations of nutrients. They can be treated furtherly to remove the remaining N and P via a variety of biological technologies like algae cultivation, nitrification, denitrification, and anammox, as reported in other studies [16, 173-176].

2.6 Antibiotics in animal manure

2.6.1 Varieties and concentrations

Global meat and dairy production have increased significantly in recent decades, thanks to the effective use of veterinary antibiotics in animal disease prevention and therapy. However, long-term use of antibiotics can pose a risk of environmental pollution via land application of animal manure [27, 28, 177]. In intensive farming areas, veterinary antibiotics have been widely found in the soil, water, and sediments with high concentrations up to μg/L. In addition, they are even detectable in plants, food, and human urine, as reported in several studies [27, 177-182]. Although the concentration of antibiotics in the environment is in ng/L to μg/L, chronically exposing in antibiotics can generate antibiotic resistance genes (ARGs) in bacteria. These substances can be transported between different bacteria using plasmid as courier, causing comprehensive pollution of ARGs over the whole ecology [183]. Hence, the overall input of antibiotics to the environment has to be limited to a safe threshold to avoid environmental pollution.

However, it is impossible to prohibit all of their use due to the economic concerns on livestock production. In the European Union, legislation has prohibited the use of antibiotics for growth promotion since 2006, yet numerous antibiotics, e.g. TCs, penicillins (PCs), and SAs, are still in use today for disease prevention [26]. There is a huge number of reports on antibiotic usage and concentrations in animal manure. Figure 2-4 shows the consumption pattern of veterinary antibiotics in Europe in 2016, summarized by the European Medicines Agency. It is found that TCs, PCs, and SAs are top three veterinary antibiotics consumed in 2016, being 32%, 26%, and 12% of the total consumption, respectively [184]. Since antibiotics are irreplaceable for animal husbandry, future studies should be focused on their removal from animal manure and minimization of the dissemination to environment.

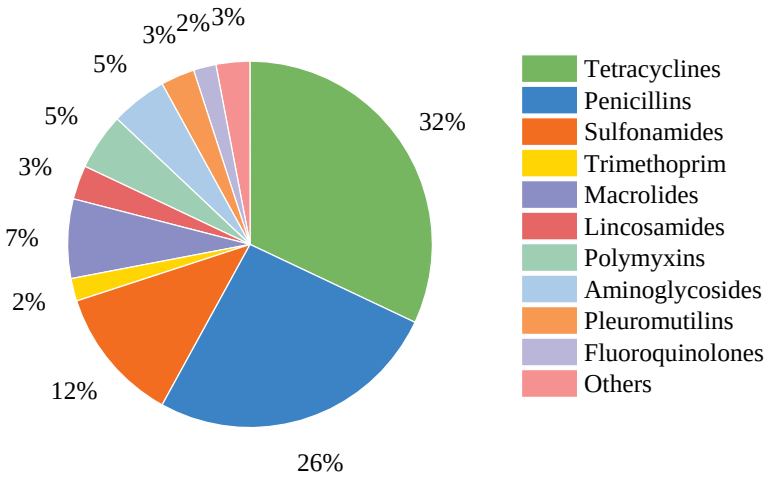

Figure 2-4. Consumption of veterinary antibiotics in European countries in 2016 [184].

Animal manure is the primary reservoir of veterinary antibiotics. Since the administered antibiotics are poorly absorbed in animal guts, the majority of the dose (30 – 90%) is excreted unchanged to the manure via urine and faeces [26]. The concentration of antibiotics in fresh animal manure can reach mg/L, depending on feeding and seasons. For instance, the concentrations of SAs in fresh pig manure were detected up to 9 mg/L in wet weight, as reported by Spielmeyer et al. [185]. The concentrations of oxytetracycline (OTC) and chlortetracycline (CTC) in pig manure have been reported in the range of 0.006 – 136 and 0.003 – 46 mg/kg in dry weight, respectively [182, 186]. The distribution of antibiotics in animal manure varies depending on their concentrations and the adsorption capacity of solids. It has been reported that around 90% of the antibiotics exist in the solid fraction of animal manure due to sorption if

their total concentration is μg/L, while the majority of them remains in the liquid fraction if the total concentration reaches mg/L [186-188]. The antibiotics in the liquid fraction of animal manure are more harmful because it can be disseminated freely from manure to the environment. In large-scale farms, animal manure is often anaerobically digested or composted prior to the land application. Serval antibiotics in animal manure are very easily degraded, such as PCs, while most of the antibiotics can remain unchanged for a very long time in anaerobic digesters or composting piles [183, 186-190]. SAs and TCs are two common antibiotics highly resistant to biological degradation. Table 2-7 summarizes the recent studies on the degradation of SAs and TCs in the AD and composting systems. It has been found that both SAs and TCs were not efficiently removed either in AD or composting systems. Therefore, high concentrations of antibiotics may exist in the raw, digested, and composted manures, which should be highly concerned prior to the land application of animal manure.

2.6.2 Removal of antibiotics from animal manure

As mentioned above, nutrient recovery from animal manure can avoid the over-fertilization of adjacent farmlands and remit P resource scarcity [63]. To date, various technologies on nutrient recovery have been demonstrated, such as ammonia stripping, struvite formation, ion exchange, and adsorption, as well as membrane separations [163]. However, most of the studies mainly have focused on their recovery efficiency, while the risk of using the recovered fertilizers has not been assessed. Previous studies have proved that long-term land application of animal manure can cause the enrichment of antibiotics and ARGs in soil [27, 28]. Most recently, it has been found that the application of struvite recovered from wastewater caused the same risk [29]. The enrichment of antibiotics in the recovered fertilizer makes its land application questionable. In general, the nutrients in animal manure can be transported to a precipitate (e.g. struvite) or a separated solution having a small volume after the recovery process. This allows the feasibility of using adsorption or oxidation as subsequent processes to eliminate antibiotics [191, 192]. The integration of antibiotics removal with nutrient recovery would be of high significance for the safe use of fertilizers.

Table 2-7. Recent studies on biological degradation of SAs and TCs.

Biological process	Days	Manures	Antibiotics	Initial concentration	Finial concentration	Removal efficiency	References
AD	40	Pig	SD	1 mg/L	-	<10%	[190]
			SMZ	1 mg/L	-	26%	
			SMX	1 mg/L	-	99%	
AD	40	Pig	SMZ	20 mg/L	17 mg/L	15%	[193]
AD	50	Pig	SCP	125 mg/kg	50-80 mg/kg	36 – 60%	[194]
AD	5	Pig	SAs	15 mg/kg	2-7 mg/kg	50 – 90%, for SD and SDM 5 – 70%, for SMZ and SMM	[195]
		Chicken	SAs	8 mg/kg	1 – 7 mg/kg	>90%, at 30 °C 0 – 60%, for 40 – 60°C	
AD	1 year continuous	-	SMZ	4 – 21 mg/kg	2.8 – 5.2 mg/kg	-	[188]
			CTC	1.7 – 3.4 mg/kg	0 – 0.7 mg/kg	-	
AD	22	Dairy	TCs	70 – 230 μg/kg	-	54%	[187]
AD	21	Pig	OTC	13 – 95 mg/kg	6 – 30 mg/kg	54 – 68%, half-life 7-14 d	[186]
			CTC	10 – 75 mg/kg	1 – 10 mg/kg	86 – 90%, half-life <7 d	
AD	33	Calve	CTC	5.9 mg/L	1.4 mg/L	75%	[196]
AD	21	Cattle	CTC	6.5 mg/L for 22 °C	6.0 mg/L	7%	[197]
				8.3 mg/L for 38 °C	1.7 mg/L	80%	
				5.9 mg/L for 55 °C	<1.0 mg/L	98%	
AD	30	Pig	CTC	20 – 500 mg/kg	0 – 228 mg/kg	50 – 90%	[198]
			OTC	20 – 501 mg/kg	0 – 249 mg/kg	50 – 90%	

AD	30	Pig	CTC	60 mg/kg	14.2 mg/kg	76.3% (59.8% during acidogenic)	[199]
			OTC	40 mg/kg	8.7 mg/kg	78.3% (41.3% during acidogenic)	
AD	60	Cattle	OTC	20 mg/kg	3.07 mg/kg	85%	[200]
Composting	42	Broiler	CTC	94.71 mg/kg	~5 mg/kg	90%, half-life 11 d	[201]
		Hog	CTC	879.6 mg/kg	~640 mg/kg	27%, half-life 86 d	
		Layer-hen	CTC	150.3 mg/kg	~20 mg/kg	90%, half-life 12 d	
Composting	52	Pig	OTC	1.5 mg/kg	0.2 mg/kg	86%	[189]
			TC	0.45 mg/kg	0.12 mg/kg	73%	
			CTC	3 mg/kg	0.7 mg/kg	77%	

Note: Tetracyclines (TCs) include oxytetracycline (OTC) and chlortetracycline (CTC); sulfanamides (SAs) include sulfadiazine (SD), sulfamethizole (SMZ), sulfamethoxazole (SMX), sulfachloropyridazine (SCP), sulfamonomethoxine (SMM), and sulfadimethoxine (SDM).

2.6.2.1 Biological and physical technologies

The most frequently studied technologies for antibiotics removal from wastewater are biological, physical, and chemical processes. The biological process includes the use of biological activated carbon, microalgae reactor, activated sludge, constructed wetland, and membrane bioreactor. These technologies have shown a wide range of antibiotics removal with the removal efficiencies varying from 20% to 95% according to the literature [202]. However, similar to AD and composting, most of the antibiotics in the wastewater are adsorbed by the sludge in biological reactors, with only a small part of them being degraded. The biological degradation of antibiotics can only take place in the AD or composting process during the manure management. In terms of the nutrient recovery from animal manure, there is no need to use the other biological processes prior to land application.

Physical processes that can remove antibiotics from wastewater include adsorption and membrane separation. Adsorption materials, including active carbon, biochar, carbon nanotube, graphite, clay minerals (e.g. bentonite), have shown very high removal efficiencies in the treatment of antibiotics contained wastewater. These technologies have been widely studied in the removal of organic contaminants from contaminated stream [203, 204]. It has been reported that biochar is the most efficient adsorption material for SAs, while carbon nanotube is efficient for TCs [205]. Adsorption is regarded as cost effective because the adsorptive materials are normally cheap and the adsorption system is simple to design and operate. The adsorption efficiencies are normally in the range of 74 – 99%, a very high level comparing with biological processes [205]. The regeneration of adsorptive materials is essential if the adsorption capacity reaches the maximum. However, these technologies are showing difficulties in the removal of antibiotics from animal manure. As aforementioned, adsorption materials can be blocked by the colloidal particles existing in animal manure. This irreversible blockage can cause complete failure in antibiotics adsorption. To date, most studies have been focused on the adsorption of antibiotics from clean water, while there have been no studies conducted on the adsorption of antibiotics from animal manure.

Many studies have reported the removal of antibiotics in membrane processes. NF and RO are two common membrane technologies being able to separate large molecules into the concentrate solution. They have been applied in the treatment of pharmaceutical

wastewater for the purpose of removing antibiotics [206]. These membrane technologies have also shown very high efficiencies in the removal of a wide range of micro-pollutants from the municipal wastewater: 23 – 99% and 93 – 99% for NF and RO, respectively [207-210]. However, similar to adsorption, these technologies cannot be directly applied to the treatment of animal manure because of the high concentrations of SS and organic matter.

2.6.2.2 Chemical technologies

Chemical technologies used for antibiotics removal are called advanced oxidation processes (AOPs). They utilize free radicals to mineralize the antibiotics and form CO_2 and H_2O. These technologies should be considered as alternatives with the intention of finding suitable technologies to further remove antibiotics after a biological process. AOPs are commonly operated in a liquid phase with several oxidants generated, achieving complete elimination of antibiotics [211, 212]. The studied AOPs on antibiotics include chlorination, ozonation, Fenton process, photolysis, electro-oxidation, and many hybrid AOPs including ferrate, electro-Fenton, photo-Fenton, and photo-catalysis processes [202, 213]. There are huge numbers of studies related to the removal of micro-pollutants from wastewater using AOPs. Their removal efficiencies are mostly close to 100% because of the high oxidizing activity of free radicals [214]. Chlorination (Cl_2 and HClO) is less reactive compared with other AOPs, while its removal efficiency can be significantly improved via the integration of UV photolysis [215, 216]. The removal efficiency of chlorination can also be enhanced by increasing chlorine dosage, extending contact time, or changing pH, while it can generate more DBPs in wastewater, such as THMs and HAAs [217]. However, the advantage of chlorination is the low cost and long-term oxidation effect. Ozonation is very efficient in micro-pollutants removal with less DBPs generated. It involves direct reaction of micro-pollutants with ozone molecules through the radicals produced from ozone in the aqueous phase. However, ozonation is also facing many challenges, like the high energy consumption, formation of some oxidative by-products, and interface of radical scavengers [202]. DBPs can be also formed during the ozonation of wastewater. UV treatment is a popular photolysis method widely used in disinfecting potable water, while direct UV photolysis on the removal of micro-pollutants is not effective [215, 216, 218]. Hybrid technologies, such as UV photolysis in the presence of H_2O_2 or

chlorine, normally show higher efficiencies in antibiotics removal that should be further studied. The situation of Fenton oxidation is quite similar. By applying only Fenton oxidation, antibiotics removal is not efficient compared with the Fenton-based hybrid technologies, such as electro-Fenton and photo-Fenton oxidation [202]. However, the problem of Fenton-based technologies also remains on the high cost of maintenance and operation.

In terms of antibiotic removal from raw animal manure, the application of AOPs is challenged by the high concentration of organic matter, which can quench the oxidant and cause low oxidation efficiencies. Hence, completely digested manure would be a better material for AOPs, since it contains less organic matter. The combination of membrane process with AOPs has shown satisfying removal of antibiotics, which has been frequently studied in recent years [202]. One of the important reasons is that the membrane technologies can retain and concentrate antibiotics, which can create an environment reducing the oxidation load of AOPs. However, the formation of DBPs should be taken into consideration as the digested manure still contains high concentration of HA.

2.7 Summary

This chapter reviews recent technologies which can be potentially used to recover nutrients from animal manure. While, nutrient recovery technologies should be adopted depending on farm size, type of animal housing, and the contents of N and P in adjacent lands. For instance, it is impossible to collect manure from grasslands, where the faeces are excreted by free range cows or sheep. In this case, the manures remain on the grasslands. Nutrient recovery technologies can be only considered for the manure generated in animal houses (e.g. pig manure), since it is stored in a manure tank and very easily collected. Nutrient recovery from animal manure is a promising option for large scale farms where the adjacent lands are insufficient to support the direct land application. Nutrients recovered can be used to produce fertilizers that can be sold on the market or transported to the lands distant from animal farms.

In terms of the nutrient recovery technologies, ammonia stripping and struvite formation are easy-operated technologies that can be selected as the best recovery

approaches nowadays. These technologies have already been implemented in full-scale plants and proved to be low energy-cost compared to membrane technologies. Amongst membrane technologies, MF and UF can be adopted as the pretreatment methods to remove particles, while NF, RO, ED, and MD are secondary membrane processes aiming at nutrient recovery. However, membrane fouling of these technologies is a problem that limits the long-term operation. In this matter, EDR and FO are promising due to their potentials of treating animal manure with high SS. Overall, all technologies have bottlenecks requiring further studies to reduce operational costs. Also, more consideration should be given to residual biomass disposal, market values, and biosafety of products. In particular, the removal of antibiotics from animal manure during nutrient recovery should be taken into consideration.

Chapter 3

Nutrient recovery from pig manure digestate using electrodialysis reversal: membrane fouling and feasibility of long-term operation

Chapter 3

3.1 Introduction

Membrane technologies are challenged by severe membrane fouling when treating animal manure digestate due to high turbidity and high concentrations of organic and inorganic matter. By frequently reversing the polarities of electrodes, EDR could be effective in mitigation of membrane fouling and scaling, providing a self-cleaning mechanism in the membrane stack. This provides a feasibility for nutrient recovery using only EDR rather than integrating filtration as a pretreatment step. To date, EDR has been applied to the desalination of seawater and industrial wastewater, while there have been no studies conducted on the treatment of pig manure digestate that has high concentrations of SS, Ca^{2+}, Mg^{2+}, and DOM. The mechanism and evolution of membrane fouling in a nutrient recovery process based on EDR remains unclear. Irreversible fouling is the main cause of a shortened membrane service life. Although there have been a few studies on the fouling of ion-exchange membranes, to the best of our knowledge, the development of irreversible fouling in EDR operation with proper cleaning protocols available has not been sufficiently investigated. Further studies on long-term use of ion-exchange membranes with proper cleaning protocols are required.

In this study, a bench-scale EDR was carried out to assess its feasibility for nutrient recovery from pig manure digestate, through a semi-continuous operation with a periodical acid cleaning protocol. Pretreatment consisted of acidification for releasing P to the liquid phase and low-speed centrifugation for removing large particles. Particle aggregation, chemical deposition, and DOM fouling on and within ion-exchange membranes were characterized systematically so as to examine the mechanisms of reversible and irreversible membrane fouling.

This chapter has been published on *Journal of Membrane Science*:

Lin Shi, Sihuang Xie, Zhenhu Hu, Guangxue Wu, Liam Morrison, Peter Croot, Hongying Hu, Xinmin Zhan. Nutrient recovery from pig manure digestate using electrodialysis reversal: membrane fouling and feasibility of long-term operation. *Journal of Membrane Science* 2019, 573, 560-569.

3.2 Materials and methods

3.2.1 Pig manure digestate

Raw pig manure was collected from a local pig farm in Co. Galway in Ireland (53.104° N, -8.306° W). It was stored in a cold room at 10 ℃ prior to being digested in laboratory-scale batch anaerobic digesters [41]. After the completion of AD (i.e. biogas was no longer generated in digesters), pig manure digestate was obtained, whose characteristics are shown in Table 3-1. Since more than 80% of P exists in the solid fraction in the form of amorphous Ca/Mg-phosphate, acidification of digestate is necessary prior to the solid-liquid separation to maximize the recovery yield of P [2, 69]. Hence, prior to being fed to EDR, pig manure digestate was pretreated to mobilize P and remove SS. The pretreatment of digestate consisted of four steps as follows: (i) acidification of digestate to pH = 5.5 using HCl; (ii) removal of sand and coarse particles using a 0.4 mm sieve; (iii) flocculation with 10 mg/L cationic polymer (Polygold®, Abbeywater, Ireland); and (iv) centrifugation at 1500 g for one minute, which mimicked the decanter centrifugation, a common solid-liquid separation practice in pig farms. The generated liquid fraction of digestate was used as the feed solution for the EDR. The characteristics of the feed solution are also listed in Table 3-1.

Table 3-1. Characteristics of pig manure digestate and feed solution of EDR.

Characteristics	Digestate	Feed solution
Total solids (TS, g/L)	45.9 ± 2.0	30.8 ± 2.2
Volatile solids (VS, g/L)	29.9 ± 1.2	20.6 ± 3.1
Suspended solids (SS, g/L)	19.3 ± 0.5	4.2 ± 0.5
Soluble COD (g/L)	2.9 ± 0.3	2.8 ± 0.2
pH	8.0 ± 0.3	5.5 ± 0.1
Volatile fatty acids (mg/L)	73.3 ± 10.2	70.2 ± 5.2
NH_4^+-N (mg/L)	2574.6 ± 1320.2	2637.0 ± 780.3
PO_4^{3-}-P (mg/L)	56.7 ± 21.2	492.4 ± 112.3
Cl^- (mg/L)	2525.2 ± 372.5	8894.5 ± 406.1

Na^+ (mg/L)	-	691.3 ± 58.7
K^+ (mg/L)	-	3258.8 ± 222.7
Ca^{2+} (mg/L)	-	1021.2 ± 56.6
Mg^{2+} (mg/L)	-	554.6 ± 29.7

3.2.2 Experimental set-up

The heterogeneous cation-exchange membrane (CM) and anion-exchange membrane (AM) used in this study were purchased from MemBrain (Czech Republic). The ion exchange groups of CM and AM were R-SO_3^- and R-$(CH_3)_3N^+$, respectively. All the membranes were statically soaked in distilled water for 48 h prior to use. The configuration of the membrane stack and operational schematics of EDR are illustrated in Figure 3-1a. The membrane stack was composed of five repeating units, and each unit contained two types of membrane sheets, i.e. CM and AM. The effective area of each membrane sheet was 200 cm^2 (20 cm × 10 cm). The membranes were isolated by 0.9 mm thick polypropylene spacers to form dilute and concentrate compartments, which were connected to different containers using silicone tubes. During the experiment, the feed solution and product solution of EDR were circulated in the dilute and concentrate compartments, respectively, at 300 mL/min by peristaltic pumps. Two graphite boards were used as the anode and cathode, and a DC power supply (Rigol, DP832) was used to provide power. The electrolytes in the anode and cathode compartments were both 0.1 M Na_2SO_4 solution.

The operational procedure of EDR included a series of alterations of two different phases, i.e. forward ED and reverse ED. During the forward ED phase, the current in the membrane stack was maintained at +3 A, and the ions were transported from the feed solution to the product solution. During the reverse ED phase, a negative current (–3 A) was applied as the polarities of electrodes were reversed. Meanwhile, the feed and product solutions in the compartments were exchanged so that the ion flux was maintained from the feed solution to the product solution. As shown in Figure 3-1b, each phase lasted for 12 minutes, followed by 3 minutes of a self-cleaning process. During this cleaning process, 300 mL of distilled water was pumped into the

concentrate compartment as the cleaning liquid to replace the feed solution. The cleaning solution was returned to the feed solution hourly.

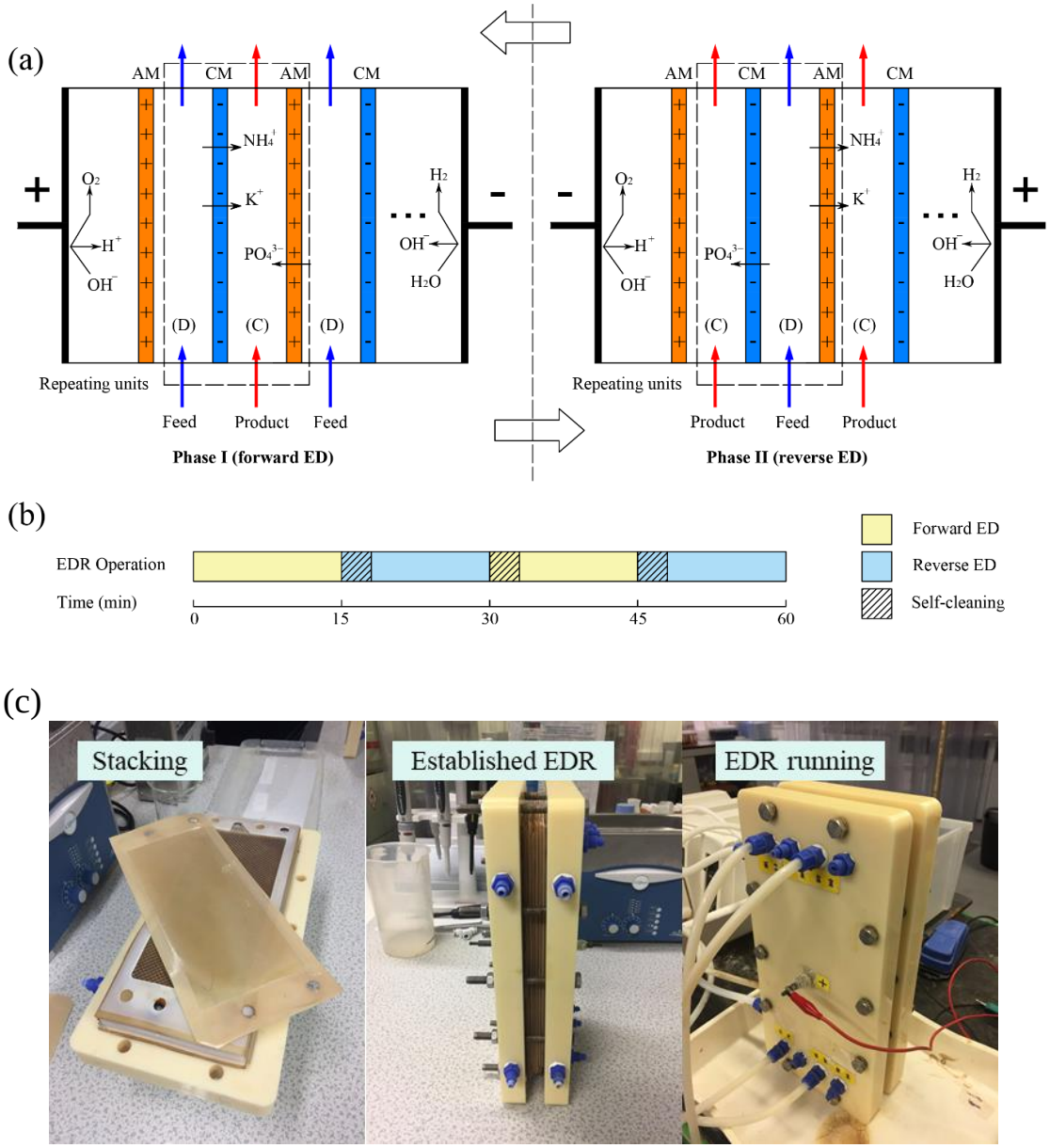

Figure 3-1. Configuration (a), operational schematic (b), and photographs (c) of EDR.
Note: The positive direction of current is from left to right in this figure.

Two experiments, Experiment I and II, were carried out in this study. Experiment I investigated the transport of ions under different volumetric ratios (the volume ratio of the feed solution to the product solution), to assess the extraction and concentration of nutrients during EDR. The volume of the product solution was 2 L, while the volume of the feed solution was 2, 4, and 6 L, which corresponded to volumetric ratios of 2/2, 4/2, and 6/2, respectively. The current was set at constant +3 or –3 A, while the voltage

increased along with the EDR desalination process till reaching 60 V. After reaching 60 V, the experiment was terminated if the current decreased to lower than 2 A, which indicated a very low conductivity of the feed solution. Experiment II was conducted in a semi-continuous mode (28 batches in total) to evaluate the feasibility of long-term operation of EDR. The volumes of the feed and product solution in each batch were both 2 L (i.e. the volumetric ratio was 2/2), and the other operating conditions remained identical as those in Experiment I. To mitigate the membrane fouling caused by DOM, a 1 M HCl solution was circulated in the membrane stack for 15 mins after each batch of EDR, namely acid cleaning. Unused virgin membranes, as well as the fouled membranes after treating with 8, 24, 40, and 56 L of the feed solution (i.e. approximate 110, 330, 550, and 770 L of pig manure digestate per m^2 membrane, respectively) were sampled for fouling characterization.

Two assays were set as the controls to consolidate the findings on membrane fouling: (i) the treatment of 2 L of the feed solution using conventional ED equipped with virgin membranes, and (ii) the treatment of 8 L of the feed solution using EDR without acid cleaning after 28 batches of EDR. The current and voltage applied were as same as those mentioned above.

3.2.3 Analytical procedures

The voltage and current during the experiment were monitored by the DC power supply. The concentration of SS was determined via weighing the microfilter (0.45 μm) before and after filtration. The concentrations of NH_4^+-N, phosphate-P (noted as PO_4^{3-}-P in this study, which was the sum of phosphorus in PO_4^{3-}, HPO_4^{2-}, and $H_2PO_4^-$), and Cl^- were measured using a Konelab nutrient analyser (ThemoFisher Scientific, USA), while the concentrations of Na^+, K^+, Mg^{2+}, and Ca^{2+} were determined using inductively coupled plasma mass spectrometry (ICP-MS, Perkin Elmer, Elan DRCe, Waltham, USA) [219, 220].

Membrane electrical conductivity was determined using direct contact AC impedance method (CHI650E electrochemical workstation), according to Kamcev's study [221]. The membranes were equilibrated in a 0.5 M NaCl solution for 2 hours prior to measurement. After equilibration, the membrane was dipped in a 5 M NaCl solution

quickly (<1s), and clamped between two laboratory-made titanium electrodes (Grade V, 25 mm in diameter) coated by 0.025 mm platinum foil for measurement. The schematic of the measurement apparatus is shown in Figure 3-2. The measurement was processed over a frequency range of 100 – 1 kHz at an amplitude of 5 mV. From the Nyquist plot, the resistance of the membrane (*R*) was taken as the real impedance when the imaginary part was zero. The membrane conductivity (mS/cm^2) was calculated according to Equation (1):

$$G = \frac{1000}{RA} \quad (1)$$

where *A* is the active area of the electrode (cm^2).

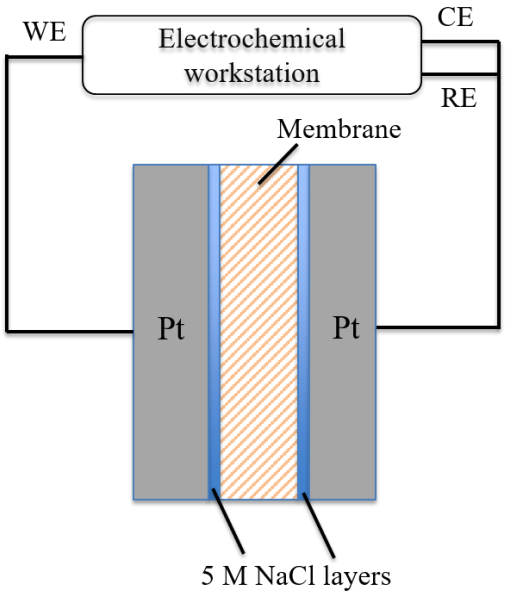

Figure 3-2. Schematic of the circuit for the measurement of membrane conductivity.

Membrane IEC was determined according to a previous method [222]. Prior to the measurement, the membranes were rinsed with distilled water and cut into small pieces (4 cm × 2 cm). For CM, the membrane piece was soaked in 30 mL of 1 M HCl solution for 1 h with agitation, followed by a water rinse for three times. Afterwards, the rinsed membrane piece was soaked in 250 mL of basic solution for 2 h. The basic solution was prepared by mixing 20 mL of 0.1 M NaOH solution and 230 mL of 0.1 M NaCl solution. The surplus OH^- in 25 mL of the basic solution was then titrated using a 0.01 M HCl solution. The IEC of CM (mmol/g) can be expressed as:

$$IEC_{\mathrm{CM}} = \frac{V_0 - V_1}{10 m_{\mathrm{CM}}} \quad (2)$$

where V_0 is the volume of 0.01 M HCl solution used to titrate the control solution without any membrane soaked in (mL), V_1 is the volume of 0.01 M HCl solution used to titrate the basic solution with CM soaked in (mL), and m_{CM} is the dry mass of the membrane piece equilibrated with Na^+ (g).

Regarding the IEC of AM, the membrane piece after acid cleaning was soaked in 30 mL of 0.1 M HCl for 1 h with agitation (while, the uncleaned membrane was soaked in 0.1 M NaCl solution), followed by rinsing with distilled water three times and soaking in 250 mL of 1 M HNO_3 solution for 12 h. The concentration of Cl^- released to the HNO_3 solution was quantified using the Konelab nutrient analyser. The IEC of AM (mmol/g) can be calculated as:

$$IEC_{\mathrm{AM}} = \frac{0.25C}{\mathrm{M_{Cl}} m_{\mathrm{AM}}} \quad (3)$$

where C is the concentration of Cl^- in the HNO_3 solution (mg/L), M_{Cl} is the molar mass of Cl^- (mol/g), and m_{AM} is the dry mass of membrane piece equilibrated with Cl^- (g).

3.2.4 Fouling characterization

Membrane fouling was investigated by characterizing both liquid samples and membranes. Particle size distribution in the liquid phase was determined by a Mastersizer 3000 laser diffraction analyser (Malvern, UK) to verify the aggregation of particles during EDR. After being rinsed by distilled water and dried in the fume hood for 48 h, the membranes were observed by a Hitachi scanning electron microscope (SEM) equipped with energy dispersive X-ray module (EDX), to characterize the chemical deposit. Liquid samples were diluted by 50 times using ultrapure water (Millipore Direct 8) and analysed by fluorescence excitation-emission matrices (EEMs, Horiba Aqualog) to determine the composition of DOM. The EEMs were obtained by measuring the fluorescence emission spectra over a range of emission wavelength (214–620 nm) at 2 nm intervals and a range of excitation wavelength (240–600 nm) at 3 nm intervals. Post-processing of the complete EEMs dataset was performed according to accepted protocols [223, 224] in the following sequence: (i) correction of instrument bias using the correction files provided by the manufacturer, (ii) subtraction of the EEM

of ultrapure water, (iii) correction of the signal for the internal absorbance of the sample, (iv) removal of Rayleigh scattering from the EEM, and (v) normalizing the fluorescence intensity to the area under the ultrapure water Raman peak (excitation 350 nm) run with each sample batch. In addition, the surfaces of unused virgin membranes, fouled membranes, acid cleaned membranes, and the interior of membranes (by scraping off the fouling layer using a knife) were analysed by a Fourier transform infrared spectroscopy equipped with an attenuated total reflection system (FTIR-ATR), to characterize the fouling caused by DOM. The cross-sectional images of membranes, which were equilibrated in 0.1 M NaCl solution for 12 h (pH was maintained at 5.5 using 0.1 M NaOH solution) prior to the observation, were obtained using an optical microscope under the same exposure intensity.

3.3 Results and discussion

3.3.1 Electrical migration and concentration of ions

Under an electric field, ions can be transported from the dilute compartment to the concentrate compartment consecutively against a concentration gradient. As shown in Figure 3-3a, the concentration of NH_4^+-N in the feed solution decreased from around 2500 to 0 mg/L at different volumetric ratios, resulting in a removal of 100%. The increase of NH_4^+-N in the product solution was correspondent to its decrease in the feed solution. The concentration of NH_4^+-N in the product solution at 2/2, 4/2, and 6/2 volumetric ratios reached 1914, 3202, and 4195 mg/L, respectively (Figure 3-3b). Similarly, the concentration of PO_4^{3-}-P in the feed solution decreased from around 500 to 50 mg/L, and it reached a maximum of 300, 522, and 700 mg/L in the product solution at 2/2, 4/2, and 6/2 volumetric ratios, respectively (Figure 3-3c and d). The transportation speed of phosphoric ions (PO_4^{3-}, HPO_4^{2-}, and $H_2PO_4^-$) was slower than that of NH_4^+, which was attributed to the larger Stokes radius and lower hydration ability of phosphoric ions in the aqueous phase [225]. In this circumstance, a higher voltage was required to maintain a desirable migration of PO_4^{3-}-P. It was observed that PO_4^{3-}-P was not fully depleted in the feed solution. This was attributed to the low power density and weak ion flux at the end of EDR process.

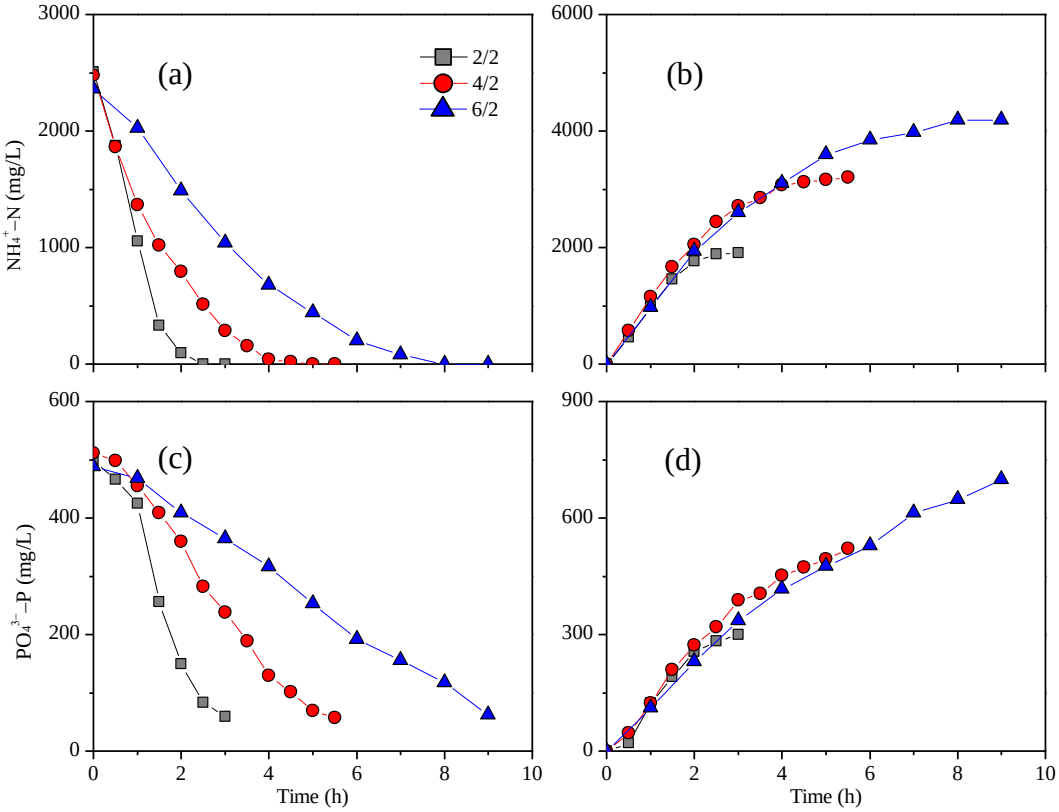

Figure 3-3. Variation of NH_4^+-N and PO_4^{3-}-P at different volumetric ratios during EDR. (a) NH_4^+-N in the feed solution; (b) NH_4^+-N in the product solution; (c) PO_4^{3-}-P in the feed solution; and (d) PO_4^{3-}-P in the product solution.

It was found that the concentrations of NH_4^+-N and PO_4^{3-}-P in the product solution were lower than the values calculated based on mass balance. For example, the concentration of NH_4^+-N in the product solution was 1914 mg/L at 2/2 volumetric ratio, lower than calculated concentration of 2500 mg/L. This phenomenon can be attributed to (i) the volume increase of the product solution, (ii) the migration of ions to the electrolyte, and (iii) the ions residing in ion-exchange membranes. The volume increase of the product solution was due to the migration of hydrated ions under the electric field [226]. In addition, a small portion of water can diffuse from the dilute compartment to the concentrate compartment due to the osmotic pressure difference at the end of EDR process [227]. In this study, the volume of product solutions at 2/2, 4/2, and 6/2 volumetric ratios increased by 0.1, 0.6, and 0.9 L, respectively, suggesting that the volume increase of the product solutions exacerbated with the increase of the volumetric ratio. Nonetheless, NH_4^+-N and phosphate-P were concentrated in the product solution at high volumetric ratios. The transportation of ions to the electrolyte

only occurred in the compartments adjacent to the electrode compartments. It can be reduced in large-scale EDR, as more repeating units would be installed in one membrane stack. The distribution of nutrients after EDR is summarized in Table 3-2. It suggested that a larger volume of the feed solution resulted in a higher recovery efficiency. Despite the volume variation, the recovery efficiencies of NH_4^+-N and PO_4^{3-}-P at 2/2 volumetric ratio were estimated as 80.1% and 63.2%, respectively. As the membranes were made from ion-exchange resins, the stock ions (Na^+ or Cl^-) of membranes can be replaced by the ions in the feed solution. Thus, a proportion of ions can reside in the membranes after EDR process. These ions can be transported from membranes to the product solution in the following batch of EDR or acid cleaning process.

Table 3-2. Distribution of NH_4^+-N and PO_4^{3-}-P after EDR at different volumetric ratios.

Nutrient	Volumetric ratio (Feed solution / Product solution)	Feed (%)	Product (%)	Electrolyte (%)	Acid cleaning (%)
NH_4^+-N	2/2	0.0	80.1	7.7	9.7
	4/2	0.0	84.0	4.0	6.9
	6/2	0.0	85.8	3.6	5.6
PO_4^{3-}-P	2/2	16.1	63.2	4.9	13.3
	4/2	13.9	66.3	6.1	12.0
	6/2	16.0	69.2	6.1	7.6

Based on the concentration of ions, the overall current efficiency at 2/2 volumetric ratio was calculated as 46.8%. In the EDR process, the low current efficiency was attributed to several factors: (i) the diffusion flux of co-ions across membranes, (ii) the protonation-deprotonation of multivalent ions, and (iii) the reversal intervals. The diffusion of co-ions is membrane independent, while the protonation-deprotonation of multivalent ions can be reduced via lowering the current density [228, 229]. In this study, the current efficiency increased to 61.3% when a current of 1 A was applied. However, it led to a long operation time, as shown in Figure 3-4(a). The protonation-deprotonation of multivalent ions cannot be completely avoided, since the EDR process led to the decrease of the limit current of the membrane stack, as shown in Figure 3-4(b).

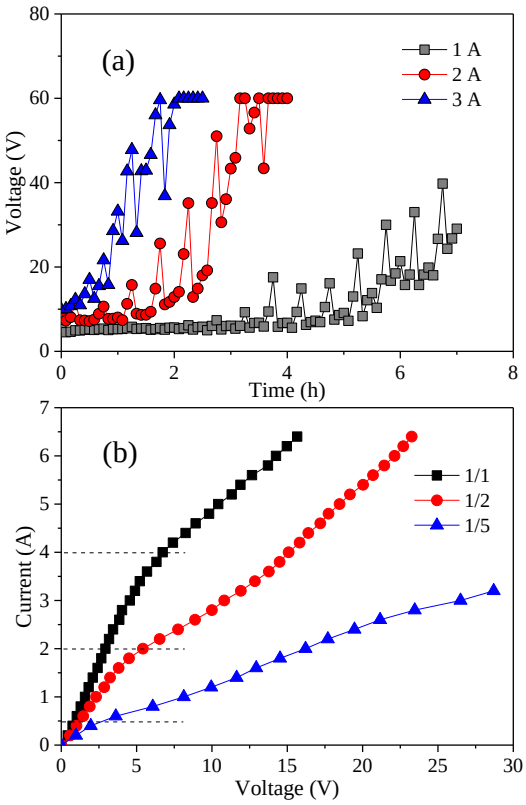

Figure 3-4. (a) Variation of voltages at the operating current of 1, 2, and 3 A, and (b) current-voltage characteristics of the membrane stack under different dilution ratios of the feed solution. *Note: In this figure, the feed solution was diluted by 1/1, 1/2, and 1/5 (v/v) times using distilled water to mimic the different stages of EDR. The low salinity of the feed solution caused a low limit current of the membrane stack, proving that a severe protonation-deprotonation of phosphate occurred at the end of EDR.*

Apart from NH_4^+ and phosphate, various ions (i.e. Na^+, K^+, Ca^{2+}, Mg^{2+}, and Cl^-) co-existed in the feed solution. Migrating along with NH_4^+ and phosphate under the electric field, these ions also migrated, consuming energy. As shown in Figure 3-5, the removal of these ions was similar to NH_4^+ as they were depleted to 0 mg/L at the end of EDR process. Ultimately, NH_4^+, K^+, and Cl^- were the dominant ions in the product solution, with the concentrations of K^+ and Cl^- reaching 2195 and 7775 mg/L, respectively. The directional movement of metal ions under the electric field is a universal phenomenon that has been reported in a plenty of studies [32, 230]. Hence, in any processes based on the electric field, ions can be removed from the feed solutions with high efficiencies in spite of their different initial concentrations. The removals of Na^+, K^+, Ca^{2+} and Mg^{2+} were mainly due to the migration driven by the electric field, because their significant concentration increases were observed in the product solution. However, for trace metal

elements, the membrane sorption may play the primary role in their removals because of the abundant sorption sites on membranes [32, 33].

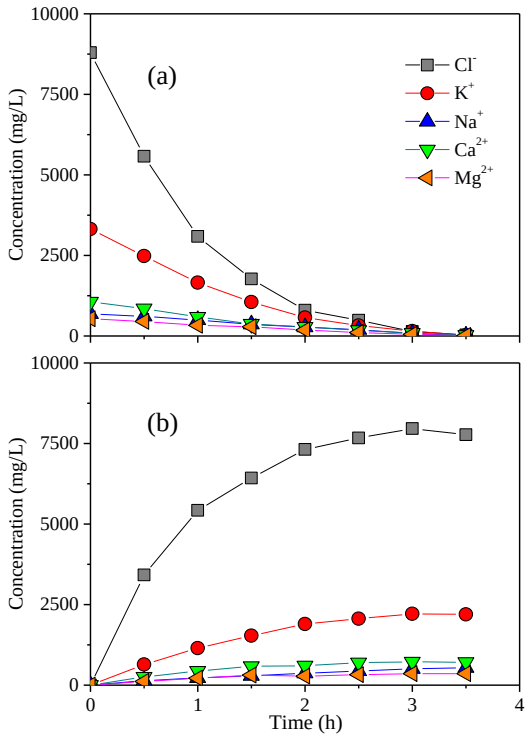

Figure 3-5. Variation of other ions in (a) feed and (b) product solutions during EDR at 2/2 volumetric ratio.

3.3.2 Fouling characterization during semi-continuous operation

3.3.2.1 Membrane characteristics

The mass, conductivity, and IEC of membranes were recorded during the semi-continuous operation of EDR, as shown in Table 3-3. The mass of both CM and AM increased in comparison with the virgin membranes, suggesting certain foulants remained on or in the membranes. In particular, the mass of AM increased from 36.8 to 41.7 mg/cm^2 on average, indicating AM was more prone to be fouled than CM (whose mass increased from 41.4 to 42.5 mg/cm^2). The conductivity of CM remained relatively stable, while that of AM decreased from 109.7 to 89.4 mS/cm^2. Similarly, a negligible decrement of IEC was observed with respect to CM, while the IEC of AM decreased from 1.73 to 1.50 mmol/g, equal to a 13.3% reduction. Since acid cleaning was applied after each batch of EDR, the increase of membrane mass and the decrease of conductivity and IEC were attributed to certain substances which remained on or in

membranes after acid cleaning. It was noteworthy that a significant decrease of IEC occurred during the treatment of initial 24 L of the feed solution, while it decreased marginally by 1.3% in the period from treating 24 L to 56 L of the feed solution, proving much slower fouling kinetics of AM after this threshold (i.e. 330 L digestate per m^2 membrane). This showed a potential feasibility of long-term use of AM with proper acid cleaning. In the control assay without acid cleaning, these three parameters all changed significantly. The conductivity of AM decreased by ~ 50%, suggesting the necessity of acid cleaning in long-term operation.

Table 3-3. Variation of dry mass, conductivity and ion-exchange capacity of membranes.

Membrane type	Feed solution treated (L)	Membrane mass (mg/cm^2)	Conductivity (mS/cm^2)	Ion-exchange capacity (mmol/g)
CM	0	41.4 ± 0.3	117.3 ± 5.6	2.43 ± 0.01
	8	41.9 ± 0.4	116.5 ± 1.0	2.36 ± 0.03
	24	41.9 ± 1.0	119.7 ± 5.9	2.43 ± 0.04
	40	42.0 ± 0.9	120.5 ± 7.1	2.42 ± 0.01
	56	42.5 ± 0.4	118.7 ± 3.0	2.46 ± 0.00
	8*	42.3 ± 0.4	105.7 ± 5.2	2.28 ± 0.03
AM	0	36.8 ± 0.0	109.7 ± 4.2	1.73 ± 0.01
	8	38.9 ± 1.2	104.8 ± 4.1	1.66 ± 0.01
	24	41.1 ± 0.3	92.6 ± 3.2	1.52 ± 0.01
	40	41.5 ± 0.5	89.6 ± 4.3	1.50 ± 0.00
	56	41.7 ± 0.4	89.4 ± 0.6	1.50 ± 0.01
	8*	43.6 ± 0.2	45.0 ± 3.6	1.11 ± 0.11

** The control assay (ii) without acid-cleaning.*

3.3.2.2 Particle aggregation

Particle deposition can cause physical fouling in ED-related technologies, by forming a layer of particle gel on the surface of membranes. In this experiment, the variation of SS in the raw digestate, the feed solution before and after EDR, as well as the product solution was assessed. As shown in Figure 3-6a, solid-liquid separation removed the SS of raw digestate by 78.5%, i.e. from 19.30 to 4.15 g/L. Effectively, particles larger than 50 μm were removed in this process (Figure 3-6b). After EDR process, it was found that the concentration of SS in the feed solution decreased. This was mainly attributed to the volume increase of the feed solution, which was due to the self-cleaning

solution being returned to the feed solution periodically in this experiment. Meanwhile, the proportion of particles smaller than 1.5 μm was significantly reduced, while there was an obvious increase in the proportion of particles in the range of 3 – 4 and 20 – 100 μm. It was noteworthy that a small portion of particles was released from the membranes to the concentrate compartments, resulting in approximately 0.15 g/L of SS in the product solution after EDR. The proportion of particles with size less than 1.5 μm in the product solution was much less than that in the feed solution, and the largest particle size was 200 μm. The change of the particle size distribution can be attributed to the aggregation of colloidal particles. As reported previously, the average electric charge of colloidal particles in pig manure is -0.70 meq/g organic solids, suggesting that they are likely to move and aggregate under the electric field [11]. In conventional ED, the aggregation of particles occurs on the surface of AM, forming a layer of gel-like deposit, thus reducing the electrical conductivity of the membrane stack [222]. However, no obvious particle deposit was observed on the membranes of EDR (Figure 3-7), proving the reversal of electrodes significantly reduced the risks of membrane fouling caused by particle deposition.

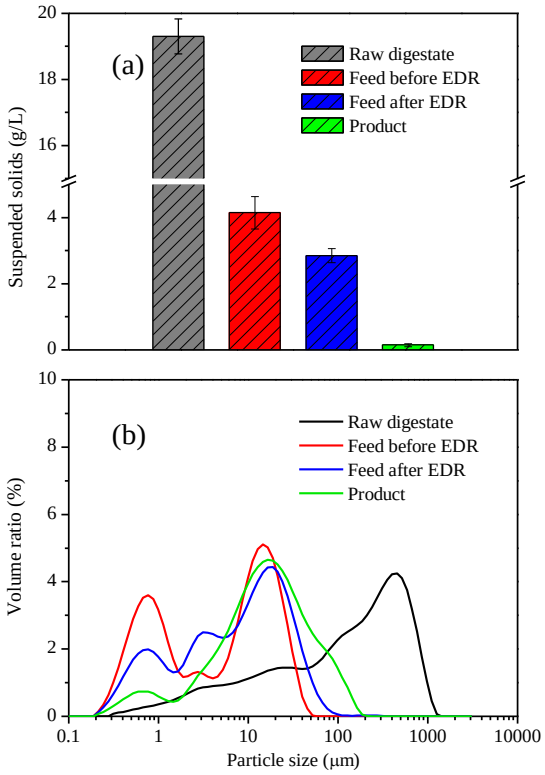

Figure 3-6. Variation of (a) SS and (b) particle size distribution in the raw digestate, the feed solutions before and after EDR, as well as the product solution.

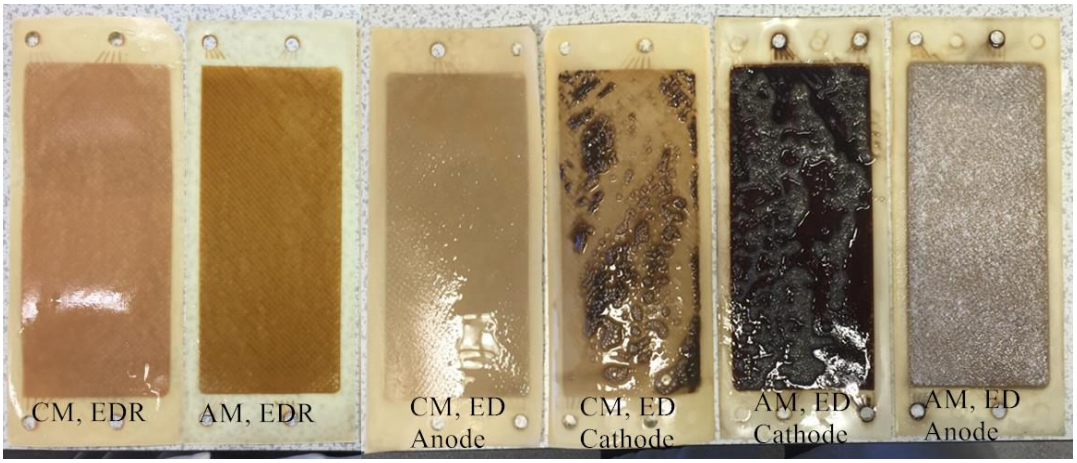

Figure 3-7. Images of ion-exchange membranes from EDR and conventional ED when treating 2 L of the feed solution.

Note: The membranes from left to right are (1) CM and (2) AM from EDR, as well as the surfaces of (3) CM toward anode, (4) CM toward cathode, (5) AM toward anode, and (5) AM toward cathode from conventional ED. Two membrane surfaces in relation to EDR are identical.

3.3.2.3 Chemical deposition

In general, both organic and inorganic deposits can be formed on the surface of membranes in ED-related processes. Figure 3-8a and b illustrate the SEM images of CM and AM after treating 56 L of the feed solution using EDR. Compared to the virgin membrane (Figure 3-8c), negligible deposits were generated on the surface of membranes. However, membranes (AM in particular) exhibited dark brown colour after EDR process (Figure 3-9), which was in accordance with the findings in other studies when treating municipal wastewater [155]. Through EDX scanning, only carbon and oxygen were identified on the surface of membranes, indicating that these foulants were likely DOM. In the control assay of conventional ED, a layer of chemical deposit was observed on the surface of AM towards the cathode, as shown in Figure 3-8d. The elemental composition of this deposit was confirmed as a mixture of C (28.1%), O (39.0 %), Ca (18.4%), P (11.2%), and Mg (3.3%), suggesting a layer of Ca/Mg-phosphate and -carbonate was formed. Similarly, previous studies have reported the formation of Ca-carbonate deposit on the membrane in conventional ED [20, 222]. The formation of this chemical deposit can be explained by the varied pH in the concentrate compartment due to the electric attraction of H^+ and OH^-, resulting in an abundant OH^- beside the AM interface in the concentrate compartment. Meanwhile, Ca^{2+} and Mg^{2+}

may precipitate in the interior of membranes, causing the likely membrane crack. By using the reversal operation of EDR, the chemical deposit was eliminated, suggesting a potential of long-term operation of EDR without chemical deposition.

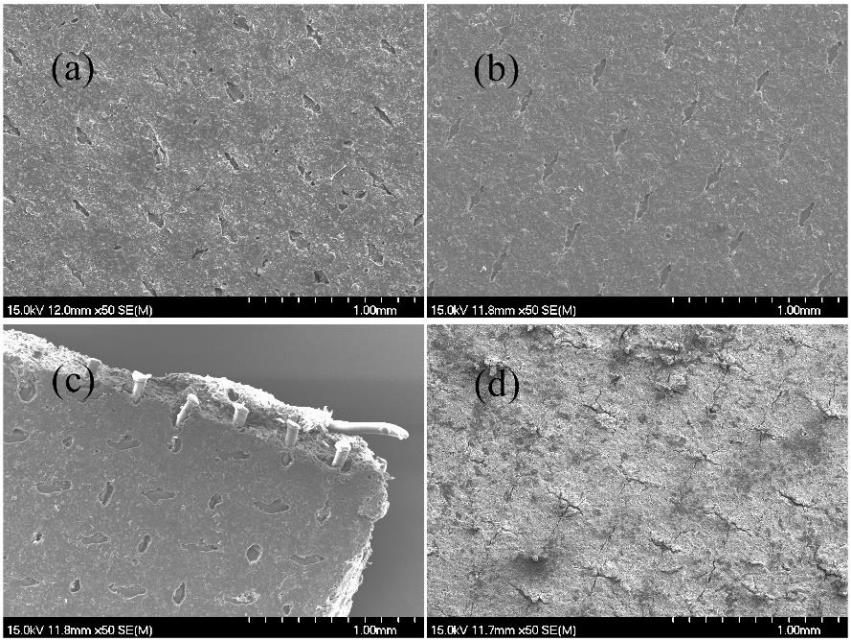

Figure 3-8. SEM images of (a) CM and (b) AM after treating 56 L digestate using EDR, (c) virgin AM, and (d) the surface of AM toward cathode after conventional ED (control assay (i)).
Note: There was no observable difference on the other surface of membranes in EDR.

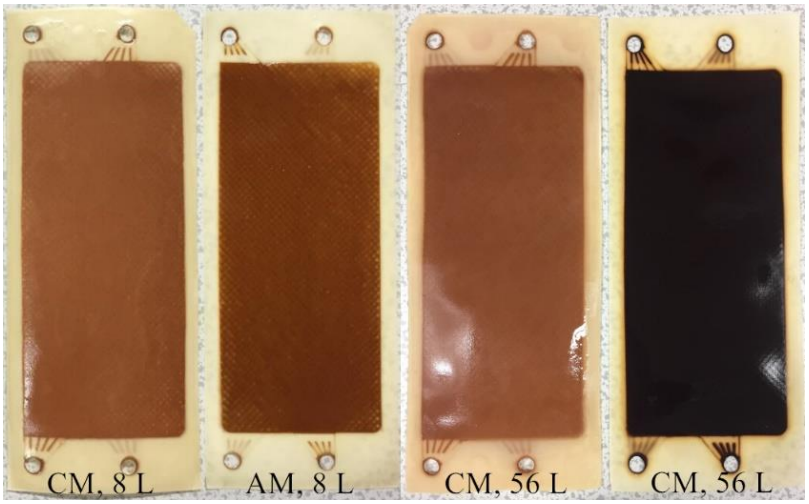

Figure 3-9. Images of ion-exchange membranes from EDR after treating 8 L and 56 L of the feed solution.
Note: The membranes from left to right are CM after treating 8 L of the feed solution, AM after treating 8 L of the feed solution, CM after treating 56 L of the feed solution, and AM after treating 56 L of the feed solution. Two surfaces of each membrane are identical.

3.3.2.4 Electric migration of DOM

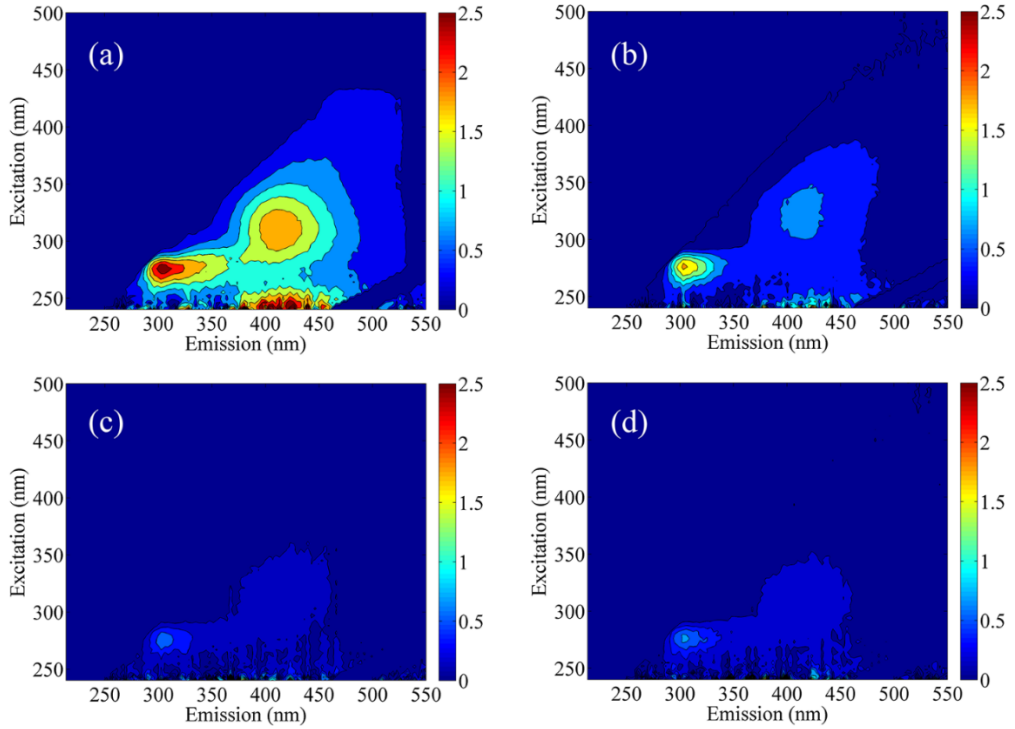

Figure 3-10. Fluorescence EEMs of the 50-times diluted samples. (a) the feed solution before EDR, (b) the feed solution after EDR, (c) the product solution, and (d) the used acid cleaning solution.

Note: The fluorescence intensities are expressed in Raman unit. The fluorophores at (270–280)/(300–310) nm and (290–325)/(390–440) nm of excitation/emission wavelength were caused by tyrosine-like proteins and terrestrial humic substances, respectively.

In addition to inorganic ions, DOM co-existing in the feed solution can migrate under the electric field, causing organic fouling of membranes. Three-dimension EEMs provided valuable insights into the composition of DOM in the feed, product, and acid cleaning solutions. As shown in Figure 3-10a, two wavelength peaks were obtained in the EEM spectra, i.e. fluorophore A and B, peaking at (270–280)/(300–310) and (290–325)/(390–440) nm, respectively. Based on the previous studies, fluorophore A was identified as a tyrosine-like substance, while fluorophore B was a terrestrial humic-like substance [231, 232]. Both substances can originate from various sources including drinking water, pig additives, and intestinal digestion products in pigs. It is noteworthy that their fluorescence intensity became weaker in Figure 3-10b, indicating that the concentrations of both components were reduced during the EDR process. This was attributed to the migration of organic substances under the electric field due to the

charged functional groups. Accordingly, the removal of bovine serum albumin (BSA) and HA from synthetic wastewater in conventional ED and EDR was assessed (Figure 3-11). The result proved that these substances were concentrated to the membrane-liquid interface in the electric field and weakly bonded with ion-exchange matrix, rather than passing through the membranes. In this study, most of the humic-like and tyrosine-like substances still remained in the feed solution of EDR due to the reversal operation, while a small proportion of them transported to the product and acid cleaning solutions (Figure 3-10c and d). The fluorescence intensities of these two components in the raw pig manure were higher than those in the feed solution, as shown in Figure 3-12. It clearly demonstrated that AD can reduce the concentrations of tyrosine-like and humic-like substances, thereby minimizing the risks of membrane fouling caused by DOM during EDR.

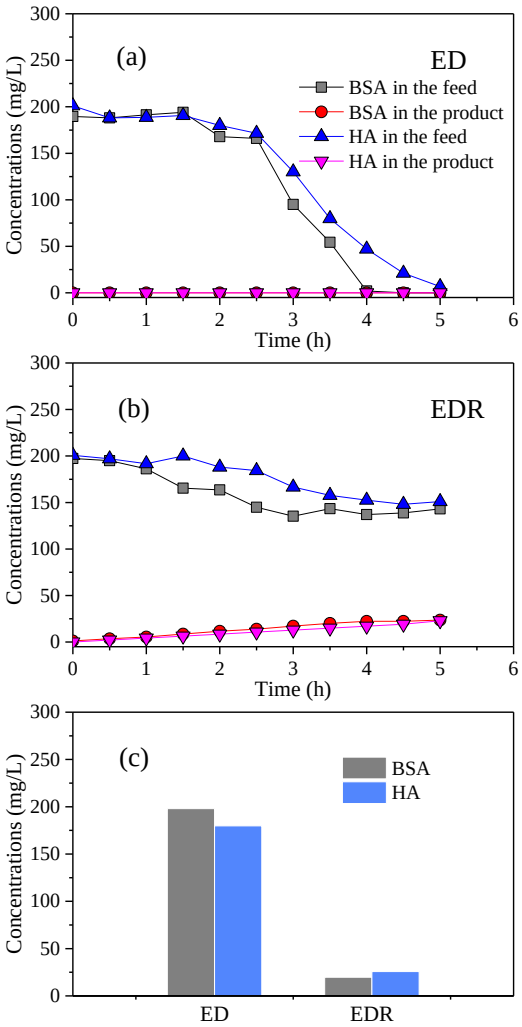

Figure 3-11. Variation of BSA and HA in the (a) conventional ED and (b) EDR processes when treating 5 L of synthetic wastewater, and (c) their concentrations in the water cleaning solutions.

Note: In this experiment, both ED and EDR were operated for 5 hours, followed by 2 minutes of membrane cleaning using 5 L of distilled water without voltage applied (i.e. water cleaning). The feed solutions used in ED and EDR were synthetic wastewater consisting of (in g/L): ammonium chloride 8.0, ammonium acetate 5.4, monopotassium phosphate 3.0, and BSA and HA 0.2. The pH of feed solution was maintained at 5.5 during the experiment. The concentration of BSA was determined using an UV spectrophotometer (Varian 50 Scan) at a wavelength of 595 nm. The preparation of samples included: (i) mixing 100 µL of the samples with 5 mL of the Coomassie protein assay reagent, and (ii) incubating the samples for 10 minutes for consistent reading. The concentration of HA was determined using the same spectrophotometer, based on its natural absorbance at 465 nm of wavelength.

In the ED process, the concentrations of BSA and HA in the feed solution decreased insignificantly at the beginning, while sharp decreases to 0 mg/L were observed in the period of 2.5 – 5.0 h. This proves the electric migration of BSA and HA mainly occurred in the late phase of ED, which was correspondent to the depletion of ions in the feed solution. However, there was no BSA or HA detected in the product solution, proving that both substances did not pass through the ion-exchange membranes. During 2 minutes of water cleaning, the concentrations of BSA and HA reached 198 and 180 mg/L, respectively, proving that the ED removed BSA and HA were mostly present in the membrane-liquid interface at high concentrations, weakly bonded with ion-exchange matrix, and easy to be cleaned. By contrast, in the EDR process, BSA and HA decreased marginally in the feed solution and their concentrations were very low in the cleaning solution, proving that the reversal operation of EDR significantly reduced the electric removal of BSA and HA.

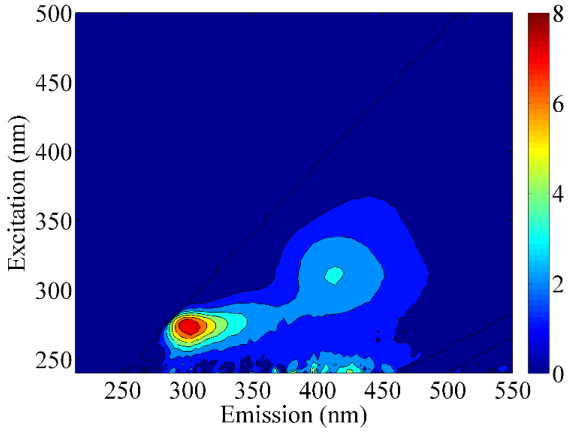

Figure 3-12. Fluorescence EEM of 50-times diluted raw pig manure before AD.
Note: The fluorescence intensity is expressed in Raman unit.

3.3.2.5 Long-term fouling caused by DOM

The organic foulants remaining on the membranes after treating 56 L of the feed solution were further characterized by FTIR-ATR, as shown in Figure 3-13a and b. A small peak can be distinguished on the spectrum of fouled CM compared to that of virgin membrane, i.e. the peak at ~ 1550 cm^{-1}. This peak was attributed to protein-like substances according to the standard FTIR spectrum of BSA reported previously, associated with the characteristic band of amide I. Another characteristic peak of proteins at ~ 1645 cm^{-1} became intensive on the spectrum of fouled CM, which has been reported as amide II [233]. On the spectrum of fouled AM, this peak was much more substantial than that on the spectrum of fouled CM, demonstrating that AM was more prone to fouling than CM. The spectra were normalized using multivariate curve resolution – alternating least squares (MCR-ALS) method [234], for a better understanding of individual peaks on each spectrum, as shown in Figure 3-14. It is noteworthy that an additional peak at ~ 1030 cm^{-1} was detected on the spectrum of fouled AM, assigned to humic-like substances [234]. It was likely that CM can resist the fouling of humic-like substances, as no significant difference was observed on the spectrum of CM at this wavenumber. This finding was consistent with previous findings in conventional ED that BSA can reduce the conductivity of both CM and AM, while the fouling of CM caused by HA solution was negligible [19]. This phenomenon is attributed to the different electric charge of protein-like and humic-like substances. In the aqueous phase, the protein-like substances have both negatively and positively charged functional groups, while the humic-like substances are negatively charged, therefore causing the variance of electrostatic and affinity interactions between foulants and the ion-exchange groups. In combination with the EEMs result, the decrease of protein-like and humic-like substances in the feed solution consolidated the FTIR findings, proving these organic substances were the major cause of membrane fouling.

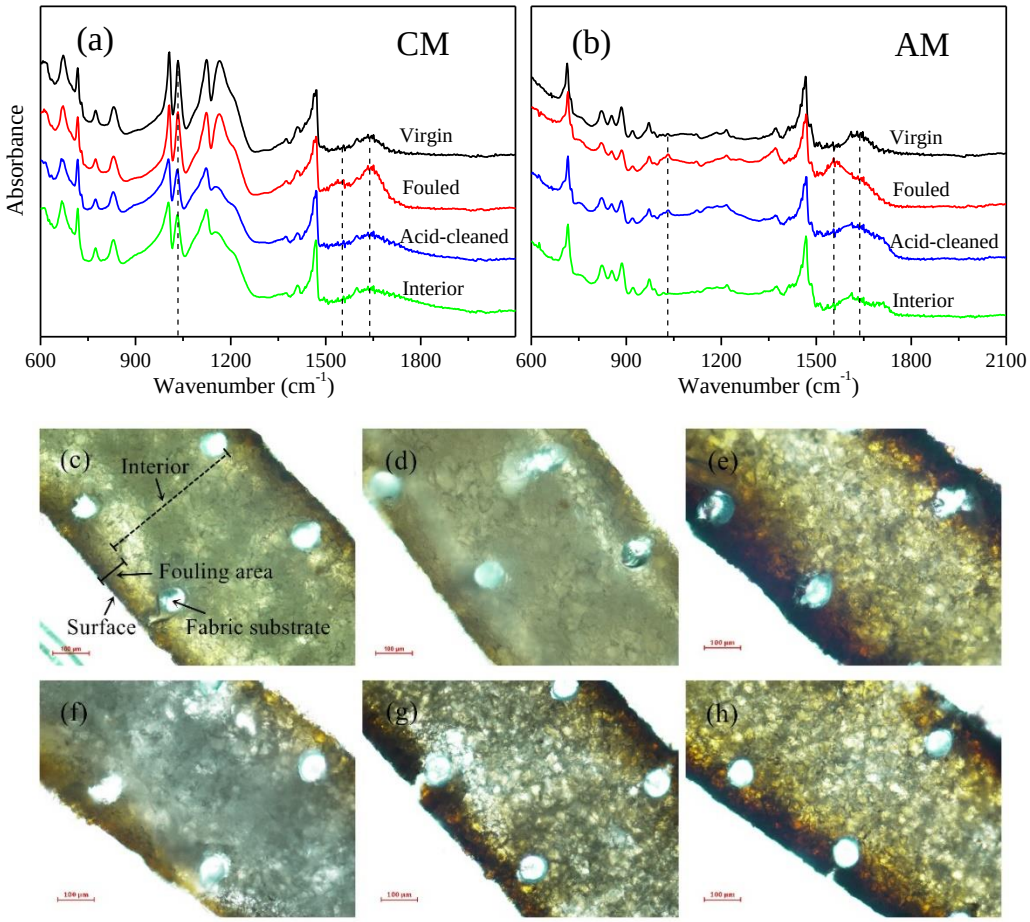

Figure 3-13. FTIR-ATR spectra of (a) CM and (b) AM, in addition to the cross-sectional microscopic images of (c) fouled CM, (d) acid cleaned CM, (e) fouled AM after treating 56 L of the feed solution, and acid cleaned AM after treating (f) 8 L, (g) 24 L, and (h) 56 L of the feed solution.

Acid cleaning was effective in the removal of protein-like substances, as the peak at ~ 1550 cm^{-1} became weakened on the spectra of cleaned CM and AM. A low pH can result in a positive charge of protein-like substances, evidenced by the isoelectric points (pI) of proteins in the range of 4 – 12 [235]. A loose fouling layer was therefore generated due to the electrical repulsive between foulants and AM at the low pH. However, the humic-like substances can be prone to their acid forms at a low pH based on the ionization equilibrium of carboxylic and phenolic groups [236]. Indeed, as reflected in Figure 3-13b, the characteristic peak of humic-like substances remained on the spectrum of AM after acid cleaning. Figure 3-13(c-h) profiles the cross-sectional views of the fouled and cleaned membranes. It was obvious that organic fouling primarily took place in the area close to the membrane surface, which was named as

"fouling area" in the membrane, where the colour of ion-exchange matrices turned dark brown. In this study, the thickness of this fouling area was around 100 μm. The formation of this fouling area was due to the rough and porous surface of the heterogeneous membranes, allowing foulants to migrate into the membrane during EDR. It stopped NH_4^+ and phosphate migrating deeper into the interior of the membrane [19, 237]. In contrast, the colour of the interior area was light green, proving that negligible fouling occurred inside the membrane. This was further validated by the FTIR spectra of the interior area, with no obvious difference compared to that of virgin membranes. It was obvious the colour of the fouling area of AM became lighter after acid cleaning (Figure 3-13e and h), suggesting the ion-exchange matrix in this area was partially regenerated.

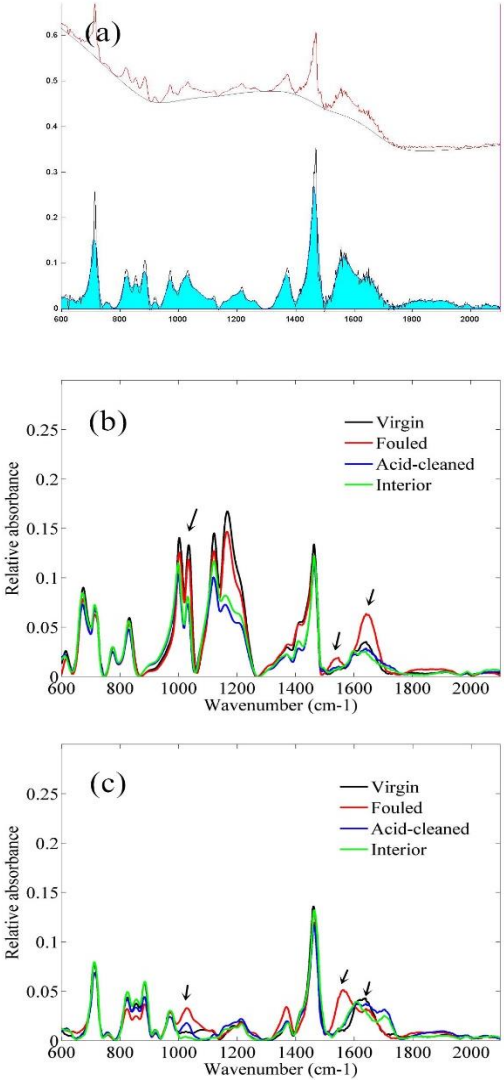

Figure 3-14. Normalization of FTIR spectra using MCR-ALS method (λ=2000). (a) Normalization process; (b) normalization of CM spectra; and (c) normalization of AM spectra.

Therefore, the fouling caused by DOM can be classified as reversible and irreversible, which were associated with the dark brown substances cleaned off AM and remaining on AM, respectively. Reversible fouling resulted from physical sorption and deposition of DOM, and this type of deposit was loose and easily cleaned by the acid. Irreversible fouling might result from chemical bonding between foulants and the ion-exchange matrix because of the permanent loss of IEC, as presented in Table 3-3. The transportation of foulants to the interior of membranes was hampered by the fouling area. As a result, the growth rate of irreversible fouling became insignificant after treating 24 L of the feed solution (i.e. 330 L/m^2 membrane), implying a promising potential of EDR in long-term operation. Few studies on ion-exchange membranes with multiple cleaning cycles have reported this phenomenon to date. However, it was similar to the previous findings on the ion-exchange resins in a batch sorption test that the decrease of IEC became insignificant after several cleaning cycles [238, 239]. In the long-term operation of EDR, reversible fouling can be formed in the fouling area and subsequently cleaned off by the acid solution, while the growth of irreversible fouling was limited after the fouling threshold (i.e. 330 L/m^2 membrane) demonstrated in this study. As reflected in Figure 3-13(f-h), the colour of the fouling area after acid cleaning changed significantly when treating the initial 24 L of the feed solution, while a negligible change was found after treating 56 L of the feed solution. Therefore, the reversible fouling dominated the fouling process after reaching this fouling threshold. This is also reflected in Table 3-3, where a substantial decrease of IEC was observed in the control assay without acid cleaning, compared to a small decrease of irreversible IEC after acid cleaning.

The overall fouling mechanisms of EDR during nutrient recovery from pig manure digestate, which had high turbidity and contained high concentrations of organic and inorganic matter, are summarized in Figure 3-15. Along with the transport of ions, the particles aggregated in the membrane-liquid interface and dissociated from the membrane surface subsequently due to the reversal of electrodes. Chemical deposition was likewise mitigated since the reversal of electrodes allowed the frequent dissolution of chemical precipitates. Tyrosine-like and humic like substances in the feed solution were transported to the membrane-liquid interface at high concentrations, and then causing the DOM fouling with dark brown foulants formed in the surface area of the membrane. These substances were partially cleaned off from the membrane by acid

solution, forming the reversible fouling of EDR, while some of them were not able to be cleaned off, forming the irreversible fouling of EDR. However, the irreversible fouling kinetics became insignificant after a threshold of 330 L/m^2 membrane, suggesting a feasibility for long-term operation.

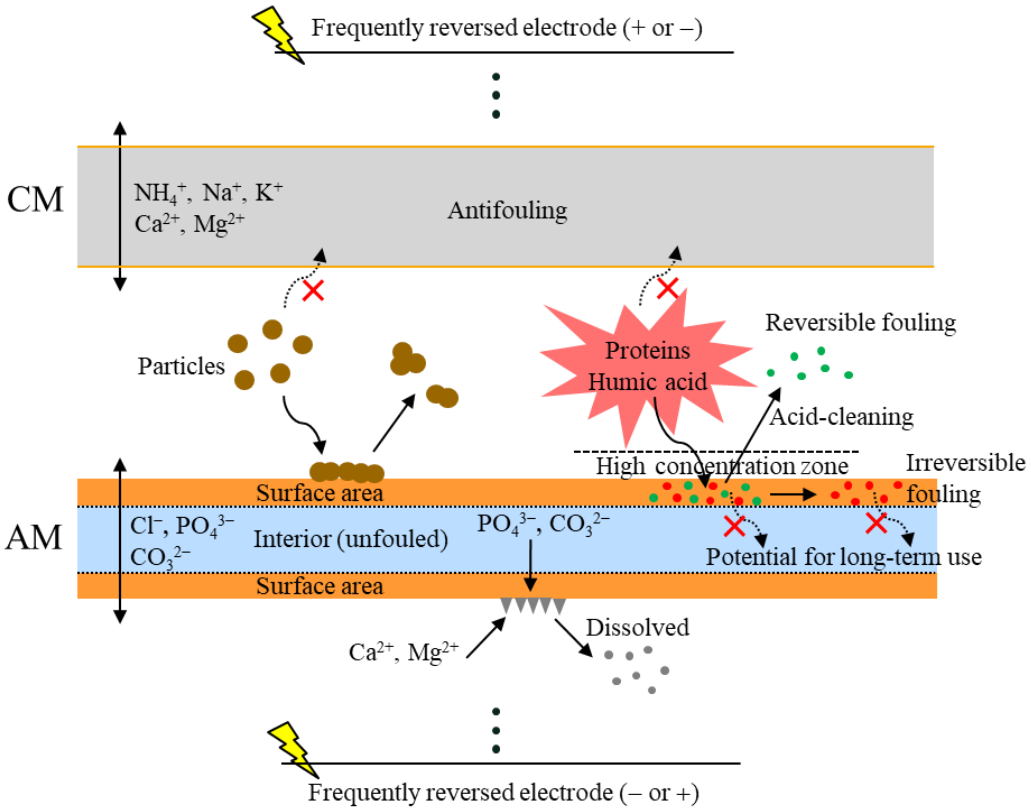

Figure 3-15. Fouling mechanisms of EDR during the nutrient recovery from pig manure digestate.

Electrodialysis reversal is often regarded as energy-intensive, and the energy consumption in this study was calculated as 0.13 kWh/L. However, it is resistant to fouling and provides an alternative to the treatment of wastewater with high SS, Ca^+, and DOM. As the chemical deposit was minimized by self-cleaning, the amount of acid used for acid cleaning was expected to be much less than that used in the conventional ED. In addition, N and P in the digestate were concentrated to the product solution via changing the volumetric ratio, thereby increasing the fertilizer effect of digestate in direct land use and reducing the transportation costs. High current efficiencies can be achieved in a small current mode, as demonstrated in this study, which was also demonstrated in bioelectrochemical reactors with a small voltage applied (0.8 – 1.4 V)

[240, 241]. However, a low current operation mode indicates a long operation time, which has to be taken into account for practical use of this EDR process.

3.4 Summary

In this study, membrane fouling during nutrient recovery from pig manure digestate using EDR was examined, in addition with nutrient recovery efficiency. EDR was able to extract NH_4^+-N and PO_4^{3-}-P with efficiencies of 100% and 84% from the high SS digestate into the product solution. During the semi-continuous operation of EDR, only significant changes of membrane mass, conductivity, and IEC were observed on AM, while they remained stable with respect to CM. Fouling caused by particle aggregation and chemical deposition was significantly mitigated by the self-cleaning of EDR. Tyrosine-like and humic-like substances were the primary cause of membrane fouling, and AM was easily fouled by these substances than CM. This type of fouling only occurred in the area close to the membrane surface, while the interior of membrane remained uncontaminated. Reversible fouling was cleaned by the acid solution, while the irreversible fouling resulted in the permanent loss of IEC. Nonetheless, the growth of irreversible fouling became insignificant after several cycles of EDR. Therefore, it is feasible to maintain the long-term operation of EDR for nutrient recovery from pig manure digestate.

In the EDR process, both NH_4^+-N and PO_4^{3-}-P were transported to and concentrated in the product solution. However, further separation and purification of the N and P in the product solution is essential for the production of marketable fertilizers. BMED is another promising ED technology that can separate NH_4^+-N and PO_4^{3-}-P into different product solutions. A base solution and a acid solution can also be produced as by-products in BMED. Hence, in the next chapter, we assessed the feasibility of BMED in nutrient recovery from pig manure, and established a novel operational method to improve the purity of products.

Chapter 4

Recovery of nutrients and volatile fatty acids from pig manure hydrolysate using two-stage bipolar membrane electrodialysis

4.1 Introduction

Pig manure hydrolysate contains abundant valuable resources including NH_4^+-N, P, and VFAs. The N and P can be recovered as fertilizers available for the plants, while VFAs can be recovered as a resource for industrial use, such as the production of bioplastics and bioenergy, as well as for biological nitrogen removal from low C/N wastewater [13]. High concentration of VFAs from initial hydrolysis during the storage renders its recovery imperative [14]. Apart from being organic matter for biogas production through AD, VFAs can be alternatively harvested as by-products, which can be potentially incorporated into the recovery processes of NH_4^+-N and P.

Bipolar membrane electrodialysis is a novel ED system equipped with a BM. It takes advantage of the specific property of a BM and effectively splits water into hydroxide ions (OH^-) and protons (H^+) under an applied electric field, thus separating cations and anions to different compartments. Ultimately, inorganic and organic salts can be converted to the corresponding acids and bases, thereby allowing the diversity of the products without chemical dosing. With efficient pretreatment to remove particles, BMED is able to recover the nutrients and VFAs from pig manure hydrolysate. In this process, a high pH in the base compartment creates suitable conditions for NH_4^+-N recovery via subsequent air-stripping, while P and VFAs migrating to the acid compartment in BMED can be recovered as weak acids. BMED has been previously applied to produce acetic acid, lactic acid, citric acid, and other organic acids for industrial uses [21-25]. However, few studies have focused on resource recovery from animal manure using BMED. Most importantly, simultaneous recovery of NH_4^+-N, P and VFAs has never been reported in the literature.

In this study, a three-compartment BMED was set up to assess the simultaneous recovery of NH_4^+-N, P and VFAs from acidified pig manure hydrolysate. The primary objectives were to (1) simultaneously recover NH_4^+-N, P and VFAs from pig manure hydrolysate using BMED; (2) establish a BMED model to simulate this process based on the ion flux balances and investigate the diffusion loss of ions; and (3) optimize the operation to separate the weak acids (phosphoric acid and VFAs) from Cl^- and SO_4^{2-} and improve the purity of products.

This chapter has been published on *Chemical Engineering Journal*:

Lin Shi, Yuansheng Hu, Sihuang Xie, Guangxue Wu, Zhenhu Hu, Xinmin Zhan. Recovery of nutrients and volatile fatty acids from pig manure hydrolysate using two-stage bipolar membrane electrodialysis. *Chemical Engineering Journal* 2018, 334, 134-142.

4.2 Materials and methods

4.2.1 Materials

Both synthetic and real pig manure hydrolysate were used as the feed wastewater to the BMED. The synthetic hydrolysate was used to investigate the fundamentals of migration of ions in BMED, in order to build up BMED modelling. The synthetic wastewater was prepared using distilled water to simulate the real pig manure hydrolysate. It consisted of (in g/L): ammonium chloride 8.02, ammonium sulfate 9.91, disodium hydrogen phosphate 3.15, sodium acetate 5.49, propionic acid 1.33, butyric acid 1.32, iso-butyric acid 1.32, valeric acid 1.02 and iso-valeric acid 1.02. The corresponding concentrations of NH_4^+, PO_4^{3-} and VFAs were 5.40 g/L, 2.09 g/L and 10.03 g/L, respectively, with NH_4^+-N and PO_4^{3-}-P being 4.20 g/L and 0.68 g/L, respectively. Pig manure hydrolysate was collected from a local pig farm in Co. Galway in Ireland (53.104° N, -8.306° W) with initial pH of 7.3. The characteristics of pig manure hydrolysate were shown in Table 4-1. It was pretreated to facilitate the release of P to the liquid fraction and to remove the solid contents. The pretreatment consisted of four steps as follows: (1) adjustment of pH to 5.0 using HCl (1 mol/L); (2) settlement for 24 h with foam removal; (3) centrifugation at 15,000 g; and (4) filtration (10 μm) and MF (0.45 μm). CM, AM and BM used in this study were heterogeneous membranes (MemBrain Company, Czech Republic). All membranes were soaked in deionized water for 48 h prior to use. The properties of the membranes used in this study are presented in Table 4-2.

Table 4-1. The characteristics of pig manure hydrolysate.

Characteristics	Concentration
Total solids (TS, %)	8.29
Volatile solids (VS, %)	6.36
Suspended solids (SS, %)	5.89
Chemical oxygen demand (COD, g/L)	52.69
Soluble chemical oxygen demand (SCOD, g/L)	21.92
Ammonium nitrogen (NH_4^+-N, g/L)	3.41
Soluble phosphorus (P, g/L)	0.58
Volatile fatty acids (VFAs, g/L)	9.54
Potassium (K, g/L)	3.32
Calcium (Ca, g/L)	1.06
Magnesium (Mg, g/L)	0.53
Sodium (Na, g/L)	0.69

Table 4-2. Properties of membranes in BMED membrane stack.

Membrane	Dry thickness (mm)	Swell difference (%)	Ion exchange group	Area resistance ($\Omega \cdot cm^2$)	Transport number of K^+ (%)	Selectivity (%)
CM	<0.45	<50	$R\text{-}SO_3^-$	<8	>95	>90
AM	<0.45	<50	$R\text{-}(CH_3)_3N^-$	<8	>95	>90
BM	0.4 ± 0.05	<22	-	-	-	-

4.2.2 BMED set-up

Figure 4-1 illustrates the schematic of the BMED apparatus used in this study. The BMED membrane stack was composed of five repeating units, and each unit contained three membrane sheets (CM, AM and BM). The active dimensions of these membranes were 20 cm in length and 10 cm in width. The membranes were isolated by 0.9 mm thick polypropylene spacers with turbulence accelerating mesh nets to form the salt, base and acid compartments. Two titanium electrodes coated by iridium were used separately as the anode and the cathode in the electrolyte compartments. The membrane compartments were connected to the salt, base, acid and electrolyte containers through

silicone tubes, respectively. Initially, the salt container was filled with 5 L of pig manure hydrolysate (synthetic or real hydrolysate), while the base and acid containers were both filled with 1 L of deionized water. The electrolyte container was filled with 1 L of Na_2SO_4 solution (0.1 mol/L). The solutions in each compartment were circulated via peristaltic pumps at 300 mL/min. A stabilized DC power supply (Rigol DP832, 60V/3A, China) was used to provide constant current density during the experiment.

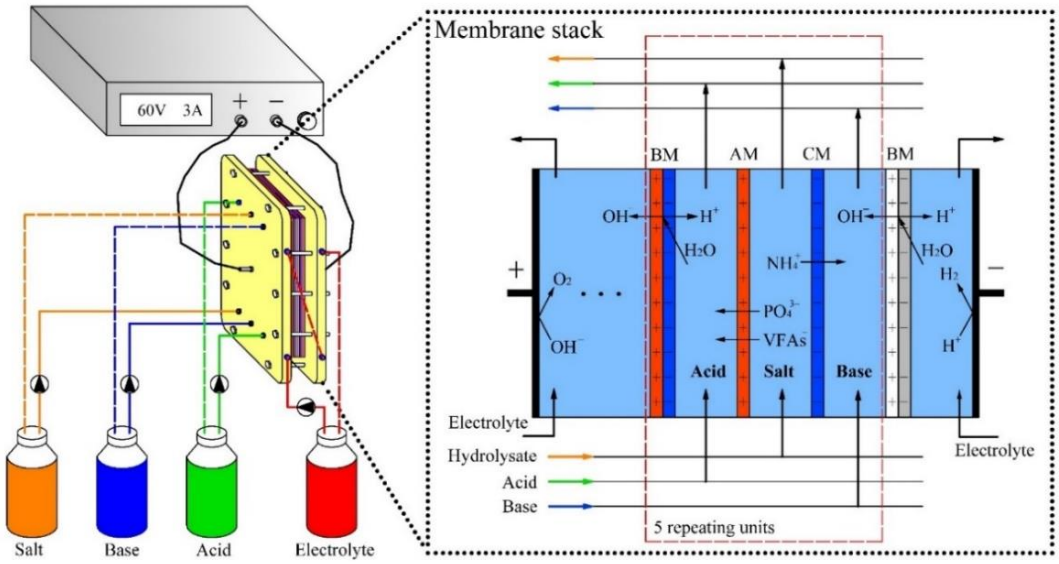

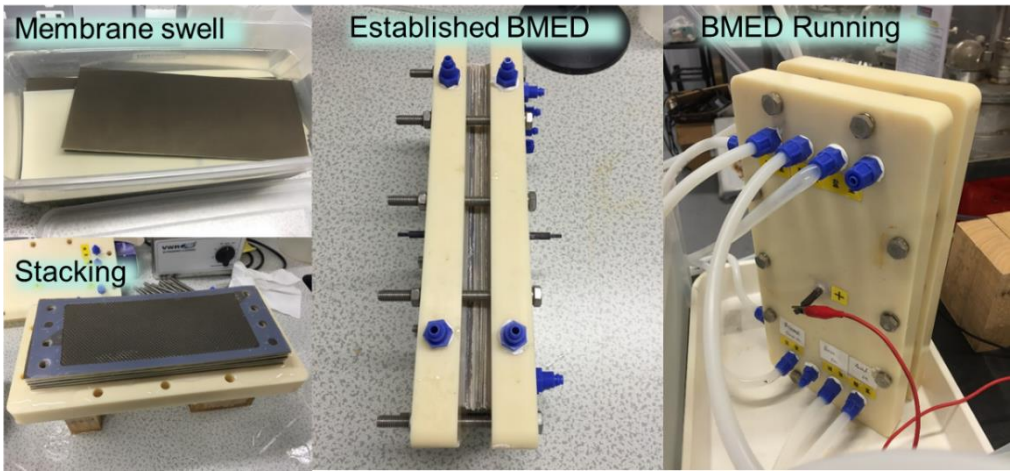

Figure 4-1. Schematic and photographs of the BMED apparatus.

4.2.3 Experimental design

Three experiments, namely Experiment I, II and III, were performed consecutively to evaluate the feasibility and efficiency of the BMED system in the recovery of nutrients

and VFAs from pig manure hydrolysate. Experiment I was performed to assess the viability of BMED in treating the synthetic pig manure hydrolysate and to provide data for modelling the BMED process. In Experiment II, a novel two-stage operation strategy was developed to separate PO_4^{3-} and VFAs anions from Cl^- and SO_4^{2-} and to improve the recovery yield of NH_4^+. The first and second stages can be distinguished during the full course of the BMED experiment by a critical time point, namely "inflection point" [226, 227], when the voltage began to increase significantly. After reaching the inflection point, the solutions in the base and acid containers were both replaced with 1 L of deionized water. Thus, two basic and two acidic solutions were produced in this experiment, namely Base I, Base II, Acid I and Acid II. In Experiment III, real pig manure was treated to further verify the results and consolidate the findings obtained from the synthetic pig manure hydrolysate.

Prior to the DC power supplied, the solution in each compartment was circulated by pumps for 5 min to eliminate visible bubbles. The current of the BMED was constant at 3 A, and the voltage was limited to less than 60 V. The liquid samples were taken from the salt, base, acid and electrolyte containers every 30 min for the measurement of ions.

4.2.4 Analytical methods

The concentrations of NH_4^+, chloride (Cl^-), sulfate (SO_4^{2-}) and phosphate (calculated as the sum of three species, i.e. $H_2PO_4^-$, HPO_4^{2-} and PO_4^{3-} and expressed as PO_4^{3-} in this study if not defined elsewhere) were measured using a Konelab analyzer (ThermoFisher Scientific, USA). The concentrations of VFAs were detected using high performance liquid chromatography (HPLC-1200 series, Agilent Technologies, USA) equipped with a UV-detector. VFAs were separated in an ion exclusion column (Aminex, HPX-87H, 300 mm × 7.8 mm) with a mobile phase (0.1% sulfuric acid) at a flow rate of 0.6 mL/min [242]. The detecting temperature was 65 °C. Protons (H^+) in the acid container were titrated using 1 mol/L of NaOH solution. The amount of H^+ in the acid was equal to the titrated value minus the concentration of weak acids (phosphoric acids and VFAs) in the acid, as weak acidic ions consumed H^+ during the titration.

4.2.5 Data analysis

The efficiency of the process performance is dependent on key parameters such as energy consumption and current efficiency. Energy consumption is calculated by the integration of the current:

$$W = \int_0^t UI\mathrm{d}t \qquad (1)$$

where W is the energy consumption of BMED (J), U is the voltage between the anode and cathode (V), I is the current applied to the membrane stack (A), and t is the reaction time (s).

Current efficiency of a specific ion is the percentage of theoretical electric charges used for transferring this ion versus total consumed electric charges. It is calculated as:

$$\eta = \frac{z_x \frac{\Delta m(t)}{M} F}{nIt} \times 100\% \qquad (2)$$

where z_x is the electrochemical valence of x ion, $\Delta m(t)$ is the total mass of transferred ion (g), M is the molar mass (g/mol), F is the Faraday constant (96485 C/mol), and n is the number of repeating units in the membrane stack.

4.2.6 BMED model

A BMED model was developed based on desired and undesired fluxes in each repeating unit (Figure 4-2 and Table 4-3), to quantify the ion fluxes and proton loss in the BMED.

According to Wilhelm [243], the balance of ion fluxes and current in each membrane is as:

$$\sum J_x^y \cdot z_x = \frac{I}{FS} \qquad (3)$$

where J_x^y is the flux of x ion through y membrane (mol/m^2·s), and S is the active area of membranes (m^2).

J_x^y can be calculated in the following equation:

$$J_x^y = \frac{V\mathrm{d}C_x}{MS\mathrm{d}t} \qquad (4)$$

where V is the volume of base or acid (L), and $\mathrm{d}C_x$ is the concentration increase of x ion (g/L) in the corresponding compartment in dt time interval (s).

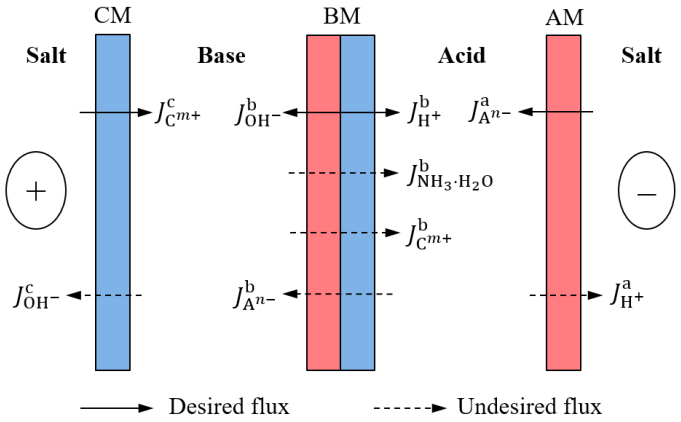

Figure 4-2. Desired and undesired fluxes in each repeating unit of BMED.

Table 4-3. Desired and undesired fluxes in the BMED model.

Flux	J_x^y	Meaning
Electro-migration (desired)	$J^{b}_{OH^-}$	Flux of OH^- produced by the BM
	$J^{b}_{H^+}$	Flux of H^+ produced by the BM
	$J^{c}_{C^{m+}}$	Flux of cations from the salt compartment to the base compartment
	$J^{a}_{A^{n-}}$	Flux of anions from the salt compartment to the acid compartment
Diffusion (undesired)	$J^{b}_{NH_3\cdot H_2O}$	Flux of $NH_3{\cdot}H_2O$ from the base compartment to the acid compartment
	$J^{b}_{C^{m+}}$	Flux of the cations from the base compartment to the acid compartment
	$J^{b}_{A^{n-}}$	Flux of the anions from the acid compartment to the base compartment
	$J^{c}_{OH^-}$	Flux of OH^- from the base compartment to the salt compartment
	$J^{a}_{H^+}$	Flux of H^+ from the acid compartment to the salt compartment

Note: J_x^y is the moles of x ions passing through y membrane per square meter per second (mol/m^2·s). y = a, b, or c, denoting AM, BM or CM, respectively. C^{m+} denotes NH_4^+, Na^+ or other cations, and A^{n-} denotes Cl^-, SO_4^{2-} or other anions.

As water is dissociated into H^+ and OH^- in BM, i.e. $J^{b}_{H^+} = J^{b}_{OH^-}$, the balance of other ions can be expressed as:

$$\sum mJ^{b}_{C^{m+}} = \sum nJ^{b}_{A^{n-}} \qquad (5)$$

where C^{m+} and A^{n-} denote cations and anions, respectively (except for H^+ and OH^-), and *m* and *n* are electrochemical valences.

As illustrated in Figure 4-2, the undesired fluxes (i.e. $J^{b}_{C^{m+}}$ and $J^{b}_{A^{n-}}$) can contribute to a positive current in BM. The flux balance in the cation layer of BM and AM are described in Equation (3). Hence, the following equations can be derived:

$$J^{b}_{H^+} + \sum mJ^{b}_{C^{m+}} + \sum nJ^{b}_{A^{n-}} = \frac{I}{FS} \qquad (6)$$

$$J^{a}_{H^+} + \sum nJ^{a}_{A^{n-}} = \frac{I}{FS} \qquad (7)$$

In the acid compartment, H_3PO_4 and VFAs were not ionized due to the low pH. Based on Equation (5) and (6), the flux balance in BM can be expressed as follows:

$$J^{b}_{H^+} + 2\left(J^{b}_{Cl^-} + 2J^{b}_{SO_4{}^{2-}}\right) = \frac{I}{FS} \qquad (8)$$

Since the phosphate in the salt compartment was mainly in the form of $H_2PO_4^-$ (as pH was 5.0), the flux balance in AM was calculated with Equation (7):

$$J^{a}_{H^+} + J^{a}_{Cl^-} + 2J^{a}_{SO_4{}^{2-}} + J^{a}_{H_2PO_4{}^-} + J^{a}_{VFAs^-} = \frac{I}{FS} \qquad (9)$$

Except for the flux of H^+, all other fluxes of ions can be calculated directly based on Equation (4). However, the flux of H^+ can be quantified according to Equation (8) and (9). The accuracy of the proposed BMED model can be examined based on the deviation between the measured and the simulated concentration of H^+ in the acid compartment.

The released flux of H^+ from BM ($J^{b}_{H^+}$) is:

$$J^{b}_{H^+} = \frac{I}{FS} - 2\left(J^{b}_{Cl^-} + 2J^{b}_{SO_4{}^{2-}}\right) \qquad (10)$$

The diffusion of H^+ from the acid compartment to the salt compartment ($J^{a}_{H^+}$) causes the undesired loss of the H^+, which can be calculated by:

$$J^{a}_{H^+} = \frac{I}{FS} - J^{a}_{Cl^-} - 2J^{a}_{SO_4{}^{2-}} - J^{a}_{H_2PO_4{}^-} - J^{a}_{VFAs^-} \quad (11)$$

Hence, the concentration of protons released from BM is:

$$C^{b}_{H^+} = \frac{1}{V}\int_0^t J^{b}_{H^+} nS\mathrm{d}t = \frac{1}{V}\int_0^t \left(\frac{I}{FS} - 2J^{b}_{Cl^-} - 4J^{b}_{SO_4{}^{2-}}\right) nS\mathrm{d}t \quad (12)$$

and the concentration of protons diffused from the acid compartment to the salt compartment is as follows:

$$C^{a}_{H^+} = \frac{1}{V}\int_0^t J^{a}_{H^+} nS\mathrm{d}t = \frac{1}{V}\int_0^t \left(\frac{I}{FS} - J^{a}_{Cl^-} - 2J^{a}_{SO_4{}^{2-}} - J^{a}_{H_2PO_4{}^-} - J^{a}_{VFAs^-}\right) nS\mathrm{d}t \quad (13)$$

The H^+ concentration in the acid compartment can be governed by $J^{b}_{H^+}$ and $J^{a}_{H^+}$. Meanwhile, the interferences from the diffusion of $NH_3{\cdot}H_2O$ from the base compartment ($J^{b}_{NH_3\cdot H_2O}$) and the presence of weak acids in the acid compartment cannot be neglected, as they can consume a significant amount of H^+. Hence, the theoretical concentration of H^+ in the acid compartment can be expressed as:

$$C^{A}_{H^+} = C^{b}_{H^+} - C^{a}_{H^+} - C^{Consumed}_{H^+} \quad (14)$$

where $C^{b}_{H^+}$ and $C^{a}_{H^+}$ are calculated based on Equations (12) and (13), respectively, and $C^{Consumed}_{H^+}$ is equal to the total concentration of NH_4^+, H_3PO_4 and VFAs in the acid compartment.

4.3 Results and discussion

4.3.1 pH variations in each compartment

In a BMED process, the base and acid solutions are formed when water is dissociated in BM at the presence of the electric field, releasing OH^- and H^+ to the adjacent compartments. During this process, NH_4^+ in the base compartment is converted into $NH_3{\cdot}H_2O$, while PO_4^{3-} and VFAs in the acid compartment are converted into their acid forms, i.e. phosphoric acid (H_3PO_4) and VFAs, respectively. The variations of pH in each compartment when treating synthetic hydrolysate are shown in Figure 4-3. The fact that pH in the salt compartment decreased marginally in this experiment

demonstrated the unbalanced migration of H^+ and OH^- in the salt compartment. The pH in the base compartment increased notably at the commencement of the BMED operation, with concomitant release of OH^- from the BM to the base compartment. However, pH started to decrease after 3.5 h probably due to the undesired diffusion and neutralization (Figure 4-2). Coincidently, the pH in the acid compartment decreased in the first 3.5 h, followed by its slight increase. The generation of base and acid solutions provided the ideal conditions for free ammonia ($NH_3 \cdot H_2O$, calculated as NH_3) recovery via subsequent air-stripping and regeneration of membranes using acid [226], while the losses of OH^- and H^+ in the base and acid compartments, as described above, adversely affected the process efficiencies.

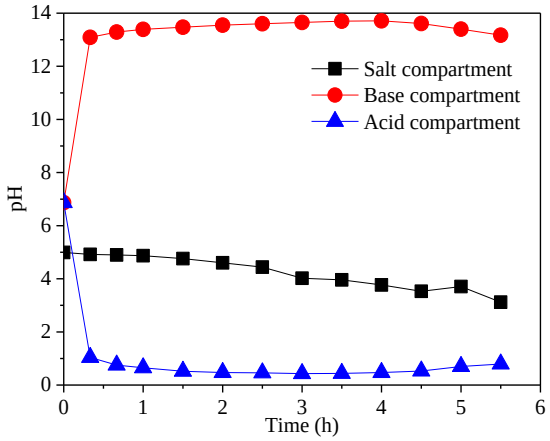

Figure 4-3. Variations of pH in the salt, base and acid compartments.

4.3.2 Variations of ions in the salt compartment

Variations of ions in the salt compartment of the BMED system are shown in Figure 4-4, when treating synthetic pig manure hydrolysate. A constant ion flux in the membrane stack was expected due to the constant current density applied. It was found that particular ions (e.g., NH_4^+, Cl^- and SO_4^{2-}) migrated faster than the others. Considerable decrease (greater than 90%) of these ions in the salt compartment was observed in the first 3.5 h. This result is consistent with the findings of other studies where a linear decrease of ions in the salt compartment was observed during the initial stage of BMED [154, 226, 227, 244]. In contrast, PO_4^{3-} and acetate (expressed as the sum of two species, CH_3COO^- and CH_3COOH, if not defined elsewhere) migrated at a much slower rate during this period. Upon the depletion of NH_4^+, Cl^- and SO_4^{2-} in the salt compartment after 3.5 h, PO_4^{3-} and acetate began to migrate considerably and their concentrations

reached 0 and 206 mg/L at 5.5 h, respectively. Other VFAs ions (i.e. propionate, iso-butyrate, butyrate, iso-valerate and valerate) exhibited a similar declining pattern as that of acetate (Figure 4-5). This study confirmed a two-stage phenomenon derived from the BMED process, being (1) the migrations of NH_4^+, Cl^- and SO_4^{2-} in the first 3.5 h, and (2) the migrations of PO_4^{3-} and acetate initiated after 3.5 h. Independently on the initial concentrations of ions, this phenomenon can be attributed to the different permselectivities of membrane towards anions depending on the Stokes radii, hydrophilicities, and ionic polarities [225]. Similar results were also obtained at 1/1 and 1/10 of concentrated ratios, i.e. the volume ratio between the salt solution and base or acid (Figure 4-6).

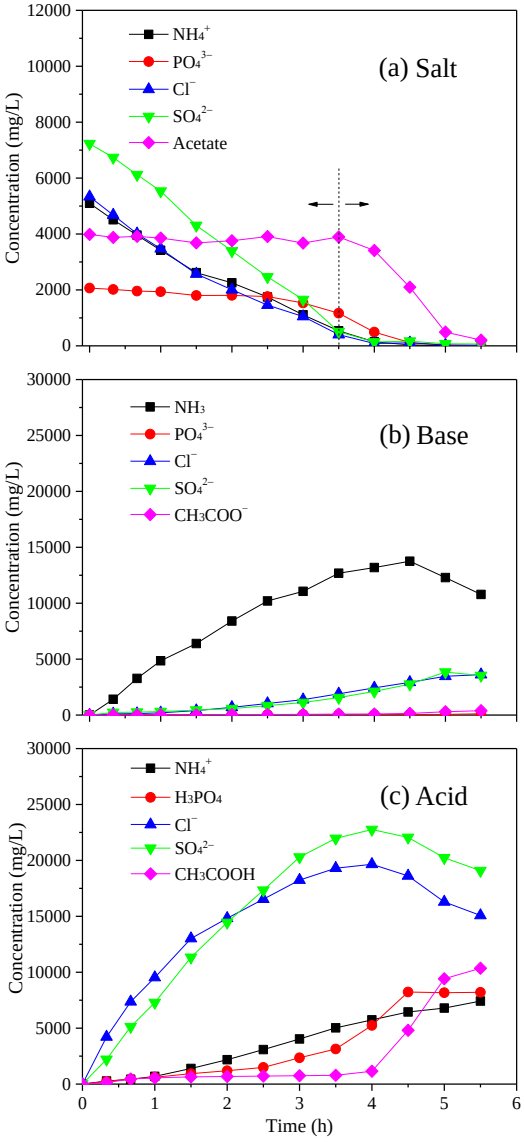

Figure 4-4. Variations of ions in the (a) salt, (b) base and (c) acid compartments.

Note: Propionate, iso-butyrate, butyrate, iso-valerate and valerate are not shown in this figure as they exhibited a similar declining pattern as that of acetate.

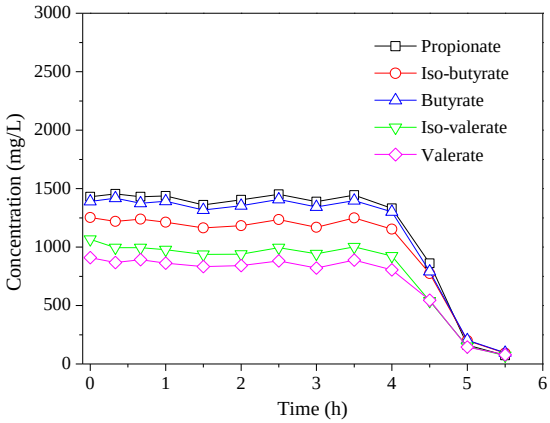

Figure 4-5. Variations of other VFAs in the salt compartment when treating 5 L synthetic pig manure hydrolysate.

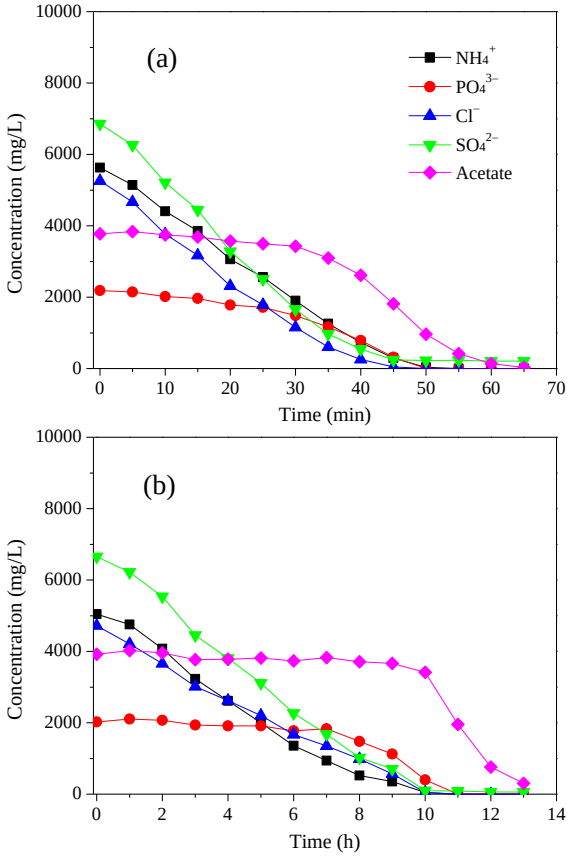

Figure 4-6. Variations of ions in the salt compartment when treating (a) 1 L and (b) 10 L synthetic pig manure hydrolysate.

Note: The volume of solutions in the base and acid compartments were both 1 L.

4.3.3 Variations of ions in the base and acid compartments

Along with the decrease of ions in the salt compartment, the concentrations of ions in the base and acid compartments increased as shown in Figure 4-4b and c. All of the ions in the base and acid compartments were derived from the salt compartment. Notably, NH_3 concentration peaked at 13757 mg/L in the base compartment, which is feasible for air-stripping recovery or using in other applications [245, 246]. It was further demonstrated in this study that using a small aeration pump and an air diffuser, 91% of NH_3 was stripped out from the base solution within 5 h. Corresponding with the decrease of Cl^-, SO_4^{2-}, PO_4^{3-} and CH_3COO^- in the salt compartment, their concentrations increased in two stages in the acid compartment as mentioned previously.

The increment of ion concentrations was nearly stable during the initial stage of the experiment due to the constant current density applied (Figure 4-7). Inevitably, anions can migrate to the adjacent base compartment and $NH_3 \cdot H_2O$ can also diffuse freely to the acid compartment through BM, namely undesired fluxes [243]. A higher concentration of ions in solutions can result in higher undesired fluxes. For example, Cl^-, SO_4^{2-} and CH_3COO^- were all detected in the base compartment and their concentrations peaked at 3614, 3842, and 388 mg/L, respectively (Figure 4-4b). Up to 7423 mg/L of NH_4^+ were detected in the acid compartment (Figure 4-4c), accounting for 48.28% of the total NH_4^+ in the feed. Indeed, the undesired fluxes accounted for the low recovery efficiency of NH_4^+, despite some NH_3 lost via evaporation in the base compartment. This is in accordance with the findings from other studies [73, 226, 246].

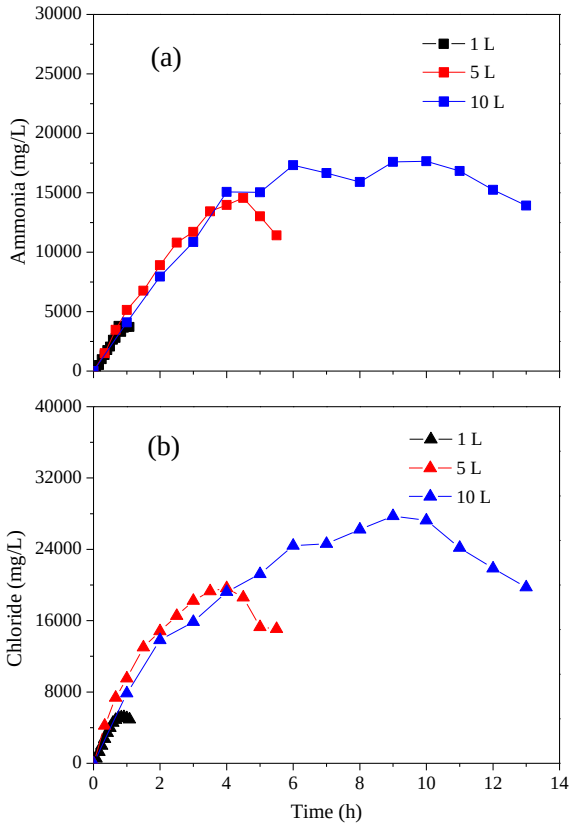

Figure 4-7. Variations of (a) NH_4^+ in the base and (b) Cl^- in the products when treating 1 L, 5 L and 10 L synthetic hydrolysate.

Note: The volume of the base and acid solutions were both 1 L.

4.3.4 Voltage, current and current efficiencies

The variations of voltage and current in the BMED are illustrated in Figure 4-8a. The voltage applied to the BMED varied due to the variation of the electric resistance of the membrane stack at a constant current of 3 A. At the commencement of the experiment, distilled water was fed to the base and acid compartments, resulting in a relatively high voltage due to the high resistance of the membrane stack, as the resistance can be governed by the compartment with the lowest concentration of ions. The voltage remained stable at 20 V and increased to 60 V after 3.5 h. The initiation of the "inflection point" was attributed to the depletion of strong acidic ions (i.e. Cl^- and SO_4^{2-} in the salt compartment). As the dominant ions in the salt compartment at the inflection point were weak acidic ions (i.e. PO_4^{3-} and VFAs anions), which have low conductivity and require higher driven force, an increase in voltage was observed. Li et al. also

reported this similar phenomenon [226]. Accordingly, the current decreased to less than 1.5 A after 5.0 h, as the voltage of the DC power supply was limited to 60 V.

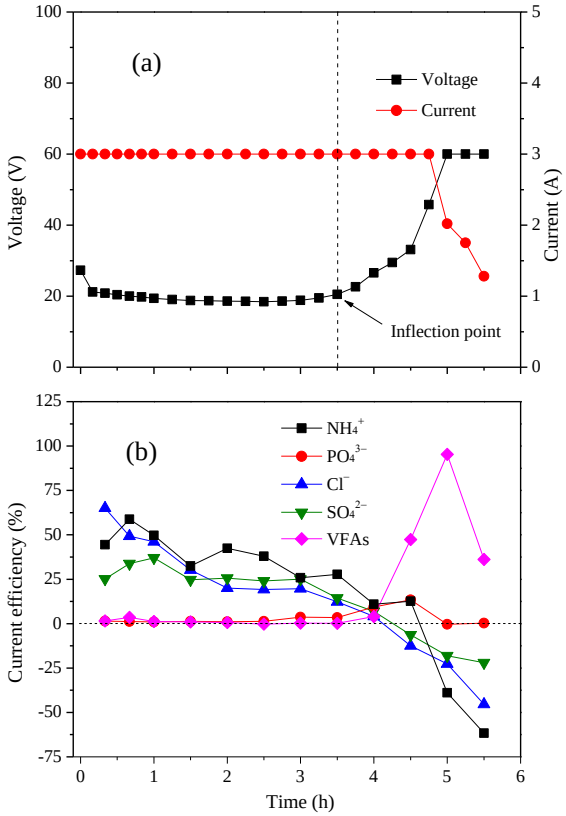

Figure 4-8. Variations of (a) voltage and current and (b) current efficiencies in BMED.

According to Equation (1), the energy consumption during this BMED experiment in Experiment I was calculated as 0.40 kWh (i.e. 1.44×10^6 J), of which 52% was used in the first stage. The average energy consumption was 0.08 kWh/L of hydrolysate treated. Current efficiency of each ion, calculated using Equation (2), is shown in Figure 4-8b. As described above, the concentration of ions in the base and acid compartments were very low during the initial stage, but they increased progressively over the course of the experiment. It is anticipated that high concentrations of ions can lead to high undesired flux, resulting in a low current efficiency. Thus, a linear decrease of current efficiencies can be therefore observed in the BMED system [244]. In this study, positive current efficiencies of NH_4^+, Cl^- and SO_4^{2-} were observed, but slightly decreasing trends before the voltage inflection point were recorded. After reaching the inflection point, current efficiencies of NH_4^+, Cl^- and SO_4^{2-} became negative because of their undesired diffusions, while the current efficiencies of PO_4^{3-} and VFAs were positive. This was

attributed to the depletion of NH_4^+, Cl^- and SO_4^{2-} and migration of weak acids in this period.

4.3.5 BMED modelling

The flux balance of H^+ in the BMED system is shown in Figure 4-9 and Table 4-4 based on Equation (14). The modelling results revealed a significant release of H^+ from BM (C_{H+}^{b}) in the experiment. Consequently, a large amount of H^+ was lost via diffusion from the acid compartment to the salt compartment (C_{H+}^{a}) and the formation of $NH_3{\cdot}H_2O$, H_3PO_4 and VFAs ($C_{H+}^{Consumed}$). By deducting these losses, the calculated concentration of H^+ well matched the detected concentration of H^+, suggesting the proposed BMED model can be used to profile the flux balance in the membrane stack. According to the model, the concentration of H^+ in the acid compartment increased rapidly at the initial stage, but it decreased after the inflection point.

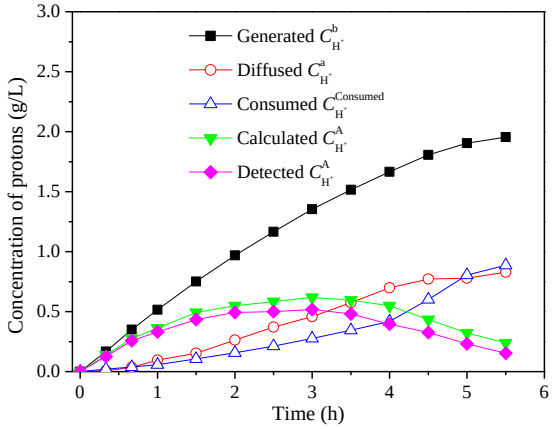

Figure 4-9. Proton flux balance calculated based on the proposed BMED model.

Table 4-4. Calculation results of the BMED model.

t(h)	*I* (A)	*I/FS* (mol/m^2·s)	$C_{H^+}^{b}$ (mol/L)	$C_{H^+}^{a}$ (mol/L)	$C_{H^+}^{Combine}$ (mol/L)	Calculated $C_{H^+}^{A}$ (mol/L)	Detected $C_{H^+}^{A}$' (mol/L)	$C_{H^+}^{A}$'/$C_{H^+}^{A}$ (%)	$C_{H^+}^{A}/C_{H^+}^{b}$ (%)
0	3.00	0	0	0	0	0	0	-	-
0.33	3.00	0.001645	0.17	0.01	0.02	0.14	0.13	92.86	76.47
0.67	3.00	0.001645	0.35	0.04	0.04	0.28	0.26	92.86	74.29
1.00	3.00	0.001645	0.52	0.10	0.06	0.36	0.33	91.67	63.46
1.50	3.00	0.001645	0.75	0.15	0.11	0.49	0.43	87.75	57.33
2.00	3.00	0.001645	0.97	0.26	0.16	0.55	0.49	89.09	50.52
2.50	3.00	0.001645	1.17	0.37	0.21	0.58	0.50	86.21	42.73
3.00	3.00	0.001645	1.35	0.46	0.28	0.62	0.52	83.87	38.51
3.50	3.00	0.001645	1.52	0.58	0.34	0.60	0.48	80.00	31.58
4.00	3.00	0.001645	1.67	0.70	0.42	0.55	0.40	72.73	23.95
4.50	3.00	0.001645	1.81	0.77	0.60	0.43	0.33	76.74	18.23
5.00	2.78	0.001524	1.90	0.78	0.80	0.32	0.23	71.87	12.11
5.50	1.65	0.000905	1.95	0.83	0.89	0.24	0.15	62.50	7.69

However, there was a marginal difference between the simulated and measured H^+, which was reflected by the decrease of $C_{H^+}^{A\prime}/C_{H^+}^{A}$ from 92.86% to 62.50% during BMED. It might be attributed to the unaccounted diffusion of cations from the acid compartment to the salt compartment (J_{Cm+}^{a}, not marked in Figure 4-2). Indeed, the overall cation flux from the salt compartment to the base compartment (J_{Cm+}^{c}) was calculated only based on the concentration decrease of cations in the salt compartment, while it should be equal to the value of $J_{Cm+}^{c\prime} - J_{Cm+}^{a}$, where $J_{Cm+}^{c\prime}$ is the real cation flux from the salt compartment to the base compartment. However, it is very difficult to detect and quantify J_{Cm+}^{a}. The decrease of $C_{H^+}^{A\prime}/C_{H^+}^{A}$ indicated that J_{Cm+}^{a} became more and more intense during BMED. The low salinity of the feed solution at the end of BMED caused a high diffusion of cations from the acid compartment to the salt compartment. Therefore, the BMED model has a better simulation in the early period of BMED than that in the late period. In addition, there was a diffusion of H^+ from the acid compartment to the electrolyte, which can also cause the inaccuracy of BMED modelling.

4.3.6 Two-stage BMED operation and products

To separate H_3PO_4 and VFAs from strong acids and improve the purity of the products, a two-stage operation of the BMED system was conducted in Experiment II based on the results obtained from Experiment I. As shown in Figure 4-10, the variations of ions in the base and acid compartments were identical to those illustrated in Figure 4-4 during the conventional one-stage operation prior to the inflection point. The acid and base solutions were replaced with deionized water at the inflection point. Thus, two base and acid solutions were generated, namely Base I and Acid I at 3.5 h, and Base II and Acid II at 6.0 h.

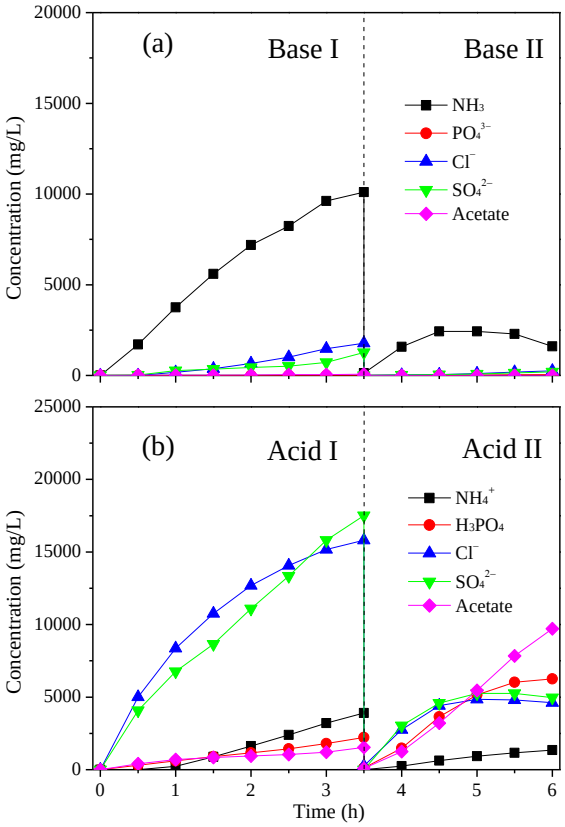

Figure 4-10. Two-stage separation of the (a) base and (b) acid solution.

Note: Propionate, iso-butyrate, butyrate, iso-valerate and valerate are not shown in this figure as they exhibited a similar declining pattern as that of acetate.

Higher impurities of Cl^- and SO_4^{2-} were observed in Base I, while Cl^- and SO_4^{2-} were almost depleted in Base II (Fig 4-10a). By replacing the Acid I with deionized water in the second stage, much lower concentrations of Cl^- and SO_4^{2-} were observed in Acid II. Consequently, this resulted in low diffusion fluxes of ions from the acid compartment to the base compartment, thereby improving the purities of products (Figure 4-10b). The diffusion of NH_3 through BM to the acid compartment was inevitable. Nevertheless, through the two-stage operation, the lost NH_4^+ in the acid compartment can be minimized to a greater extent. As the concentration of NH_3 did not peak at 3.5 h, additional 2,500 mg/L of NH_4^+ in Base II can be potentially recovered (Figure 4-4a). Given this consideration, a supplementary experiment was performed to replace the base solution with deionized water at 4.25 h, and a higher NH_3 recovery rate up to 78% was achieved in Base I (Figure 4-11).

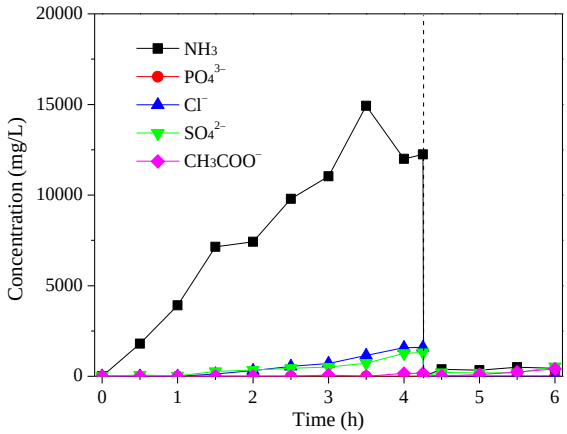

Figure 4-11. Variations of ions in the base compartment with two-stage operation (separation occurred at 4.25 h).

Strong acidic ions (i.e. Cl^- and SO_4^{2-} dominated in Acid I and their concentrations were up to 15,805 mg/L and 17,551 mg/L, respectively. It is noteworthy that it is inefficient to separate Cl^- from SO_4^{2-} using non-selective membranes, despite their different electro-migration rates. The initial electro-migration rates for Cl^- and SO_4^{2-} were calculated as 5.65 mol/min and 1.70 mol/min, respectively, decreasing gradually towards the end of the experiment. Even with monovalent selective membranes, the separation efficiency between Cl^- from SO_4^{2-} remained lower than 60% [247]. In contrast, PO_4^{3-} and VFAs dominated in Acid II, demonstrating a successful two-stage operation of the BMED system. Although 20% of the Cl^- and SO_4^{2-} migrated and remained in Acid II (Figure 4-10b), the enriched PO_4^{3-} concentration and its purity were much higher than that reported by Zhang et al. [154] using a selective membrane.

The ion distribution in the products from the one- and two-stage operation of BMED systems is shown in Figure 4-12. During the one-stage BMED operation (Experiment I), only 52% of NH_4^+ migrated to the base compartment. In contrast, during the two-stage BMED operation (Experiment II), 61% of the NH_4^+ migrated to the base compartment forming Base I. The recovery rate of NH_4^+ was further optimized up to 78% when the solution replacement time was postponed to 4.25 h in this study. Indeed, the two-stage operation minimized the diffusion loss of NH_4^+ in Stage II and generated a base solution more effectively for NH_3 air-stripping. The acid solution generated from the one-stage BMED operation exhibited a mixture of strong and weak acidic ions, while this acid was separated into Acid I rich in Cl^- and SO_4^{2-}, and Acid II rich in PO_4^{3-}

and VFAs. Acid I and II can be regarded as the spilt solutions of the acid in Experiment I.

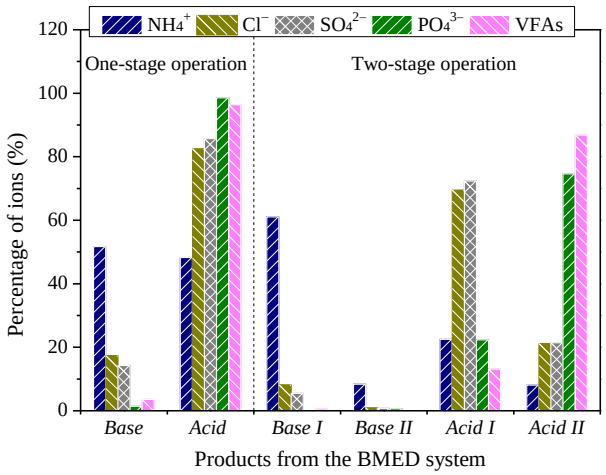

Figure 4-12. Ions distribution in the products from the BMED system.
Note: The percentage of NH_3 in Base I increased to 78% if the replacing time was 4.25 h.

As to the acid production, a trade-off between higher recovery concentrations and higher purities of the products need to be considered. In this study, higher recovery concentrations of PO_4^{3-} and VFAs were achieved in the acid solution derived from Experiment I, while the purities of PO_4^{3-} and VFAs were much higher in Acid II than those in the acid solution from Experiment I. Nevertheless, Acid I exhibited a higher potential on the perspective of applying the strong acids (i.e. HCl and H_2SO_4) for membrane cleaning due to a higher concentration of H^+ remaining in the solutions.

4.3.7 Treatment of real pig manure hydrolysate

To assess the feasibility of two-stage operation of the BMED system in resource recovery, real pig manure hydrolysate was pretreated and fed to the BMED system. A low pH of 5.0 promoted the separation efficiency of VFAs, as they were mostly presented in their acid forms (zero-charged) in acidic conditions. This reduced their migration rates during the first stage before 30 minutes (Figure 4-13). In addition, the pretreatment facilitated the release of P from the solid to the liquid fraction, resulting in more than 90% of P in the liquid fraction. In this study, after the pH adjustment to 5.0, the concentration of PO_4^{3-} in pig manure hydrolysate increased dramatically from 187 mg/L to 1773 mg/L.

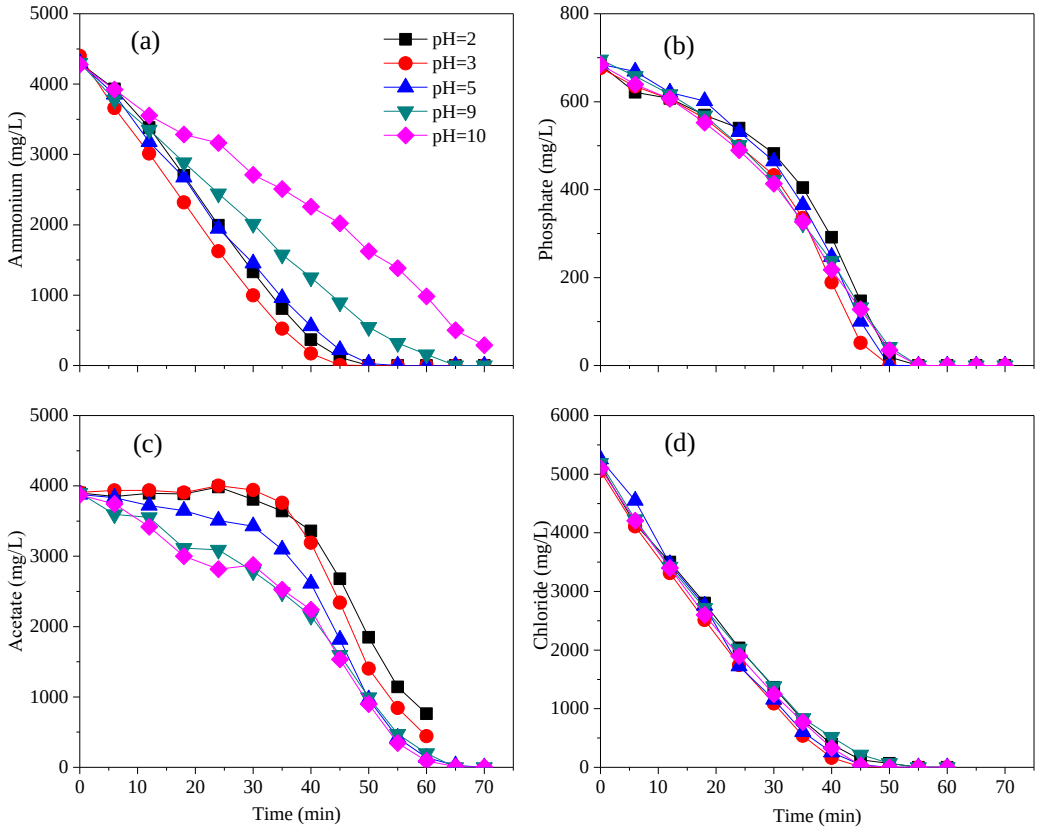

Figure 4-13. Variations of (a) NH_4^+, (b) PO_4^{3-}, (c) acetate and (d) Cl^- when treating 1 L synthetic pig manure hydrolysate under different pH values.

The variations of ions in the salt compartment when treating real pig manure hydrolysate are shown in Figure 4-14. The concentrations of NH_4^+ and Cl^- decreased rapidly, whereas the concentrations of PO_4^{3-} and acetate remained unchanged during the initial stage. The profile of ions in the salt compartment during BMED operation was similar to that when using synthetic hydrolysate, indicating the potential application of the two-stage operation. The two-stage separation of real pig manure hydrolysate is presented in Figure 4-15. Further attention needs to be paid to tackle membrane fouling, which may occur after a long-term operation [20, 222]. It is noteworthy that potassium (K), magnesium (Mg), calcium (Ca) and carbonate co-exist in the real pig manure hydrolysate [2, 93, 94, 248]. These ions can migrate under the same electrical field, consuming an insignificant proportion of electrical energy in this study. Nevertheless, these ions had no major impact on the purity of products generated in the BMED system. It was observed that Mg and Ca co-precipitated in the base solution, and carbonate was converted to CO_2 during the acidification of pig manure at the pH of 5.0.

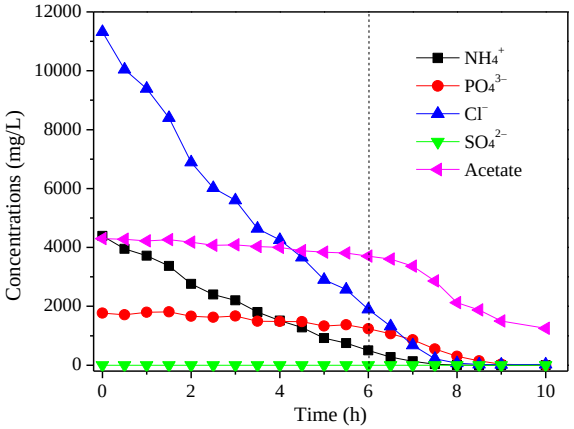

Figure 4-14. Variations of ions in real pig manure hydrolysate in the salt compartment of the BMED system.

Note: The inflection point of voltage was at 6.0 h.

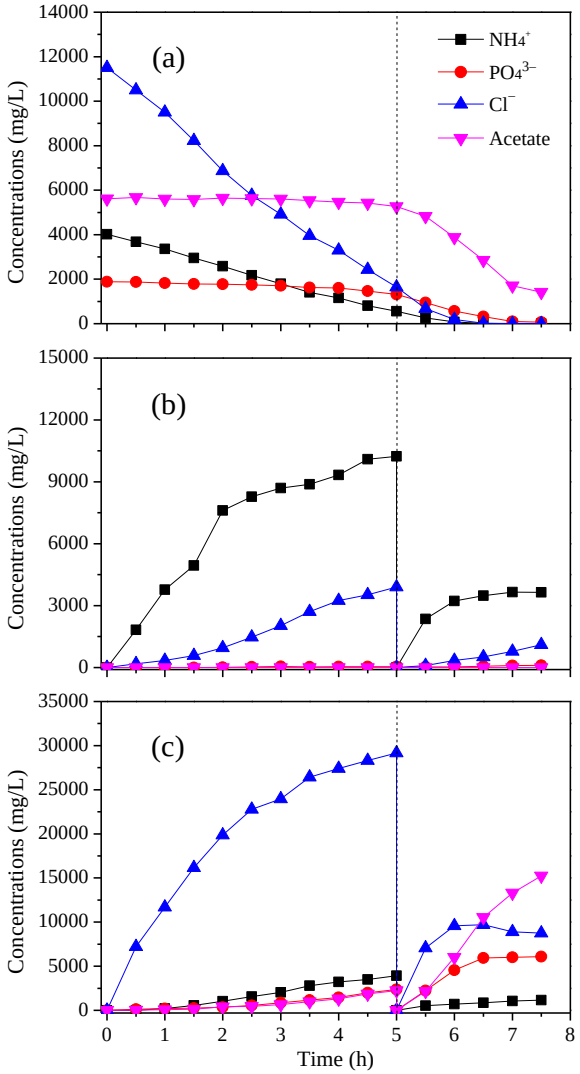

Figure 4-15. Variation of ions in the (a) salt, (b) base and (c) acid compartment when treating real pig manure hydrolysate using two-stage BMED.

After the two-stage BMED operation, Base I was further processed with air stripping to recover NH_3 and Acid I was reused *in situ* to acidify the raw pig manure. In addition, the separation of P from Acid II should be considered due to aforementioned global P depletion. P can be harvested via mixing Acid II with the remaining solution of Base I and Base II after stripping of NH_3, which can provide sufficient Mg^{2+} (in the form of MgOH) for struvite formation as shown in SEM and EDX analysis (Figure 4-16). Alternatively, the low pH in Acid II would offer the potential to separate phosphoric acid and VFAs via certain evaporation process, such as azeotropic distillation and MD [150, 249]. Based on this concept, a holistic technical process focusing on resources recovery from pig manure hydrolysate using two-stage BMED is proposed and illustrated in Figure 4-17.

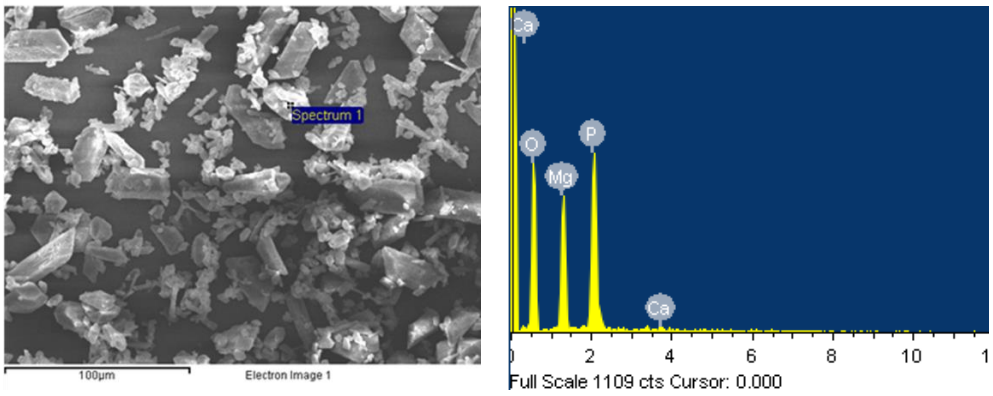

Figure 4-16. Scanning electron microscope image of phosphorus precipitate formed in the product and corresponding spectrum scanned by energy dispersive X-ray detector (EDX).

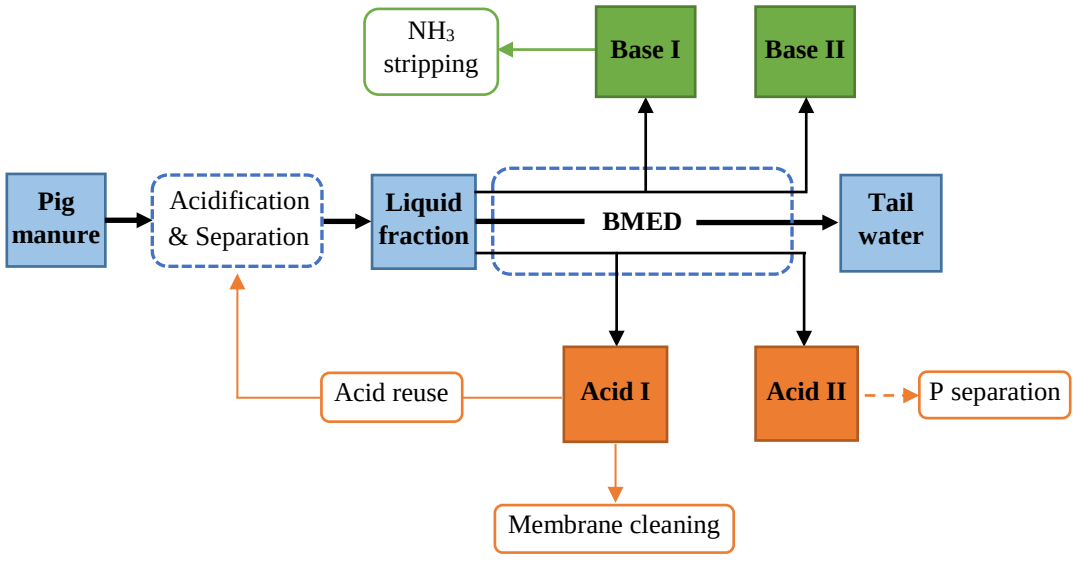

Figure 4-17. Schematic flow chart of two-stage BMED process.

4.4 Summary

The application of BMED system to recover valuable resources from pig manure hydrolysate was systematically assessed and demonstrated in this study. The proof-of-concept BMED system treating pig manure hydrolysate could simultaneously extract NH_4^+, PO_4^{3-} and VFAs to the base and acid compartments. Through a proposed BMED model, ion flux balance in the BMED membrane stack was successfully simulated, revealing that the undesired fluxes of ions contributed to low current efficiencies and the H^+ loss in the acid compartment. The undesired fluxes can be effectively minimized via a novel two-stage BMED operation, through which the recovery yield of NH_4^+ increased from 52% to 78%, and most of the PO_4^{3-} and VFAs were concentrated into Acid II. This study suggested that the two-stage BMED system is applicable to the nutrients and VFAs recovery from pig manure hydrolysate.

From the results in Chapter 3 and 4, it was found that both EDR and BMED can be used to recover nutrients from pig manure, while they have different applications. EDR is suitable for the treatment of pig manure containing high concentrations of SS, Ca^{2+}, and Mg^{2+}, while BMED requires a cleaner feed solution and a more frequent membrane cleaning than EDR. Efficient solid-liquid separation is necessary prior to BMED process. However, apart from the migration of nutrients, antibiotics can be potentially transported to and concentrated in the product solution in either EDR or BMED process. In the next chapter, we investigated the sorption and migration of antibiotics in ED technologies, so as to provide information on the fate of antibiotics during the development of the nutrient recovery process.

Chapter 5

Antibiotics in the process of nutrient recovery from pig manure using electrodialysis reversal: sorption and migration influenced by membrane fouling

Chapter 5

5.1 Introduction

Animal manure is the primary reservoir of veterinary antibiotics. Since the administered antibiotics are poorly absorbed in animal guts, the majority of the dose is excreted unchanged to the animal manure via urine and faeces [26]. SAs and TCs are two typical groups of antibiotics widely used in pig farming. High concentrations of SAs and TCs are present either in the fresh or digested pig manure, since these two compounds can persist for a long time in anaerobic digesters. Nutrient recovery from pig manure is a promising alternative to manure land-spreading. Most recently, it has been reported that the application of struvite recovered from wastewater induced the enrichment of antibiotics and antibiotic resistant genes (ARGs) in soil [29]. This indicates the antibiotics in animal manure can be potentially transported to the product in a nutrient recovery process. EDR is able to recover N and P from pig manure (either in the form of digestate or hydrolysate). In this process, the antibiotics in the feed solution may be transported and concentrated to the product solution. If the concentrating of antibiotics occurs, the recovered fertilizers will become much riskier for land application. The migration and concentrating of antibiotics in EDR should be examined for the safe use of fertilizers.

This chapter established an EDR process for nutrient recovery from pig manure with SD and TC spiked, two representative compounds of SAs and TCs, respectively. Raw pig manure without complete digestion (being stored in the manure tank for several weeks) was selected as the feeding material for EDR. A conventional ED process without electrode reversal was set up as the control group. The overall objectives of this study were: (i) to investigate the variation of SD and TC during the nutrient recovery process in EDR; (ii) to study the mechanism of sorption and migration of SD and TC in EDR; and (iii) to explore the influence of membrane fouling on the sorption and migration of SD and TC.

5.2 Materials and methods

5.2.1 Experimental materials

In this chapter, both synthetic wastewater and the liquid fraction of pig manure were used as the feed solution of ED and EDR. The synthetic wastewater was used to investigate the sorption and migration of antibiotics in the absence of particles, which was prepared with ultrapure water using (in g/L): ammonium chloride 8.02, ammonium acetate 5.39, monopotassium phosphate 2.99, and propionic acid 4.00, to mimic the liquid fraction of pig manure. In addition, 200 mg/L of HA (prepared using sodium humate) and BSA were added to the synthetic wastewater as the dissolved organic foulants for membranes. The pH value of the synthetic wastewater was adjusted to 5.5 using 1 M NaOH prior to use. Raw pig manure was collected from a settling tank beneath pig houses in a local farm in Co. Carlow, Ireland. The pig manure had been stored in the tank for several weeks before the collection. The liquid fraction of pig manure was obtained after a pre-treatment procedure consisting of (i) acidification to pH=5.5 to release P to the liquid phase; (ii) flocculation using 10 mg/L cationic polymer (Polygold®, Abbeywater, Ireland); and (iii) centrifugation at 1500 g for one minute to remove coarse particles. The separated liquid fraction of pig manure contained (in mg/L): NH_4^+-N 2897 ± 305, PO_4^{3-}-P 158 ± 19, Cl^- 7696 ± 119, DM 8.88 ± 0.07, and SS 1.20 ± 0.05. SD and TC standards were purchased from Sigma-Aldrich, and their physiochemical characteristics are outlined in Table 5-1, according to previous reports [250, 251]. The dosage of SD and TC in the feed solution varied from 0.05 to 5 mg/L depending on the experimental design. Heterogeneous CM and AM were purchased from MemBrain, Czech Republic, containing sulphon R-SO_3^- and quaternary ammonium R-$(CH_3)_3N^+$ as their ion-exchange functional groups, respectively. The membranes were soaked in distilled water for 48 h of free swell prior to use.

Table 5-1. Physiochemical characteristics of sulfadiazine and tetracycline.

Property	Sulfadiazine	Tetracycline
Formula	$C_{10}H_{10}N_4O_2S$	$C_{22}H_{24}N_2O_8$
Molecular weight (g/mol)	250.05	444.44
Solubility (mg/L, 25°C)	77	231
pK_{a1}, pK_{a2}, pK_{a3}	2.5, 6.5, -	3.3, 7.7, 9.7
LogK_{ow}	-0.1	-2.2 ~ -1.3
Hydrogen acceptors	2	9
Hydrogen donors	6	6
Structure	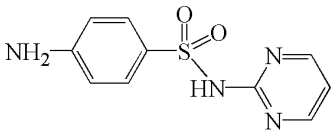	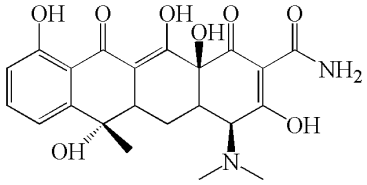

5.2.2 Electrodialysis reversal set-up

The ED and EDR membrane stack had an identical configuration, both had one membrane stack containing 5 repeating membrane units, and each unit was composed of one CM and one AM, as shown in Figure 5-1. The membranes were isolated by 0.9 mm thick polypropylene spacers to form the dilute and concentrate compartments. One pair of 3 mm thick titanium electrodes coated by iridium were used as the electrodes. The active working area of membranes and electrodes was 200 cm^2 (20 cm × 10 cm). During the experiment, the dilute compartment was fed with 5 L synthetic wastewater or the liquid fraction of pig manure as the feed solution, while the concentrate compartment was fed with 1 L ultrapure water as the product solution. The anode and cathode compartments were both fed with 0.1 M Na_2SO_4 solution as electrolytes. The solution in each compartment was circulated by peristaltic pumps at a flow speed of 300 mL/min. A DC power supply (Rigol, DP832) provided a maximum output voltage of 60 V and a maximum output current of 3 A to the membrane stack during the experiment. The experiment was conducted until the current decreased to less than 2.0

A, which indicated a very low conductivity of the feed solution at the end of the experiment. In the EDR process, the polarities of electrodes were reversed and the feed solution and product solution were swapped in every 15 mins, namely self-cleaning in this context, so as to remit the membrane fouling formed. The operational procedure of self-cleaning was as same as that in Chapter 3 [252].

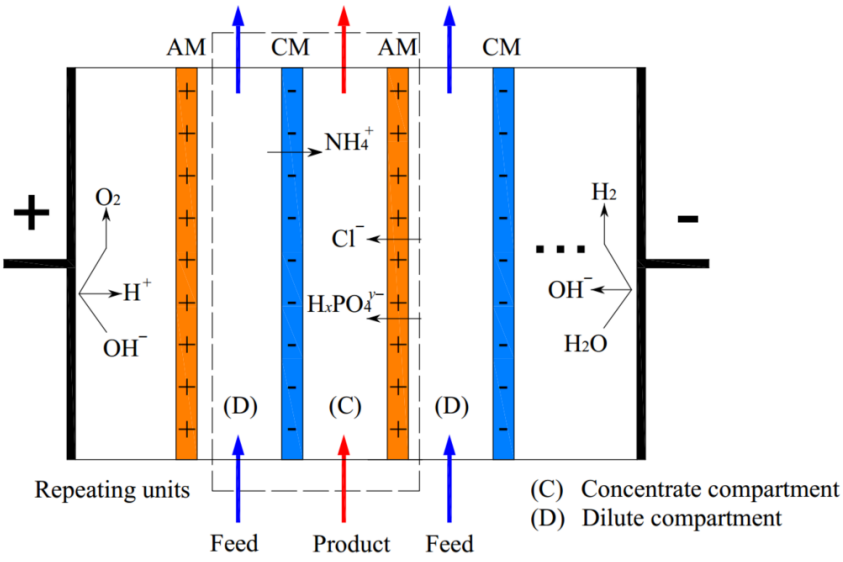

Figure 5-1. Schematic configuration of EDR membrane stack.

5.2.3 Experimental design

This study involved two experiments, i.e. experiment I and II. Experiment I was to investigate the migration of antibiotics in the ED and EDR processes using synthetic wastewater. After the ED and EDR processes were completed for nutrients removal, a cleaning protocol was applied to the membrane stack to assess the antibiotics cleaned off the membranes. The cleaning protocol contained three steps as follows: (i) 2 mins of water cleaning using 1 L of ultrapure water; (ii) 15 mins of acid cleaning using 1 L of 0.1 M HCl solution; and (iii) 15 mins of base cleaning using 1 L of 0.1 M NaOH solution. Two additional groups were set as control. Control group (i) was to investigate the sorption of antibiotics in the absence of the electric field. The raw and 1/10 diluted synthetic wastewater, as well as ultrapure water, all were spiked with 5 mg/L SD and TC, and used as the feed solutions to mimic the different stages of ED and EDR since the salinity of feed solutions decreased gradually over time during ED and EDR. The product solutions in the concentrate compartments were identical as the feed solutions

but did not contain SD and TC. Control group (ii) was to investigate the sorption capacity of membranes in different pH conditions. The virgin membranes were cut into small pieces (10 cm^2 for each), and placed in conical flasks with 100 mL SD and TC solutions added (5 mg/L). The conical flasks were shaken in 220 rpm for 5 hours, during which the pH value in each flask was maintained stable using 0.1 M NaOH or HCl solutions.

Experiment II was to investigate the fate of antibiotics using real pig manure. In this experiment, 5 mg/L, 500 μg/L and 50 μg/L of SD and TC were spiked to the separated liquid fraction of pig manure to mimic the pig manure containing three different concentration levels of antibiotics. After the ED and EDR process, the membrane stack was disassembled and the particle fouling and chemical deposit on the membranes were scraped off for antibiotics determination. The SD and TC sorbed by the membranes were determined after cleaning the membranes for four times using the cleaning protocol aforementioned (to ensure most of the SD and TC were cleaned off). After treating 56 L of pig manure using EDR, the membranes before and after cleaning were cut into small pieces (10 cm2 each) for the determination of the sorption capacity, in order to explore the influence of long-term organic fouling on antibiotics sorption. The cleaned membranes were equilibrated in a 5 M NaCl solution for 2 hours before the test, to ensure that the stock ions in the cleaned membranes were identical as those in the virgin membranes.

5.2.4 Analytical methods

The voltage and current during the experiment were monitored by the DC power supply. The solution conductivity was measured using a portable conductivity meter. The concentrations of NH_4^+-N, PO_4^{3-}-P (the sum of P in the form of $H_2PO_4^-$, HPO_4^{2-}, and PO_4^{3-}), and Cl^- were determined by a Konelab ions analyser (ThemoFisher Scientific, USA). The concentration of total proteins was measured at 595 nm of wavelength using Coomassie brilliant blue as the chromogenic reagent. The concentration of HA was expressed by the absorbancy at 465 nm of wavelength. The concentrations of SD and TC in the synthetic wastewater were determined at 265 nm of UV wavelength using HPLC (Agilent 1200 HPLC). The separation of SD and TC was performed in a C18 chromatographic column (ACE 5 C18, 150 × 4.6 mm i.d.) with a mobile solution

flowing at 1.0 mL/min constantly. The mobile solution consisted of 50 mmol/L KH_2PO_4, 10% methanol, 20% acetonitrile, and 0.1% formic acid. The concentrations of SD and TC in the real wastewater and fouling deposit were determined using liquid chromatography tandem mass spectrometry (Agilent 6460 Triple Quad LC-MS). The samples were processed with a solid phase extraction (SPE) to remove the HA and salts before being injected to the LC-MS. The SPE procedure and LC-MS measuring parameters are detailed as follows:

- The pretreatment of samples before SPE had the following steps: (i) the pH of each sample was adjusted to 4.0 using acetic acid; (ii) 5 mL of each sample was collected and mixed with 1 mL EDTA-McIlvaine buffer (pH=4.0) and 5 mL methanol in 15 mL centrifuge tube; (iii) the tube was vortexed for 60 s and placed in a ultrasonic bath for 10 min of extraction; (iv) the tube was centrifuged at 15 000 rpm and the supernatant was decanted into a 300 mL beaker; (v) repeating the procedure twice and the collected supernatant was diluted to 300 mL using ultrapure water to reduce the methanol content.

- The SPE consisted of an NH_2 cartridge (Hypersep, 500mg/2.5mL) for HA removal and an HLB cartridge (Supelco, 200mg/6mL) for antibiotics extraction. The operational procedure included: (i) the cartridges were activated by 10 mL methanol and 10 mL ultrapure water containing 0.1% formic acid; (ii) the samples were percolated through the NH_2 and HLB cartridges successively, at a flow rate of 2 mL/min; (iii) the NH_2 cartridge was discarded, while the HLB cartridge was rinsed by 10 mL ultrapure water containing 0.1 % formic acid, dried in air flow for 10 min, and eluted by 10 mL methanol; and (vi) the eluent from HLB cartridge was purged using gentle N_2 steam in a 40 °C water bath till the volume was concentrated to 1 mL for LC-MS measurement.

- Quantification of antibiotics by LC-MS. Sulfamerazine and demeclocycline were used as the internal standards for the quantification of SD and TC, respectively. The separation of different antibiotics was accomplished at a flow rate of 0.2 mL/min with solvents A and B employing a linear gradient, using a C18 chromatographic column (Agilent RRHT, 50 × 2.1 mm i.d.). Solvent A was ultrapure water containing 0.1% formic acid and solvent B was acetonitrile containing 0.1% formic acid. The gradient was 10% B for the first minute, then

ramped to 100% B at 10 minutes and kept at 100% B for one minute. Then the system was equilibrated for 6 mins at 10% B. Mass spectral analysis was conducted in the positive mode using an electrospray ionization (ESI) source.

5.3 Results and discussion

5.3.1 Removal of nutrients, antibiotics, and organic foulants from synthetic wastewater

5.3.1.1 Removal of nutrients from synthetic wastewater

The removals of NH_4^+ and PO_4^{3-} in the ED and conventional EDR processes are presented in Figure 5-2. Apparently, the NH_4^+ and PO_4^{3-} in the feed solutions of ED and EDR were both removed efficiently. The concentration of NH_4^+-N in the feed solution decreased from around 2700 mg/L to 0, alongside a decrease of PO_4^{3-}-P from around 650 mg/L to 30 mg/L at the same time. The NH_4^+ and PO_4^{3-} were concentrated in the product solution. The concentrations of NH_4^+-N and PO_4^{3-}-P in the product solution of ED reached around 7856 mg/L and 1669 mg/L, respectively. It is noteworthy that EDR had a longer operation time than ED, and the concentrations of nutrients in the product solution of EDR were lower than those in the ED, which was attributed to the dilution effect caused by the self-cleaning process of EDR. In each reversal cycle of EDR, the membrane stack was processed with 3 minutes of cleaning using water, causing the volume of the feed solution to increase from 5.0 to 5.5 L in this experiment and slow removal of ions. In addition to nutrients, the other salt ions (e.g. Cl^- and Na^+) were also removed from the feed solution (data not shown), resulting in the decrease in the conductivity of the feed solution. In this experiment, the conductivity of the feed solution decreased from 30.2 to 0.1 mS/cm, while the conductivity of the product solution increased from 0 to 83.3 mS/cm.

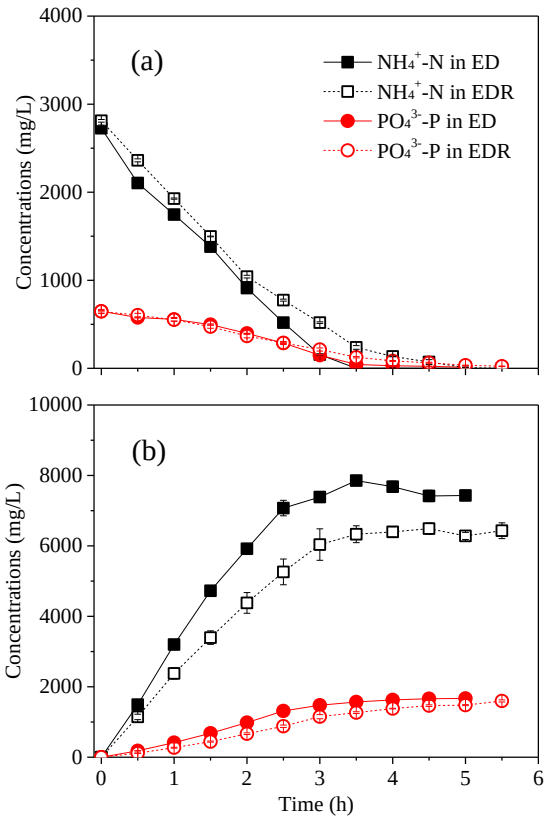

Figure 5-2. Variation of NH_4^+-N and PO_4^{3-}-P in the (a) feed and (b) product solutions of ED and EDR using synthetic wastewater.

5.3.1.2 Removal of antibiotics and organic foulants from synthetic wastewater

Figure 5-3a shows the variation of SD and TC in the feed solutions during nutrient recovery from synthetic wastewater. In the control group (i.e. ED process), the SD and TC in the feed solution decreased by around 90%, but their decrease rates were slower than those of NH_4^+ and PO_4^{3-} (the variation of nutrients in the feed solution is shown in Figure 5-2). Their slow decrease rates might be due to the large molecular weight and stokes radii of SD and TC. It is noteworthy that SD and TC were relative stable in the initial 2 hours but then decreased fast to the end. The initial concentration plateaus of SD and TC showed that the main process at the beginning of ED was the migration of nutrients and other salts but not antibiotics. In the EDR process, the decrease of SD and TC in the feed solution were similar to those in ED. However, SD and TC were completely removed from both the feed solutions of ED and EDR. At the end of ED and EDR experiments, the salts in the feed solutions were almost totally removed, leading to the low conductivities of the feed solutions and low current densities in the

membrane stack. This caused the slow decrease rates of SD and TC at the end of the experiments.

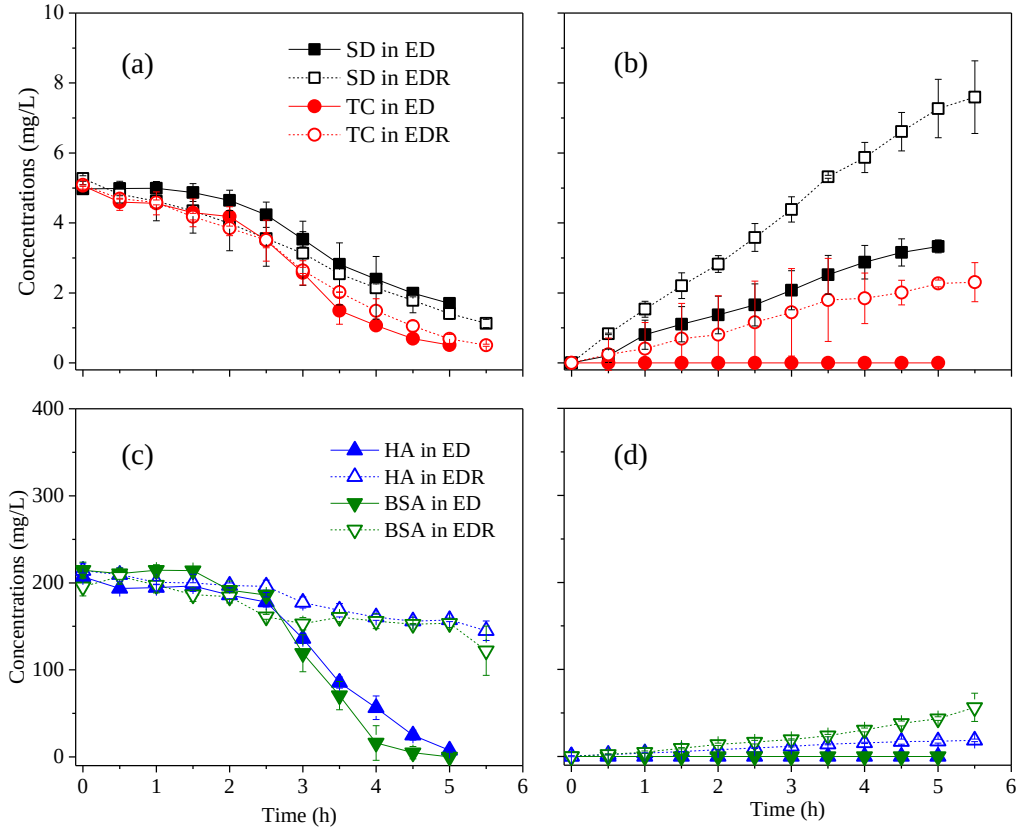

Figure 5-3. Variation of antibiotics in the (a) feed and (b) product solutions, as well as dissolved organic foulants in the (c) feed and (d) product solutions using synthetic wastewater.

The variation of SD and TC in the feed solution was almost identical, but there was a difference between them in the product solution, as shown in Figure 5-3b. In the ED process, there was no TC detected in the product solution, indicating that TC could not pass through the membranes. It is inferred that the removed TC from the feed solution should be retained by the membranes. Around 3 mg/L SD was detected in the product solution of ED. This was probably attributed to the smaller molecular size of SD compared with TC. The ionization of SD and TC in the liquid phase might also impact their migration under the electric field, which will be discussed later in this chapter. In the EDR process, 2.3 mg/L of TC was detected in the product solution. This was attributed to the reversal operation in EDR, which released TC from the membranes to the product solution in each reversal cycle. The concentration of SD in the product solution of EDR reached 7.6 mg/L, which was higher than that in the ED process,

proving that the reversal operation of EDR caused a higher transport of SD to the product solution.

The HA and BSA in the feed solution showed different decrease patterns (Figure 5-3c and 3d). In the ED process, the HA and BSA in the feed solution decreased sharply to 0 after 2.5 h. This was coincidental with the high voltage (Figure 5-4) and low salt concentration in the late stage of ED. However, there was no HA and BSA detected in the product solution of ED, indicating that the HA and BSA remained in or on the membranes rather than passed through the membranes, which was similar to the migration of TC aforementioned. In the EDR process, the concentrations of HA and BSA in the feed solution only decreased by around 34%, and a small amount of HA and BSA was observed in the product solution. The reversal operation of EDR caused most of the HA and BSA remaining in the feed solution and a small proportion of them released to the product solution. Similar to SD and TC, a proportion of HA and BSA were also retained by the membranes in EDR.

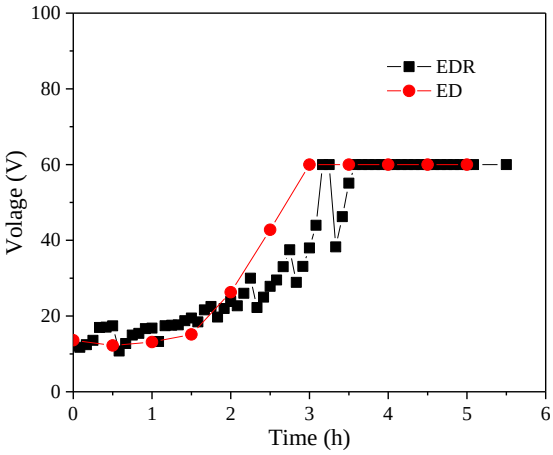

Figure 5-4. Variation of voltage during ED and EDR.

5.3.1.3 Antibiotics and organic foulants retained by the membranes

After the ED and EDR processes, the SD and TC retained by the membranes were cleaned off using the proposed cleaning protocol, as shown in Figure 5-5a. The ultrapure water can clean the molecules weakly bonded on the membrane surface, while the acid and base solutions can clean the molecules strongly bonded in the membranes (for example via ion-exchange). In both ED and EDR, a very low amount of SD was cleaned from the membranes by water, while the amounts of SD cleaned by the acid and base solutions were much higher. Hence, most of the SD retained by the membrane

was strongly bonded in the membranes. By contrast, a higher concentration of TC was cleaned from the membranes by water cleaning. In the ED experiment, up to 7.4 mg/L of TC was cleaned from the membranes, indicating that a high amount of TC was weakly bonded on the membrane surface. While this part of TC in EDR was lower because of the reversal operation. Figure 5-5b shows the HA and BSA cleaned from the membranes. In the ED process, a very high amount of HA and BSA (around 750 mg/L for each) was cleaned from the membranes by water, in contrast with a very small amount cleaned by the acid and base solutions. Therefore, most of the HA and BSA retained by the membranes were also weakly bonded on the membrane surface, which can be released to the water easily in the absence of the electric field. The high amounts of HA and BSA on the membrane surface was attributed to the electric force in the membrane stack, which can concentrate HA and BSA to the membrane-solution interface with high concentrations. In the EDR experiment, around 150 mg/L of HA and BSA were cleaned from the membranes by water, which were far lower than those cleaned from ED membranes. The reversal operation in EDR released most of the HA and BSA back to the feed solution.

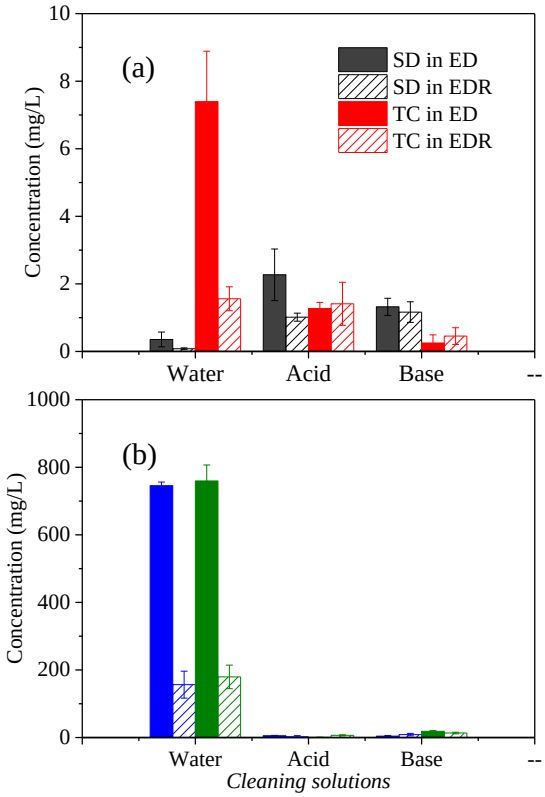

Figure 5-5. Distribution of (a) antibiotics and (b) organic foulants in the cleaning solutions.
Note: Each cleaning solution used was 1 L.

It was found that the cleaning of TC was similar to HA and BSA: they all presented high concentrations in the water cleaning solution. Hence, it is inferred that the spatial distribution of TC in ED and EDR was associated with the organic foulants. In the solution without HA and BSA, the amount of TC cleaned by water was far less. Only around 1.3 mg/L of TC was cleaned from the membranes by water (data was not shown), further indicating the association between TC and organic foulants in the feed solution. Certain molecular bonding might exist between TC and organic foulants. Different from TC, a very small amount of SD was cleaned by water, so the migration and distribution of SD were not associated with the organic foulants. The concentrations of SD and TC in the acid and base solutions were higher than those of HA and BSA, indicating that SD and TC were easier to be transported to the membrane interior than HA and BSA.

5.3.2 Mechanisms of antibiotics removal in the feed solution

5.3.2.1 Membrane sorption of antibiotics in the absence of electric field

Ion-exchange membrane can sorb organic molecules in the ED system [32-35]. In the ED and EDR processes, the nutrients and other ions in the dilute compartment were removed gradually over time, causing the decrease of solution salinity. Hence, it is necessary to investigate the sorption of SD and TC in the dilute compartment under different salinities, since the salts can affect the sorption of organic molecules on ion-exchange membranes [253, 254]. The sorption of SD and TC in the dilute compartment using raw solution (the prepared synthetic solution without dilution, high salinity), 1/10 diluted solution (low salinity), and ultrapure water were profiled in Figure 5-6. Using raw solution, low sorption amounts of SD and TC were observed. The concentrations of SD and TC in the raw solution only decreased by 0.7 and 1.0 mg/L, respectively. It proves that weak sorption of SD and TC occurred at the beginning of ED and EDR, because the deceases of SD and TC were also insignificant in this stage. The concentrations of SD and TC in the 1/10 diluted solution and ultrapure water decreased faster than those in the raw solution, indicating the membrane sorption capabilities for SD and TC were higher at the low salinity. In general, high ionic strength can weaken

the sorption of antibiotics on sorbents [250]. In this experiment, the competitive salt cations or anions reduced the active sorption sites for SD and TC on the membranes. It was found that the sorption of TC was more intensive than that of SD, which was reflected by the lower concentration of TC remaining in the feed solution. In the ultrapure water without salts added, the concentration of TC decreased to 0.75 mg/L after 5 hours of sorption, almost equal to the concentrations of TC in the feed solutions at the end of ED and EDR experiments (Figure 5-3). This indicates that the sorption of TC dominated its removal in the late period of ED and EDR rather than electric migration. This finding was consolidated by Figure 5-7, where the electric field had negligible impacts on the sorption of TC on the membranes. By contrast, the SD in the ultrapure water did not reach such a low concentration as TC by sorption. Hence, it is inferred that the sorption of SD played less than 50% of its removal in ED and EDR. The removal of SD was also caused by the electric field, which can transport the SD from the feed solution to the membrane interior and release it to the product solution subsequently. During five batches of ED operation (Figure 5-8), the SD in the product solution increased gradually, showing that SD was transported in the ion-exchange membrane very slowly. The SD in the feed solution can pass through the membrane and reach the product solution. However, the TC remained in the feed solution and no TC was detected in the product solution. At the beginning of each batch in Figure 5-8, the TC on the membranes was released back to the feed solution because of the high salinity, causing the TC desorption in the dilute compartment.

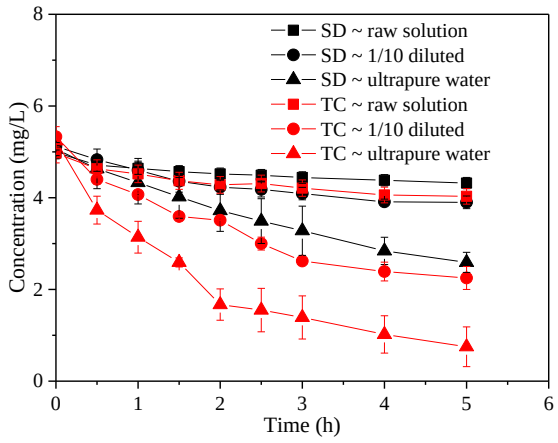

Figure 5-6. Five-hour sorption of antibiotics in the dilute compartment under different salinities. *Note: The raw solution, 1/10 diluted solution, and ultrapure water (the concentration of organic foulants in each solution was same) were used to mimic the feed solution at the beginning, the 3rd, and 5th hour of the ED and EDR processes.*

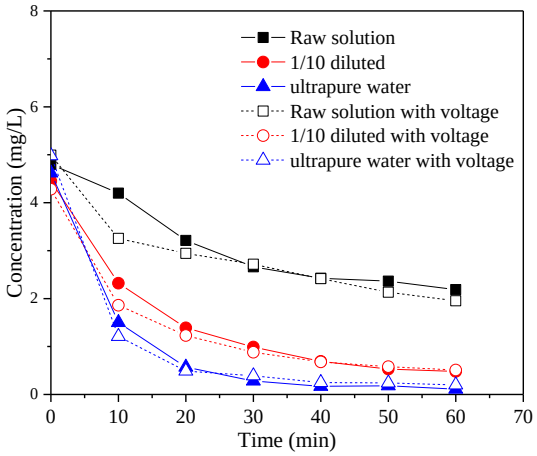

Figure 5-7. Sorption of TC in the membrane stack with and without external voltage applied.

Note: The feed solution (1 L) was circulated in both the dilute and concentrate compartment. It has been proved that TC cannot pass through the membrane in Figure 5-3. If electric migration occurred, the TC should be transported from the feed solution to the membrane surface gradually, causing a significant decrease of TC in the feed solution. However, it was observed that there was no difference in the sorption of TC with and without electric field, proving the electric migration of TC was negligible in the membrane stack. The decrease of TC in the feed solution was mainly because of the membrane sorption. This experiment cannot be made using SD, because SD can pass through the membrane gradually.

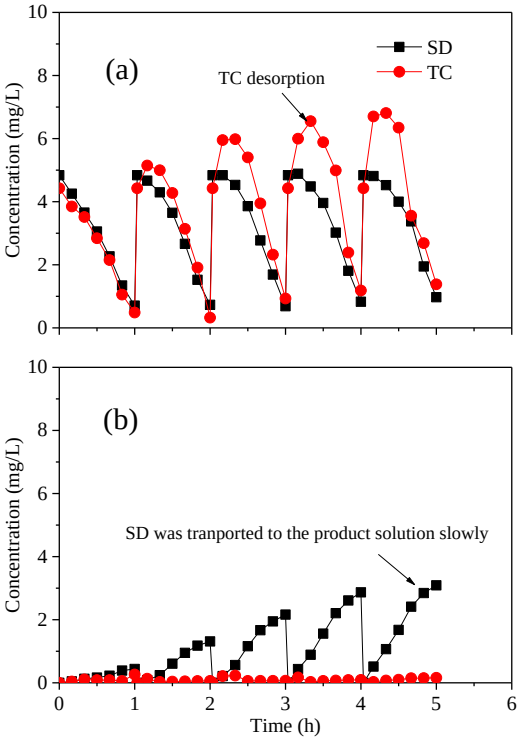

Figure 5-8. Variation of antibiotics in the (a) feed and (b) product solutions during five batches of ED using synthetic wastewater.

5.3.2.2 Sorption of antibiotics on CM and AM

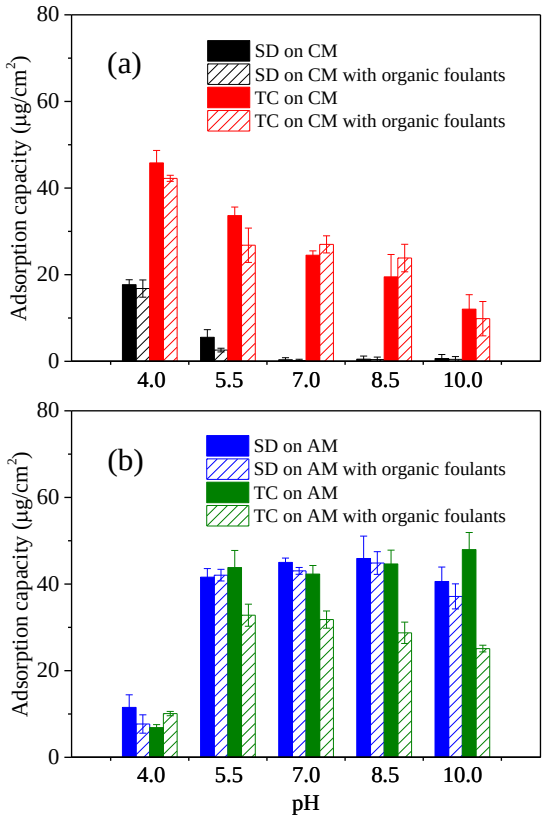

Figure 5-9. Sorption of antibiotics on virgin (a) CM and (b) AM under different pH conditions.

It is necessary to explore the sorption behaviours of antibiotics on the CM and AM separately, so as to explain the sorption mechanisms. Figure 5-9 shows the sorption capacities of SD and TC on the virgin membranes under different pH conditions. In the condition of pH = 4.0, the sorption capacities of SD and TC on the CM were far higher than those on the AM. This can be explained by the positive ionization of SD and TC at pH = 4.0 (the ionization species of SD and TC are shown in Figure 5-10), which led to an electrostatic attraction to the CM but a repulsion to the AM. The SD and TC converted to their negative forms at higher pH values, causing the increase of their sorption on the AM. TC was easier to be sorbed by the CM than SD over a wide range of pH values, while their sorption capacities on the AM were almost identical. The sorption capacity of TC on the AM became lower in the solution containing HA and BSA, indicating that organic foulants can weaken the sorption of TC by AM. Particularly in the condition of pH = 10.0, a significant decrease of the sorption capacity of TC on the AM was observed. The decrease of sorption can be explained by the decrease of active sorption sites on the membrane surface caused by HA and BSA.

However, the presence of HA and BSA did not reduce the sorption of SD on the AM significantly, indicating that organic foulants did not impact SD sorption. The SD in the feed solution can pass through the fouling zone freely and migrate into the interior of the AM, forming the mechanism of ion-exchange in AM.

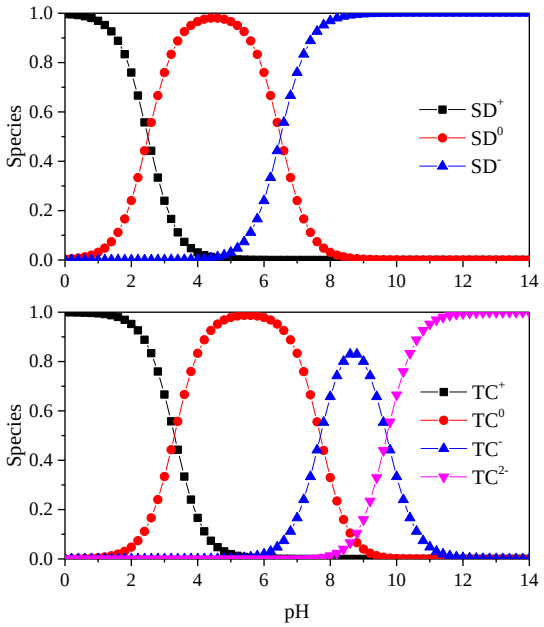

Figure 5-10. Ionization species of SD and TC in the aqueous phase.

The sorption mechanism of organic molecules is complex, which can be impacted by various molecular interactions, such as electrostatic interaction, hydrogen bonding, hydrophilicity, cation-π, and van der Waals forces [35]. Figure 5-11 shows the electrostatic interactions and possible hydrogens bonding between the antibiotics and membrane matrices in the experimental conditions (pH = 5.5). SD has two functional groups that can be ionized in the liquid phase. The R–NH_2 group can be converted to R–NH_3^+ by combining one H^+, while the R–NH group can release one H^+ and form R–N^-. In the experimental conditions, the R–NH_3^+ group existed as R–NH_2 based on the low pK_{a1} of SD, but the R–NH was converted to R–N^- according to pK_{a2}. Hence, the overall electrical charge of SD was negative, causing the electrostatic repulsion to the R–SO_3^- group in CM, but an electrostatic attraction to the R–$N(CH_3)_3^+$ group in AM. In addition, the hydrogen bonding between SD and AM can be formed, which can increase the chance of SD sorption on the AM. The existence of ionization equilibrium constants of TC, i.e. pK_{a1}, pK_{a2}, and pK_{a3}, were based on the ionization of three different functional groups. Different from SD, TC performed as a zwitterion in the experimental conditions because of these functional groups. It is hypothesized that the hydrogen

bonding played vital roles on TC sorption because the overall electrostatic attraction between zwitterions and membranes were weak. On the CM, the hydrogen bonding could take place between the functional groups of TC and the R–S=O group of membrane, while on the AM, it could take place between the R–C=O group of TC and the R–CH_3 group of membrane. In this circumstance, TC can be sorbed via weak molecular interactions rather than electrostatic attraction because of the zwitterionic properties [34]. Overall, the pH could influence the ionization and molecular interactions between the antibiotics and membranes, causing the differences in antibiotics removal. However, the removal of antibiotics in ED was not impacted by pH too much. As shown in Figure 5-12, the SD and TC in the feed solutions were both removed with high efficiencies over a wide pH range. It was noticed that a small amount of TC passed the membrane to the product solution when the pH was 3.0. However, since the pH value of the feed solution is in the range of 5.5 – 8.5 in practice, the sorption of TC on the AM can be maintained at a high level.

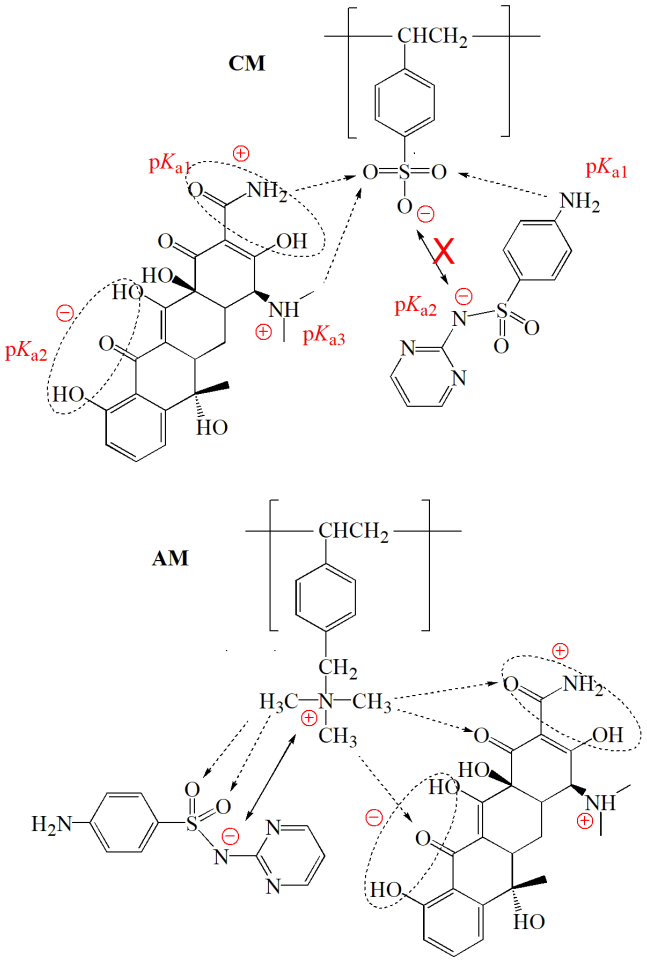

Figure 5-11. Electrostatic interactions and possible hydrogen bondings between the antibiotics and membrane matrices in the experimental conditions.

Note: The solid arrow denotes electrostatic attraction and the dash arrow denotes hydrogen bonding. Hydroxyl groups can be either the hydrogen donors or accepters but are not marked in this figure. If the ions are positively or negatively charged, electrostatic interactions occur on and inside the membranes via ion-exchange. If the ions are zwitterionic, electrostatic interactions are weak, and the molecular bonding only occurs on membrane surfaces since the ions cannot migrate into the membranes.

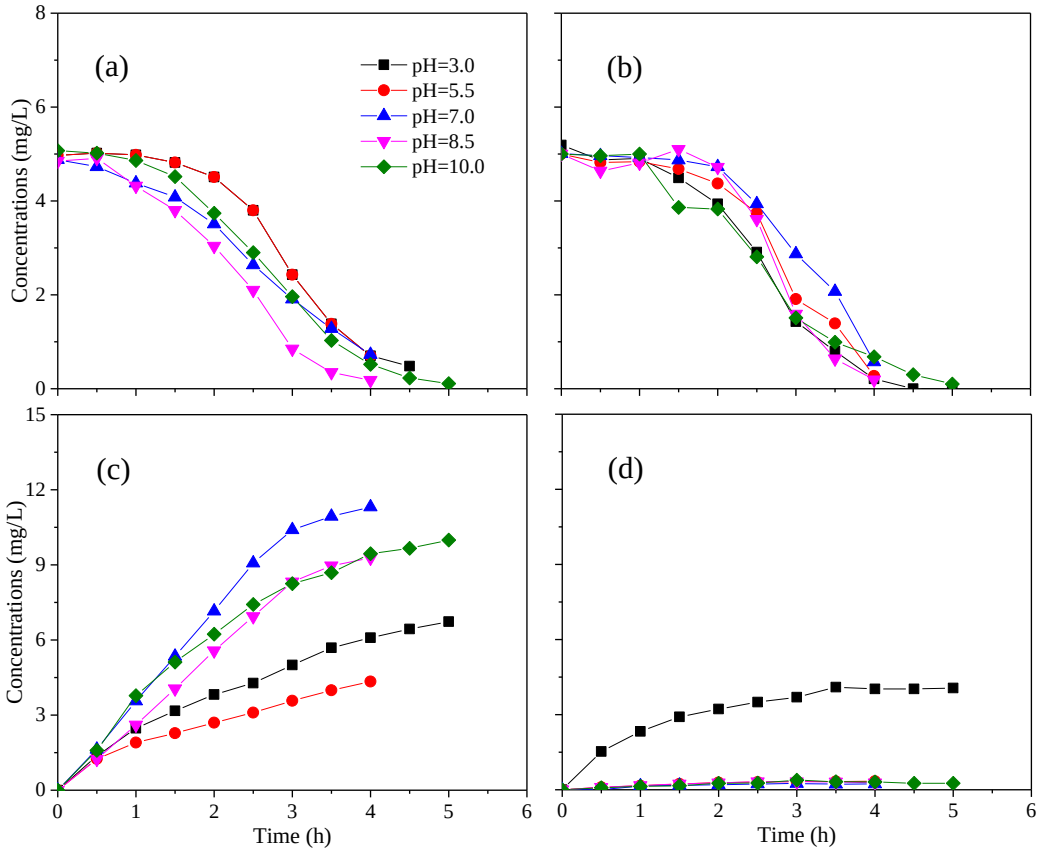

Figure 5-12. Removal of SD and TC under different pH values in the ED process. (a) SD in the feed solution; (b) TC in the feed solution; (c) SD in the product solution; and (d) TC in the product solution.

5.3.3 Removal of SD and TC from pig manure

Figure 5-13 shows the distribution of SD and TC after the ED and EDR processes for nutrient recovery from real pig manure. It was found that around 51% of the SD and 36% of the TC remained in the feed solution of EDR, which were higher than their corresponding amounts remaining in the feed solution using synthetic wastewater (Figure 5-3). The sorption and migration of SD and TC in pig manure can be hindered

by various factors, because the composition of pig manure was much more complex than that of synthetic wastewater. In pig manure, the SD and TC can be sorbed by the suspended particles, which can cause more SD and TC remaining in the feed solution. The formed particle fouling was dense due to the compaction effect under the electric field, so it can hinder the migration of antibiotics towards membranes. It was observed that the fouling cake of ED contained 17% of TC. Also, a very high absorbancy at 465 nm was observed in the fouling cake of ED. In the product solutions of ED, SD reached 32% of the total spiked amount, but TC was not detected in the product solution of ED. This is consistent with the finding aforementioned that TC cannot pass through the membranes. However, in EDR, TC was transported to the product solution via sorption and desorption due to the reverse operation. If the product solution is used on farmlands as fertilizer directly, additional treatment must be applied to reduce its ecological risks. The membranes sorbed antibiotics, so a large amount of antibiotics were detected in the cleaning solutions. The disposal of cleaning solutions containing antibiotics should also be taken into account. The spatial distributions of SD and TC obtained at different initial concentrations spiked (500 and 50 μg/L) were similar, as shown in Figure 5-14. Similar percentages of SD and TC still remained in the feed solution at very low spiked concentrations.

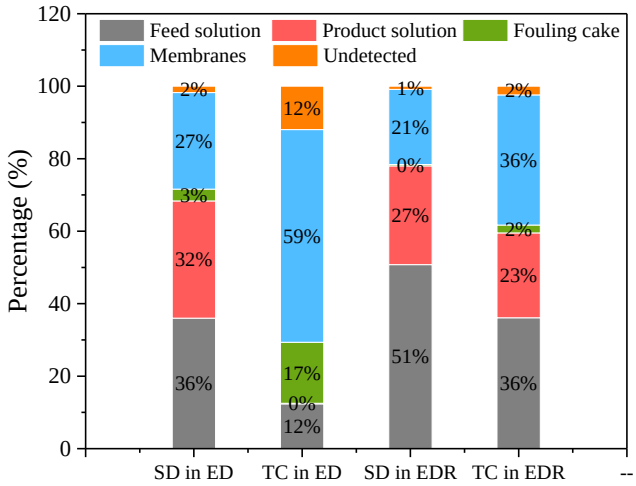

Figure 5-13. Distribution of SD and TC after the ED and EDR processes with 5 mg/L of initial concentrations spiked.

Note: There was no SD and TC detected in the chemical deposit.

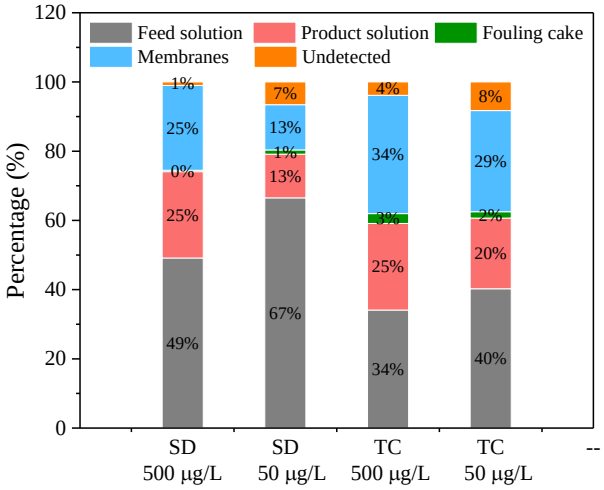

Figure 5-14. Distribution of SD and TC after the EDR process using 500 and 50 μg/L as the initial concentrations.

5.3.4 Sorption of antibiotics on the fouled membranes

As demonstrated in Chapter 3, the irreversible fouling of EDR became stable after treating 56 L pig manure. It is necessary to investigate the sorption of antibiotics after this threshold, so as to provide referential data for long-term operation. Figure 5-15 shows the sorption capacities of SD and TC on the fouled membranes before and after being cleaned by the proposed protocol twice. Comparing with Figure 5-9, it is clear that the sorption capacities of SD and TC on the fouled membranes before cleaning were far lower than those on the virgin membranes. This consolidated the findings in Figure 5-13, i.e. a large amount of SD and TC remained in the feed solutions because of the weak sorption at the end of ED and EDR. However, the sorption capabilities of membranes were mostly regenerated via membrane cleaning. In particular, the sorption of SD on the cleaned AM decreased negligibly in comparison with the virgin membranes. As demonstrated in Chapter 3, the cleaned membranes had an irreversible fouling zone around the membrane surfaces. The high sorption of SD on the cleaned membranes indicated that SD can pass through this fouling zone and migrated into the interior of membranes. The sorption of TC on the fouled CM and AM were still lower than those on the virgin membranes, proving that the cleaning procedure cannot fully regenerate the sorption of TC on the membranes. The deterioration of sorption can be attributed to the weakened molecular interaction between the antibiotics and membranes, particularly in the irreversible fouling zone around the membrane surfaces.

Nonetheless, since the irreversible fouling became stable after treating 56 L of pig manure, a relatively high sorption capability of antibiotics can be maintained if the periodical cleaning is applied. Using the cleaned membranes after treating 56 L pig manure, the removal of SD and TC in the dilute compartment showed negligible difference comparing with the experiment using virgin membranes (Figure 5-16). This indicates the sorption and migration of SD and TC in each batch of EDR during a long-term operation will be mostly identical but have a small decrease in sorption capabilities.

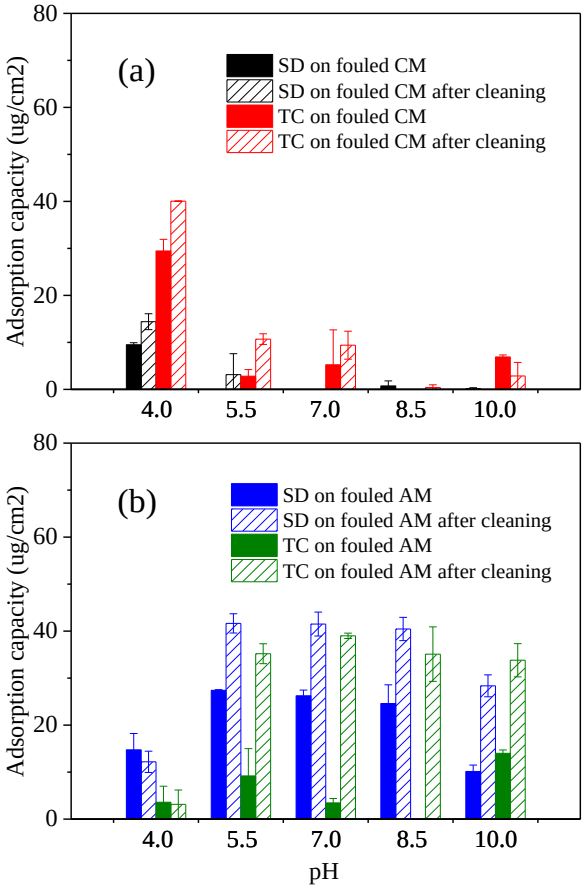

Figure 5-15. Sorption of antibiotics on the fouled (a) AM and (b) CM.

Note: The fouled membranes were collected from the EDR membrane stack after treating 56 L pig manure. The fouled membranes were cleaned by the proposed cleaning protocol twice prior to the test.

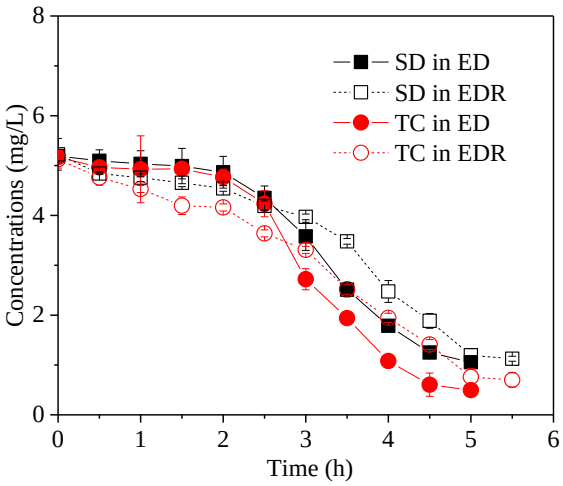

Figure 5-16. Removal of antibiotics from synthetic wastewater using the fouled membranes after cleaning.

5.3.5 Impact of fouling formation on antibiotics migration

The sorption and migration of antibiotics and their association with membrane fouling are illustrated in Figure 5-17. In the membrane stack, the application of electric field caused the directional movement of the ions, organic foulants, and colloidal particles. The particles can be enriched and aggregate on the surface of AM, forming a layer of fouling cake existing in the interface of membrane and solution. Similarly, organic foulants can be concentrated to this interface with high concentrations, forming a mixture of particle fouling and organic foulants. Because of the molecular interactions, TC sorption and migration were impacted by the organic and particle fouling in the feed solution. Therefore, in the experimental conditions, a high concentration of TC was found in the particle fouling zone. Meanwhile, a small part of TC can be sorbed by the CM due to the hydrogen bonding or other molecular interactions. A proportion of organic foulants can be sorbed by the AM, forming the irreversible organic fouling on the surface of AM. However, negatively ionized SD can pass through this fouling zone and migrate into the membrane interior till being released to the product solution on the other side of membrane. In the EDR process, because of the electrode reversal, the particle fouling can be on-line cleaned off. In this circumstance, the particles, organic foulants, and antibiotics in particle fouling and organic fouling zones can be mostly released to the self-cleaning solution, therefore being returned to the feed solution

subsequently. Only a small proportion of the organic foulants and antibiotics in the organic fouling zone can be released to the product solution.

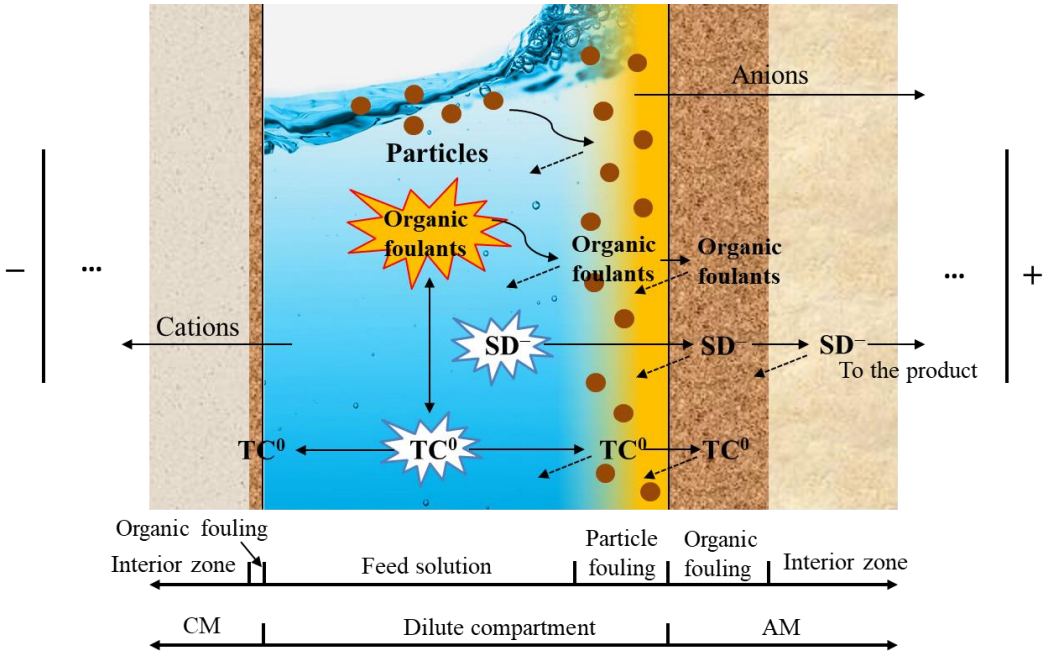

Figure 5-17. Schematics of membrane fouling and antibiotics migration in the membrane stack.

Note: Dash arrows denote the molecule movement after reversing the electrodes.

In practice, the membranes can provide enough sorption sites for antibiotics. The sorbed antibiotics can remain in the membranes during batch operations till the maximum sorption capacities are reached. A large amount of antibiotics sorbed by the membranes will be transported to the cleaning solution eventually. In this study, the product solution contained approximate 30% of the total spiked antibiotics. It means the amount of antibiotics in the recovered products will be lower than the total amount of antibiotics in the raw pig manure. Although the antibiotics can be concentrated in the product of EDR, using the recovered product solution as fertilizer can reduce the total antibiotics input to the lands than using raw pig manure. If proper post treatment for antibiotics removal from the recovered product is applied, the recovered products would be much safer for land application.

5.4 Summary

In this study, the migration of SD and TC in ED and EDR for nutrient recovery from pig manure was investigated. In the synthetic wastewater, around 90% of SD and TC can be removed from the feed solution. Membrane sorption played the primary role in their removal, while it was impacted by the salinity of feed solution. The low salinity at the end of EDR resulted in intensive sorption of antibiotics. AM can sorb both SD and TC, while CM can only sorb TC. The sorbed SD can be transported to the product through membranes, while TC was retained in the membrane-solution interface. The liquid fraction of pig manure was used as the feed solution for the practical test. The particle fouling caused a low removal efficiency of SD and TC from the feed solution. High concentration of TC was transported to the cleaning solutions, showing that particle fouling and organic foulants impacted its sorption on membranes. The fouled membranes after a long-term operation still presented a high sorption capacity almost identical to the virgin membranes. This study can provide the industry with valuable information on the sorption and migration of antibiotics during the nutrient recovery using ED/EDR technologies.

In ED technologies, antibiotics can be transported to the product solution via sorption and electric migration. Hence, further treatment is necessary to improve the biosafety of the recovered fertilizer prior to being used on lands. In the next chapter, we developed a novel method based on advanced oxidation. The hypothesis was that the antibiotics in pig manure can be oxidized and removed from the ED system.

Chapter 6

In-situ anodic oxidation for antibiotics removal, pathogen inactivation, and fouling mitigation during nutrient recovery from pig manure digestate

6.1 Introduction

In general, ED technologies are regarded as energy intensive due to their high energy consumption on the transportation of ions through membranes [255, 256]. For this reason, almost 90% of sea and saline water desalination facilities use multistage flash distillation and RO rather than ED technologies [257]. In most cases, researchers and engineers only focus on the migration of ions through membranes in ED, while the anode and cathode are ignored with electrode gas generated and wasted. From the perspective of nutrient recovery, ED should be regarded as a hybrid technology being able to achieve multiple purposes. The membrane section can be used for nutrient extraction, while the anode and cathode can be regarded as a separate functional section that can be potentially utilized for other purposes.

It is hypothesized that the anode in ED technologies (including EDR and BMED) might be utilized in-situ to oxidize the antibiotics in animal manure because of the generation of anodic oxidants, such as Cl_2 and ·OH. The generated gas might also mitigate the membrane fouling via gas bubbling [45-47]. It has been reported that the anodic oxidation can inactivate the pathogens in toilet wastewater with acceptable DBPs generated [40]. If the hypothesis is correct, it would provide a possibility to reclaim the feed solution after ED for on-farm use. Therefore, in this study, we developed the in-situ utilization of anode in an ED membrane stack designed for the nutrient recovery from pig manure digestate, namely anode-ED. Although anodic oxidation can generate DBPs, such as THMs and HAAs, it is expected that the DBPs can be adsorbed by the membranes and a safer effluent can be obtained (the effluent is the feed solution after ED treatment). The objectives of this chapter were to: (i) investigate the anodic oxidation of antibiotics in the developed anode-ED; (ii) assess the fouling mitigation and pathogen inactivation in anode-ED; and (iii) assess the DBPs generated in the feed and product solutions of anode-ED.

6.2 Materials and methods

6.2.1 Experimental materials

Synthetic wastewater was used to investigate the oxidation rate of SD and TC, which was prepared using deionized ultrapure water to mimic the liquid fraction of pig manure digestate, which consisted of (in mg/L): ammonium chloride 8020, ammonium sulfate 4080, monopotassium phosphate 299, SD 5, and TC 5. In addition, different concentrations of sodium bicarbonate, sodium acetate, and HA were added into the synthetic wastewater depending on the experimental design. The pH of the synthetic wastewater was adjusted to 5.5 prior to use. Synthetic wastewater without Cl^- was tested, ammonium sulfate was used to replace ammonium chloride, while the other ingredients were not changed. Raw pig manure used in this study was as same as that used in Chapter 3. The digestate was also obtained after mesophilic AD of pig manure with an inoculum ratio of 4/1 (manure/sludge) in the laboratory. The liquid fraction of pig manure and of digestate was obtained from a solid-liquid separation process including (i) acidification to pH=5.5 for the release of P to the liquid phase; (ii) flocculation using 10 mg/L cationic polymer (Polygold®, Abbeywater, Ireland); and (iii) centrifugation at 1500 g for one minute to remove coarse particles. The separated liquid fraction was used as the feed solution of ED. Heterogeneous CM and AM used in this study were purchased from MemBrain, Czech Republic, containing sulphon R-SO_3^- and quaternary ammonium R-$(CH_3)_3N^+$ as ion-exchange functional groups, respectively. The membranes were soaked in deionized ultrapure water for at least 48 h prior to use.

6.2.2 Experimental apparatus

Two apparatuses were used in this study, i.e. single-compartment (SC) reactor and ED membrane stack. The SC reactor was designed to investigate the efficiency and mechanisms of anodic oxidation in the absence of membranes. As shown in Figure 6-1a, it only contained one pair of iridium-coated titanium electrodes with a gap of 1.8 mm between them, forming one electrode compartment in the reactor. The feed solution flowed through the reactor, and the gas generated was bubbled in the feed solution. The

ED membrane stack used in this study was as same as that used in Chapter 3. It consisted of five repeating membrane units clamped between the titanium electrodes used in the SC reactor. The membranes were isolated by 0.9 mm thick polypropylene spacers to form the dilute and concentrate compartments. The active working area of membranes and electrodes was 200 cm^2 (20 cm × 10 cm). The dilute compartment was fed with 2 L pig manure digestate as the feed solution, while the concentrate compartment was fed with 1 L deionized ultrapure water as the product solution. The anode and cathode compartments were fed with 0.1 M Na_2SO_4 solution as electrolytes. The solutions in each compartment were circulated at a constant flow rate of 300 mL/min using peristaltic pumps. A DC power supply (Rigol, DP832) provided a maximum voltage of 60 V and a constant current of 3 A (current density was 15 mA/cm^2) to the membrane stack during the experiment.

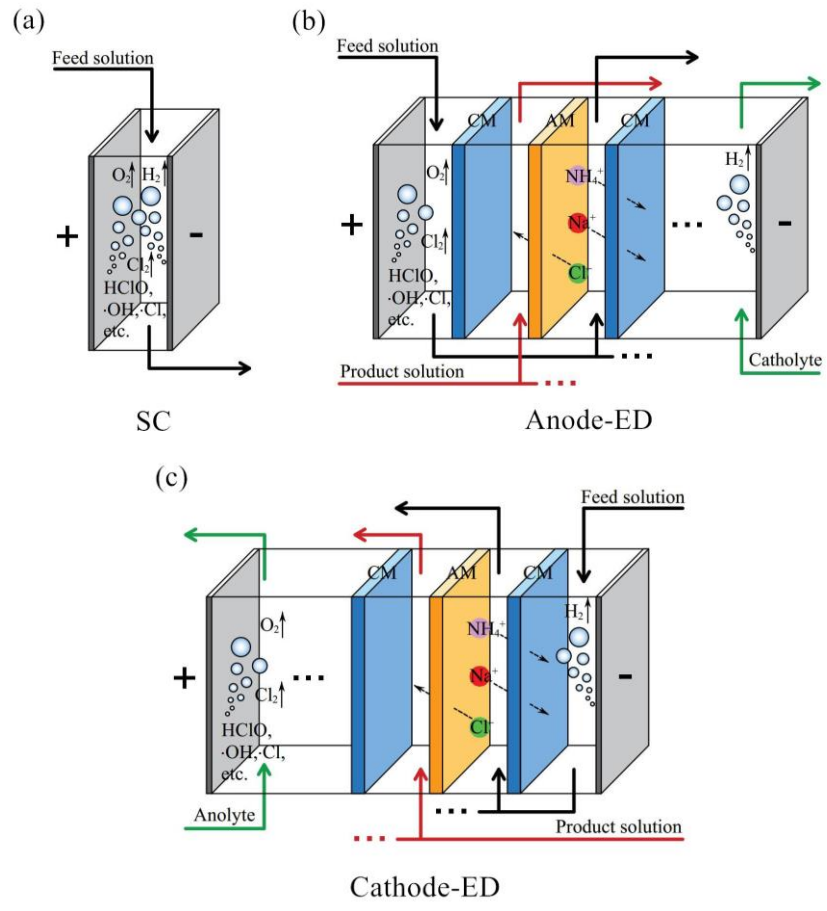

Figure 6-1. Schematic configuration of (a) the SC reactor and the ED membrane stack operated under the (b) anode-ED and (c) cathode-ED flowing modes.

In order to utilize the anode in the ED membrane stack, an anode-ED flowing mode was adopted by pumping 2 L feed solution to the anode compartment and flowing to

the dilute compartment subsequently, as shown in Figure 6-1b. In this mode, the anodic oxidation and nutrient recovery can be processed simultaneously in the ED membrane stack. The cathode compartment was fed with 0.1 M Na_2SO_4 solution, and the generated H_2 was exhausted to the fume hood. In addition, a cathode-ED flowing mode was set up as the control to investigate the mechanism of fouling mitigation. In this mode, the feed solution flowed to the cathode and dilute compartment successively, forming the cathodic gas bubbling in the feed solution. The cathodic gas was generated at the same rate as the anodic gas generated in anode-ED, because the current densities used in the two flowing modes were both 15 mA/cm^2. By comparing the formed fouling in these two flowing modes, the mitigation of membrane fouling caused by anodic oxidation and gas bubbling can be distinguished. The pH of feed solution in these two flowing modes was maintained at 5.5.

6.2.3 Experimental design

Firstly, an SC experiment was conducted to investigate the mechanism of anodic oxidation of antibiotics. Synthetic wastewater was used as the feed solution, and SD and TC were spiked as the target compounds. The oxidation of SD and TC in the feed solutions was investigated at different current intensities (1 – 15 mA/cm^2) and different concentrations of Cl^-, carbonate, acetate, and HA. In addition, tert-butyl alcohol (*t*BuOH) was used as the quencher to probe the functions of ·OH and ·Cl during oxidation [215]. Secondly, an anode-ED experiment was conducted to assess the efficiency of anodic oxidation in ED membrane stack. The liquid fraction of pig manure digestate spiked with 5 mg/L of SD and TC was used as the feed solution. Three control experiments were also operated: (i) the conventional ED without anodic or cathodic gas bubbling, (ii) cathode-ED experiment, and (iii) SC experiment. The pH of the feed solution was maintained at 5.5 during the experiment. After the experiment, the membrane stack was dissembled and the fouling cake formed on the membranes was scraped off and weighed after drying under 105 °C overnight. In order to assess pathogen inactivation, 10^4 – 10^5 of *E. coli* and *Enterococcus* were inoculated to the feed solution, to replicate an environment rich in pathogens. The samples were collected from the reactor at 0, 10, 20, 30, 60, and 120 min for the analysis of pathogens. The colonies of *E. coli* and *Enterococcus* in the samples were counted after culturing in agar

plates under 37 and 45 °C, respectively, which were expressed as colony forming unit per mL (CFU/mL) in the context.

6.2.4 Analytical method

During the experiment, the liquid samples were collected from the reactors, immediately quenched with 10 mmol/L sodium thiosulfate, and placed in the ice bath for at least 10 mins to eliminate the residual disinfectants. The concentrations of NH_4^+-N, PO_4^{3-}-P (including the form of $H_2PO_4^-$, HPO_4^{2-}, and PO_4^{3-}), and Cl^- were determined by a Konelab ions analyser (ThemoFisher Scientific). The concentrations of free chlorine and total chlorine were measured according to the N, N-diethyl-p-phenylenediamine colorimetric standard method using a spectrometer (Varian 50 scan). The concentrations of SD and TC were determined using HPLC (Agilent 1200) equipped with a UV detector scanning at 265 nm of wavelength. The separation of SD and TC was performed in a C18 chromatographic column (ACE 5 C18, 150 × 4.6 mm i.d.) at a flow rate of 1.0 mL/min. The mobile phase was composed of 50 mmol/L monopotassium phosphate, 10% methanol, 20% acetonitrile, and 0.1% formic acid. The concentration of DOM was expressed by UV_{254} determined with the wavelength of 254 nm in a spectrometer after 10-time dilution of the samples. Also, the 10-time diluted samples were analysed by fluorescence EEMs (Shimadzu, RF-6000) for the analysis of DOM composition. EEMs were obtained by measuring the fluorescence spectra over a range of 240 - 550 nm excitation wavelength and a range of 214 - 500 nm emission wavelength using 2 nm intervals.

The oxidation intermediate products were identified using HPLC tandem Q-ToF mass spectrometry (HPLC-MS/MS, Angilent 6540). The separation column was a C18 chromatographic column (ACE 3 C18-PFP, 100 × 2.1 mm i.d.). The mobile phase was composed of ultrapure water (A) and acetonitrile (B) both containing 0.1 % formic acid, and the elution gradient was as follows: 0-2 min, 95% A and 5% B; 2-10 min, B ramped to 100% with A decreased to 0%; 10-13 min, B 100%. The electromic spray ion-source was operated in a positive mode and MS/MS collosion energy was 30 eV. The MS/MS spectrum of each compound were searched in PubChem and biological databases using SIRIUS method established recently [258]. Prior to the measurement, the samples were processed with a SPE as pretreatment using an HLB cartridge (Supelco, 200 mg, 6 mL).

Breifly, 200 mL samples (pH was adjusted to 4.0) flowed through the HLB cartridges (activated using 10 mL methanol prior to use) and then eluted by 10 mL methanol for determination.

The generated DBPs, including THMs and HAAs, were quantified using gas chromatography equipped with an electron capture detector (GC-ECD, Shimadzu 2010 Plus). The separation of THMs and HAAs was performed in a DB-1 and DB-1701 capillary column, respectively. Prior to the measurement, the samples were processed with a liquid-liquid extraction using me thyl tertiary butyl ether (MTBE), based on the US EPA 551.1 and 552.2 standard methods. The detection limits for THMs and HAAs were less than 1 μg/L for each compound. The concentrations of chloral hydrate (CH) and dichloroacetonitrile (DCAN) were also obtained from the chromatogram of THMs.

6.3 Results and discussion

6.3.1 Mechanism of anodic oxidation

6.3.1.1 Anodic oxidation of nutrients and antibiotics in the SC experiment

In an anodic oxidation process, the anodic oxidation might influence the efficiency of nutrient recovery, because NH_4^+ in the digestate can be oxidized by HClO in the anode compartment, which can be expressed as:

$$Cl_2 + H_2O \leftrightarrow HClO + H^+ + Cl^- \qquad (1)$$

$$NH_4^+ + HClO \rightarrow N_2 \uparrow + 2H_2O + 6H^+ + 2Cl^- \qquad (2)$$

The variations of Cl^-, NH_4^+-N, PO_4^{3-}-P, SD, and TC in the SC experiment are shown in Figure 6-2. After 120 min of anodic oxidation (the current intensity was 15 mA/cm^2), the concentrations of Cl^- and NH_4^+-N only decreased by 326 and 293 mg/L, equal to 6.7% and 10.6% of the total Cl^- and NH_4^+-N in the feed solution, respectively. This is consistent with a previous finding that a current intensity of 15 mA/cm^2 resulted in around 200 mg/L of NH_4^+-N being removed, while significant oxidation of NH_4^+-N was only found at a current intensity up to 90 mA/cm^2 [259]. As demonstrated in Chapter 3, the Cl^- in the feed solution can be completely removed during the 120 min

of the ED process. If the anodic oxidation was integrated into ED, the Cl^- in the feed solution would be sufficient to support the anodic oxidation, since the consumption of Cl^- on anode was very slow compared with Cl^- migration. There was no decrease of PO_4^{3-}-P observed and a small proportion of NH_4^+-N consumed, indicating that the impact of anodic oxidation on nutrient recovery was negligible. It has been reported that free chlorine (i.e. HClO, and ClO^-) can react with NH_3 and form chloramines. The concentrations of free chlorine and total chlorine are shown in Figure 6-3. It showed that a huge amount of chlorine up to 142 mg/L was converted to the chloramines, while the concentration of free chlorine was relatively stable at around 4 mg/L. The pH value of the feed solution was 5.5 in this experiment. Although NH_3 was mostly converted to NH_4^+ at this pH value, a high concentration of chloramines was detected in the feed solution.

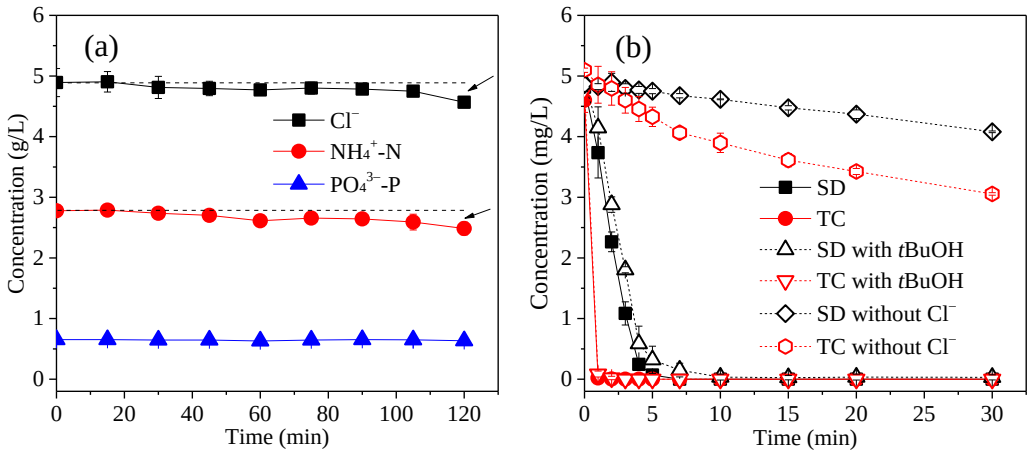

Figure 6-2. Variations of (a) Cl^-, NH_4^+-N, PO_4^{3-}-P, and (b) SD and TC in the feed solution of the SC reactor. The current density was 15 mA/cm^2.

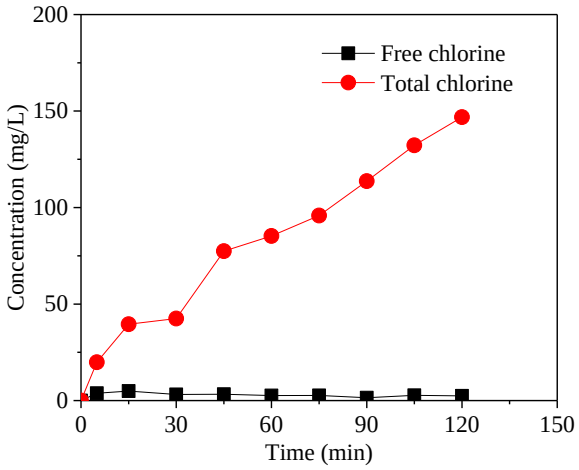

Figure 6-3. Free chlorine and total chlorine in the SC experiment. The current density was 15 mA/cm^2.

Note: The gap between total and free chlorine was chloramines.

Remarkable decreases of SD and TC were found in the feed solution, as shown in Figure 6-2b. The concentrations of SD and TC decreased by more than 90 % in the first 5 and 1 min, respectively. It proved that the oxidation of these two antibiotics was very fast compared with Cl^- and NH_4^+ oxidation, and SD was slower to be oxidized than TC. Figure 6-4 shows the oxidation of SD and TC under different current densities. The higher current intensity, the faster removal rates of SD and TC obtained. The generated Cl_2 can form many different oxidants available for oxidation, e.g. HClO, ClO^-, ·OH, ·Cl, and chloramines. In the experiments with the addition of 100 mM *t*BuOH, which has been reported to be used as an efficient quencher of ·OH and ·Cl [215], no significant impacts on the oxidation of SD and TC were observed, proving that the generation of ·OH and ·Cl was negligible in this experiment. In the experiment with synthetic wastewater not containing Cl^-, the oxidation of SD and TC was very slow, indicating that Cl^- was essential for anodic oxidation. Therefore, the chlorine generated on the anode played the primary role in the oxidation of antibiotics in the reactor; in particular, the free chlorine was considered more efficient than chloramines [260]. The existence of ·OH and ·Cl can favour the oxidation of antibiotics, because these radicals have higher oxidation activity than free chlorine [202]. The generation of ·OH and ·Cl can be achieved via the modification of electrodes or upgrading of the oxidation method (e.g. integrating UV into the anode compartment), while it was not the main focus of this study.

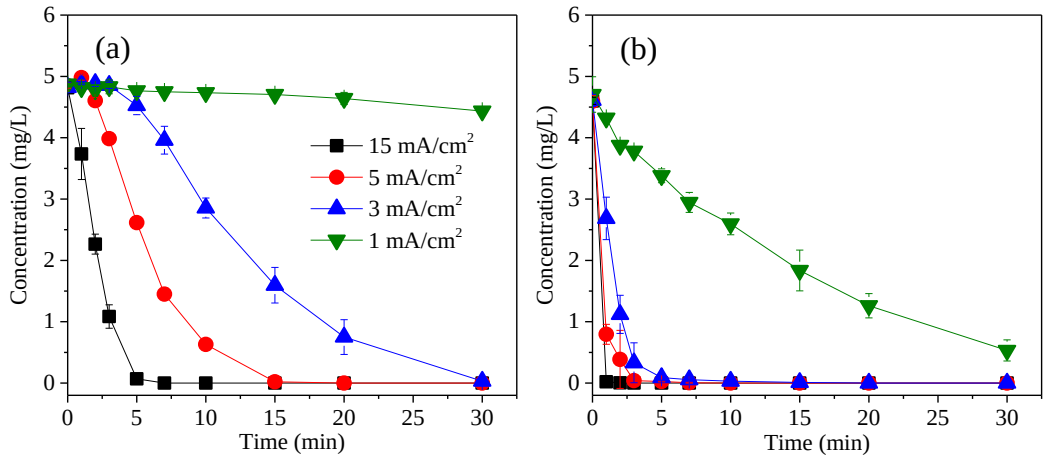

Figure 6-4. Anode oxidation of (a) SD and (b) TC under different current intensities.

6.3.1.2 Effect of solution parameters on anodic oxidation in the SC experiment

The effect of pH on anodic oxidation of SD and TC in the SC experiment is shown in Figure 6-5a and b, respectively. The fastest oxidation of SD was found at pH=6.0, while it became slower when pH was 4.0 and 8.0. According to the ionization species of free chlorine in Figure 6-6, the optimal pH range of chlorination is 4.0 – 6.0, because the relative abundance of HClO reaches the maximum. However, in this pH range, lower pH reduced the solubility of Cl_2, leading to less HClO dissolved in the solution and more Cl_2 emitting alongside anodic bubbles. This is why the oxidation rate of SD at pH=4.0 was lower than that at pH=6.0. At pH=10.0, the oxidation of SD was significantly inhibited (Figure 6-5a). A similar phenomenon was found in relation to TC, while TC was oxidized very fast in the acidic conditions (Figure 6-5b).

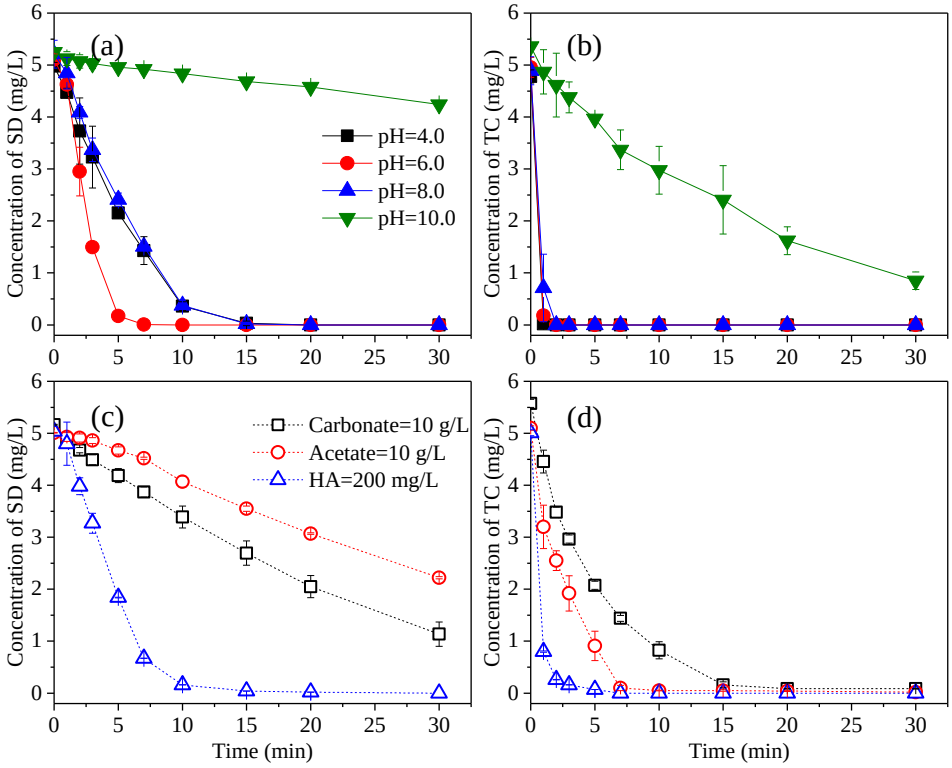

Figure 6-5. Effect of pH on the oxidation of (a) SD and (b) TC, as well as the effects of carbonate, acetate, and HA on the oxidation of (c) SD and (d) TC in the SC experiment.

Note: The assays of acetate and HA were conducted at pH=6.0, while the assay of carbonate was conducted at pH=8.0. This is because the carbonate can be converted to CO_2 at pH=6.0. The assay of carbonate was set as the control to investigate the oxidation process in the digestate without acidification.

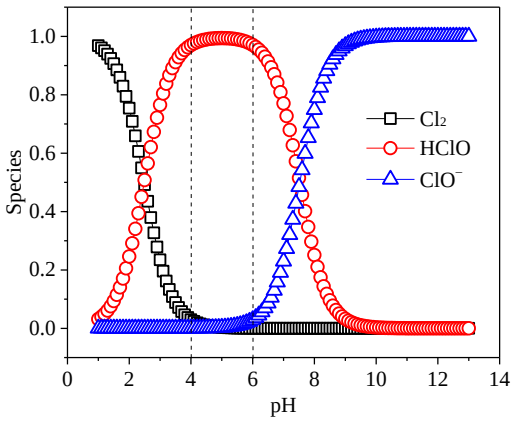

Figure 6-6. Ionization of free chlorine in the experimental conditions.

Note: The ionization was based on two equations as follows [261] :

$Cl_2 + H_2O \leftrightarrow HClO + H^+ + Cl^-$ $\quad K_{a1} = 4.0 \times 10^{-4}$

$HClO \leftrightarrow H^+ + ClO^-$ $\quad K_{a2} = 3.2 \times 10^{-8}$

It has been reported that carbonate and organic matter can inhibit the oxidation process [215]. In this experiment, the effects of carbonate, acetate, and HA on the anodic oxidation of SD and TC were investigated, and the results are shown in Figure 6-5c and d. The maximum concentrations of carbonate, acetate, and HA added to the solution were 10, 10, and 0.2 mg/L, respectively, aiming at mimicking the real conditions of raw pig manure and pig manure digestate. It shows that 10 g/L carbonate significantly hampered the oxidation of antibiotics. The carbonate can consume HClO due to the reaction with H^+, and quench the free radicals [262]. Hence, the high alkalinity of pig manure digestate can adversely reduce the oxidation efficiency. During the pretreatment of digestate, the carbonate was consumed since the pH of feed solution was adjusted to 5.5. This approach not only increased the concentration of P in the feed solution, but also increased the oxidation efficiency due to the removal of carbonate. It was found that 10 g/L acetate also hampered the oxidation significantly, indicating that the presence of VFAs in the feed solution (pig manure or pig manure digestate) would be detrimental to the anodic oxidation. The higher concentration of VFAs, the more significant inhibition occurred. By contrast, 200 mg/L of HA showed less serious inhibition to the anodic oxidation compared with carbonate and acetate.

6.3.1.3 Oxidation intermediates of antibiotics

In this study, the generated oxidation intermediates of SD and TC were determined by HPLC-MS/MS. The ion chromatograms and MS/MS spectra of intermediates are shown in Appendix B. Comparing with the ion chromatograms before oxidation (chromatograms at 0 min), five oxidation intermediates of SD were distinguished from the chromatograms, i.e. the compounds with *m/z* ($[M+H]^+$) of 172, 188, 202, 433, and 497. Six oxidation intermediates of TC were also distinguished from the ion chromatograms, i.e. the compounds with *m/z* ($[M+H]^+$) of 399, 415, 429, 459, 487, and 511. The MS/MS spectra for each compound were searched and compared in the database for the confirmation of chemical structures. Figure 6-7 profiles the possible chemical structures of the oxidation intermediates of SD. The MS/MS spectra of *m/z* 172 and 202 had good similarities up to 68% with the chemical structures in the database. The compound with *m/z* 188 cannot be found in the database, while its chemical structure can be inferred from the spectrum by comparing the MS/MS fragments with the other products. All the compounds had the fragments with *m/z* 170, and 80, indicating that certain fragments of the products were identical. The compounds with *m/z* 433 and 497 can be regarded as the combination of SD with intermediates and Na^+. According to the previous study, SO_2 extrusion and rearrangement should be the possible mechanism for SD oxidation [263]. However, there are huge numbers of isomers for each compound with the same similarities. Particularly for TC, it is very difficult to know the accurate chemical structures only based on the MS/MS spectra. Generally, HClO is reduced to H_2O and Cl^- in the reaction with organic matters where outer sphere electron transfer occurs [264]. New organic substances are formed after a series of reactions, such as hydroxylation, carbonylation, carboxylation, and amine cleavage, etc. These reactions can be inferred from the differences between the chemical structures of intermediates. The relative abundances of intermediates during the oxidation are summarized in Figure 6-8. It can be found that the abundances of oxidation intermediates increased at the beginning, while they were all undetectable at the end of the experiment. This is reflected in the ion chromatograms after 120 min of oxidation, where no peaks of intermediate products were observed (the extracted ion chromatograms for each *m/z* were checked). However, the slow decrease of total organic carbon (TOC), which was decreased by around 20%, indicated a slow loss of carbon via CO_2, which is in line with the low concentrations of radicals generated. This

indicates that the oxidation intermediates were further oxidized into smaller molecules in the reactors. No chlorine contained products (CCPs) were generated during the oxidation of SD based on the MS spectra, while two CCPs were observed during the oxidation of TC, i.e. *m/z* 487 and *m/z* 511.

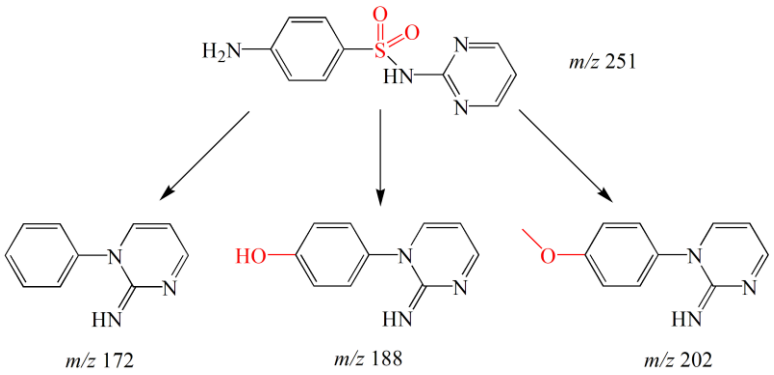

Figure 6-7. Possible intermediates during the oxidation of SD.

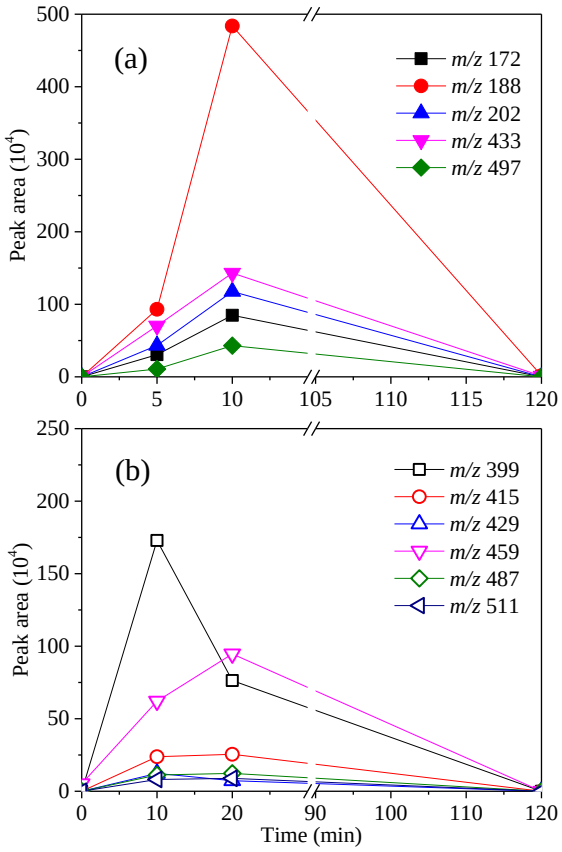

Figure 6-8. Variation in the abundance of oxidation intermediates with the reaction time during the oxidation of (a) SD and (b) TC.

Note: Because the oxidation of SD and TC were too fast at 15 mA/cm^2, current intensities of 3 and 1 mA/cm^2 were applied to the reactor for the determination of the oxidation intermediates of SD and TC, respectively.

6.3.2 Integration of anodic oxidation into ED

6.3.2.1 Anodic oxidation of antibiotics

Figure 6-9 shows the removal of SD and TC in the conventional ED and anode-ED processes, using the liquid fraction of pig manure digestate as the feed solutions. In the ED process, the SD and TC concentrations in the feed solution decreased negligibly in the first 60 min. As demonstrated in Chapter 5, the decrease of SD and TC in ED technologies was attributed to the electric migration and membrane sorption. The decrease of SD and TC became more significant after 60 min, which was attributed to the increase of the electric field and the decrease of salinity. While only around 50% of SD and TC were removed from the feed solution in ED. With anodic oxidation integrated, the SD and TC in anode-ED were efficiently removed in the initial 60 min, indicating that anodic oxidation played the primary role in antibiotic removal. The removal of SD and TC in pig manure digestate was slower than that in the synthetic wastewater, which was attributed to the complex composition of digestate. In this experiment, the soluble COD of digestate was 2108 ± 296 mg/L, indicating that certain DOM in the digestate can quench the oxidants. Nonetheless, the antibiotics were completely removed at the beginning of the anode-ED process, proving that anodic oxidation is efficient in antibiotics removal from pig manure digestate. Using the raw pig manure (before AD) as the feed solution, the SD and TC cannot be efficiently oxidized due to the high concentration of VFAs (Figure 6-10). It indicates that the digestate would be a better material for oxidation than raw pig manure in terms of antibiotics removal.

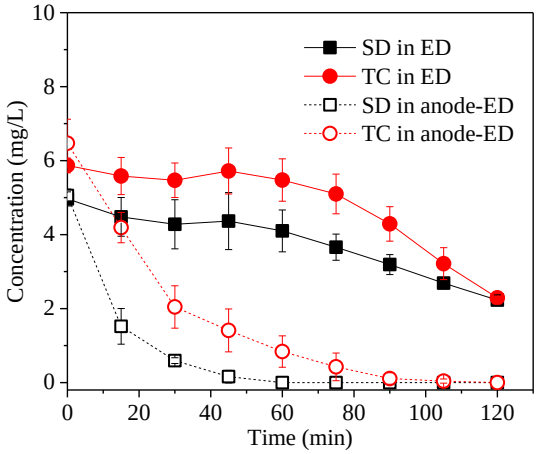

Figure 6-9. Removal of SD and TC in the conventional ED and anode-ED processes.

Note: The liquid fraction of pig manure digestate was used as the feed solution.

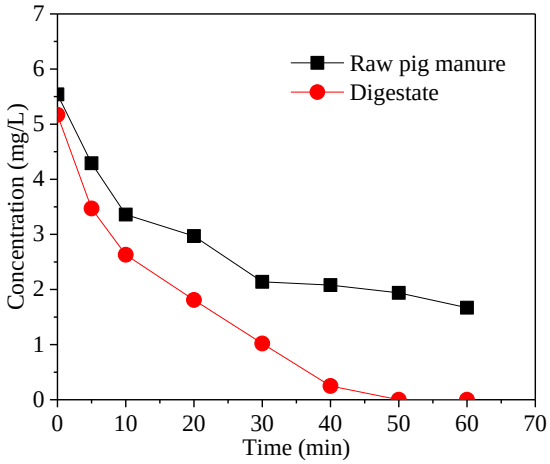

Figure 6-10. Removal of SD from raw pig manure and pig manure digestate in anode-ED.

6.3.2.2 Fouling mitigation

In the ED technologies, colloidal particles can aggregate under the electric field due to their negetive charges. They can form a layer of fouling cake on the membranes and block the membrane stack. The bubbles generated in the anode compartment can increase the turbulence in the feed solution, therefore mitigating the particle fouling in the membrane stack. As shown in Figure 6-11a, the particle fouling formed on the membranes in the conventional ED was around 1.8 g, while it was around 0.6 g on the membranes of anode-ED (the pictures of particle fouling are shown in Figure 6-12). The particle fouling was also around 0.6 g in the cathode-ED, proving that the primary mechanism of fouling mitigation was gas bubbling rather than oxidation. DOM can cause the organic fouling of ion-exchange membranes. In conventional ED processes, the UV_{254} of the feed solution decreased by around 40% because of the eletric migration and sorption of DOM on the membranes. The DOM in the feed solution can be concentrated to the liquid-membrane interface with a small portion forming irreversible organic fouling on the membrane [252]. It was found that both anode-ED and cathode-ED removed more DOM from the feed solution, compared with conventional ED. This was probably because the mitigation of particle fouling led to more DOM adsorbed by the membranes (the compacted fouling cake in concentional ED can hinder the DOM sorption on the membranes). DOM was not decomposed by the anodic gas, because the UV_{254} of the feed solution did not decrease in the SC experiment. This is consistent with the previous findings that the chlorine cannot decrease the UV_{254} of organic matter significantly as only the electrophilic substitution reaction occurs [262]. However, it

seemed that the anodic oxidation changed the compositation of DOM. According to the EEMs spectra in Figure 6-11b and c, two fluoresence peaks can be distinguished in the digestate before oxidation, i.e. fluorophore at (270-280)/(300-310) and (290-325)/(390-440) nm. These two fluorophores were attributed to the tyrosine-like substances and humic-like substances, respectively. The fluorophore of tyrosine-like substances was eliminated in the SC experiment, while the fluorophore of humic-like substances became less intensive and presented a shift in excitation wavelength by around 10 nm. This indicated that the melecular distribution of humic-like substances was changed, being probably from the decomposition of large melecules to smaller ones [216].

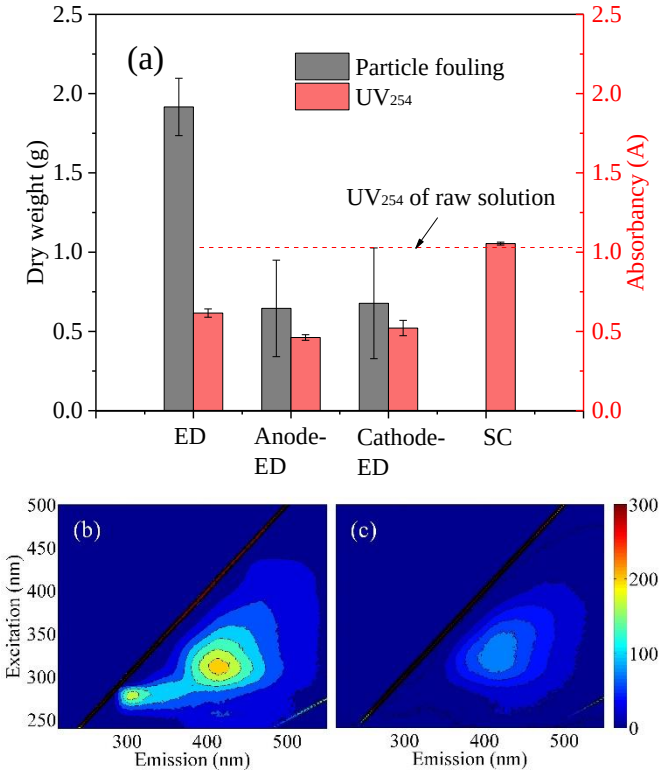

Figure 6-11. Fouling mitigation in different reactors. (a) the dry weight of particle fouling and UV_{254} of the feed solution after 2 hours of experiments in different reactors; (b) the EEM spectrum of feed digestate before oxidation; and (c) the EEM spectrum after 2 hours of oxidation in the SC experiment.

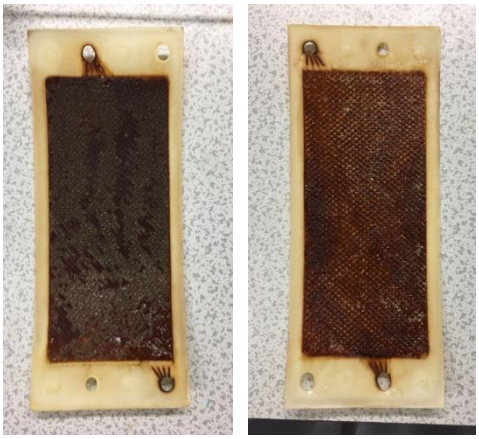

Figure 6-12. Fouling cake formed on AM in conventional ED (left) and anode-ED (right).

6.3.2.3 Pathogen inactivation

Table 6-1 shows the pathogen inactivation in the anode-ED and SC experiment with 10^4 – 10^6 CFU/mL of *E. coli* and *Enterococcus* inoculated in the pig manure digestate. *E. coli* and *Enterococcus* were both effeciently inactivated in the first 30 min. After 30 min of treatment, the *E. coli* and *Enterococcus* in the feed solution of anode-ED became undetectable, and only 5 ± 2 CFU/mL of *E. coli* and 3 ± 1 CFU/mL of *Enterococcus* were detected in SCR. The faster inactivation of pathogens in the anode-ED might be due to the electric attraction and membrane sorption, because pathogens were negatively charged in the feed solution. However, the electric field was not effective in the removal of pathogens without anodic oxidation, which was evidenced by the 10^3 – 10^4 CFU/mL of *E. coli* and *Enterococcus* remaining after 5 hours of EDR with pig manure digestate (Figure 6-13). The effective pathogen inactivation ensured that the effluent (the feed solution after treatment) of anode-ED can meet the EU regulations on animal by-products and derive products (<10^3 CFU/g fresh matter) [265]. A similar phenomenon was also observed in Huang's study, in which *E. coli* and *Enterococcus* were found mainly inactivated in the first 30 mins of electrochemical disinfection of toilet wastewater [40]. *E. coli* and *Enterococcus* were undetectable after the anode-ED process, showing that the effluent is safe for water reuse regading the pathogen levels. In addition, the high concentration of chloramines generated favours long-term disinfection after the anode-ED process.

Table 6-1. Pathogen inactivation over time during anodic oxidation in the anode-ED and SC processes.

Time (min)	Anode-ED		SC	
	E. coli (CFU/mL)	*Enterococcus* (CFU/mL)	*E. coli* (CFU/mL)	*Enterococcus* (CFU/mL)
0	$(1.5 \pm 0.1) \times 10^5$	$(1.5 \pm 0.4) \times 10^4$	$(2.4 \pm 0.1) \times 10^5$	$(2.5 \pm 0.4) \times 10^4$
10	$(7.2 \pm 1.2) \times 10^4$	$(3.5 \pm 0.4) \times 10^2$	$(7.0 \pm 0.5) \times 10^4$	$(4.8 \pm 0.8) \times 10^3$
20	72 ± 1	5 ± 1	$(8.2 \pm 0.7) \times 10^2$	$(2.2 \pm 0.2) \times 10^2$
30	-	-	5 ± 2	3 ± 1
60	-	-	-	-
120	-	-	-	-

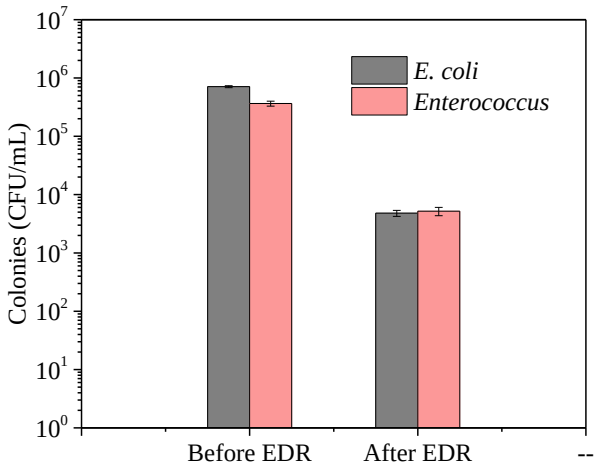

Figure 6-13. Pathogen inactivation after 5 hours of EDR without anodic oxidation.
Note: The feed solution was 5 L of pig manure digestate.

6.3.2.4 Formation of DBPs

Figure 6-14 shows the concentrations of THMs, HAAs, and other DBPs in different solutions of anode-ED and SC experiment. In the SC experiment, very high concentrations of DBPs were detected in the feed solution. The concentrations of THMs and HAAs reached up to 2116 and 8305 μg/L. The maximum formation potential of TCM, DCAA, TCAA, and CH of the raw digestate were measured as 106, 45, 258, and 5 mg/L, respectively, showing that around 2% of THMs and HAAs were formed in this system. However, in the anode-ED process, the feed solution contained only around 134 μg/L of THMs and 192 μg/L of HAAs, far lower than those in the SC experiment. It has been reported that the ion-exchange membranes can adsorb micro-containments

from the wastewater, such as the pesticides and heavy metals [33-35]. In this study, the low concentrations of DBPs in anode-ED were probably because of the membrane sorption. The concentrations of DBPs in the feed solution of anode-ED were lower than those reported in Huang et al's study, in which the concentrations of THMs and HAAs can reach 347 and 739 μg/L, respectively, after the electrochemical disinfection of toilet wastewater. In addition, the current density in this study was 15 mA/cm^2, far higher than that used in Xiao et al's study (2.4 mA/cm^2). Therefore, the developed anode-ED can generate a feed solution with more chlorine but less DBPs. The concentrations of DBPs were also lower than those measured in the reclaimed water after a UV/chlorination process [216]. In the product solution, a relatively high concentration of DCAA was detected. It was probably because of the migration of DCAA from the diluted compartment to the product. Around 20 μg/L of CH and 79 μg/L of DCAN were detected in the feed solution, while they remained undetectable in the product solution.

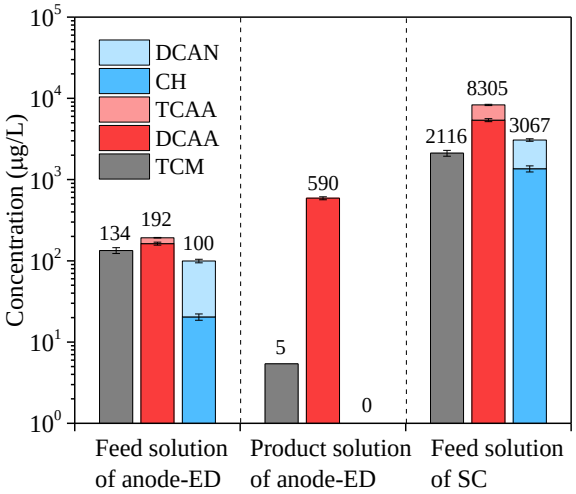

Figure 6-14. Concentrations of DBPs generated in anode-ED and SC processes.
Note: The detectable THMs only contained trichloromethane (TCM), while the HAAs included dichloroacetic acid (DCAA), trichloroacetic acid (TCAA).

6.4 Summary

Overall, it was found that the anode-ED reactor was effecient in antibiotics removal, fouling mitigation, and pathogen inactivation. This approach can utilize the energy consumed on the electrodes and improve the energy efficiency of ED technologies. THMs and HAAs were generated alongside the anodic oxidation process, while the

membranes equipped in the anode-ED reactor can adsorb them, thereby significantly reducing the emission of DBPs to the envrionment. The effluent after the anode-ED process can be recycled for farm use, i.e. manure flushing. However, the DBPs adsorbed on the membrane should be further considered when the sorption capacity of the membrane reached the maximum threshold. In practice, the membranes are cleaned by the acid or base solutions periodically, so the DBPs will be transported to the cleaning solution that needs further treatment.

Chapter 7

Conclusions and recommendations

7.1 Overview

In this Ph.D. research, the application of EDR and BMED into nutrient recovery from pig manure was assessed. The sorption and migration of antibiotics during the nutrient recovery process were investigated. In addition, an anode-ED technology was developed for the in-situ antibiotics removal, fouling mitigation, and pathogen inactivation.

7.2 Main conclusions

- ***Nutrient recovery from pig manure digestate using EDR***

(1) Electrodialysis reversal can extract 100% of NH_4^+ and 84% of PO_3^- from the pig manure digestate to the product solution efficiently.

(2) During semi-continuous operation, particle fouling and chemical deposition were significantly mitigated, while tyrosine-like and humic-like substances fouled AM gradually. CM was resistant to the fouling caused by DOM.

(3) With periodical HCl cleaning, the fouling of AM ceased after treating the digestate at a capacity of 330 L/m^2 membrane when its conductivity and ion-exchange capacity decreased by 18.5% and 13.3% compared with the virgin membrane, respectively.

(4) The organic foulants existed in the fouling area around the membrane surface, rather than migrating deeper into the interior of the membrane.

- ***Recovery of nutrients and VFAs from pig manure hydrolysate using BMED***

(1) Bipolar membrane electrodialysis can extract 52% of NH_4^+ to the base compartment, and 98% of PO_4^{3-} and 95% of VFAs to the acid compartment.

(2) The BMED model substantiated that the low recovery efficiencies of NH_4^+ and the impurity of acid solution were primarily caused by the undesired diffusion of ions through BM.

(3) Through a two-stage BMED, the recovery efficiency of NH_4^+ increased to 78%, and 75% of PO_4^{3-} and 87% of VFAs were separated from Cl^- and SO_4^{2-} in the acid compartment. Real pig manure hydrolysate was tested and the variations of ions in the BMED were consistent as those using synthetic wastewater.

- ***Antibiotics removal in EDR for nutrient recovery from pig manure***

(1) Using synthetic wastewater, around 90% of SD and TC can be removed from the feed solution and transported to the product solution. Membrane sorption played the primary role in their removal, while it was impacted by the salinity and pH of the feed solution. The low salinity at the end of EDR resulted in stronger sorption of antibiotics.

(2) It was proved that anion membrane can adsorb both SD and TC, while the cation membrane can only adsorb TC. The adsorbed SD was transported to the product solution through membranes, while TC was retained in the membrane-solution interface.

(3) Membrane fouling hindered the sorption and migration of antibiotics in EDR. High concentrations of TC were transported to the membrane cleaning solutions, showing its association with particle fouling and organic foulants.

(4) With periodical membrane cleaning, the membranes after a long-term operation still presented a high sorption capacity almost identical to that of virgin membranes.

- ***In-situ anodic oxidation in ED for antibiotics removal, fouling mitigation, and pathogen inactivation during the nutrient recovery from pig manure digestate***

(1) Negligible decreases were observed on Cl^-, NH_4^+-N, and PO_4^{3-}-P in contrast with the rapid removal of SD and TC from the feed solution. HClO was evidenced as the dominant oxidant, and a small amount of ·OH and ·Cl were generated.

(2) The optimal pH for anodic oxidation was 6.0, but the oxidation efficiency decreased with the presences of carbonate, acetic acid, and HA.

(3) Several oxidation intermediates of SD and TC were detected, and they were all eliminated at the end of the experiment. Chlorine contained intermediates were only observed during the oxidation of TC.

(4) Particle fouling was significantly mitigated due to the gas bubbling. *E. coli* and *Enterococcus* were efficiently inactivated in the first 30 min of oxidation.

(5) Despite a high generation potential of DBPs, THMs and HAAs in the effluent (feed solution) were only 134 and 192 μg/L, respectively, because of the membrane sorption in anode-ED.

7.3 Summary

Electrodialysis reversal can be applied to the nutrient recovery from pig manure containing high concentrations of SS, Ca^{2+}, Mg^{2+}, and DOM. The particle fouling and chemical deposit were efficiently mitigated by the self-cleaning process during EDR. With efficient solid-liquid separation, two-stage BMED can be applied to the nutrient recovery from pig manure with acid and base solution produced. VFAs can be harvested as a by-product if the hydrolysate was used as the raw materials for nutrient recovery. Antibiotics in animal manure were transported to the product solution during the nutrient recovery in EDR. Their sorption and migration were associated with membrane fouling during the recovery and cleaning processes. In-situ anodic oxidation can be utilized for antibiotics elimination in ED technologies. This approach can also mitigate particle fouling and inactivate pathogens. The generated DBPs in the feed solution can be adsorbed by ion-exchange membranes.

7.4 Contributions to pig manure management

Currently, the management of excessive pig manure is a worldwide issue requiring further studies. Membrane technologies are efficient in the nutrient recovery from pig manure, while their applications are limited by severe membrane fouling. This Ph.D. research systematically assessed the nutrient recovery from pig manure using ED technologies, including EDR and BMED, for the first time. It can provide promising options to the disposal of excessive pig manure. In addition, this Ph.D. research investigated the fate of antibiotics during the nutrient recovery from pig manure, very valuable information regarding biosafety. It reveals the potential risk of recovering nutrients from pig manure containing antibiotics. Based on this, the in-situ utilization

of anode in the ED technologies has been proposed for the first time. This research provides with an effective method to remove the antibiotics and reduce the overall energy cost of ED processes.

7.5 Recommendations for future research

Based on the results obtained in this research, several recommendations for future research directions are proposed.

(1) *Long-term operation of EDR.* EDR can be used to recover the nutrients from pig manure, while a long-term operation is essential. Demonstrations with pilot-scale EDR are needed to probe the membrane service life.

(2) *The integration of BMED to other technologies.* BMED relies on efficient filtration as pretreatment, because it cannot reverse the electrodes like EDR. Hence, BMED can be used in the treatment of pig manure containing less SS or integrated with other technologies (e.g. after EDR) to increase the product diversity.

(3) *The utilization of by-products generated in BMED.* BMED can produce acid and base solutions, which can be potentially used for membrane cleaning. The utilization of these by-products requires further tests.

(4) The disposal of feed solution. With ED processes, the nutrients in the feed solution are mostly extracted. However, around 10 – 20% of P cannot be extracted by ED. Further studies are needed on the recovery of this part of P. Alternatively, the solution after extraction can be potentially used for farm flushing.

(5) *Optimization of anodic oxidation in ED technologies.* In-situ utilization of anode in ED is effective, while it needs to be optimized to reduce the generation of DBPs. Anodic oxidation can be upgraded to a hybrid technology rich in ·OH (e.g. changing anode materials or the integration with UV), which will be more efficient in antibiotics removal. A low current density and short contact time can be applied to anode-ED, in order to reduce the generation of DBPs. The cleaning frequency of membranes and the disposal of cleaning solutions also need further studies.

(6) *Cost-benefit analysis and life cycle assessment.* According to the experimental results, the energy cost of nutrient recovery from pig manure using ED technologies should be assessed.

(7) *Kinetics analysis and modelling of complex ED system.* Up to date, no studies have succeeded in the simulation of complex ED systems containing various ions, while the kinetics analysis and modelling will be useful to provide a universal understanding of the migration of ions in the ED system.

7.6 Career development plan

Soon after this thesis submitted, I am leaving the environmental research group in the National University of Ireland, Galway, and will join the Trinity College Dublin as a postdoctoral researcher. I will steadily continue to work in the field of environmental engineering with the interests in developing novel technologies to remove emerging contaminants from wastewater.

Over the past four years, my interest have gradually inclined to this area. As demonstrated, ED technologies have the potential to remove antibiotics alongside nutrient recovery. The key of extending ED technologies to practical scale is to reduce the overall energy input. There is always a question – "cost and benefits", on any proposed novel technologies. ED technologies offer the potential of reducing energy via utilizing the anode and cathode, and it can also remove the emerging contaminants from wastewater via membrane sorption and cleaning. My Ph.D. study is a good start leading me to explore further in this research area.

My ambition is to pursue a successful academic career, in other words, to become a leading scholar that can find out or invent something useful in wastewater treatment. Exploring new research areas independently is an important skill towards this goal. It always involves the abilities of project application, management, data analysis, communication, dissemination and leadership. Research is not everything in my life, but life is nothing without research from the very beginning. With the enthusiasm and optimism, I believe I can achieve more than research.

Bibliography

[1] B. Ben-Belhassen, C. Calpe, A. Abbassian, Food Outlook: Biannual Report on Global Food Markets, 2018.

[2] M. Hjorth, K.V. Christensen, M.L. Christensen, S.G. Sommer, Solid-liquid separation of animal slurry in theory and practice. a review, Agron. Sustain. Dev. (2010) 30: 153-180.

[3] S.M. Heilmann, J.S. Molde, J.G. Timler, B.M. Wood, A.L. Mikula, G.V. Vozhdayev, E.C. Colosky, K.A. Spokas, K.J. Valentas, Phosphorus reclamation through hydrothermal carbonization of animal manures, Environ. Sci. Technol. (2014) 48: 10323-10329.

[4] I. Sárvári Horváth, M. Tabatabaei, K. Karimi, R. Kumar, Recent updates on biogas production - a review, Biofuel Res. J. (2016) 3: 394-402.

[5] C. Dennehy, P.G. Lawlor, Y. Jiang, G.E. Gardiner, S. Xie, L.D. Nghiem, X. Zhan, Greenhouse gas emissions from different pig manure management techniques: a critical analysis, Front. Env. Sci. Eng. (2017) 11.

[6] Y. Jiang, C. Dennehy, P.G. Lawlor, Z. Hu, X. Zhan, G.E. Gardiner, Inactivation of enteric indicator bacteria and system stability during dry co-digestion of food waste and pig manure, Sci. Total Environ. (2017) 612: 293-302.

[7] S. Xie, P.G. Lawlor, P. Frost, C.D. Dennehy, Z. Hu, X. Zhan, A pilot scale study on synergistic effects of co-digestion of pig manure and grass silage, Int. Biodeterior. Biodegrad. (2017) 123: 244-250.

[8] OJEC Directive, Council Directive 91/676/EEC of 12 December 1991 concerning the protection of waters against pollution caused by nitrates from agricultural sources (1991).

[9] S.I.610, S.I.610, Statutory Instruments-Good Agricultural Practice for Protection of Waters Regulations (2010).

[10] S.I. No. 610 of 2010, European Communities (Good Agricultural Practice for Protection Of Waters) Regulations 2010.

[11] M.L. Christensen, M. Hjorth, K. Keiding, Characterization of pig slurry with reference to flocculation and separation, Water Res. (2009) 43: 773-783.

[12] D. Fangueiro, M. Hjorth, F. Gioelli, Acidification of animal slurry - a review, J. Environ. Manage. (2015) 149: 46-56.

[13] W.S. Waste ManagLee, A.S.M. Chua, H.K. Yeoh, G.C. Ngoh, A review of the production and applications of waste-derived volatile fatty acids, Chem. Eng. J. (2014) 235: 83-99.

[14] C. Dennehy, P.G. Lawlor, T. Croize, Y. Jiang, L. Morrison, G.E. Gardiner, X. Zhan, Synergism and effect of high initial volatile fatty acid concentrations during food waste and pig manure anaerobic co-digestion, Waste Manage. (2016) 56: 173-180.

[15] A. Zarebska, D. Romero Nieto, K.V. Christensen, L. Fjerbæk Søtoft, B. Norddahl, Ammonium fertilizers production from manure: a critical review, Crit. Rev. Env. Sci. Technol. (2015) 45: 1469-1521.

[16] E. Monfet, G. Aubry, A.A. Ramirez, Nutrient removal and recovery from digestate: a review of the technology, Biofuels (2017) 1-16.

[17] K. Möller, T. Müller, Effects of anaerobic digestion on digestate nutrient availability and crop growth: a review, Eng. Life Sci. (2012) 12: 242-257.

[18] H. Guo, F. You, S. Yu, L. Li, D. Zhao, Mechanisms of chemical cleaning of ion exchange membranes: a case study of plant-scale electrodialysis for oily wastewater treatment, J. Membr. Sci. (2015) 496: 310-317.

[19] W. Wang, R. Fu, Z. Liu, H. Wang, Low-resistance anti-fouling ion exchange membranes fouled by organic foulants in electrodialysis, Desalination (2017) 417: 1-8.

[20] M. Xie, H.K. Shon, S.R. Gray, M. Elimelech, Membrane-based processes for wastewater nutrient recovery: technology, challenges, and future direction, Water Res. (2016) 89: 210-221.

[21] X. Tongwen, Y. Weihua, Citric acid production by electrodialysis with bipolar membranes, Chem. Eng. Process. (2002) 41: 519-524.

[22] X. Wang, Y. Wang, X. Zhang, H. Feng, T. Xu, In-situ combination of fermentation and electrodialysis with bipolar membranes for the production of lactic acid: Continuous operation, Bioresour. Technol. (2013) 147: 442-448.

[23] X. Zhang, C. Li, Y. Wang, J. Luo, T. Xu, Recovery of acetic acid from simulated acetaldehyde wastewaters: bipolar membrane electrodialysis processes and membrane selection, J. Membr. Sci. (2011) 379: 184-190.

[24] Y. Zhou, H. Yan, X. Wang, Y. Wang, T. Xu, A closed loop production of water insoluble organic acid using bipolar membranes electrodialysis (BMED), J. Membr. Sci. (2016) 520: 345-353.

[25] C. Li, G. Wang, H. Feng, T. He, Y. Wang, T. Xu, Cleaner production of niacin using bipolar membranes electrodialysis (BMED), Sep. Purif. Technol. (2015) 156: 391-395.

[26] I.T. Carvalho, L. Santos, Antibiotics in the aquatic environments: a review of the European scenario, Environ. Int. (2016) 94: 736-757.

[27] S.R. Joy, S.L. Bartelt-Hunt, D.D. Snow, J.E. Gilley, B.L. Woodbury, D.B. Parker, D.B. Marx, X. Li, Fate and transport of antimicrobials and antimicrobial resistance genes in soil and runoff following land application of swine manure slurry, Environ. Sci. Technol. (2013) 47: 12081-12088.

[28] R. Marti, A. Scott, Y.-C. Tien, R. Murray, L. Sabourin, Y. Zhang, E. Topp, The impact of manure fertilization on the abundance of antibiotic-resistant bacteria and frequency of

detection of antibiotic resistance genes in soil, and on vegetables at harvest, Appl. Environ. Microbiol. (2013) 01682-01613.

[29] Q.L. Chen, X.L. An, Y.G. Zhu, J.Q. Su, M.R. Gillings, Z.L. Ye, L. Cui, Application of struvite alters the antibiotic resistome in soil, rhizosphere, and phyllosphere, Environ. Sci. Technol. (2017) 51: 8149-8157.

[30] H. Lu, W. Zou, P. Chai, J. Wang, L. Bazinet, Feasibility of antibiotic and sulfate ions separation from wastewater using electrodialysis with ultrafiltration membrane, J Clean Prod (2016) 112: 3097-3105.

[31] S. Gabarron, W. Gernjak, F. Valero, A. Barcelo, M. Petrovic, I. Rodriguez-Roda, Evaluation of emerging contaminants in a drinking water treatment plant using electrodialysis reversal technology, J. Hazard. Mater. (2016) 309: 192-201.

[32] C. Onorato, L.J. Banasiak, A.I. Schäfer, Inorganic trace contaminant removal from real brackish groundwater using electrodialysis, Sep. Purif. Technol. (2017) 187: 426-435.

[33] L.J. Banasiak, A.I. Schäfer, Removal of boron, fluoride and nitrate by electrodialysis in the presence of organic matter, J. Membr. Sci. (2009) 334: 101-109.

[34] L.J. Banasiak, B. Van der Bruggen, A.I. Schäfer, Sorption of pesticide endosulfan by electrodialysis membranes, Chem. Eng. J. (2011) 166: 233-239.

[35] L.J. Banasiak, A.I. Schäfer, Sorption of steroidal hormones by electrodialysis membranes, J. Membr. Sci. (2010) 365: 198-205.

[36] B. Gomez-Ruiz, S. Gómez-Lavín, N. Diban, V. Boiteux, A. Colin, X. Dauchy, A. Urtiaga, Efficient electrochemical degradation of poly- and perfluoroalkyl substances (PFASs) from the effluents of an industrial wastewater treatment plant, Chem. Eng. J. (2017) 322: 196-204.

[37] H. Särkkä, A. Bhatnagar, M. Sillanpää, Recent developments of electro-oxidation in water treatment - a review, J. Electroanal. Chem. (2015) 754: 46-56.

[38] S. Liang, H. Lin, X. Yan, Q. Huang, Electro-oxidation of tetracycline by a Magnéli phase Ti4O7 porous anode: kinetics, products, and toxicity, Chem. Eng. J. (2018) 332: 628-636.

[39] C. Han, Y. Ye, G. Wang, W. Hong, C. Feng, Selective electro-oxidation of phenol to benzoquinone/hydroquinone on polyaniline enhances capacitance and cycling stability of polyaniline electrodes, Chem. Eng. J. (2018) 347: 648-659.

[40] X. Huang, Y. Qu, C.A. Cid, C. Finke, M.R. Hoffmann, K. Lim, S.C. Jiang, Electrochemical disinfection of toilet wastewater using wastewater electrolysis cell, Water Res. (2016) 92: 164-172.

[41] C. Dennehy, P.G. Lawlor, M.S. McCabe, P. Cormican, J. Sheahan, Y. Jiang, X. Zhan, G.E. Gardiner, Anaerobic co-digestion of pig manure and food waste; effects on digestate

biosafety, dewaterability, and microbial community dynamics, Waste Manage. (2018) 71: 532-541.

[42] G. Fongaro, A. Kunz, M.E. Magri, A. Viancelli, C.D. Schissi, M.C. da Silva Lanna, M. Hernández, D. Rodríguez-Lázaro, M.C. García-González, C.R.M. Barardi, Evaluation of the effective inactivation of enteric bacteria and viruses from swine effluent and sludge at tropical temperatures, Water, Air, Soil Pollut. (2018) 229.

[43] D. Masse, Y. Gilbert, E. Topp, Pathogen removal in farm-scale psychrophilic anaerobic digesters processing swine manure, Bioresour. Technol. (2011) 102: 641-646.

[44] V. Orzi, B. Scaglia, S. Lonati, C. Riva, G. Boccasile, G.L. Alborali, F. Adani, The role of biological processes in reducing both odor impact and pathogen content during mesophilic anaerobic digestion, Sci. Total Environ. (2015) 526: 116-126.

[45] L. Bohm, A. Drews, H. Prieske, P.R. Berube, M. Kraume, The importance of fluid dynamics for MBR fouling mitigation, Bioresour. Technol. (2012) 122: 50-61.

[46] A. Eliseus, M.R. Bilad, N. Nordin, Z.A. Putra, M.D.H. Wirzal, Tilted membrane panel: A new module concept to maximize the impact of air bubbles for membrane fouling control in microalgae harvesting, Bioresour. Technol. (2017) 241: 661-668.

[47] T.M. Qaisrani, W.M. Samhaber, Impact of gas bubbling and backflushing on fouling control and membrane cleaning, Desalination (2011) 266: 154-161.

[48] A.J. McAfee, E.M. McSorley, G.J. Cuskelly, B.W. Moss, J.M. Wallace, M.P. Bonham, A.M. Fearon, Red meat consumption: an overview of the risks and benefits, Meat Sci. (2010) 84: 1-13.

[49] W.L. Claeys, S. Cardoen, G. Daube, J. De Block, K. Dewettinck, K. Dierick, L. De Zutter, A. Huyghebaert, H. Imberechts, P. Thiange, Y. Vandenplas, L. Herman, Raw or heated cow milk consumption: review of risks and benefits, Food Control (2013) 31: 251-262.

[50] U. Nations, World population prospects: the 2017 revision, Population division of the department of economic and social affairs of the United Nations Secretariat, New York (2017).

[51] L. Shiming, The utilization of human excreta in Chinese agriculture and the challenge faced, (2002).

[52] M. Balter, Researchers discover first use of fertilizer, Sicence: origins of civilization, 2013.

[53] D. Chadwick, J. Wei, T. Yan'an, Y. Guanghui, S. Qirong, C. Qing, Improving manure nutrient management towards sustainable agricultural intensification in China, Agr. Ecosyst. Environ. (2015) 209: 34-46.

[54] M.A. Vázquez, D. de la Varga, R. Plana, M. Soto, Integrating liquid fraction of pig manure in the composting process for nutrient recovery and water re-use, J. Clean Prod. (2015) 104: 80-89.

[55] R. Li, J.J. Wang, Z. Zhang, F. Shen, G. Zhang, R. Qin, X. Li, R. Xiao, Nutrient transformations during composting of pig manure with bentonite, Bioresour. Technol. (2012) 121: 362-368.

[56] W.-T. Tsai, C.-I. Lin, Overview analysis of bioenergy from livestock manure management in Taiwan, Renew Sust. Energ. Rev. (2009) 13: 2682-2688.

[57] R. Li, N. Duan, Y. Zhang, Z. Liu, B. Li, D. Zhang, T. Dong, Anaerobic co-digestion of chicken manure and microalgae Chlorella sp.: Methane potential, microbial diversity and synergistic impact evaluation, Waste Manage. (2017).

[58] P. Kuttner, A. Weißböck, V. Leitner, A. Jäger, Examination of commercial additives for biogas production, Agron. Res. (2015) 13: 337-347.

[59] S. Cheng, Z. Li, H.-P. Mang, E.-M. Huba, R. Gao, X. Wang, Development and application of prefabricated biogas digesters in developing countries, Renew Sust. Energ. Rev. (2014) 34: 387-400.

[60] X. Wang, X. Lu, G. Yang, Y. Feng, G. Ren, X. Han, Development process and probable future transformations of rural biogas in China, Renew Sust. Energ. Rev. (2016) 55: 703-712.

[61] Bioenergy Supply in Ireland 2015-2035: an update of potential resource quantities and costs, Sustainable Energy Authority of Ireland, 2016.

[62] F. Boysan, Ç. Özer, K. Bakkaloğlu, M.T. Börekçi, Biogas Production from Animal Manure, Procedia Earth Planet Sci. (2015) 15: 908-911.

[63] D. Cordell, A. Rosemarin, J.J. Schroder, A.L. Smit, Towards global phosphorus security: a systems framework for phosphorus recovery and reuse options, Chemosphere (2011) 84: 747-758.

[64] B.K. Mayer, L.A. Baker, T.H. Boyer, P. Drechsel, M. Gifford, M.A. Hanjra, P. Parameswaran, J. Stoltzfus, P. Westerhoff, B.E. Rittmann, Total value of phosphorus recovery, Environ. Sci. Technol. (2016) 50: 6606-6620.

[65] M.B. Van Weelden, D.S. Andersen, B.J. Kerr, S.L. Trabue, L.M. Pepple, Impact of fiber source and feed particle size on swine manure properties related to spontaneous foam formation during anaerobic decomposition, Bioresour. Technol. (2016) 202: 84-92.

[66] H.B. Møller, S.G. Sommer, B.K. Ahring, Separation efficiency and particle size distribution in relation to manure type and storage conditions, Bioresour. Technol. (2002) 85: 189-196.

[67] H.B. Møller, I. Lund, S.G. Sommer, Solid–liquid separation of livestock slurry: efficiency and cost, Bioresour. Technol. (2000) 74: 223-229.

[68] M. Hjorth, M.L. Christensen, P.V. Christensen, Flocculation, coagulation, and precipitation of manure affecting three separation techniques, Bioresour. Technol. (2008) 99: 8598-8604.

[69] S. Piveteau, S. Picard, P. Dabert, M.L. Daumer, Dissolution of particulate phosphorus in pig slurry through biological acidification: A critical step for maximum phosphorus recovery as struvite, Water Res. (2017) 124: 693-701.

[70] L. Zhang, D. Jahng, Enhanced anaerobic digestion of piggery wastewater by ammonia stripping: effects of alkali types, J. Hazard. Mater. (2010) 182: 536-543.

[71] A. Bonmatí, X. Flotats, Air stripping of ammonia from pig slurry: characterisation and feasibility as a pre- or post-treatment to mesophilic anaerobic digestion, Waste Management (2003) 23: 261-272.

[72] M. Laureni, J. Palatsi, M. Llovera, A. Bonmatí, Influence of pig slurry characteristics on ammonia stripping efficiencies and quality of the recovered ammonium-sulfate solution, J. Chem. Technol. Biot. (2013) 88: 1654-1662.

[73] M. Mondor, L. Masse, D. Ippersiel, F. Lamarche, D.I. Masse, Use of electrodialysis and reverse osmosis for the recovery and concentration of ammonia from swine manure, Bioresour. Technol. (2008) 99: 7363-7368.

[74] W. Huang, T. Yuan, Z. Zhao, X. Yang, W. Huang, Z. Zhang, Z. Lei, Coupling hydrothermal treatment with stripping technology for fast ammonia release and effective nitrogen recovery from chicken manure, ACS Sustain. Chem. Eng. (2016) 4: 3704-3711.

[75] P.L. Kaparaju, J.A. Rintala, Effects of solid-liquid separation on recovering residual methane and nitrogen from digested dairy cow manure, Bioresour. Technol. (2008) 99: 120-127.

[76] D. Fangueiro, S. Surgy, J. Coutinho, E. Vasconcelos, Impact of cattle slurry acidification on carbon and nitrogen dynamics during storage and after soil incorporation, J. Plant Nutri. Soil Sci. (2013) 176: 540-550.

[77] Y. Yao, L. Yu, R. Ghogare, A. Dunsmoor, M. Davaritouchaee, S. Chen, Simultaneous ammonia stripping and anaerobic digestion for efficient thermophilic conversion of dairy manure at high solids concentration, Energy (2017) 141: 179-188.

[78] L. Liu, C. Pang, S. Wu, R. Dong, Optimization and evaluation of an air-recirculated stripping for ammonia removal from the anaerobic digestate of pig manure, Process Saf. Environ. (2015) 94: 350-357.

[79] G. Provolo, F. Perazzolo, G. Mattachini, A. Finzi, E. Naldi, E. Riva, Nitrogen removal from digested slurries using a simplified ammonia stripping technique, Waste Manage. (2017) 69: 154-161.

[80] S. Kizito, S. Wu, W. Kipkemoi Kirui, M. Lei, Q. Lu, H. Bah, R. Dong, Evaluation of slow pyrolyzed wood and rice husks biochar for adsorption of ammonium nitrogen from piggery manure anaerobic digestate slurry, The Science of the total environment (2015) 505: 102-112.

[81] C. Ledda, A. Schievano, S. Salati, F. Adani, Nitrogen and water recovery from animal slurries by a new integrated ultrafiltration, reverse osmosis and cold stripping process: a case study, Water Res. (2013) 47: 6157-6166.

[82] D. Bolzonella, F. Fatone, M. Gottardo, N. Frison, Nutrients recovery from anaerobic digestate of agro-waste: Techno-economic assessment of full scale applications, J. Environ. Manage. (2017).

[83] S.G. Sommer, M. Maahn, H.D. Poulsen, M. Hjorth, J. Sehested, Interactions between phosphorus feeding strategies for pigs and dairy cows and separation efficiency of slurry, Environ. Technol. (2008) 29: 75-80.

[84] V. Beaudette, D.I. Massé, L. Masse, M. Muir, Size distribution and compositation of particles in raw and anaerobically digested swine manure, T. Asae (2005) 48: págs. 1943-1949.

[85] J.I. Houghton, T. Stephenson, Effect of influent organic content on digested sludge extracellular polymer content and dewaterability, Water Res. (2002) 36: 3620-3628.

[86] S. Xie, Evaluation of biogas production from anaerobic digestion of pig manure and grass silage, National University of Ireland, Galway (2012).

[87] M.P. Bernal, J.A. Alburquerque, R. Moral, Composting of animal manures and chemical criteria for compost maturity assessment. a review, Bioresour. Technol. (2009) 100: 5444-5453.

[88] G.H. Li, H.G. Li, P.A. Leffelaar, J.B. Shen, F.S. Zhang, Characterization of phosphorus in animal manures collected from three (dairy, swine, and broiler) farms in China, Plos. One (2014) 9.

[89] R. Nkoa, Agricultural benefits and environmental risks of soil fertilization with anaerobic digestates: a review, Agron. Sustain. Dev. (2013) 34: 473-492.

[90] R. Zhang, H.M. El-Mashad, K. Hartman, F. Wang, G. Liu, C. Choate, P. Gamble, Characterization of food waste as feedstock for anaerobic digestion, Bioresour. Technol. (2007) 98: 929-935.

[91] O. Oenema, A. Bannink, S.G. Sommer, J. Van Groenigen, G. Velthof, Gaseous nitrogen emissions from livestock farming systems, nitrogen in the environment: sources, problems, and management, second edition, JL Hatfield & RF Follett (Eds.) Acad. Press, Amsterdam (2008) 395-441.

[92] M.L. Daumer, S. Picard, P. Saint-Cast, P. Dabert, Technical and economical assessment of formic acid to recycle phosphorus from pig slurry by a combined acidification-precipitation process, J. Hazard. Mater. (2010) 180: 361-365.

[93] M.S. Romero-Güiza, S. Astals, J.M. Chimenos, M. Martínez, J. Mata-Alvarez, Improving anaerobic digestion of pig manure by adding in the same reactor a stabilizing agent formulated with low-grade magnesium oxide, Biomass Bioenergy (2014) 67: 243-251.

[94] C.Y. Lin, C.H. Lay, Effects of carbonate and phosphate concentrations on hydrogen production using anaerobic sewage sludge microflora, Int. J. Hydrogen Energy (2004) 29: 275-281.

[95] A. Zarebska, D. Romero Nieto, K.V. Christensen, L. Fjerbæk Søtoft, B. Norddahl, Ammonium fertilizers production from manure: a critical review, Crit. Rev. Env. Sci. Technol (2015) 45: 1469-1521.

[96] W. Powers, L. Flatow, Flocculation of swine manure: influence of flocculant, rate of addition, and diet, in: 2002 ASAE Annual Meeting, American Society of Agricultural and Biological Engineers, pp (2002).

[97] J. Sherman, H. Van Horn, R. Nordstedt, Use of flocculants in dairy wastewaters to remove phosphorus, Appl. Eng. Agr. (2000) 16: 445.

[98] H. Moller, J.D. Hansen, C. Sorensen, Nutrient recovery by solid-liquid separation and methane productivity of solids, T. Asae (2007) 50: 193-200.

[99] R. Sneath, M. Shaw, A. Williams, Centrifugation for separating piggery slurry 1. The performance of a decanting centrifuge, J. Agr. Eng. Res. (1988) 39: 181-190.

[100] P.A. Vadas, Distribution of phosphorus in manure slurry and its infiltration after application to soils, J. Environ. Quality (2006) 35: 542-547.

[101] Stephen Gilkinson, P. Frost, Evaluation of mechanical separation of pig and cattle slurries by a decanting centrifuge and a brushed screen separator, in, Agri-Food and Biosciences Institute, Hillsborough, Northern Ireland, (2007).

[102] C.H. Burton, C. Turner, Manure management: treatment strategies for sustainable agriculture, Editions Quae, 2003.

[103] R.D. Holmberg, D. Hill, T. Prince, N. Van Dyke, Potential of solid-liquid separation of swine wastes for methane production, T. Asae (1983) 26: 1803-1807.

[104] J. Pieters, G. Neukermans, M. Colanbeen, Farm-scale membrane filtration of sow slurry, J. Agr. Eng. Res. (1999) 73: 403-409.

[105] R. Hegg, R. Larson, J. Moore, Mechanical liquid-solid separation in beef, dairy and swine waste slurries, T. ASAE (1981) 24: 159-0163.

[106] H.B. Møller, S.G. Sommer, B.K. Ahring, Separation efficiency and particle size distribution in relation to manure type and storage conditions, Bioresour. Technol. (2002) 85: 189-196.

[107] Z. Wu, Phosphorus and nitrogen distribution of screw press separated dairy manure with recovery of bedding material, Appl. Eng. Agr. (2007) 23: 757-762.

[108] P.M. Ndegwa, J. Zhu, A. Luo, Effects of solid levels and chemical additives on removal of solids and phosphorus in swine manure, J. Environ. Eng. (2001) 127: 1111-1115.

[109] D. Meyer, P. Ristow, M. Lie, Particle size and nutrient distribution in fresh dairy manure, Appl. Eng. Agr. (2007) 23: 113-118.

[110] M. Hjorth, M.L. Christensen, Evaluation of methods to determine flocculation procedure for manure separation, T. Asabe (2008) 51: 2093-2103.

[111] S.G. Sommer, S. Génermont, P. Cellier, N.J. Hutchings, J.E. Olesen, T. Morvan, Processes controlling ammonia emission from livestock slurry in the field, Eur. J. Agron. (2003) 19: 465-486.

[112] J.R. Köster, K. Dittert, K.-H. Mühling, H. Kage, A. Pacholski, Cold season ammonia emissions from land spreading with anaerobic digestates from biogas production, Atmos. Environ. (2014) 84: 35-38.

[113] D. Fangueiro, H. Ribeiro, J. Coutinho, L. Cardenas, H. Trindade, C. Cunha-Queda, E. Vasconcelos, F. Cabral, Nitrogen mineralization and CO_2 and N_2O emissions in a sandy soil amended with original or acidified pig slurries or with the relative fractions, Biol. Fert. Soils (2010) 46: 383-391.

[114] J. Eriksen, A.J. Andersen, H.V. Poulsen, A.P.S. Adamsen, S.O. Petersen, Sulfur turnover and emissions during storage of cattle slurry: effects of acidification and sulfur addition, J. Environ. Quality (2012) 41: 1633-1641.

[115] M. Hjorth, G. Cocolo, K. Jonassen, S.G. Sommer, Acidifications effect on transformations in and composition of animal slurry, in: RAMIRAN 2013-15th International Conference, pp (2013).

[116] S.O. Petersen, A.J. Andersen, J. Eriksen, Effects of cattle slurry acidification on ammonia and methane evolution during storage, J. Environ. Quality (2012) 41: 88-94.

[117] P. Kai, P. Pedersen, J.E. Jensen, M.N. Hansen, S.G. Sommer, A whole-farm assessment of the efficacy of slurry acidification in reducing ammonia emissions, Eur. J. Agron. (2008) 28: 148-154.

[118] P. Sørensen, J. Eriksen, Effects of slurry acidification with sulphuric acid combined with aeration on the turnover and plant availability of nitrogen, Agr. Ecosyst. Environ. (2009) 131: 240-246.

[119] L. Zeng, C. Mangan, X. Li, Ammonia recovery from anaerobically digested cattle manure by steam stripping, Water Sci. Technol. (2006) 54: 137-145.

[120] P. Liao, A. Chen, K. Lo, Removal of nitrogen from swine manure wastewaters by ammonia stripping, Bioresour. Technol. (1995) 54: 17-20.

[121] X. Li, J. Guo, R. Dong, B.K. Ahring, W. Zhang, Properties of plant nutrient: Comparison of two nutrient recovery techniques using liquid fraction of digestate from anaerobic digester treating pig manure, Sci. Total Environ. (2016) 544: 774-781.

[122] K.S. Le Corre, E. Valsami-Jones, P. Hobbs, S.A. Parsons, Phosphorus recovery from wastewater by sruvite crystallization: a review, Crit. Rev. Env. Sci. Technol. (2009) 39: 433-477.

[123] A. Capdevielle, E. Sykorova, B. Biscans, F. Beline, M.L. Daumer, Optimization of struvite precipitation in synthetic biologically treated swine wastewater--determination of the optimal process parameters, J. Hazard. Mater. (2013) 244-245: 357-369.

[124] W. Tao, K.P. Fattah, M.P. Huchzermeier, Struvite recovery from anaerobically digested dairy manure: A review of application potential and hindrances, J. Environ. Manage. (2016) 169: 46-57.

[125] M. Cerrillo, J. Palatsi, J. Comas, J. Vicens, A. Bonmatí, Struvite precipitation as a technology to be integrated in a manure anaerobic digestion treatment plant - removal efficiency, crystal characterization and agricultural assessment, J. Chem. Technol. Biot. (2015) 90: 1135-1143.

[126] T. Tervahauta, R.D. van der Weijden, R.L. Flemming, L. Hernandez Leal, G. Zeeman, C.J. Buisman, Calcium phosphate granulation in anaerobic treatment of black water: a new approach to phosphorus recovery, Water Res. (2014) 48: 632-642.

[127] S. Guštin, R. Marinšek-Logar, Effect of pH, temperature and air flow rate on the continuous ammonia stripping of the anaerobic digestion effluent, Process Saf. Environ. (2011) 89: 61-66.

[128] J. Bousek, D. Scroccaro, J. Sima, N. Weissenbacher, W. Fuchs, Influence of the gas composition on the efficiency of ammonia stripping of biogas digestate, Bioresour. Technol. (2016) 203: 259-266.

[129] W. Tao, A.T. Ukwuani, Coupling thermal stripping and acid absorption for ammonia recovery from dairy manure: Ammonia volatilization kinetics and effects of temperature, pH and dissolved solids content, Chem. Eng. J. (2015) 280: 188-196.

[130] Q.-B. Zhao, J. Ma, I. Zeb, L. Yu, S. Chen, Y.-M. Zheng, C. Frear, Ammonia recovery from anaerobic digester effluent through direct aeration, Chem. Eng. J. (2015) 279: 31-37.

[131] X. Lei, N. Sugiura, C. Feng, T. Maekawa, Pretreatment of anaerobic digestion effluent with ammonia stripping and biogas purification, J. Hazard. Mater. (2007) 145: 391-397.

[132] A. Limoli, M. Langone, G. Andreottola, Ammonia removal from raw manure digestate by means of a turbulent mixing stripping process, J. Environ. Manage. (2016) 176: 1-10.

[133] S. Kataki, H. West, M. Clarke, D.C. Baruah, Phosphorus recovery as struvite from farm, municipal and industrial waste: Feedstock suitability, methods and pre-treatments, Waste Manage. (2016) 49: 437-454.

[134] Y.H. Song, G.L. Qiu, P. Yuan, X.Y. Cui, J.F. Peng, P. Zeng, L. Duan, L.C. Xiang, F. Qian, Nutrients removal and recovery from anaerobically digested swine wastewater by struvite crystallization without chemical additions, J. Hazard. Mater. (2011) 190: 140-149.

[135] C. Vaneeckhaute, A.T. Zeleke, F.M.G. Tack, E. Meers, Comparative Evaluation of Pre-treatment Methods to Enhance Phosphorus Release from Digestate, Waste Biomass Valori. (2016) 8: 659-667.

[136] Y. Shen, J. Ogejo, K. Bowers, Abating the effects of calcium on struvite precipitation in liquid dairy manure, T. Asabe (2011) 54: 325-336.

[137] H. Zhang, V.K. Lo, J.R. Thompson, F.A. Koch, P.H. Liao, S. Lobanov, D.S. Mavinic, J.W. Atwater, Recovery of phosphorus from dairy manure: a pilot-scale study, Environ. Technol. (2015) 36: 1398-1404.

[138] X. Guo, L. Zeng, X. Li, H.S. Park, Removal of ammonium from RO permeate of anaerobically digested wastewater by natural zeolite, Sep. Sci. Technol. (2007) 42: 3169-3185.

[139] B. Tao, J. Donnelly, I. Oliveira, R. Anthony, V. Wilson, S.R. Esteves, Enhancement of microbial density and methane production in advanced anaerobic digestion of secondary sewage sludge by continuous removal of ammonia, Bioresource Technol. (2017) 232: 380-388.

[140] C. Takaya, L. Fletcher, S. Singh, K. Anyikude, A. Ross, Phosphate and ammonium sorption capacity of biochar and hydrochar from different wastes, Chemosphere (2016) 145: 518-527.

[141] S. Kizito, S. Wu, W.K. Kirui, M. Lei, Q. Lu, H. Bah, R. Dong, Evaluation of slow pyrolyzed wood and rice husks biochar for adsorption of ammonium nitrogen from piggery manure anaerobic digestate slurry, Sci. Total Environ. (2015) 505: 102-112.

[142] L. Masse, D. Masse, Y. Pellerin, The effect of pH on the separation of manure nutrients with reverse osmosis membranes, J. Membr. Sci. (2008) 325: 914-919.

[143] M.L. Gerardo, N.H. Aljohani, D.L. Oatley-Radcliffe, R.W. Lovitt, Moving towards sustainable resources: recovery and fractionation of nutrients from dairy manure digestate using membranes, Water Res. (2015) 80: 80-89.

[144] S. Carretier, G. Lesage, A. Grasmick, M. Heran, Water and nutrients recovering from livestock manure by membrane processes, Can. J. Chem. Eng. (2015) 93: 225-233.

[145] D. Karakashev, J.E. Schmidt, I. Angelidaki, Innovative process scheme for removal of organic matter, phosphorus and nitrogen from pig manure, Water Res. (2008) 42: 4083-4090.

[146] M.-J. Luján-Facundo, J.-A. Mendoza-Roca, B. Cuartas-Uribe, S. Álvarez-Blanco, Membrane fouling in whey processing and subsequent cleaning with ultrasounds for a more sustainable process, J. Clean Prod. (2017) 143: 804-813.

[147] X. Shi, G. Tal, N.P. Hankins, V. Gitis, Fouling and cleaning of ultrafiltration membranes: a review, J. Water Process Eng. (2014) 1: 121-138.

[148] J. Mulder, Basic principles of membrane technology, Springer Science & Business Media, 2012.

[149] L. Shi, Y. Hu, S. Xie, G. Wu, Z. Hu, X. Zhan, Recovery of nutrients and volatile fatty acids from pig manure hydrolysate using two-stage bipolar membrane electrodialysis, Chem. Eng. J. (2018) 334: 134-142.

[150] P. Wang, T.-S. Chung, Recent advances in membrane distillation processes: Membrane development, configuration design and application exploring, J. Membr. Sci. (2015) 474: 39-56.

[151] J.L. Soler-Cabezas, J.A. Mendoza-Roca, M.C. Vincent-Vela, M.J. Luján-Facundo, L. Pastor-Alcañiz, Simultaneous concentration of nutrients from anaerobically digested sludge centrate and pre-treatment of industrial effluents by forward osmosis, Sep. Purif. Technol. (2018) 193: 289-296.

[152] D. Ippersiel, M. Mondor, F. Lamarche, F. Tremblay, J. Dubreuil, L. Masse, Nitrogen potential recovery and concentration of ammonia from swine manure using electrodialysis coupled with air stripping, J. Environ. Manage. (2012) 95 Suppl: S165-169.

[153] R. Liu, Y. Wang, G. Wu, J. Luo, S. Wang, Development of a selective electrodialysis for nutrient recovery and desalination during secondary effluent treatment, Chem. Eng. J. (2017) 322: 224-233.

[154] Y. Zhang, E. Desmidt, A. Van Looveren, L. Pinoy, B. Meesschaert, B. Van der Bruggen, Phosphate separation and recovery from wastewater by novel electrodialysis, Environ. Sci. Technol. (2013) 47: 5888-5895.

[155] N.B. Goodman, R.J. Taylor, Z. Xie, Y. Gozukara, A. Clements, A feasibility study of municipal wastewater desalination using electrodialysis reversal to provide recycled water for horticultural irrigation, Desalination (2013) 317: 77-83.

[156] K. Yadav, K. Morison, M.P. Staiger, Effects of hypochlorite treatment on the surface morphology and mechanical properties of polyethersulfone ultrafiltration membranes, Polym. Degrad. Stabil. (2009) 94: 1955-1961.

[157] Q. He, G. Yu, W. Wang, S. Yan, Y. Zhang, S. Zhao, Once-through CO 2 absorption for simultaneous biogas upgrading and fertilizer production, Fuel Process Technol. (2017) 166: 50-58.

[158] S. Kim, D.W. Lee, J. Cho, Application of direct contact membrane distillation process to treat anaerobic digestate, J. Membr. Sci. (2016) 511: 20-28.

[159] Q. He, T. Tu, S. Yan, X. Yang, M. Duke, Y. Zhang, S. Zhao, Relating water vapor transfer to ammonia recovery from biogas slurry by vacuum membrane distillation, Sep. Purif. Technol. (2018) 191: 182-191.

[160] D.L. Shaffer, J.R. Werber, H. Jaramillo, S. Lin, M. Elimelech, Forward osmosis: Where are we now?, Desalination (2015) 356: 271-284.

[161] M. Xie, L.D. Nghiem, W.E. Price, M. Elimelech, Toward Resource Recovery from Wastewater: Extraction of Phosphorus from Digested Sludge Using a Hybrid Forward Osmosis–Membrane Distillation Process, Environ. Sci. Technol. Letters (2014) 1: 191-195.

[162] A.J. Ansari, F.I. Hai, W.E. Price, L.D. Nghiem, Phosphorus recovery from digested sludge centrate using seawater-driven forward osmosis, Sep. Purif. Technol. (2016) 163: 1-7.

[163] C. Vaneeckhaute, V. Lebuf, E. Michels, E. Belia, P.A. Vanrolleghem, F.M.G. Tack, E. Meers, Nutrient recovery from digestate: systematic technology review and product classification, Waste Biomass Valori. (2016) 8: 21-40.

[164] K.B. Cantrell, P.G. Hunt, M. Uchimiya, J.M. Novak, K.S. Ro, Impact of pyrolysis temperature and manure source on physicochemical characteristics of biochar, Bioresour. Technol. (2012) 107: 419-428.

[165] K.U. Suwelack, D. Wüst, P. Fleischmann, A. Kruse, Prediction of gaseous, liquid and solid mass yields from hydrothermal carbonization of biogas digestate by severity parameter, Biomass Convers. Bior. (2015) 6: 151-160.

[166] M. Toufiq Reza, A. Freitas, X. Yang, S. Hiibel, H. Lin, C.J. Coronella, Hydrothermal carbonization (HTC) of cow manure: carbon and nitrogen distributions in HTC products, Environ. Prog. Sustain. (2016) 35: 1002-1011.

[167] U. Ekpo, A.B. Ross, M.A. Camargo-Valero, L.A. Fletcher, Influence of pH on hydrothermal treatment of swine manure: Impact on extraction of nitrogen and phosphorus in process water, Bioresour. Technol. (2016) 214: 637-644.

[168] R. Huang, Y. Tang, Speciation Dynamics of Phosphorus during (Hydro)Thermal Treatments of Sewage Sludge, Environ. Sci. Technol. (2015) 49: 14466-14474.

[169] H. Kahiluoto, M. Kuisma, E. Ketoja, T. Salo, J. Heikkinen, Phosphorus in manure and sewage sludge more recyclable than in soluble inorganic fertilizer, Environ. Sci. Technol. (2015) 49: 2115-2122.

[170] K. Wu, Y. Gao, G. Zhu, J. Zhu, Q. Yuan, Y. Chen, M. Cai, L. Feng, Characterization of dairy manure hydrochar and aqueous phase products generated by hydrothermal carbonization at different temperatures, J. Anal. Appl. Pyrol. (2017) 127: 335-342.

[171] M. Nyström, Mobile biomass HTC-processing unit, (2016).

[172] M. Lucian, L. Fiori, Hydrothermal carbonization of waste biomass: process design, modeling, energy efficiency and cost analysis, Energies (2017) 10: 211.

[173] E. Sforza, E. Barbera, F. Girotto, R. Cossu, A. Bertucco, Anaerobic digestion of lipid-extracted microalgae: enhancing nutrient recovery towards a closed loop recycling, Biochem. Eng. J. (2017) 121: 139-146.

[174] M. Zhang, P.G. Lawlor, Z. Hu, X. Zhan, Nutrient removal from separated pig manure digestate liquid using hybrid biofilters, Environ. Technol. (2013) 34: 645-651.

[175] K. Carney, M. Rodgers, P. Lawlor, X. Zhan, Treatment of separated piggery anaerobic digestate liquid using woodchip biofilters, Environ. Technol. (2013) 34: 663-670.

[176] M. Zhang, P.G. Lawlor, G. Wu, B. Lynch, X. Zhan, Partial nitrification and nutrient removal in intermittently aerated sequencing batch reactors treating separated digestate liquid after anaerobic digestion of pig manure, Bioproc. Biosyst. Eng. (2011) 34: 1049-1056.

[177] R.P. Tasho, J.Y. Cho, Veterinary antibiotics in animal waste, its distribution in soil and uptake by plants: a review, Sci. Total Environ. (2016) 563-564: 366-376.

[178] Y.M. Awad, S.-C. Kim, S.A.M. Abd El-Azeem, K.-H. Kim, K.-R. Kim, K. Kim, C. Jeon, S.S. Lee, Y.S. Ok, Veterinary antibiotics contamination in water, sediment, and soil near a swine manure composting facility, Environ. Earth Sci. (2013) 71: 1433-1440.

[179] X. Liu, H. Zhang, L. Li, C. Fu, C. Tu, Y. Huang, L. Wu, J. Tang, Y. Luo, P. Christie, Levels, distributions and sources of veterinary antibiotics in the sediments of the Bohai Sea in China and surrounding estuaries, Mar. Pollut. Bull. (2016) 109: 597-602.

[180] N. Li, K.W.K. Ho, G.G. Ying, W.J. Deng, Veterinary antibiotics in food, drinking water, and the urine of preschool children in Hong Kong, Environ. Int. (2017) 108: 246-252.

[181] X. Liu, J.C. Steele, X.Z. Meng, Usage, residue, and human health risk of antibiotics in Chinese aquaculture: A review, Environ. Pollut. (2017) 223: 161-169.

[182] C. Li, J. Chen, J. Wang, Z. Ma, P. Han, Y. Luan, A. Lu, Occurrence of antibiotics in soils and manures from greenhouse vegetable production bases of Beijing, China and an associated risk assessment, Sci. Total Environ. (2015) 521-522: 101-107.

[183] P. Grenni, V. Ancona, A. Barra Caracciolo, Ecological effects of antibiotics on natural ecosystems: a review, Microchem. J. (2018) 136: 25-39.

[184] ESVAC-Sales of veterinary antimicrobial agents in 30 European countries in 2016, trends from 2010 to 2016, European Medicines Agency, (2018).

[185] A. Spielmeyer, J. Ahlborn, G. Hamscher, Simultaneous determination of 14 sulfonamides and tetracyclines in biogas plants by liquid-liquid-extraction and liquid chromatography tandem mass spectrometry, Analyt. Bioanalyt. Chem. (2014) 406: 2513-2524.

[186] J.A. Alvarez, L. Otero, J.M. Lema, F. Omil, The effect and fate of antibiotics during the anaerobic digestion of pig manure, Bioresour. Technol. (2010) 101: 8581-8586.

[187] J.S. Wallace, E. Garner, A. Pruden, D.S. Aga, Occurrence and transformation of veterinary antibiotics and antibiotic resistance genes in dairy manure treated by advanced

anaerobic digestion and conventional treatment methods, Environ. Pollut. (2018) 236: 764-772.

[188] A. Spielmeyer, B. Breier, K. Groissmeier, G. Hamscher, Elimination patterns of worldwide used sulfonamides and tetracyclines during anaerobic fermentation, Bioresour. Technol. (2015) 193: 307-314.

[189] X. Wu, Y. Wei, J. Zheng, X. Zhao, W. Zhong, The behavior of tetracyclines and their degradation products during swine manure composting, Bioresour. Technol. (2011) 102: 5924-5931.

[190] L. Feng, M.E. Casas, L.D.M. Ottosen, H.B. Møller, K. Bester, Removal of antibiotics during the anaerobic digestion of pig manure, Sci. Total Environ. (2017) 603-604: 219-225.

[191] W. Ben, Y. Shi, W. Li, Y. Zhang, Z. Qiang, Oxidation of sulfonamide antibiotics by chlorine dioxide in water: Kinetics and reaction pathways, Chem. Eng. J. (2017) 327: 743-750.

[192] F. Yu, Y. Li, S. Han, J. Ma, Adsorptive removal of antibiotics from aqueous solution using carbon materials, Chemosphere (2016) 153: 365-385.

[193] S.M. Mitchell, J.L. Ullman, A.L. Teel, R.J. Watts, C. Frear, The effects of the antibiotics ampicillin, florfenicol, sulfamethazine, and tylosin on biogas production and their degradation efficiency during anaerobic digestion, Bioresour. Technol. (2013) 149: 244-252.

[194] R. Zhang, J. Gu, X. Wang, X. Qian, M. Duan, W. Sun, Y. Zhang, H. Li, Y. Li, Relationships between sulfachloropyridazine sodium, zinc, and sulfonamide resistance genes during the anaerobic digestion of swine manure, Bioresour. Technol. (2017) 225: 343-348.

[195] H. Lin, J. Zhang, H. Chen, J. Wang, W. Sun, X. Zhang, Y. Yang, Q. Wang, J. Ma, Effect of temperature on sulfonamide antibiotics degradation, and on antibiotic resistance determinants and hosts in animal manures, Sci. Total Environ. (2017) 607-608: 725-732.

[196] O.A. Arikan, Degradation and metabolization of chlortetracycline during the anaerobic digestion of manure from medicated calves, J. Hazard. Mater. (2008) 158: 485-490.

[197] V. Varel, J. Wells, W. Shelver, C. Rice, D. Armstrong, D. Parker, Effect of anaerobic digestion temperature on odour, coliforms and chlortetracycline in swine manure or monensin in cattle manure, J. Applied Microbiol. (2012) 112: 705-715.

[198] F. Yin, H. Dong, C. Ji, X. Tao, Y. Chen, Effects of anaerobic digestion on chlortetracycline and oxytetracycline degradation efficiency for swine manure, Waste Manage. (2016) 56: 540-546.

[199] F. Yin, H. Dong, W. Zhang, Z. Zhu, B. Shang, Antibiotic degradation and microbial community structures during acidification and methanogenesis of swine manure

containing chlortetracycline or oxytetracycline, Bioresour. Technol. (2018) 250: 247-255.

[200] Ç. Akyol, O. Ince, Z. Cetecioglu, F.U. Alkan, B. Ince, The fate of oxytetracycline in two ‐ phase and single ‐ phase anaerobic cattle manure digesters and its effects on microbial communities, J. Chem. Technol. Biot. (2016) 91: 806-814.

[201] Y. Bao, Q. Zhou, L. Guan, Y. Wang, Depletion of chlortetracycline during composting of aged and spiked manures, Waste Manage. (2009) 29: 1416-1423.

[202] M.B. Ahmed, J.L. Zhou, H.H. Ngo, W. Guo, N.S. Thomaidis, J. Xu, Progress in the biological and chemical treatment technologies for emerging contaminant removal from wastewater: A critical review, J. Hazard. Mater. (2017) 323: 274-298.

[203] R. Han, D. Ding, Y. Xu, W. Zou, Y. Wang, Y. Li, L. Zou, Use of rice husk for the adsorption of congo red from aqueous solution in column mode, Bioresour. Technol. (2008) 99: 2938-2946.

[204] V. Homem, L. Santos, Degradation and removal methods of antibiotics from aqueous matrices–a review, J. Environmental Manage. (2011) 92: 2304-2347.

[205] M.B. Ahmed, J.L. Zhou, H.H. Ngo, W. Guo, Adsorptive removal of antibiotics from water and wastewater: Progress and challenges, Sci. Total Environ. (2015) 532: 112-126.

[206] A. Deegan, B. Shaik, K. Nolan, K. Urell, M. Oelgemöller, J. Tobin, A. Morrissey, Treatment options for wastewater effluents from pharmaceutical companies, Int. J. Environ. Sci. Technol. (2011) 8: 649-666.

[207] Y. Luo, W. Guo, H.H. Ngo, L.D. Nghiem, F.I. Hai, J. Zhang, S. Liang, X.C. Wang, A review on the occurrence of micropollutants in the aquatic environment and their fate and removal during wastewater treatment, Sci. Total Environ. (2014) 473-474: 619-641.

[208] V. Yangali-Quintanilla, S.K. Maeng, T. Fujioka, M. Kennedy, Z. Li, G. Amy, Nanofiltration vs. reverse osmosis for the removal of emerging organic contaminants in water reuse, Desalin. Water Treat. (2011) 34: 50-56.

[209] M. Röhricht, J. Krisam, U. Weise, U.R. Kraus, R.A. Düring, Elimination of carbamazepine, diclofenac and naproxen from treated wastewater by nanofiltration, CLEAN–Soil, Air, Water (2009) 37: 638-641.

[210] E. Sahar, I. David, Y. Gelman, H. Chikurel, A. Aharoni, R. Messalem, A. Brenner, The use of RO to remove emerging micropollutants following CAS/UF or MBR treatment of municipal wastewater, Desalination (2011) 273: 142-147.

[211] C. Comninellis, A. Kapalka, S. Malato, S.A. Parsons, I. Poulios, D. Mantzavinos, Advanced oxidation processes for water treatment: advances and trends for R&D, J. Chem. Technol. Biotechnol. (2008) 83: 769-776.

[212] I.A. Balcıoğlu, M. Ötker, Treatment of pharmaceutical wastewater containing antibiotics by O3 and O3/H2O2 processes, Chemosphere (2003) 50: 85-95.

[213] J.L. Wang, L.J. Xu, Advanced oxidation processes for wastewater treatment: formation of hydroxyl radical and application, Crit. Rev. Env. Sci. Technol. (2012) 42: 251-325.

[214] J. Wang, S. Wang, Removal of pharmaceuticals and personal care products (PPCPs) from wastewater: A review, J. Environ. Manage. (2016) 182: 620-640.

[215] W.-L. Wang, Q.-Y. Wu, N. Huang, T. Wang, H.-Y. Hu, Synergistic effect between UV and chlorine (UV/chlorine) on the degradation of carbamazepine: Influence factors and radical species, Water Res. (2016) 98: 190-198.

[216] W.L. Wang, X. Zhang, Q.Y. Wu, Y. Du, H.Y. Hu, Degradation of natural organic matter by UV/chlorine oxidation: Molecular decomposition, formation of oxidation byproducts and cytotoxicity, Water Res. (2017) 124: 251-258.

[217] C. Noutsopoulos, E. Koumaki, D. Mamais, M.-C. Nika, A.A. Bletsou, N.S. Thomaidis, Removal of endocrine disruptors and non-steroidal anti-inflammatory drugs through wastewater chlorination: the effect of pH, total suspended solids and humic acids and identification of degradation by-products, Chemosphere (2015) 119: S109-S114.

[218] D. Vogna, R. Marotta, A. Napolitano, R. Andreozzi, M. d'Ischia, Advanced oxidation of the pharmaceutical drug diclofenac with UV/H2O2 and ozone, Water Res. (2004) 38: 414-422.

[219] J. Ratcliff, A. Wan, M. Edwards, A. Soler-Vila, M. Johnson, M.H. Abreu, L. Morrison, Metal content of kelp (Laminaria digitata) co-cultivated with Atlantic salmon in an integrated multi-trophic aquaculture system, Aquaculture (2016) 450: 234-243.

[220] M. Healy, P. Ryan, O. Fenton, D. Peyton, D. Wall, L. Morrison, Bioaccumulation of metals in ryegrass (Lolium perenne L.) following the application of lime stabilised, thermally dried and anaerobically digested sewage sludge, Ecotox. Environ. Safe. (2016) 130: 303-309.

[221] J. Kamcev, R. Sujanani, E.-S. Jang, N. Yan, N. Moe, D.R. Paul, B.D. Freeman, Salt concentration dependence of ionic conductivity in ion exchange membranes, J. Membr. Sci. (2018) 547: 123-133.

[222] M. Mondor, D. Ippersiel, F. Lamarche, L. Masse, Fouling characterization of electrodialysis membranes used for the recovery and concentration of ammonia from swine manure, Bioresour. Technol. (2009) 100: 566-571.

[223] K.R. Murphy, K.D. Butler, R.G. Spencer, C.A. Stedmon, J.R. Boehme, G.R. Aiken, Measurement of dissolved organic matter fluorescence in aquatic environments: an interlaboratory comparison, Environ. Sci. Technol. (2010) 44: 9405-9412.

[224] A.J. Lawaetz, C. Stedmon, Fluorescence intensity calibration using the Raman scatter peak of water, Appl. Spectrosc. (2009) 63: 936-940.

[225] T. Xu, Z. Liu, W. Yang, Fundamental studies of a new series of anion exchange membranes: membrane prepared from poly(2,6-dimethyl-1,4-phenylene oxide) (PPO) and triethylamine, J. Membr. Sci. (2005) 249: 183-191.

[226] Y. Li, S. Shi, H. Cao, X. Wu, Z. Zhao, L. Wang, Bipolar membrane electrodialysis for generation of hydrochloric acid and ammonia from simulated ammonium chloride wastewater, Water Res. (2016) 89: 201-209.

[227] J. Shen, J. Huang, L. Liu, W. Ye, J. Lin, B. Van der Bruggen, The use of BMED for glyphosate recovery from glyphosate neutralization liquor in view of zero discharge, J. Hazard. Mater. (2013) 260: 660-667.

[228] E.D. Belashova, N.D. Pismenskaya, V.V. Nikonenko, P. Sistat, G. Pourcelly, Current-voltage characteristic of anion-exchange membrane in monosodium phosphate solution. Modelling and experiment, J. Membr. Sci. (2017) 542: 177-185.

[229] E.D. Melnikova, N.D. Pismenskaya, L. Bazinet, S. Mikhaylin, V.V. Nikonenko, Effect of ampholyte nature on current-voltage characteristic of anion-exchange membrane, Electrochimica Acta (2018) 285: 185-191.

[230] L. Xu, F. Dong, H. Zhuang, W. He, M. Ni, S.-P. Feng, P.-H. Lee, Energy upcycle in anaerobic treatment: Ammonium, methane, and carbon dioxide reformation through a hybrid electrodeionization–solid oxide fuel cell system, Energ. Convers. Manage. (2017) 140: 157-166.

[231] S.A. Baghoth, S.K. Sharma, G.L. Amy, Tracking natural organic matter (NOM) in a drinking water treatment plant using fluorescence excitation-emission matrices and PARAFAC, Water Res. (2011) 45: 797-809.

[232] L. Yang, J. Hur, W. Zhuang, Occurrence and behaviors of fluorescence EEM-PARAFAC components in drinking water and wastewater treatment systems and their applications: a review, Environ. Sci. Pollut. Res. (2015) 22: 6500-6510.

[233] S. Mikhaylin, L. Bazinet, Fouling on ion-exchange membranes: Classification, characterization and strategies of prevention and control, Adv. Colloid Interfac. Sci. (2016) 229: 34-56.

[234] B.C. Huang, Y.F. Guan, W. Chen, H.Q. Yu, Membrane fouling characteristics and mitigation in a coagulation-assisted microfiltration process for municipal wastewater pretreatment, Water Res. (2017) 123: 216-223.

[235] A.A. Maldonado, J.M. Ribeiro, A. Sillero, Isoelectric point, electric charge, and nomenclature of the acid–base residues of proteins, Biochem. Mol. Biol. Edu. (2010) 38: 230-237.

[236] E.A. Ghabbour, G. Davies, Humic substances: structures, models and functions, Royal Society of chemistry, 2007.

[237] Z. Zhao, S. Shi, H. Cao, B. Shan, Y. Sheng, Property characterization and mechanism analysis on organic fouling of structurally different anion exchange membranes in electrodialysis, Desalination (2018) 428: 199-206.

[238] J.N. Apell, T.H. Boyer, Combined ion exchange treatment for removal of dissolved organic matter and hardness, Water Res. (2010) 44: 2419-2430.

[239] K.M. Walker, T.H. Boyer, Long-term performance of bicarbonate-form anion exchange: removal of dissolved organic matter and bromide from the St. Johns River, FL, USA, Water Res. (2011) 45: 2875-2886.

[240] Y. Zhang, I. Angelidaki, Recovery of ammonia and sulfate from waste streams and bioenergy production via bipolar bioelectrodialysis, Water Res. (2015) 85: 177-184.

[241] Y. Zhang, I. Angelidaki, Submersible microbial desalination cell for simultaneous ammonia recovery and electricity production from anaerobic reactors containing high levels of ammonia, Bioresour. Technol. (2015) 177: 233-239.

[242] S. Xie, P.G. Lawlor, J.P. Frost, Z. Hu, X. Zhan, Effect of pig manure to grass silage ratio on methane production in batch anaerobic co-digestion of concentrated pig manure and grass silage, Bioresour. Technol. (2011) 102: 5728-5733.

[243] F.G. Wilhelm, Bipolar membrane electrodialysis-membrane development and transport characteristics, Twente University Press, 2001.

[244] J.-n. Shen, J. Yu, J. Huang, B. Van der Bruggen, Preparation of highly pure tetrapropyl ammonium hydroxide using continuous bipolar membrane electrodialysis, Chem. Eng. J. (2013) 220: 311-319.

[245] D.P. Holmes, Ammonia Air Stripping, in: Proceedings of the Water Environment Federation, (2003). 926-932.

[246] M. Ali, M. Rakib, S. Laborie, P. Viers, G. Durand, Coupling of bipolar membrane electrodialysis and ammonia stripping for direct treatment of wastewaters containing ammonium nitrate, J. Membr. Sci. (2004) 244: 89-96.

[247] B. Van der Bruggen, A. Koninckx, C. Vandecasteele, Separation of monovalent and divalent ions from aqueous solution by electrodialysis and nanofiltration, Water Res. (2004) 38: 1347-1353.

[248] J. Meng, L. Wang, X. Liu, J. Wu, P.C. Brookes, J. Xu, Physicochemical properties of biochar produced from aerobically composted swine manure and its potential use as an environmental amendment, Bioresour. Technol. (2013) 142: 641-646.

[249] G. Li, Determination and Correlation of Vapor–Liquid Equilibria for the Phosphoric Acid + Water + Cyclohexane + Ethanol System, J. Chem. Eng. Data (2017) 62: 1161-1167.

[250] P. Chang, W. Jiang, Z. Li, J. Jean, C. Kuo, Antibiotic tetracycline in the environments - a review, Res. Rev. J. Pharm. Analy. (2015).

[251] C. Zarfl, Chemical Fate of Sulfadiazine in Soil: Mechanisms and Modelling Approaches, Shaker, 2008.

[252] L. Shi, S. Xie, Z. Hu, G. Wu, L. Morrison, P. Croot, H. Hu, X. Zhan, Nutrient recovery from pig manure digestate using electrodialysis reversal: Membrane fouling and feasibility of long-term operation, J. Membr. Sci. (2019) 573: 560-569.

[253] D.H. Kim, S.-H. Moon, J. Cho, Investigation of the adsorption and transport of natural organic matter (NOM) in ion-exchange membranes, Desalination (2003) 151: 11-20.

[254] H.-J. Lee, D.H. Kim, J. Cho, S.-H. Moon, Characterization of anion exchange membranes with natural organic matter (NOM) during electrodialysis, Desalination (2003) 151: 43-52.

[255] T. Xu, C. Huang, Electrodialysis-based separation technologies: a critical review, AIChE J. (2008) 54: 3147-3159.

[256] F.C. Yen, S.J. You, T.C. Chang, Performance of electrodialysis reversal and reverse osmosis for reclaiming wastewater from high-tech industrial parks in Taiwan: A pilot-scale study, J. Environ. Manage. (2017) 187: 393-400.

[257] A.D. Khawaji, I.K. Kutubkhanah, J.-M. Wie, Advances in seawater desalination technologies, Desalination (2008) 221: 47-69.

[258] K. Duhrkop, M. Fleischauer, M. Ludwig, A.A. Aksenov, A.V. Melnik, M. Meusel, P.C. Dorrestein, J. Rousu, S. Bocker, SIRIUS 4: a rapid tool for turning tandem mass spectra into metabolite structure information, Nature Methods (2019) 16: 299-302.

[259] A. Cabeza, A. Urtiaga, M.-J. Rivero, I. Ortiz, Ammonium removal from landfill leachate by anodic oxidation, J. Hazard. Mater. (2007) 144: 715-719.

[260] G.J. Kirmeyer, Optimizing chloramine treatment, American Water Works Association, 2004.

[261] R.L. Jolley, J.H. Carpenter, Aqueous chemistry of chlorine: chemistry, analysis, and environmental fate of reactive oxidant species, in, Oak Ridge National Lab., TN (USA), pp (1982).

[262] Y. Yang, J. Jiang, X. Lu, J. Ma, Y. Liu, Production of sulfate radical and hydroxyl radical by reaction of ozone with peroxymonosulfate: a novel advanced oxidation process, Environ. Sci. Technol. (2015) 49: 7330-7339.

[263] Y. Ji, Y. Shi, L. Wang, J. Lu, C. Ferronato, J.M. Chovelon, Sulfate radical-based oxidation of antibiotics sulfamethazine, sulfapyridine, sulfadiazine, sulfadimethoxine, and sulfachloropyridazine: Formation of SO2 extrusion products and effects of natural organic matter, Sci. Total Environ. (2017) 593-594: 704-712.

[264] M.J. Celestine, L.S. Joseph, A.A. Holder, Kinetics and mechanism of the oxidation of a cobaloxime by sodium hypochlorite in aqueous solution: is it an outer-sphere mechanism?, Inorg. Chim. Acta (2017) 454: 254-265.

[265] E. Commission, Commission Regulation (EU) No 142/2011 of 25 February 2011 implementing Regulation (EC) No 1069/2009 of the European Parliament and of the Council laying down health rules as regards animal by‐products and derived products not intended for human consumption and implementing Council Directive 97/78/EC as regards certain samples and items exempt from veterinary checks at the border under that Directive, Off J Eur Commun (2011) 50: 1-254.

Appendix A

Coagulation and flocculation of pig manure

A.1 Acidification of pig manure

A.1.1 Zeta potential

As shown in Figure A-1, the zeta potentials of pig manure were measured in different pH conditions during acidification. The zeta potentials of pig manure were minus in the pH range of 2.0 – 7.5, showing that the colloidal particles in pig manure were negatively charged. It was found that the lower pH caused higher zeta potentials. The zeta potential became positive when the pH was higher than 2.0. However, pig manure cannot be acidified to such a low pH value in practice.

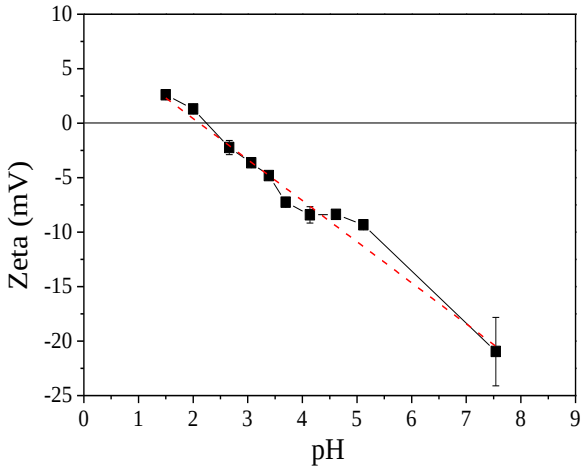

Figure A-1. Zeta potentials of pig manure in different pH conditions.

A.1.2 Nutrients and acetate

Figure A-2 shows the concentrations of nutrients and acetate in pig manure under different pH conditions. It was found that 90% of PO_4^{3-}-P was released to the liquid phase when the pH was lower than 6.0, and PO_4^{3-}-P was completely released to the liquid phase when the pH reached 5.5. The acidification process did not impact the concentration of NH_4^+-N in the liquid phase.

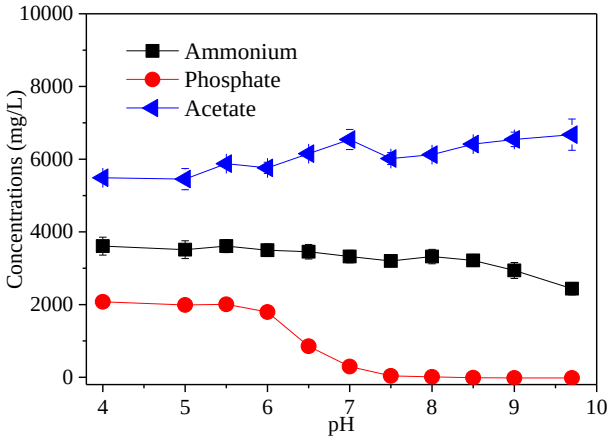

Figure A-2. The concentrations of nutrients and acetate in pig manure under different pH conditions.

A.1.3 Coagulation of pig manure

Figure A-3 shows the turbidity of pig manure with different dosage of ployaluminium chloride (PAC). It was observed that PAC did not work efficiently in the raw pig manure (pH=7.2), the turbidity could not decrease to a low level even if a very high dosage of PAC was applied. This was attributed to the carbonate in pig manure, which can react with PAC and generate CO_2 during the coagulation (Figure A-4). Using the acidified pig manure (pH=5.5), the turbidity was efficiently reduced to a very low level. However, up to 1200 mg/L of PAC were needed to support the coagulation (up to 3000 mg/L of aluminum sulfate were also tested), which is considered not cost-effective. In addition, the soluble P was removed due to the coagulation, which is unexpected for P recovery (Figure A-5).

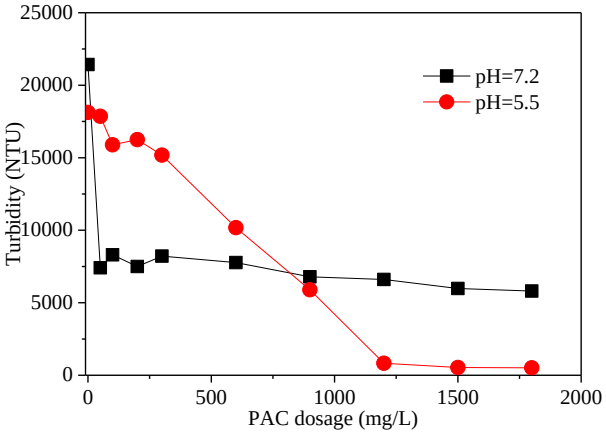

Figure A-3. Turbidity of pig manure with different dosage of PAC.

Note: The turbidity was measured after a series of dilution of pig manure.

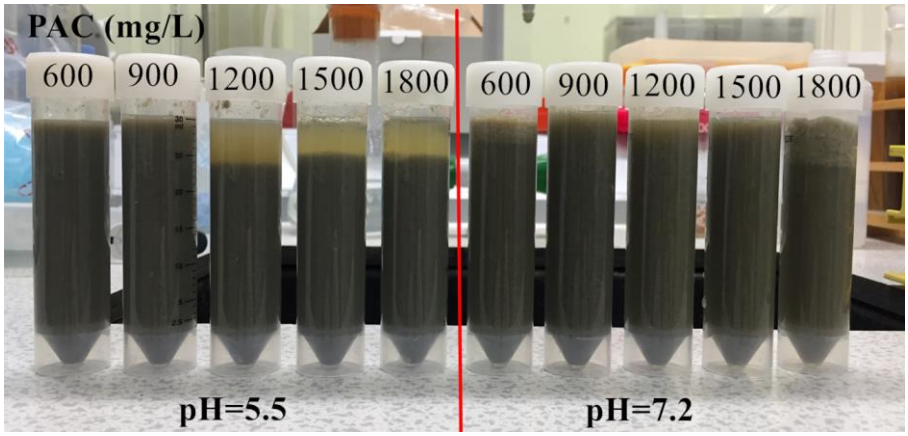

Figure A-4. Coagulation of pig manure using PAC.

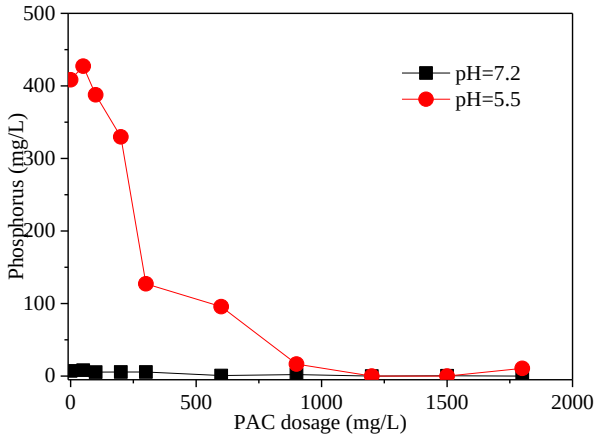

Figure A-5. Concentration of P in pig manure after coagulation with different dosage of PAC.

A.1.4 Flocculation of pig manure

Figure A-5 shows the turbidity of acidified pig manure after flocculation using polyacrylamide (PAM). The results showed that PAM was effective in the solids removal. However, PAM cannot reduce the turbidity to a very low level, because pig manure is rich in colloidal particles (Figure A-6). The separated liquid fraction of pig manure was still turbid. The nutrients all remained in the solutions.

Appendix

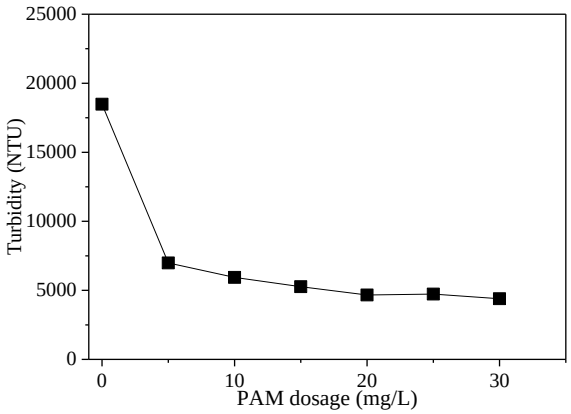

Figure A-5. Turbidity of pig manure with different dosage of PAM.

Figure A-6. Flocculation of acidified pig manure using 10 mg/L PAM.

Appendix B

HPLC-MS/MS spectra of intermediate products

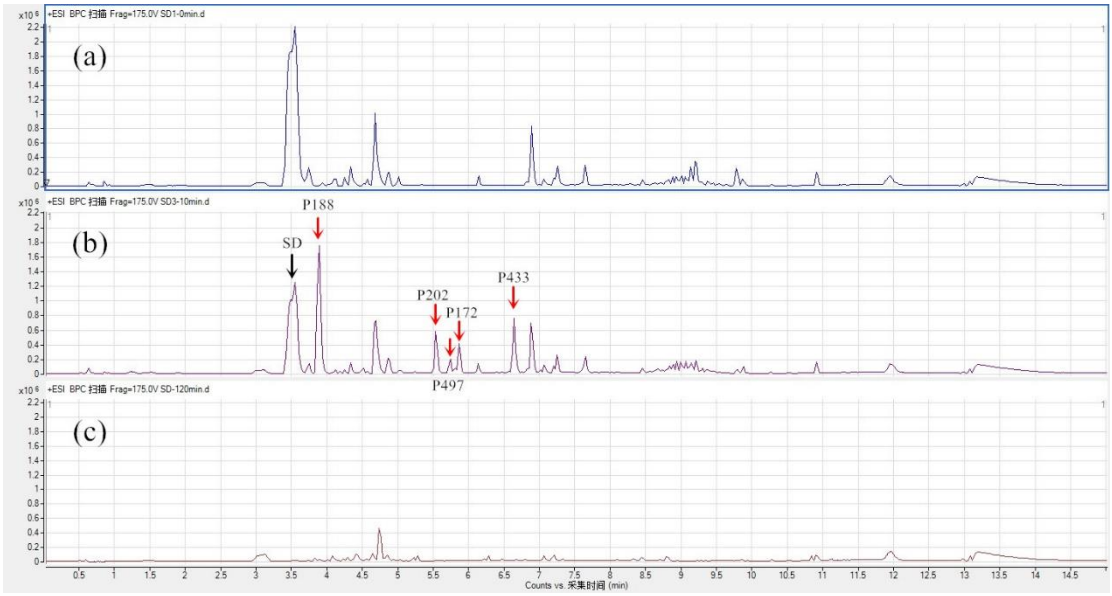

Figure B-1. Ion choromatography of samples during the oxidation of SD. (a) 0 min; (b) 10 min; (c) 120 min. The other peaks are background from the reator, HLB colums, and glassware.

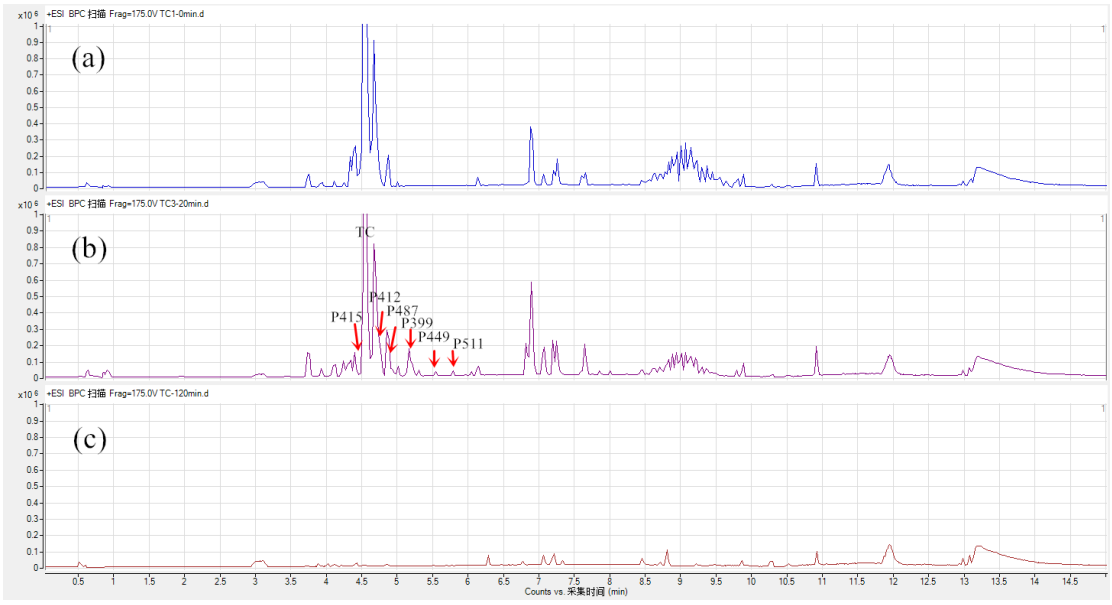

Figure B-2. Ion choromatography of samples during the oxidation of TC. (a) 0 min; (b) 20 min; (c) 120 min. The other peaks are background from the reator, HLB colums, and glassware.

Appendix

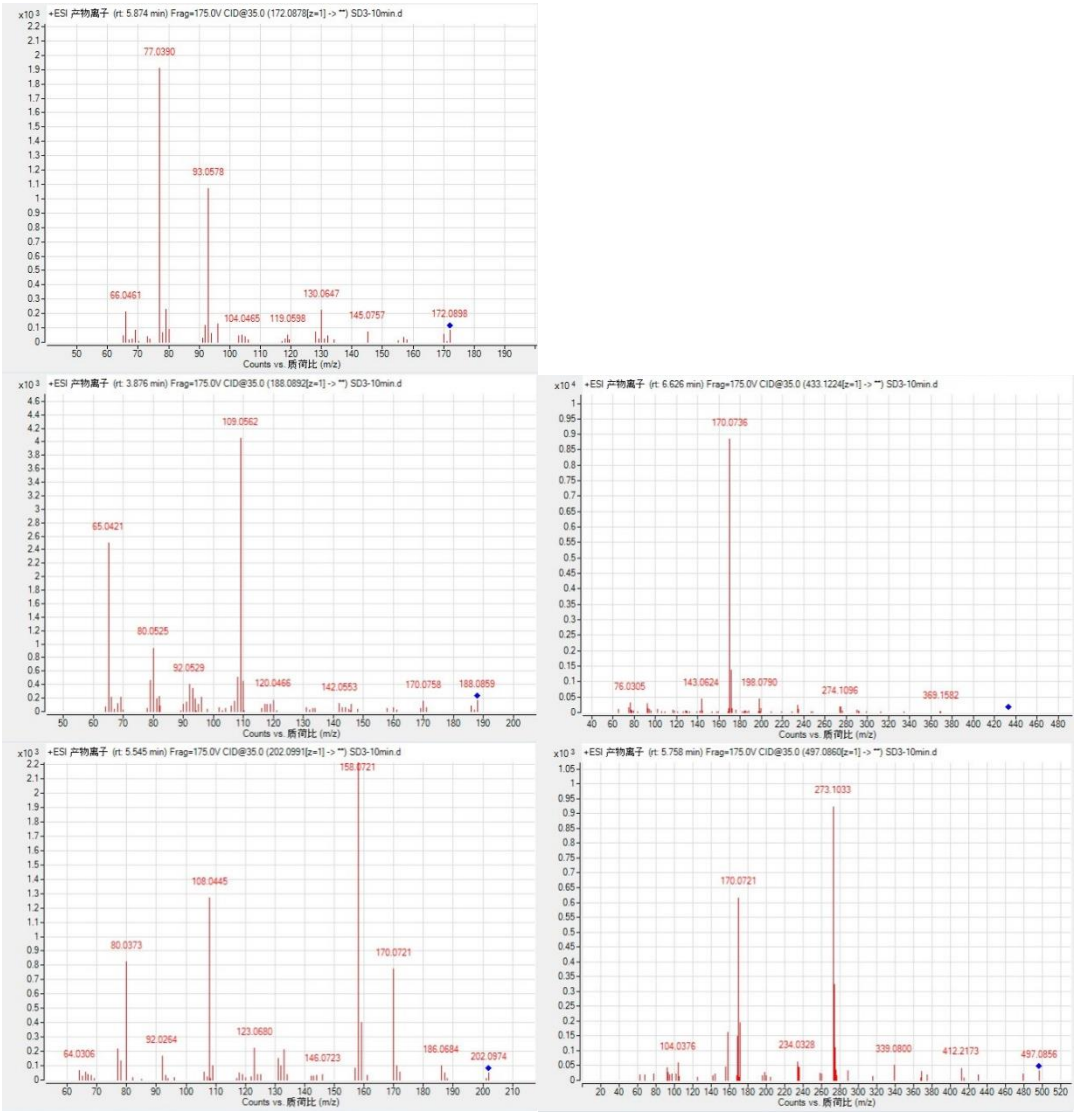

Figure B-3. MS/MS spectra of intermidiate products during the oxidation of SD. The blue dots denote the precursor ions.

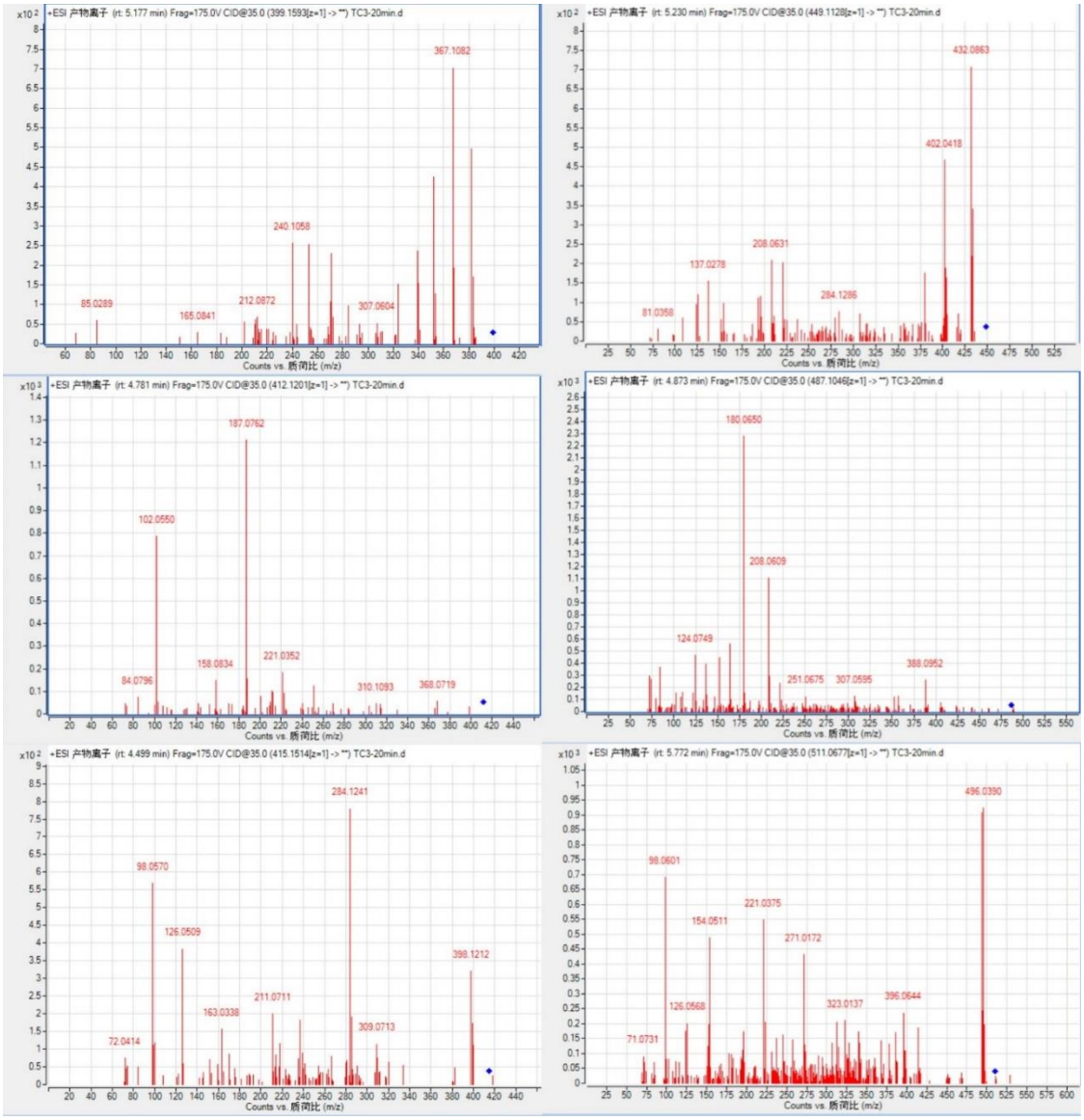

Figure B-4. MS/MS spectra of intermidiate products during the oxidation of SD. The blue dots denote the precursor ions.